Monitoring Survey at the Isles of Shoals North Disposal Site, August/September 2022

Disposal Area Monitoring System - DAMOS

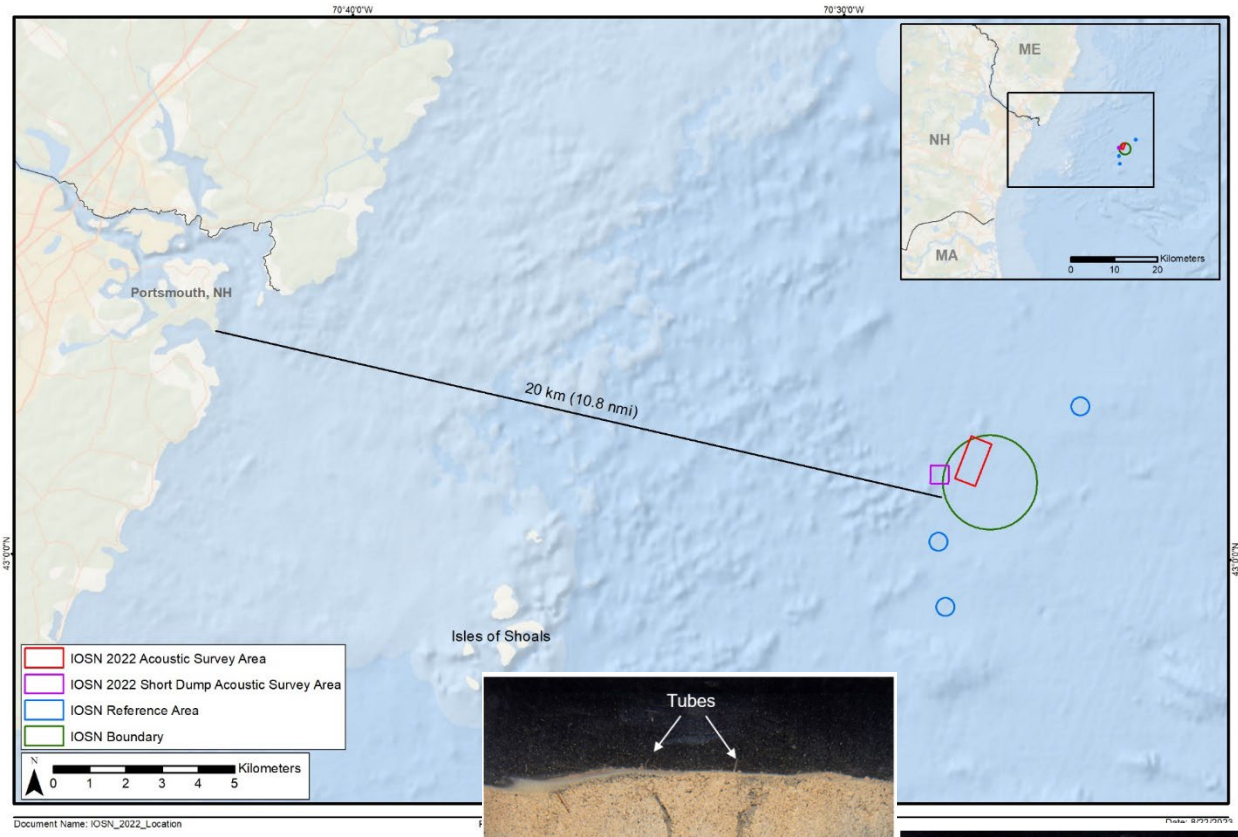

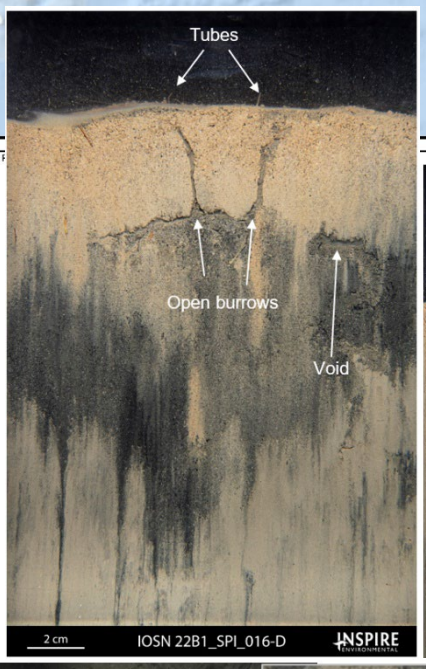

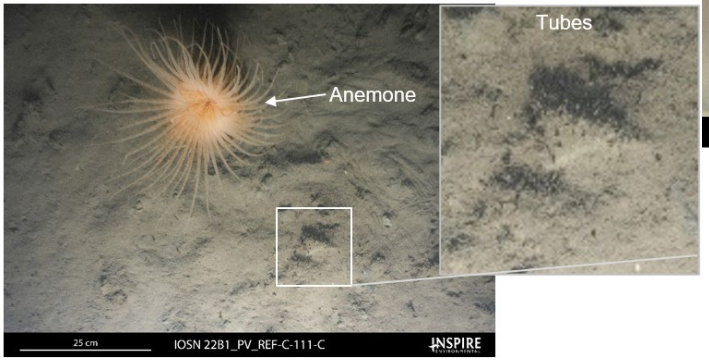

US Army Corps of Engineers
New England District

D A M O S
DISPOSAL AREA MONITORING SYSTEM

Contribution 217
December 2023

REPORT DOCUMENTATION PAGE

form approved OMB No. 0704-0188

1. AGENCY USE ONLY (LEAVE BLANK)	2. REPORT DATE	3. REPORT TYPE AND DATES COVERED
	December 2023	FINAL Contribution, August/September 2022

4. TITLE AND SUBTITLE
Monitoring Survey at the Isles of Shoals North Disposal Site, August/September 2022

5. FUNDING NUMBERS
Contract No. W912WJ-19-D-0010

6. AUTHOR(S)
Kaitlin Sylvester, INSPIRE Environmental

7. PERFORMING ORGANIZATION NAME(S) AND ADDRESS(ES)
INSPIRE Environmental
513 Broadway
Newport, RI 02840

8. PERFORMING ORGANIZATION REPORT NUMBER

9. SPONSORING/MONITORING AGENCY NAME(S) AND ADDRESS(ES)
US Army Corps of Engineers-New England District
696 Virginia Rd
Concord, MA 01742-2751

10. SPONSORING/MONITORING AGENCY REPORT NUMBER
Contribution No. 217

11. SUPPLEMENTARY NOTES
Available from DAMOS Program Manager, Environmental Branch
USACE-NAE, 696 Virginia Rd, Concord, MA 01742-2751

12a. DISTRIBUTION/AVAILABILITY STATEMENT
Approved for public release; distribution unlimited

12b. DISTRIBUTION CODE

13. ABSTRACT

INSPIRE Environmental (INSPIRE) conducted a monitoring survey of the Isles of Shoals North Disposal Site (IOSN) in August and September 2022. The objective of the 2022 IOSN survey was to conduct a confirmatory study at three areas within IOSN: (1) at Mound A, an area that received approximately 46,200 cubic meters (m^3) (60,400 cubic yards [yd3]) of dredged material from 2020 to 2021, (2) at Mound B, an area that received approximately 530,900 m^3 (694,390 yd^3) of dredged material from 2021 to 2022, and (3) at Mound C, an area that received approximately 27,600 m^3 (36,099 yd^3) of rocky dredged material from 2021 to 2022. Survey activities consisted of Sediment Profile Imaging and Plan View (SPI/PV) imagery collection at six stations at Mound A, eight stations at Mound B, and four stations in each of the three reference areas. The study also included acoustic data collection at Mound B and Mound C. A focused study was conducted at an area just outside of the western boundary of the site, where an erroneous disposal of dredged material occurred (short dump). The study consisted of acoustic data collection and adaptive SPI/PV imagery collection.

The confirmatory acoustic survey was conducted over the active portion of the site and covered a 600 x 1,250-meter (m) (1,970 x 4,100-foot [ft]) area. Bathymetric data revealed a relatively flat surface ranging from 92.5 to 94.0 m (303.5 to 308.4 ft) with two distinct features, newly formed Mounds B and C, rising from the ambient seafloor. The bathymetric elevation change model revealed that Mound B is greater than 7 m (23 ft) in height, and Mound C is approximately 2 m (6.6 ft) in height. The acoustic backscatter for both mounds displayed footprints of coarser material disbursed radially around the disposal target.

Acoustic data was also collected over a 500 x 500-m (1,640 x 1,640-ft) area over a reported short-dump location. Bathymetric data revealed a relatively flat surface with a moderate depression visible in the central portion of the short-dump survey area, which correlated with the location of the errant disposal from the scow data log. Backscatter and side-scan sonar data revealed a discrete signature of stronger returns located in the central portion of the short-dump survey area corresponding spatially to the depression observed in the bathymetric data, and with the short-dump disposal record.

SPI/PV survey results provided several lines of evidence indicating benthic recovery was progressing as expected following dredged material disposal at Mound B. Mean maximum successional stage rank at Mound B was statistically equivalent to that of the reference areas. The apparent Redox Potential Discontinuity (aRPD) depths were often indeterminate and could not be statistically compared to the reference areas. This was largely due to the physical nature of the sediment types (e.g., mixture of porous very fine to coarse sands, hard substrate) and may be further complicated by the relatively recent disposal activities at the Site; consolidation is likely to occur over time as the material settles. However, additional lines of evidence derived from SPI/PV indicated benthic recovery including the prevalence of surficial tubes, relatively deep bioturbation depths, and the presence of large epifauna including lobster, crab, and shrimp, demonstrating the habitat is becoming colonized by a variety of taxa.

At Mound A in 2022, approximately two years after dredged material placement, the signature of dredged material persisted, and signs of benthic recovery were evident. In 2022, the mean maximum infaunal successional stage rank at Mound A was statistically equivalent to the reference areas. Further, at Mound A, the mean maximum infaunal successional stage rank in 2022 was statistically more advanced than in 2021. Similar to the findings observed in 2021, in 2022 the measured aRPD depths at Mound A were statistically inequivalent (shallower) than aRPD depths measured at the reference areas. Additionally, the aRPD depths at Mound A were shallower in the 2022 data compared to those measured in 2021, eight months after disposal. However, a similar reduction of mean aRPD depths was observed at the reference sites from 2021 to 2022 indicating a temporal change may have occurred that affected aRPD depth values for both the site and reference areas during this time. The increase in successional stage between years at Mound A follows the successional stage paradigm, with more advanced successional stage developing over time since disturbance. This suggests that the area is still trending toward recovery and an equilibrium with the benthic communities from the undisturbed surrounding areas.

Results of the 2022 surveys led to the following recommendations:

R1: Future dredged material can be placed throughout the disposal site and should continue to be targeted to specific areas to limit temporary impacts to the benthic community. Scow disposal speeds should be monitored for compliance with permit conditions and contract specifications to limit the spread of material beyond target areas.

R2: Mound B should be revisited to determine if aRPD depths are measurable after additional time has passed since disposal events. This will provide additional information on whether additional time and consolidation will result in measurable aRPD depths associated with the mixed/porous dredged material.

R3: Mound C should be monitored under a hard bottom habitat-specific recovery protocol, focusing on benthic colonization and species recruitment of the harder substrate at this mound.

R4: Another SPI/PV survey at Mound A paired with the next monitoring survey, prior to placing additional dredged material in this area, would provide further temporal resolution on the recovery timeline at the Site.

R5: Targeted acoustic data collection, coupled with SPI/PV sampling, should continue to be used to investigate any future short-dump events.

14. SUBJECT TERMS	15. NUMBER OF TEXT PAGES:
DAMOS, dredged material, IOSN, Isles of Shoals, acoustic, multibeam, backscatter, side-scan sonar, SPI, PV, sediment profile imaging, short dump	61 pp plus Figures and Appendices
	16. PRICE CODE

17. SECURITY CLASSIFICATION OF REPORT	18. SECURITY CLASSIFICATION OF THIS PAGE	19. SECURITY CLASSIFICATION OF ABSTRACT	20. LIMITATION OF ABSTRACT
Unclassified			

MONITORING SURVEY AT THE ISLES OF SHOALS NORTH DISPOSAL SITE AUGUST/SEPTEMBER 2022

CONTRIBUTION #217

December 2023

Contract No. W912WJ-19-D-0010

Funded and Managed by:
New England District
U.S. Army Corps of Engineers
696 Virginia Road
Concord, MA 01742-2751

Prepared by:
INSPIRE Environmental
513 Broadway
Newport, RI 02840

This report should be cited as:

USACE. 2023. Monitoring Survey at the Isles of Shoals North Disposal Site, August/September 2022. DAMOS Contribution No. 217. Prepared by INSPIRE Environmental, Newport, RI for the U.S. Army Corps of Engineers, New England District, Concord, MA. 61 pp plus Figures and Appendices.

Note on units of this report: As a scientific data summary, information and data are presented in the metric system. However, given the prevalence of English units in the dredging industry of the United States, conversions to English units are provided for general information in Section 1.0. A table of common conversions can be found in Appendix A.

TABLE OF CONTENTS

Page

Page

LIST OF TABLES

LIST OF FIGURES

Figure Page

Figure Page

Figure Page

Figure Page

LIST OF ACRONYMS

ANOVA	Analysis of Variance
aRPD	apparent Redox Potential Discontinuity
ASCII	American Standard Code for Information Interchange
CCBDS	Cape Cod Bay Disposal Site
CI	confidence interval
CLT	Central Limit Theorem
cm	centimeter
CTD	conductivity, temperature, and depth
DAMOS	Disposal Area Monitoring System
DGPS	Digital Global Positioning System
FNP	Federal Navigation Project
ft	feet
GIS	Geographic information system
GNSS	Global Navigation Satellite System
GPS	Global Positioning System
INSPIRE	INSPIRE Environmental
IOSN	Isles of Shoals North Disposal Site
kHz	kilohertz
km	kilometer
m	meter
mm	millimeter
MBES	multibeam echosounder
MLLW	Mean Lower Low Water
MMS	Mobile Mapping Suite
MPRSA	Marine Protection, Research, and Sanctuaries Act
NAD 1983	North American Datum of 1983
NAVD88	North American Vertical Datum of 1988
NAE	USACE, New England Division

NEF	Nikon Electronic Format
nmi	nautical mile
NOAA	National Oceanic and Atmospheric Association
NOS	National Ocean Service
ODMDS	Ocean Dredged Material Disposal Site
PSD	Photoshop Document
PV	Plan View
QAPP	Quality Assurance Project Plan
RISDS	Rhode Island Sound Disposal Site
RMS	Root Mean Square
RTK	Real Time Kinematic
R/V	research vessel
SBET	Smoothed Best Estimate of Trajectory
SD	standard deviation
SMMP	Site Management and Monitoring Plan
SOP	Standard Operating Procedures
SPI	Sediment Profile Imaging
TIF	tagged image file
TOST	two one-sided tests
USACE	U.S. Army Corps of Engineers
VDATUM	Vertical Datum Transformation
WAAS	Wide Area Augmentation System
yd	yard

EXECUTIVE SUMMARY

INSPIRE Environmental (INSPIRE) conducted a monitoring survey of the Isles of Shoals North Disposal Site (IOSN) in August and September 2022. The objective of the 2022 IOSN survey was to conduct a confirmatory study at three areas within IOSN: (1) at Mound A, an area that received approximately 46,200 cubic meters (m^3) (60,400 cubic yards [yd^3]) of dredged material from 2020 to 2021, (2) at Mound B, an area that received approximately 530,900 m^3 (694,390 yd^3) of dredged material from 2021 to 2022, and (3) at Mound C, an area that received approximately 27,600 m^3 (36,099 yd^3) of rocky dredged material from 2021 to 2022. Survey activities consisted of Sediment Profile Imaging and Plan View (SPI/PV) imagery collection at six stations at Mound A, eight stations at Mound B, and four stations in each of the three reference areas. The study also included acoustic data collection at Mound B and Mound C. A focused study was conducted at an area just outside of the western boundary of the site, where an erroneous disposal of dredged material occurred (short dump). The study consisted of acoustic data collection and adaptive SPI/PV imagery collection.

The confirmatory acoustic survey was conducted over the active portion of the site and covered a 600 x 1,250-meter (m) (1,970 x 4,100-foot [ft]) area. Bathymetric data revealed a relatively flat surface ranging from 92.5 to 94.0 m (303.5 to 308.4 ft) with two distinct features, newly formed Mounds B and C, rising from the ambient seafloor. The bathymetric elevation change model revealed that Mound B is greater than 7 m (23 ft) in height, and Mound C is approximately 2 m (6.6 ft) in height. The acoustic backscatter for both mounds displayed footprints of coarser material disbursed radially around the disposal target.

Acoustic data was also collected over a 500 x 500-m (1,640 x 1,640-ft) area over a reported short-dump location. Bathymetric data revealed a relatively flat surface with a moderate depression visible in the central portion of the short-dump survey area, which correlated with the location of the errant disposal from the scow data log. Backscatter and side-scan sonar data revealed a discrete signature of stronger returns located in the central portion of the short-dump survey area corresponding spatially to the depression observed in the bathymetric data, and with the short-dump disposal record.

SPI/PV survey results provided several lines of evidence indicating benthic recovery was progressing as expected following dredged material disposal at Mound B. Mean maximum successional stage rank at Mound B was statistically equivalent to that of the reference areas. The apparent Redox Potential Discontinuity (aRPD) depths were often indeterminate and could not be statistically compared to the reference areas. This was

largely due to the physical nature of the sediment types (e.g., mixture of porous very fine to coarse sands, hard substrate) and may be further complicated by the relatively recent disposal activities at the Site; consolidation is likely to occur over time as the material settles. However, additional lines of evidence derived from SPI/PV indicated benthic recovery including the prevalence of surficial tubes, relatively deep bioturbation depths, and the presence of large epifauna including lobster, crab, and shrimp, demonstrating the habitat is becoming colonized by a variety of taxa.

At Mound A in 2022, approximately two years after dredged material placement, the signature of dredged material persisted, and signs of benthic recovery were evident. In 2022, the mean maximum infaunal successional stage rank at Mound A was statistically equivalent to the reference areas. Further, at Mound A, the mean maximum infaunal successional stage rank in 2022 was statistically more advanced than in 2021. Similar to the findings observed in 2021, in 2022 the measured aRPD depths at Mound A were statistically inequivalent (shallower) than aRPD depths measured at the reference areas. Additionally, the aRPD depths at Mound A were shallower in the 2022 data compared to those measured in 2021, eight months after disposal. However, a similar reduction of mean aRPD depths was observed at the reference sites from 2021 to 2022 indicating a temporal change may have occurred that affected aRPD depth values for both the site and reference areas during this time. The increase in successional stage between years at Mound A follows the successional stage paradigm, with more advanced successional stage developing over time since disturbance. This suggests that the area is still trending toward recovery and an equilibrium with the benthic communities from the undisturbed surrounding areas.

Results of the 2022 surveys led to the following recommendations:

R1: Future dredged material can be placed throughout the disposal site and should continue to be targeted to specific areas to limit temporary impacts to the benthic community. Scow disposal speeds should be monitored for compliance with permit conditions and contract specifications to limit the spread of material beyond target areas.

R2: Mound B should be revisited to determine if aRPD depths are measurable after additional time has passed since disposal events. This will provide additional information on whether additional time and consolidation will result in measurable aRPD depths associated with the mixed/porous dredged material.

R3: Mound C should be monitored under a hard bottom habitat-specific recovery protocol, focusing on benthic colonization and species recruitment of the harder substrate at this mound.

R4: Another SPI/PV survey at Mound A paired with the next monitoring survey, prior to placing additional dredged material in this area, would provide further temporal resolution on the recovery timeline at the Site.

R5: Targeted acoustic data collection, coupled with SPI/PV sampling, should continue to be used to investigate any future short-dump events.

1.0 INTRODUCTION

INSPIRE Environmental (INSPIRE) conducted acoustic and Sediment Profile and Plan View Imaging (SPI/PV) monitoring surveys at the Isles of Shoals North Disposal Site (IOSN) in August and September 2022 as part of the U.S. Army Corps of Engineers (USACE) New England District (NAE) Disposal Area Monitoring System (DAMOS) Program. DAMOS is a comprehensive monitoring and management program designed and conducted to address environmental concerns surrounding the placement of dredged material at aquatic disposal sites throughout the New England region. An introduction to the DAMOS Program and IOSN, including brief descriptions of previous dredged material disposal and site monitoring activities, is provided below.

1.1 Overview of the DAMOS Program

The DAMOS Program features a tiered management protocol designed to ensure that any potential adverse environmental impacts associated with dredged material disposal are promptly identified and addressed (Germano et al. 1994). For over 40 years, the DAMOS Program has collected and evaluated dredged material disposal site data throughout New England. Based on these data, patterns of physical, chemical, and biological responses of seafloor environments to dredged material disposal activity have been documented (Fredette and French 2004).

DAMOS monitoring surveys fall into two general categories: confirmatory studies and focused studies. The data collected and evaluated during these studies provide answers to strategic questions in determining next steps in the disposal site management process. DAMOS monitoring results guide the management of disposal activities at existing sites, support planning for use of future sites, and evaluate the long-term status of historical sites (Wolf et al. 2012).

Confirmatory studies are designed to test hypotheses related to expected physical and ecological response patterns following placement of dredged material on the seafloor at established, active disposal sites. Two primary goals of DAMOS confirmatory monitoring surveys are to document the physical location and stability of dredged material placed into the aquatic environment and to evaluate the biological recovery of the benthic community following placement of dredged material. Several survey techniques are employed in order to characterize these responses to dredged material placement. Sequential acoustic monitoring surveys (including bathymetric, acoustic backscatter, and side-scan sonar data

collection) are performed to characterize the height and spread of discrete dredged material deposits or mounds created at open-water sites as well as the accumulation/consolidation of dredged material into confined aquatic disposal cells.

SPI and PV imaging surveys are performed in confirmatory studies to provide further physical characterization of the material and to support evaluation of seafloor (benthic) habitat conditions and recovery over time. Each type of data collection activity is conducted periodically at disposal sites, and the conditions found after a defined period of disposal activity are compared with the long-term data set at specific sites to determine the next step in the disposal site management process (Germano et al. 1994).

Focused studies are periodically undertaken within the DAMOS Program to evaluate candidate sites, as baseline surveys at new sites, to evaluate inactive or historical disposal sites, and to contribute to the development of dredged material management and monitoring techniques. Focused DAMOS monitoring surveys often feature additional types of data collection activities as deemed appropriate to achieve specific survey objectives, such as grab or core sampling of sediment for physical/chemical/biological analyses, sub-bottom profiling, or video image collection.

The 2022 IOSN survey included confirmatory monitoring over the active portion of the site and at the south-central portion of the site where material was placed in 2021. A focused study was also conducted to assess seafloor conditions at a location just outside of the IOSN site boundary where dredged material was inadvertently released (the short-dump location). The confirmatory study over the active portion of the site paired an acoustic survey with SPI/PV imagery to support an assessment of physical modifications and the initial benthic community response to dredged material placement. Additionally, SPI/PV imagery was collected within the south-central portion of the site where material was placed in 2021 to further monitor benthic recovery as well as within the three designated reference areas for comparative purposes. The focused study was conducted at the short-dump location and included paired acoustic data collection with adaptive SPI/PV imagery collection to delineate the dredged material footprint on the seafloor resulting from the documented short-dump event.

1.2 Introduction to the Isles of Shoals North Disposal Site

IOSN is located approximately 20 kilometers (km) (10.8 nautical miles [nmi]) east of Portsmouth, New Hampshire, in the Gulf of Maine (Figure 1-1). IOSN is circular in shape and approximately 2.5 km (1.3 nmi) in diameter. Current conditions at IOSN include water

depths that range from approximately 90 meters (m) (295 feet [ft]) Mean Lower Low Water (MLLW) on the western boundary to 100 m (328 ft) in the eastern portion of the site. The seafloor at IOSN slopes gradually, increasing in water depth from the western boundary to the eastern boundary of the site (Figure 1-2). There was a moderate (0.7 m [2.3 ft]) elevation change at the south-central portion of the site following the placement of approximately 46,000 m^3 of dredged material in 2020-2021, referred to as Mound A (USACE 2022). Outside of the IOSN boundaries to the northwest and southeast, hard bottom features rise approximately 10 to 20 m (33 to 66 ft) above the surrounding seafloor (Guarinello et al. 2016). Three reference areas (REF-A, REF-B, and REF-C) are defined as 250-m (~820-ft) radius circles and are located to the southwest and northeast of the site (Figure 1-2). Water depths at the reference areas range from 93 to 95 m (305 to 312 ft).

IOSN was designated as an Ocean Dredged Material Disposal Site (ODMDS) in September 2020 by the U.S. Environmental Protection Agency Region 1 (EPA Region 1) under Section 102(c) of the Marine Protection, Research, and Sanctuaries Act (MPRSA). The site is managed by EPA Region 1 and USACE NAE following the Site Management and Monitoring Plan (SMMP) (USACE/EPA 2020). The site began receiving material in November 2020 from the Rye Harbor dredging project (USACE 2022).

1.3 Previous IOSN Monitoring Events

The DAMOS Program conducted baseline surveys of IOSN in 2015, 2019, and 2020 to support the site designation process and to characterize the site and reference areas prior to disposal activities (Guarinello et al. 2016; USACE 2021a). A confirmatory survey was conducted in 2021 after initial placement of dredged material at Mound A (Table 1-1; USACE 2022). The 2021 IOSN survey included the collection of high-resolution acoustic data and SPI/PV imagery around the area of recent disposal activity at Mound A (material from Rye Harbor). Additional SPI/PV imagery was collected in baseline areas of the site and the three reference areas. These surveys found that dredged material distribution was limited to the planned target area. Measured apparent redox potential discontinuity (aRPD) depths at Mound A were statistically less than those at the reference areas, however successional stage was statistically similar, indicating that the area where recent disposal material had been placed was progressing towards recovery. The baseline conditions documented within IOSN during the 2021 survey were observed to be similar to those at the reference areas.

1.4 Recent Dredged Material Disposal Activity

Since the September 2021 survey at IOSN, approximately 558,500 cubic meters (m^3) (730,490 cubic yards [yd^3]) of dredged material have been placed at IOSN (Table 1-2; Figure 1-3). This material originated from the improvement dredging of the Portsmouth Harbor and Piscataqua River Federal Navigation Project (FNP). Dredged material consisted of fine-grained sediment, sand, and glacial till which was placed in the west-central portion of the site (referred to as Mound B). A small volume of the total placement amount (27,600 m^3 [36,099 yd^3]) was rock blasted as part of the improvement project and directed to a separate target in the northern portion of the site (referred to as Mound C). The target was designed with the intention of beneficially using the blasted rock to create hard bottom habitat at the site and was selected to be adjacent to existing hard bottom features outside the northern boundary of IOSN to facilitate recruitment and colonization of the new rock reef.

A detailed record of dredged material disposal activity at IOSN from November 2021 to April 2022, including the origin, volume, and disposal location, is provided in Appendix B.

1.5 Short-Dump Disposal

Approximately 3,800 m^3 (5,000 yd^3) of dredged material was inadvertently released west of IOSN in a documented short-dump event from one scow (Figure 1-3). This material also originated from the improvement dredging of the Portsmouth Harbor and Piscataqua River FNP and was reported to consist of fine-grained sediments.

1.6 2022 Survey Objectives

The overall objective of the 2022 IOSN monitoring effort was to conduct a confirmatory survey and a focused investigation designed to address the following:

- Characterize the seafloor topography and surficial features over the active portion of IOSN (Mound B and Mound C) using acoustic data;
- Use SPI/PV imaging to assess the recolonization status of benthic organisms and surficial sediment characteristics at the active areas of IOSN (Mound B and Mound C), the previously active area (Mound A), and three references areas; and
- Assess seafloor conditions and delineate potential dredged material deposits using acoustic data and adaptive SPI/PV sampling at the short-dump location.

Table 1-1.

Overview of Survey Activities at IOSN

Date	Purpose of Survey	Bathymetry Area	SPI Stations (location - #)	Additional Data	DAMOS Report/ Contribution No.	Reference
Sept 2015	Baseline Acoustic and SPI/PV	3,500 x 3,500 m	45	-	2015-D-01	Guarinello et al. 2016
Sept/Oct 2019 and Sept 2020	Baseline Sediment Characterization, Benthic Community Structure, and Water Quality	-	-	17 Sediment Grab Samples 4 Water Quality Profiles/Samples	DR-2020-1	USACE 2021a
Oct 2021	Monitoring Survey	1,000 x 1,000 m	IOSN – 15 REF Areas - 9	-	Contribution 214	USACE 2022

Table 1-2.

Disposal Activity at IOSN November 25, 2021 to April 15, 2022
(per dredged material disposal logs provided by USACE, August 2022)

Permit number	Project Name	Disposal Location	Disposal Dates	Load volume (m^3)	Load volume (yd^3)
W912WJ-21-C-0027	Portsmouth Piscataqua FNP	Mound B	11/25/2021 – 04/15/2022	530,868	694,349
W912WJ-21-C-0027	Portsmouth Piscataqua FNP	Mound C (Rock)	1/21/2022 – 2/21/2022	27,600	36,099
			Total	**558,468**	**730,448**
W912WJ-21-C-0027	Portsmouth Piscataqua FNP	Short Dump	3/20/2022	3,931	5,141

2.0 METHODS

The acoustic data collection was completed by Substructure, Inc. onboard the 32-foot research vessel (R/V) *Orion* on 25 August 2022. The SPI/PV imagery was collected by INSPIRE Environmental onboard the 50-foot R/V *Gulf Challenger* on 13-14 September 2022.

2.1 Acoustic Survey

The acoustic survey featured use of a multibeam echosounder (MBES) to collect bathymetric, acoustic backscatter, and side-scan sonar measurements over an approximately 600 x 1,250 m area of the site and an approximately 500 x 500 m area covering the reported short-dump location. Fishing gear observations were made during the acoustic survey to quantify fishing activity in and around IOSN.

2.1.1 Navigation and Onboard Data Acquisition

During survey operations, vessel navigation and orientation data were controlled by an Applanix 320 POSMV on the *R/V Orion* that received Real Time Kinematic (RTK) differential Global Navigation Satellite System (GNSS) correctors from a local Trimble R10 base station (established over a survey mark at the Portsmouth, NH Marina) via a dedicated NTRIP caster network (Table 2-1). During survey operations, the POSMV vessel navigation, heading, and motion data were logged within the QPS QINSy hydrographic survey software, and the raw POSMV observables were continuously recorded throughout the survey period to enable post-processing using the Applanix POSPac Mobile Mapping Suite (MMS) software. The POSPac post-processed horizontal position error Root Mean Square (RMS) was consistently below 2.0 centimeters (cm), and the vertical error RMS was below 3.0 cm.

Bathymetric, acoustic backscatter (snippets), and side-scan sonar (Truepix) data were acquired using an R2Sonic 2024 MBES as detailed in the Program Quality Assurance Project Plan (QAPP; INSPIRE 2020) and in the standard operating procedures (SOP) for acoustic surveys (Substructure 2022). This 200-450 kilohertz (kHz) system forms 256 0.5- to 1-degree beams (frequency dependent) distributed equiangularly or equidistantly across up to a 160-degree swath. For this survey, the sonar frequency was set to 300 kHz and a sonar swath opening of 70 degrees was used, resulting in swath coverage approximately 1.4 times the water depth. The narrower swath opening was used for this survey to

improve data density and to reduce the beam footprint in the deeper waters (80 to 95 m) that characterize this site.

Corrections of sounding depth and position (range and azimuth) for refraction due to water column speed of sound differences were applied using a series of four conductivity, temperature, and depth (CTD) profiles acquired periodically during the survey operations. The CTD profiles were generally consistent across the survey period, and the profiles were applied directly within the survey program during data acquisition. The observed speed of sound differences resulted in very minor outer beam differences that had no effect on the usable swath of the multibeam data.

2.1.2 Acoustic Data Collection

The acoustic surveys within the active disposal area of IOSN (Mounds B and C) and at the short-dump area were executed to provide greater than 200-percent coverage by running a series of north-south oriented lines spaced at 50-m intervals across the IOSN survey area and the short-dump location, totaling thirteen and ten lines, respectively (Figure 2-1). Adequate survey coverage was confirmed by closely monitoring the 2-m real-time sounding grid. In addition, four perpendicular east-west oriented cross-check sounding lines (cross-lines) were acquired across both survey areas.

2.1.3 Bathymetric Data Processing

Bathymetric data were processed using Applanix POSPac MMS, QPS Qimera, and HYPACK HYSWEEP® software. Processing components are described below and included:

- Post-processing of real-time POSMV solution with POSPac MMS using POSMV raw observables and local base station Trimble R10 GNSS data;
- Application of POSPac Smoothed Best Estimate of Trajectory (SBET) file to raw multibeam data files;
- Conversion of the SBET ellipsoidal height reference to MLLW via Geoid Model 12B and published North American Vertical Datum of 1988 (NAVD88) to MLLW offset for the survey area from the National Oceanic and Atmospheric Administration's (NOAA) VDatum application;
- Comparison of SBET height reference to the NOAA Seavey Island tide observations;

- Application of speed of sound profiles to account for differences in the water column during the survey period;
- Removal of spurious points associated with water column interference or system errors;
- Development of a grid surface representing depth solutions;
- Statistical estimation of sounding solution uncertainty; and
- Generation of data visualization products.

The combined uncertainties associated with all system elements, including calibrations, tide corrections, and refraction caused by water column stratification, were quantified by comparing primary survey transects with perpendicular cross-line transects.

Comparisons were made using the Qimera Cross Check program to show the observed differences by beam angle between the 2-m grid surface (computed from the primary survey transects) and the cross-line survey point data. This comparison used a 70-degree swath opening for the main lines and a 50-degree opening for the cross-lines which was consistent with the swath opening used for final grid development. This resulted in approximately 3.8 million mainstay versus cross-check comparison points, with a mean difference of -0.032 m, a standard deviation (SD) of 0.167 m, and a mean 95% RMS (2-sigma) confidence limit uncertainty of 0.366 m. Mean elevation changes across the swaths ranged from -3.38 m to 2.68 m with the greatest changes observed in the outer beam overlap areas. This comparison indicates negligible tide bias with only slightly increased outer swath uncertainty associated with minor refraction impacts. This analysis shows compliance with USACE accuracy recommendations and National Ocean Service (NOS) standards. Note that the NOS standard for this project depth (Special Order) specifies a 95th percentile confidence interval (95% CI) of ±0.731 m at the maximum survey depths.

Reduced bathymetric data were exported in American Standard Code for Information Interchange (ASCII) text format at a resolution of 2 m x 2 m with fields for easting, northing, and MLLW elevation (meters). All data were projected to the North American Datum of 1983 (NAD 1983) Maine West State Plane Coordinate System meters. A variety of data visualizations were generated using a combination of HYPACK, QPS Fledermaus, and ESRI ArcGIS Pro. Visualizations and data products included:

- ASCII data files of all processed soundings including MLLW depths and elevations;

- 3-dimensional surface maps of the seabed created using 5x vertical exaggeration and artificial illumination to highlight fine-scale features not visible on contour layers (delivered in grid and Tagged Image File [TIF] formats); and
- An acoustic relief map of the survey area created using 5x vertical exaggeration, delivered in georeferenced TIF format.

2.1.4 Backscatter Data Processing

MBES backscatter data were processed using the QPS Fledermaus GeoCoder Toolkit implementation of the GeoCoder algorithms, originally developed by NOAA's Center for Coastal and Ocean Mapping Joint Hydrographic Center. GeoCoder uses beam-angle varying gain algorithms to normalize the MBES snippet beam time-series data across the full swath. The resulting backscatter intensity data for IOSN were exported in ASCII format with fields for easting, northing, and backscatter intensity (in decibel units) at a grid resolution of 1 m and as a seamless 1-m backscatter mosaic in GeoTIF format. A Gaussian filter was applied to backscatter data to minimize nadir artifacts and the filtered data were used to develop backscatter visualization draped over hillshaded relief.

2.1.5 Side-Scan Sonar Data Processing

MBES pseudo side-scan sonar (TruePix) data were processed using Chesapeake Technology SonarWiz software. The TruePix data (16-bit QINSy QPD files) were imported into SonarWiz and each transect was manually bottom- and far-field tracked. Slant-range corrections and nadir filters were applied to the bottom-tracked data, and then empirical gain normalization was applied across the full dataset to create a seamless side-scan sonar mosaic. The deeper depths associated with this site and the resulting separation between the sonar and the seafloor limited the effectiveness of the pseudo side-scan sonar data. The side-scan sonar mosaic was exported at a 1-m resolution in GeoTIF format to complement the MBES backscatter mosaic.

2.1.6 Acoustic Data Analysis

The processed bathymetric grids were converted to rasters, and bathymetric contour lines and acoustic relief models were generated and displayed using GIS. The backscatter mosaics and filtered backscatter grid were combined with acoustic relief models in GIS to facilitate visualization of relationships between acoustic datasets. This was done by rendering images and color-coded grids with sufficient transparency to allow the three-dimensional acoustic relief model to be visible underneath.

Surfer software was used to calculate elevation change grids between the 2022 bathymetric dataset and the DAMOS survey conducted in 2015. Elevation change grids were calculated by subtracting the earlier survey elevation estimates from the 2022 survey depth estimates at each point throughout the grid. The resulting elevation changes were contoured and displayed using GIS.

2.2 Sediment Profile and Plan View Imaging Survey

Sediment profile imaging and plan view imaging (SPI/PV) are monitoring techniques used to provide data on the physical characteristics of the seafloor and the status of the benthic biological community.

2.2.1 Navigation and Onboard Data Acquisition

Navigation for the SPI/PV survey was carried out by INSPIRE. A Hemisphere VS330 GNSS compass with dual antennas using Wide Area Augmentation System (WAAS) differential correctors was used to accurately record vessel heading as well as position accuracy within a meter. During operations, HYPACK® LITE software received Differential Global Positioning System (DGPS) data and transmitted a visual display to the helm, guiding the captain to maneuver the vessel to each sampling station. The GNSS was interfaced to HYPACK® software via laptop serial ports to provide a method to record actual sampling locations. Throughout the survey, the HYPACK® data acquisition system received GNSS positioning data. The incoming data stream was digitally integrated and stored on the PC's hard drive. Actual SPI/PV sampling locations were recorded using this system.

For survey activities at the reference areas and within IOSN, the vessel was positioned at each station's target coordinates and the camera was deployed within a defined 7.5-m radius station tolerance. At the reported short-dump location to the west of IOSN, the vessel was aligned according to sea conditions and drifted along a transect, beginning before the acoustic signature of the short dump, which was identified after review of the preliminary acoustic data (see Section 3.1), and continuing beyond it.

When the camera contacted the seafloor, the SPI/PV technicians signaled via handheld radio that the camera was on the bottom. The navigator recorded the time and position of the camera electronically in HYPACK® as well as in the written field log. After all stations were sampled, the navigator exported all recorded positional data into a Microsoft

Excel© spreadsheet, including the station name, date, time, and position of every SPI/PV pair collected.

2.2.2 SPI and PV Survey Planning

The IOSN SPI/PV survey featured image collection at 26 stations. Fourteen stations were distributed within IOSN; eight stations were positioned over the active disposal area, Mound B, that recently received dredged material (within the acoustic survey footprint), and six stations were positioned within the area of the site that received material in 2020/2021, Mound A. Four stations were randomly located within each of the three reference areas (REF A, REF B, and REF C; Figure 2-2). Four SPI/PV stations were proposed over a rock pile area (Mound C) within the active disposal area; however, these samples were not collected due to weather constraints.

A focused SPI/PV survey of the short-dump area included the collection of 15 individual, paired SPI/PV images along a transect line (Figure 2-2). SPI and PV imagery were collected at the short-dump survey area to locate and delineate dredged material on the seafloor. SPI/PV target station locations are provided in Table 2-2, and actual SPI/PV station replicate locations are provided in Appendix C. The methodology for data acquisition and analysis for these images was consistent with the sampling methods described in detail in the Project QAPP (INSPIRE 2020) and INSPIRE SPI/PV SOPs (INSPIRE 2019).

2.2.3 Sediment Profile Imaging

Sediment profile imaging (SPI) is a monitoring technique used to provide data on the physical characteristics of the seafloor and the status of the benthic biological community. The technique involves deploying an underwater camera system to photograph a cross section of the sediment–water interface. In the 2022 survey at IOSN, high-resolution SPI images were acquired using a Nikon® D7200 digital single-lens reflex camera mounted inside an Ocean Imaging® Model 3731 pressure housing system. The pressure housing sat atop a wedge-shaped steel prism with a plexiglass front faceplate and a back mirror. The mirror was mounted at a 45-degree angle to reflect the profile of the sediment–water interface. The camera lens looked down at the mirror, which reflected the image from the faceplate. The prism had an internal strobe mounted inside at the back of the wedge to provide illumination for the image; this chamber was filled with distilled water, so the camera always had an optically clear path. The descent of the prism into the sediment was controlled by a hydraulic piston. As the prism penetrated the seafloor, a trigger activated a time-delay circuit that fired an internal strobe to obtain a cross-sectional image of the upper

15–20 cm of the sediment column (Figure 2-3). The camera remained on the seafloor for approximately 20 seconds to ensure that a successful image had been obtained.

Test exposures of a Color Calibration Target were made on deck at the beginning and end of the 2022 survey to verify that all internal electronic systems consistently met design specifications and to provide a color standard against which final images could be checked to ensure proper color balance. Details of the camera settings for each digital image are available in the associated parameters file embedded in each electronic image file. For this survey, the ISO-equivalent was set at 640, shutter speed was 1/250, f-stop was f13, and storage was in compressed raw Nikon Electronic Format (NEF) files (approximately 30 MB each). All camera settings and any setting changes were recorded in the field log.

Each time the camera system was brought onboard, the frame counter was checked to ensure that the requisite number of replicates had been obtained. In addition, a prism penetration depth indicator on the camera frame was checked to verify that the optical prism had penetrated the bottom to a sufficient depth. If images were missed or the penetration depth was insufficient, the camera frame stop collars were adjusted and/or weights were added or removed, and additional replicate images were taken. Frame counts, time of image acquisition, and the number of weights used were recorded in the field log for each replicate image.

Each image was assigned a unique time stamp in the digital file attributes by the camera's data logger and cross-checked with the time stamp in the navigational system's computer data file. In addition, the field crew kept redundant written sample logs. Images were downloaded periodically to verify successful sample acquisition and/or to assess what type of sediment/depositional layer was present at a particular station. Digital image files were renamed with the appropriate station names after downloading as a further quality assurance step.

2.2.4 Plan View Imaging

An Ocean Imaging® Model DSC24000 plan view underwater camera (PV) system with two Ocean Imaging® Model 400-37 Deep Sea Scaling lasers was attached to the sediment profile camera frame and used to collect plan view images of the seafloor surface. Both SPI and PV images were collected during each "drop" of the system. The PV system consisted of a Nikon D7200 encased in an aluminum housing, a 24 VDC autonomous power pack, a 500 W strobe, and a bounce trigger. A weight was attached to the bounce trigger with a stainless-steel cable so that the weight hung below the camera frame; the scaling

lasers projected two red dots that are separated by a constant distance (26 cm) regardless of the field of view of the PV system. The field of view can be varied by increasing or decreasing the length of the trigger wire and, thereby, the camera height above the bottom when the picture is taken. As the SPI/PV camera system was lowered to the seafloor, the weight attached to the bounce trigger contacted the seafloor prior to the camera frame reaching the seafloor and triggered the PV camera (Figure 2-3).

During set-up and testing of the PV camera, the positions of lasers on the PV camera were checked and calibrated to ensure separation of 26 cm. Test images were also captured to confirm proper camera settings for site conditions. Details of the camera settings for each digital image are available in the associated parameters file embedded in each electronic image file; for this survey, the ISO-equivalent was set at 640. The additional camera settings used were as follows: shutter speed 1/20, f18, white balance set to flash, color mode set to Adobe RGB, sharpening set to none, noise reduction off, and storage in compressed raw NEF files (approximately 30 MB each). Images were checked periodically throughout the survey to confirm that the initial camera settings were still resulting in the highest quality images possible. All camera settings and any setting changes were recorded in the field log.

Prior to field operations, the internal clock in the digital PV system was synchronized with the GPS navigation system and the SPI camera. For each PV image, a time stamp was recorded in the digital file and redundant time notes were made in the field and navigation logs. Throughout the survey, PV images were downloaded at the same time as the SPI images and evaluated to confirm image acquisition and image clarity.

The ability of the PV system to collect usable images was dependent on the clarity of the water column. Water conditions at IOSN allowed use of a 0.9 m (3 ft) trigger wire, resulting in a mean image width of 0.9 m and a mean field of view of 0.6 m^2.

2.2.5 SPI and PV Data Collection

The SPI/PV survey was conducted at IOSN and reference areas on 13 and 14 September 2022 onboard the R/V *Gulf Challenger*. At least four replicate SPI and PV images were collected at each station. The three replicate images with the best quality (adequate prism penetration, no or minimal sampling artifacts) at each station were selected for analysis (Appendices D and E). The single-drop SPI/PV image pairs were opportunistic along the transect (i.e., there were no predetermined locations or station tolerances) and designed to delineate the presence and extent of the short-dump material. All single-drop SPI/PV image pairs were selected for analysis (Appendix D and E).

The DGPS described above was interfaced to HYPACK® software via laptop serial ports to provide a method to locate target coordinates and record actual sampling locations. Throughout the survey, the HYPACK® data acquisition system received DGPS data. The incoming data stream was digitally integrated and stored on the PC's hard drive. Actual SPI/PV sampling locations were recorded using this system.

2.2.6 Image Conversion and Calibration

Following completion of field operations, quality control checks were conducted on the field log, image date/time stamps were verified, and project-specific filenames were generated. After these procedures, the NEF raw image files were color calibrated in Adobe Camera Raw® by synchronizing the raw color profiles to the Color Calibration Target that was photographed prior to field operations with the SPI camera. The raw SPI and PV images were then converted to high-resolution Photoshop Document (PSD) format files, using a lossless conversion file process and maintaining an Adobe RGB (1998) color profile. The PSD images were then calibrated and analyzed in Adobe Photoshop®. Length and area measurements were recorded as number of pixels and converted to scientific units using the calibration information. Detailed results of all SPI and PV image analyses are presented in Appendices D and E.

2.2.7 SPI and PV Data Analysis

Computer-aided analysis of the resulting images provided a set of standard measurements to allow comparisons between different locations and different surveys. The DAMOS Program has successfully used this technique for over 30 years to map the distribution of disposed dredged material and to monitor benthic recolonization at disposal sites (Germano et al. 2011).

Measured parameters for SPI and PV images were recorded in Microsoft Excel© spreadsheets. These data were subsequently checked by one of INSPIRE's senior scientists as an independent quality assurance/quality control review before final interpretation was performed. Spatial distributions of SPI and PV parameters were mapped using ESRI ArcGIS 10.5. Map backgrounds, unless otherwise indicated in the figure footnote, use ESRI Oceans regional hillshaded model accessed through the ArcGIS Online platform.

2.2.7.1 Sediment Profile Image Analysis Parameters

The parameters discussed below were assessed and/or measured and recorded for each replicate SPI image selected for analysis (Appendix D). Descriptive comments were also recorded for each. Many variables can be seen and annotated in context in SPI images from soft bottom coastal and estuarine environments (Figure 2-4). Single-drop SPI images at the short-dump site received an abbreviated analysis for dredged material variables only.

Sediment Type – The sediment grain size major mode and range were estimated visually from the images using a grain size comparator at a similar scale. Results were reported using the phi scale. Conversion to other grain size scales is provided in Appendix F. The presence and thickness of disposed dredged material were also assessed as described below.

Penetration Depth – The depth to which the camera penetrated into the seafloor was measured to provide an indication of the sediment density and bearing capacity. The penetration depth can range from a minimum of 0 cm (i.e., no penetration on hard substrata) to a maximum of 20 cm (full penetration on very soft substrata).

Surface Boundary Roughness–Surface boundary roughness is a measure of the vertical relief of features at the sediment–water interface in the sediment profile image. Surface boundary roughness was determined by measuring the vertical distance between the highest and lowest points of the sediment–water interface. The surface boundary roughness (sediment surface relief) measured over the width of sediment profile images typically ranges from 0 to 4 cm, and may be related to physical structures (e.g., ripples, rip-up structures, mud clasts) or biogenic features (e.g., burrow openings, fecal mounds, foraging depressions). Biogenic roughness typically changes seasonally and is related to the interaction of bottom turbulence and bioturbation activities.

Apparent Redox Potential Discontinuity (aRPD) Depth – The aRPD depth provides a measure of the integrated time history of the balance between near-surface oxygen conditions and biological reworking of sediments. Sediment particles exposed to oxygenated waters oxidize and lighten in color to brown or light gray. As the particles are buried or moved down by biological activity, they are exposed to reduced oxygen concentrations in subsurface pore waters and their oxic coating slowly reduces, changing color to dark gray or black. When biological activity is high, the aRPD depth increases; when it is low or absent, the aRPD depth decreases. The aRPD depth was measured by assessing color and reflectance boundaries within the images.

Mud Clasts – When fine-grained, cohesive sediments are disturbed, either by physical bottom scour or faunal activity (e.g., decapod foraging) intact clumps of sediment are often scattered across the seafloor. The number of clasts observed at the sediment–water interface was counted and their oxidation state assessed. The detection of reduced mud clasts in an obviously aerobic setting suggests a recent origin (Germano 1983). Mud clasts that are artifacts of SPI sampling (mud clots can fall off the back of the prism or wiper blade) are not recorded in the analysis sheet but may be noted in the "Comments" field.

Dredged Material Layer Depth and Thickness – The depth below the sediment–water interface that the top of dredged material layer occurred was measured. Additionally, the thickness of the dredged material layer, from 1 millimeter (mm) to 20 cm (the height of the SPI optical window) was measured. If the layer extended below the depth of prism penetration, it was noted.

Biological Mixing – The depth to which sediments are bioturbated, or the biological mixing depth, can be an important parameter for studying nutrient or contaminant flux, as well as organic enrichment, in sediments. In this study, the maximum linear distances from the sediment surface to subsurface voids was measured. This parameter represents the maximum observed particle mixing depth of head-down feeders, mainly polychaetes. The presence of subsurface voids were noted for each SPI replicate.

Sediment oxygen demand (SOD) – Represents the overall rate of biological and chemical oxygen consumption in the sediment column. Organic loading results in increased SOD and reduced sediments. The relative amount of organic enrichment is indicated by sediment color; darker coloration indicates more reduced sediments with greater organic loading (Fenchel 1969; Rhoads 1974; Lyle 1983; Bull and Williamson 2001; Sturdivant and Shimizu 2017). SOD levels (i.e., none, low, medium, and high) were assessed for all images.

Low Dissolved Oxygen – Images in which dark gray or black reduced sediments were in contact with the water column across the entire length of the sediment–water interface were recorded as having low dissolved oxygen condition.

Sedimentary Methane – If organic loading is extremely high, porewater sulfate is depleted and methanogenesis occurs. The process of methanogenesis is indicated by the appearance of methane bubbles in the sediment column. These gas-filled voids are readily discernable in SPI images because of their irregular, generally circular aspect and glassy texture (due to the reflection of the strobe off the gas bubble). The presence of subsurface methane bubbles were noted.

Thiophilic Bacteria (*Beggiatoa*) – The presence of sulfur-oxidizing bacterial colonies indicates hypoxic dissolved oxygen concentrations in the water column at the benthic boundary-layer (Rosenberg and Diaz 1993; Sturdivant et al. 2012). The presence and extent (e.g., threads, trace, patches, mat) of *Beggiatoa* or *Beggiatoa*-like colonies were noted.

Infaunal Successional Stage – Infaunal successional stage is a measure of the biological community inhabiting the seafloor. Current theory holds that organism–sediment interactions in fine-grained sediments follow a predictable sequence of development after a major disturbance (e.g., dredged material disposal) (Pearson and Rosenberg 1978; Rhoads and Germano 1982; Rhoads and Boyer 1982). This continuum has been divided subjectively into four stages: Stage 0, indicative of a sediment column that is largely devoid of macrofauna, occurs immediately following a physical disturbance or in close proximity to an organic enrichment source; Stage 1 is the initial recolonizing of tiny, densely populated polychaete assemblages; Stage 2 is the start of the transition to head-down deposit feeders; and Stage 3 is the mature, equilibrium community of deep-dwelling, head-down deposit feeders (Figure 2-5). Successional stage was assigned by assessing the types of species and related activities (e.g., feeding voids) apparent in the images. Biogenic particle mixing depths can be estimated by measuring the maximum and minimum depths of imaged fauna, burrows, or feeding voids in the sediment column.

A successional stage rank variable was applied to each image to evaluate successional stages numerically. A rank value of 3 was assigned to Stage 3, 2 on 3, and 1 on 3 designations, a value of 2 was applied to Stage 2 and 1 on 2, a value of 1 was applied to Stage 1, intermediate ranks were assigned to the transitional assemblages (2.5 for Stage 2 transitioning to Stage 3, and 1.5 for Stage 1 transitioning to Stage 2), and images from which the stage could not be determined were excluded from calculations. The maximum successional stage rank among replicates was used to represent the station value.

Station means and ranges for the quantitative SPI parameters were calculated and mapped. Station means, calculated from three replicates per station, were used in statistical analyses.

2.2.7.2 Plan View Image Analysis Parameters

The PV images provided a much larger field of view than the SPI images and provided valuable information about the landscape ecology and sediment topography in the area where the pinpoint “optical core” of the sediment profile was taken (Figure 2-6). Atypical surface sediment layers, textures, or structures detected in any of the sediment

profile images can be interpreted within the larger context of surface sediment features observed in the paired PV images, i.e., is a surface layer or topographic feature a regularly occurring feature and typical of the bottom in this general vicinity or just an isolated anomaly. The scale information provided by the underwater lasers allows for accurate density counts of attached epifaunal colonies, sediment burrow openings, or larger macrofauna or fish which may have been missed in the sediment profile cross section. Information on sediment transport dynamics and bedform wavelength were also available from PV image analysis.

For each replicate PV image selected for analysis, analysts calculated the image size and field of view, and the following were recorded: sediment type; oxidation state of the surface sediment; presence and type of bedforms; presence of *Beggiatoa* and estimates of cover extent; dredged material presence; presence of burrows, tubes, tracks/trails, and debris; types of epifauna and flora; number of fish; and descriptive comments (Appendix E).

2.2.8 Data Quality Assurance and Quality Control

Measures were taken both during field data collection and during post-collection analysis for data quality assurance and control in alignment with the project QAPP (INSPIRE 2020). These included but were not limited to:

- Systems were tested prior to and during survey activities to ensure calibration and operation,
- A full backup system (including tools, parts, and electronics) was carried in the field, and
- Collected imagery was time stamped both digitally and in hand-written logs to ensure proper identification and synchronization with navigational data.

2.2.9 Statistical Analyses

One objective of the 2022 SPI/PV survey at IOSN was to assess the biological status of two areas that have received dredged material, Mound A and more recently Mound B, relative to reference area conditions. Statistical analyses were conducted to compare Mound A, Mound B, and the reference areas using the following SPI variables: 1) aRPD depth and 2) successional stage rank. The aRPD depth and successional stage rank were used in this comparison because they are known to be key indicators of infaunal activity measured by SPI within soft-sediment environments, such as those at IOSN. Standard boxplots were generated to provide a visual assessment of the central tendency and variability of these two

metrics at Mound A, Mound B, and the reference areas. Tests evaluating the inequivalence between the reference and disposal areas in 2022 were conducted and described in detail below.

Traditionally, the objective of this study would be addressed using point null hypotheses of the form "There is no difference in benthic conditions between the reference area and the disposal target areas." However, in this instance, a bioequivalence or interval testing approach was considered more informative than the point null hypothesis test of "no difference" (Germano 1999). One reason is that there is always some small difference between areas, and the statistical significance of this difference may or may not be ecologically meaningful. Without an associated power analysis, the results of traditional point null hypothesis testing often provide an inadequate ecological assessment.

In this application of bioequivalence (interval) testing the null hypothesis is chosen as one that presumes the difference is great, i.e., an inequivalence hypothesis (e.g., McBride 1999). This is recognized as a "proof of safety" approach because rejection of this inequivalence null hypothesis requires sufficient proof that the difference is actually small. The null and alternative hypotheses to be tested were:

$$H_0: \ d \leq -\delta \ \text{ or } \ d \geq \delta \text{ (presumes the difference is great)}$$

$$H_A: \ -\delta < d < \delta \text{ (requires proof that the difference is small)}$$

where d is the difference between a reference mean and a disposal site mean. If the null hypothesis is rejected, then it can be concluded that the two means are equivalent to one another within ±δ units. The size of δ should be determined from historical data and/or best professional judgment to identify a maximum difference that is within background variability/noise and is therefore not ecologically meaningful. Previously established δ values of 1.00 cm for aRPD depth, and 0.5 for successional stage rank on the 0–3 scale were used.

The test of this interval hypothesis can be broken down into two one-sided tests (TOST; McBride 1999 after Schuirmann 1987) which are based on the normal distribution, or on Student's *t*-distribution when sample sizes are small and variances must be estimated from the data (the typical case in the majority of environmental monitoring projects). The statistics used to test the interval hypotheses shown here are based on such statistical

foundations as the Central Limit Theorem (CLT) and basic statistical properties of random variables. A simplification of the CLT states that the mean of any random variable is normally distributed. Linear combinations of normal random variables are also normal, so a linear function of means is also normally distributed. When a linear function of means is divided by its standard error the ratio follows a *t*-distribution with degrees of freedom associated with the variance estimate. Hence, the *t*-distribution can be used to construct a confidence interval around any linear function of means.

In the sampling design for the 2022 survey, five distinct areas were sampled: three of which were categorized as reference areas (REF-A, REF-B, REF-C) and two were locations within the disposal site (Mound A and Mound B). The difference equation of interest was the linear contrast of the average of the reference means minus the disposal area mean, or

$$\hat{d} = [1/3 \text{ x } (\text{Mean}_{\text{REF-A}} + \text{Mean}_{\text{REF-B}} + \text{Mean}_{\text{REF-C}}) - (\text{Mean}_{\text{Mound}})] \qquad \text{[Eq. 1]}$$

where $\text{Mean}_{\text{Mound}}$ was the mean for the disposal site mound. Each disposal mound was tested against the reference areas separately.

The three reference areas collectively represented ambient conditions, but if the means were different among these three areas, then pooling them into a single reference group would inflate the variance estimate. Inflation would occur because it would include the variability between areas, rather than only the variability between stations within a single homogeneous area. The effect of keeping the three reference areas separate [Eq. 1] had no effect on the grand reference mean when sample size was equal among these areas, and it ensured that the variance was truly the residual variance within a single population, with a constant mean.

The standard error of each difference equation was calculated from the fact that the variance of a sum is the sum of the variances for independent variables, or

$$se(\hat{d}) = \sqrt{\sum_j \left(S_j^2 c_j^2 / n_j \right)} \qquad \text{[Eq. 2]}$$

Where:

$se(\hat{d})$ standard error of the difference equation

$\hat{d}$ observed difference in means between the reference areas and the disposal area

c_j coefficients for the j means in the difference equation, $\hat{d}$ (i.e., for [Eq. 1] shown above, the coefficients were 1/3 for each of the three reference locations, and -1 for the disposal area.

S_j^2 variance for the j^{th} area. If we can assume equal variances, a single pooled residual variance estimate can be substituted for each group, equal to the mean square error from an Analysis of Variance (ANOVA).

n_j number of stations for the j^{th} area

The inequivalence null hypothesis was rejected (and equivalence was concluded) if the confidence interval on the difference of means, $\hat{d}$, was fully contained within the interval [–δ, +δ].

Thus, the decision rule was to reject H_0 if

$$D_L = \hat{d} - t_{\alpha,\upsilon} se(\hat{d}) > -\delta \qquad \text{and} \qquad D_U = \hat{d} + t_{\alpha,\upsilon} se(\hat{d}) < \delta \qquad \text{[Eq. 3]}$$

where:

$t_{\alpha,\upsilon}$ upper (1-α)*100th percentile of a Student's t-distribution with υ degrees of freedom (α = 0.05)

$se(\hat{d})$ standard error of the difference ([Eq. 2])

υ degrees of freedom for the standard error. If a pooled residual variance estimate was used, it was the residual degrees of freedom from an ANOVA on all groups (total number of samples minus the number of groups); if separate variance estimates were used, degrees of freedom were calculated based on the Welch-Satterthwaite estimation (Satterthwaite 1946).

Validity of the normality and equal variance assumptions were tested using Shapiro-Wilk's test for normality on the area residuals (α=0.05) and Levene's test for equality of variances among the four areas (α =0.05). If normality was not rejected but equality of variances was, then the variance for the difference equation was based on separate variances for each group. If systematic deviations from normality were identified, then a non-parametric bootstrapped interval was used. Bootstrapping methodology is outlined in Appendix G.

2.2.10 aRPD and Successional Stage Temporal Statistical Methods

Temporal statistical analyses were conducted to compare key SPI variables between two survey years, 2021 and 2022, for Mound A. Similar to the comparisons described above (Section 2.2.9) the aRPD depth and successional stage rank were used in these temporal comparisons. Standard boxplots were generated for visual assessment of the central tendency and variation of these variables within each area for both years. Tests evaluating the inequivalence between the 2021 and 2022 conditions for Mound A were conducted, using the methods detailed in Section 2.2.9.

The difference equation of interest here was the linear contrast of the location mean in 2021 minus the location mean in 2022, or

$$\hat{d} = [\ (\text{Mean}_{2021}) - (\text{Mean}_{2022})] \qquad \text{[Eq. 4]}$$

where Mean_{20xx} was the mean in year 2021 or 2022, for Mound A.

Table 2-1.

Navigation and Data Acquisition Equipment

Measurement	Equipment
Vessel Navigation and Motion	Applanix 320 POSMV
Local GNSS Base Station	Trimble R10 dual-frequency GNSS
MBES	R2Sonic 2024
Sound Velocity	Valeport Mini SVS and YSI Castaway

Table 2-2.

IOSN 2022 Survey Target SPI/PV Station Locations

Station ID	Latitude (NAD 1983)	Longitude (NAD 1983)	X (NAD 83 State Plane ME West meters)	Y (NAD 83 State Plane ME West meters)
Mound C (Rock)				
001*	43.027948	-70.455691	876444.1479	21659.8529
002*	43.027808	-70.454972	876502.6532	21644.1015
003*	43.02716	-70.455052	876495.9026	21572.0949
004*	43.028537	-70.454948	876504.9035	21725.1089
Mound B				
005	43.021118	-70.457453	876297.8846	20901.5336
006	43.021767	-70.457097	876327.1372	20973.5401
007	43.020472	-70.456484	876376.6418	20829.5269
008	43.021363	-70.456681	876360.8903	20928.5361
009	43.021567	-70.455771	876435.1471	20951.0381
010	43.022191	-70.457624	876284.3833	21020.7945
011	43.021458	-70.458973	876174.1233	20939.7871
012	43.023043	-70.457048	876331.6377	21115.3031
Mound A				
013	43.012	-70.450316	876876.1875	19886.6907
014	43.012248	-70.448385	877033.7019	19913.6932
015	43.010363	-70.448984	876984.1973	19704.424
016	43.010596	-70.452822	876671.4187	19731.4265
017	43.012178	-70.451918	876745.6755	19906.9426
018	43.013537	-70.45129	876797.4303	20057.7064
Reference				
REF-A-101	42.98981	-70.465604	875621.1562	17425.9216
REF-A-102	42.98733	-70.466518	875545.5984	17150.6754
REF-A-103	42.986998	-70.46334	875804.6537	17112.8965
REF-A-104	42.987821	-70.464535	875707.5079	17204.6452
REF-B-105	43.005644	-70.467071	875507.8195	19185.339
REF-B-106	43.004386	-70.465079	875669.729	19045.0173
REF-B-107	43.002875	-70.466991	875513.2164	18877.7108
REF-B-108	43.004524	-70.467926	875437.6586	19061.2083
REF-C-109	43.039086	-70.419878	879366.6642	22887.6711
REF-C-110	43.037779	-70.417621	879550.1617	22741.9525
REF-C-111	43.037822	-70.419939	879361.2672	22747.3495
REF-C-112	43.036801	-70.420597	879307.2974	22634.0128

*Stations were not sampled.

3.0 RESULTS

In August 2022, an acoustic survey was conducted over the northwest portion of IOSN, at Mounds B and C, and at a short-dump site located just outside the western border of the disposal site. In September 2022, SPI/PV imagery was collected at the northwest portion of IOSN (Mound B), at the southern portion of the site (Mound A), at the short-dump site, and within the three reference areas. The results from these surveys are presented below.

3.1 Acoustic Survey

3.1.1 Bathymetry

The 2022 multibeam bathymetric data were rendered as an acoustic relief model to provide a detailed representation of the seafloor surface within the active portion of IOSN (Mounds B and C) (Figure 3-1). The 2022 bathymetry of the active portion of IOSN revealed a relatively flat surface except for two distinct topographic features, Mounds B and C. Ambient depths within this portion of the site ranged from 92.5 to 94.0 m. One feature, Mound B, was located in the southern portion of the survey area and was about 7 to 8 m above the ambient seafloor to depths of approximately 85 m. Mound B was circular with a diameter of approximately 200 m. Smaller-scale, high-relief topographic features indicative of coarser materials were seen in the central part of the mound and to the east and northeast of the mound. Mound C, the second prominent circular feature, was observed on the seafloor in the northern portion of the survey area, approximately 2 m above the ambient seafloor to depths of approximately 91 m and had a diameter of approximately 150 m.

The bathymetric relief model at the short-dump survey area revealed two rocky outcrops along the western and southern boundaries at depths of approximately 82 m (Figure 3-1). In the central portion of the short-dump survey area, a moderate depression in the ambient seafloor was visible and measured approximately 120 x 100 m. The depression had a crater-like shape with the edges of the feature slightly elevated above the ambient seafloor.

3.1.2 Acoustic Backscatter and Side-Scan Sonar

Acoustic backscatter data provides a relative estimate of surface sediment texture (hard or soft; rough or smooth). Stronger backscatter returns are indicative of coarser-grained, rougher, or harder sediment relative to areas with weaker backscatter returns, which are indicative of finer-grained, smoother, or softer sediment.

The unfiltered backscatter data collected over the active portion of IOSN showed two distinct disposal footprints (Mounds B and C) evident by stronger acoustic returns relative to the surrounding seafloor (Figure 3-2). One footprint, Mound B, occurred in the southern portion of the survey extent, while a smaller disposal footprint, Mound C, occurred in the northern portion of the surveyed area (Figure 3-2). Similarly, the filtered backscatter data highlighted these two areas of stronger backscatter returns (displayed in red and yellow) at Mounds B and C, which varied in texture from the surrounding seafloor that was characterized by weaker backscatter returns (shown in blue; Figure 3-3).

The two features, Mounds B and C, evident in the backscatter data were consistent in location with the topographic features apparent in the bathymetric data but differed in size and extent between the two data types. While both features exhibited discrete footprints of topographic relief visible in the bathymetric data (Section 3.1.1), the size of the stronger backscatter signal of non-native sediments in both areas extended beyond that of the topographic relief footprint associated with each feature (Figures 3-1 and 3-3).

The backscatter had a relatively high return around Mound B that was oblong in shape and extended approximately 200 m to the west and 600 m to the east from the edge of the bathymetric relief footprint (Figures 3-1 and 3-3). In general, a stronger backscatter return was observed to the east of disposal Mound B. The backscatter return associated with Mound C was observed an additional 200 to 300 m from the mound, also extending further to the east (Figure 3-3). Several elongated narrow trails of relatively strong backscatter return were visible radiating to the northeast of Mound C (Figure 3-3).

Within the short-dump survey area, stronger backscatter returns were present at the two surficial outcroppings compared with the surrounding seafloor (Figure 3-3). In the center of the short-dump survey area, a discrete signature of stronger backscatter return was observed coinciding spatially with the small-scale surface relief (crater-like shape noted in Section 3.1.1) observed in the bathymetric relief layer (Figures 3-1 and 3-3). This relatively strong backscatter return was approximately 250 m in diameter.

Side-scan sonar data are higher resolution and more responsive to minor surface textural features and slope than backscatter results and can often reveal additional information about topographic and textural properties of the seafloor. Side-scan sonar imagery collected at IOSN displayed the same distinct footprints within the active site (Mounds B and C) as seen in the backscatter dataset (Figures 3-3 and 3-4). At the short-dump site, rough topographic features were seen where the rock outcroppings were observed

in the bathymetry and backscatter datasets. Additionally, a higher return area was observed coinciding with the reported short-dump placement event in the central portion of the survey area (Figures 1-3 and 3-3).

3.1.3 Comparison with Previous Bathymetry

The 2022 bathymetric data were quantitatively compared to 2015 bathymetric data to assess elevation changes between the two surveys (Figure 3-5). Bottom depths measured during the 2015 survey were subtracted from those measured during the 2022 survey to obtain an elevation change map of each survey point throughout the overlapping study areas. Elevation changes between the two datasets (2015 and 2022) of +0.5/-0.5 m are considered statistically insignificant based on model uncertainties. Positive values (represented as shades of yellow and green) between surveys indicated an increase in elevation (i.e., sediment accumulation). Negative elevation change values (represented in shades of blue and purple) between surveys indicated a decrease in elevation (i.e., compaction, redistribution, smoothing).

Results of the elevation change calculations displayed a positive increase in elevation from 2015 to 2022 at the two discrete areas that correspond spatially with Mounds B and C, as previously described (Sections 3.1.1) (Figures 3-1 and 3-5). Mound B increased in elevation to a maximum height of greater than 7 m above ambient seafloor, while Mound C increased in elevation to a maximum height of approximately 2 m above ambient seafloor (Figure 3-5). The sediment dispersion observed at Mound B was greater than that observed at Mound C and was indicated by approximately 1 m of sediment accumulation, which extended roughly 400 m east of the mound's center. This elevation change observation corresponded with the acoustic data, where an area of rough topographic appearance and stronger backscatter returns was apparent (Figure 3-5).

In the short-dump area, a small area of compaction, approximately 20 m in diameter, was observed at the apparent disposal location/crater center. This visible elevation change of -0.6 m was observed in the elevation change model between the 2015 and 2022 survey data outside of the model uncertainty range of +0.5/-0.5 m (Figure 3-5).

3.2 Fishing Gear Observations

The fishing gear observations made during the acoustic survey resulted in the identification of six fishing surface markers (buoys). Four buoys were located within the 2022 acoustic survey area, one buoy was located within IOSN but outside of the 2022

acoustic survey area, and one buoy was located just outside of the western boundary of IOSN along the southern boundary of the 2022 short-dump acoustic survey area (Figure 3-6).

3.3 Sediment Profile and Plan View Imaging

The primary purpose of the SPI/PV image collection at IOSN was to assess the status of benthic colonization following dredged material placement in two specific areas of the disposal site, Mounds A and B, at which dredged material was placed during different years. Dredged material placement occurred most recently at Mound B (the active portion of the site); here, results of the SPI/PV imagery were compared with the three reference areas. At Mound A, where dredged material placement was completed in March 2021, SPI/PV image results were compared to the three reference areas, as well as to the 2021 SPI/PV results from this area. This temporal comparison provided additional insight into the recovery of the benthic community approximately a year and a half following the last dredged material placement event. Station summaries of selected physical and biological parameters from the SPI/PV images can be found in Tables 3-1 through 3-6, and complete sets of SPI/PV results are provided in Appendices D and E.

The primary purpose of the short-dump investigation was to delineate and confirm the presence of dredged material outside the IOSN boundary using single-drop SPI/PV image pairs collected along a transect across the suspected short-dump location. Images were analyzed for prism penetration, dredged material depth, and dredged material thickness. Dredged material presence and a brief description of dredged material observed on the sediment surface were noted from the PV imagery (Appendix E). Station summaries for these parameters for the short-dump investigation are provided in Table 3-7; a complete set of SPI/PV results are provided in Appendices D and E.

Below, SPI/PV results including results of the specific statistical comparisons are presented by sampling area: reference areas, Mound B, Mound A, and the short-dump area.

3.3.1 Reference Area Stations

A total of twelve SPI/PV stations, four stations in each area, were sampled across the three references areas (REF-A, REF-B, and REF-C) during the September 2022 survey (Tables 3-1 and 3-2; Figure 3-7). Paired SPI and PV image collection occurred at all stations, and images were analyzed in triplicate for each station. The data collected within the reference areas are intended to provide a representative sampling of baseline sediment conditions to compare with the soft bottom disposal sites (Mounds A and B).

3.3.1.1 Physical Sediment Characteristics

Sediment grain size major mode at all reference area stations was consistently classified as silt/clay (Table 3-1; Figure 3-8). Camera prism penetration depth ranged from 9.5 cm at REF-C Station 112 to 19.7 cm at REF-B Station 107 (Table 3-1; Figures 3-9 and 3-10). At REF-C, a clay deposit layer observed at depth likely limited camera penetration depths compared to the other reference area stations (Figure 3-10). The clay-like material was observed at depth at all stations within REF-C (Figure 3-10C; Table 3-1).

Boundary roughness values across the reference areas ranged from a station average of 0.6 cm at REF-A Station 104 to 2.7 cm at REF-C Station 110, with an overall reference area mean of 1.3 cm (Table 3-1; Figure 3-11). At REF-A and REF-B, the small-scale boundary roughness variability was likely attributable to biological processes and features such as small burrow openings, pits, mounds, etc., formed as a result of surface and subsurface benthic species activity (Table 3-1; Figures 3-10 and 3-12). Two stations at REF-C (Stations 110 and 112) had pebbles scattered at the sediment surface, which physically influenced boundary roughness in a few SPI replicates, generally resulting in increased boundary roughness at these stations (Figure 3-11).

3.3.1.2 Biological Conditions

The biological characteristics of the seafloor observed in SPI and PV were similar across the three reference areas sampled in 2022. Surficial sediment tracks, burrows, and tubes were observed in PV images at every station across all three reference areas (Table 3-2; Figure 3-12). Epifauna observations were not common in these soft sediment habitats, however, when present, anemones and bryozoans/hydroids were most frequently observed (Table 3-2; Figure 3-12).

The average aRPD depth at the reference areas was 2.8 cm; a maximum value of 3.4 cm was observed at REF-A Station 102, and a minimum value of 2.0 cm was observed at REF-B Station 105 (Table 3-2; Figures 3-13 and 3-14). No evidence of low oxygen, methane, or *Beggiatoa* were recorded at any of the reference stations (Appendices D and E).

Evidence of mature, deposit-feeding (Successional Stage 3) assemblages were observed at all reference stations, recorded as subsurface feeding voids, large burrows, and/or bioturbation deep in the sediment column, generally from the presence of head-down, deposit-feeding polychaetes (Figures 3-15 through 3-17). Stage 1 on 3 communities were most frequently observed at REF-A and REF-B, which were characterized by deep

burrowing polychaetes and/or subsurface feeding voids concurrent with small Stage 1 tubes at the sediment–water interface (Table 3-2). Stage 2 on 3 was the most common successional stage noted at REF-C (Table 3-2). The presence of Stage 3 fauna observed in the SPI was corroborated by features observed in the PV images, including large burrow openings (Figure 3-12). Mean station maximum bioturbation depths ranged from 7.8 cm at REF-C Station 112 to 18.2 cm at REF-A Station 102 and at REF-B Station 107 (Figure 3-16; Table 3-2). In general, REF-C stations had shallower maximum bioturbation depths relative to the other reference areas (Figure 3-16).

3.3.2 IOSN Active Site (Mound B) SPI/PV Stations

A total of eight SPI/PV stations were sampled at Mound B, the currently active portion of IOSN (Tables 3-3 and 3-4; Figure 3-7). This area received new dredged material between November 2021 and April 2022 (Table 1-2); targeted SPI/PV collection had not been completed in this area prior to the September 2022 survey.

3.3.2.1 Physical Sediment Characteristics

Evidence of dredged material was observed at all eight stations sampled at Mound B (Table 3-3; Figures 3-18 through 3-20). The dredged material signature at the active portion of the site varied in composition, and included white clay, fine to coarse sand, and gravels (pebbles, cobbles, and boulders). At all stations surveyed at Mound B, white clay was observed in SPI as subsurface sediment layers and/or in PV as large clay deposits on the sediment surface (Figures 3-21 and 3-22; Appendices D and E). Coarse dredged material (i.e., rock, including blasted rock [angular fragments], pebbles, and boulders) was observed at four stations at Mound B (Stations 005, 006, 008, 009) (Appendix E; Table 3-3; Figures 3-21 and 3-22). The presence of coarse dredged material inhibited the camera prism penetration at Stations 006 and 008 (Figures 3-9, 3-21, and 3-22). At stations where the SPI prism penetrated the sediment column and dredged material was assumed to be below the maximum penetration depth, dredged material thickness was assumed to be greater than the SPI prism penetration. The depth at which dredged material resided below the sediment water interface was measured as zero for Mound B stations; (i.e., not buried by native material) (Table 3-3; Figures 3-18, 3-19, and 3-20).

In general, the sediment composition was heterogeneous, including mixtures of a wide range of sediment types at all stations surveyed at Mound B. Sediment grain size major mode across Mound B varied, consisting of sand (ranging from very fine sand to coarse sand), white clay, and rock visible in SPI and PV images (Table 3-3; Figures 3-8, 3-21, and

3-22). Small-scale sediment type layering, with coarser material overlying finer material, was observed at several stations at Mound B (Stations 007, 011, and 012) (Figures 3-8, 3-21B, and 3-21C). Camera prism penetration depths for stations with measurable penetration at Mound B ranged from 6.2 cm at Station 007 (fine sand over silt/clay, on the mound apron) to 10.7 cm at Station 011 (very fine sand over silt/clay, on the mound apron). Stations 006 and 008 had no measurable penetration and were located on the central part of the mound feature (Table 3-3; Figures 3-9 and 3-21A).

Boundary roughness ranged from 0.9 cm at Station 012 to 1.8 cm at Station 009 (Table 3-3; Figure 3-11). Mean boundary roughness across stations at Mound B was 1.3 cm (Table 3-3). In general, areas of the greatest elevation change at Mound B exhibited boundary roughness that was driven by physical processes, while boundary roughness at stations along the apron of the mound feature were driven by biological processes, such as burrows and foraging depressions.

3.3.2.2 Biological Conditions and Benthic Recolonization

Only two stations within the active area of the site (Mound B) had measurable aRPD depths (Table 3-4). Indeterminate aRPD depths at Mound B were mainly due to the surficial sediment type, which was generally a heterogeneous sandy mixture of porous grain sizes (Figures 3-13 and 3-21). Stations 011 and 009 were the only stations where aRPD depths were distinguishable; at each of these two stations only a single SPI replicate had a measurable aRPD depth, resulting in station values of 1.8 cm and 2.1 cm, respectively (Table 3-4; Figure 3-13; Appendix D). There was no evidence of low dissolved oxygen; methane and *Beggiatoa* were not observed (Appendices D and E).

Tubes were present at all stations sampled at Mound B, observed in relatively high abundances at Stations 006, 007, and 012 (25-75% cover) (Table 3-4; Figure 3-23; Appendix E). Surficial tracks and burrows were not frequently observed; though where present these biological features tended to be less dense than tubes (Table 3-4; Figure 3-23). Bryozoa/hydroids and shrimp were the most common epifauna and were observed in images collected at Stations 005, 006, 008, 009, 010, and 011 (Table 3-4). Several other types of crustaceans such as a lobster and hermit crab were observed at Station 006 in the PV imagery, where harder substrate (boulders) were present (Table 3-4; Figure 3-22B). A crab was observed on the soft sediments in the PV imagery collected at Station 011 (Table 3-4; Figure 3-22C).

Infaunal successional stage was variable within the active disposal area, with Stage 2, Stage 2 on 3, Stage 1 on 3, and Stage 2->3 all documented at Mound B (Table 3-4). In general, Stage 2 and Stage 2 on 3 were the most documented infaunal successional stages. Evidence of Stage 3 taxa was observed in at least one image replicate at five (Stations 005, 009, 010, 011, and 012) of the eight stations, and the majority of the remaining replicates at these stations were classified as Stage 2 assemblages. Station 007 was classified as Stage 2 in all replicates (Table 3-4; Figure 3-15). Stage 2 assemblages were characterized by tubes at the sediment–water interface (Figure 3-24). Evidence of Stage 3 infauna included the presence of burrowing worms and/or deep voids in the sediment column, often concurrent with Stage 2 tubes at the surface (i.e., Stage 2 on 3) (Figure 3-24). The mean maximum bioturbation depths ranged from 5.7 cm at Station 007, where prism penetration was relatively shallow (6.2 cm), to 9.4 cm at Station 011, where prism penetration was relatively deep (10.7 cm) (Tables 3-3 and 3-4; Figures 3-9, 3-16, and 3-24). Infaunal successional stage was not able to be determined at Stations 006 and 008 due to the lack of prism penetration; however, several types of crustaceans and other epifauna were observed at these generally hard bottom stations, indicating benthic colonization of these areas (Table 3-4; Figures 3-9, 3-15, and 3-22).

3.3.2.3 Statistical Comparisons

Statistical comparisons of data collected at Mound B were planned to be conducted on two variables: aRPD depth and successional stage rank. Both variables are quantifiable metrics indicative of the health of a benthic community. Generally, deeper aRPD depths and high infaunal successional stage ranks are indications of a healthy and functioning benthic community. These statistical analyses explored one hypothesis related to the 2022 survey objectives at the active site (Mound B):

1. The benthic community at the active portion of IOSN (Mound B) in 2022 was ecologically dissimilar to the benthic community at the reference areas in 2022, based on aRPD depths and successional stage ranks.

There were two measurable aRPD depth observations from the active disposal area (Mound B) and therefore reliable statistical results could not be generated for aRPD depth at this location (Table 3-8). When calculated using the two available values, area mean aRPD depth at the active disposal area (Mound B) was 1.9 cm, which was lower than the grand mean of the reference areas, 2.8 cm (Tables 3-2 and 3-4; Figure 3-25). The active disposal

area at Mound B had less variability in aRPD depth compared to the reference areas (SD of 0.3 and 0.4, respectively).

The maximum successional stage rank among replicates was used to represent station values and used in the statistical comparison between Mound B and the reference areas (see Section 2.2.7.1). Results of the normality test indicated that area mean maximum successional stage ranks were significantly different from a normal distribution (Shapiro-Wilk's test, p-value <0.001, $\alpha = 0.05$) and did not have equal variances (Levene's test, p-value = 0.03, $\alpha = 0.05$). Therefore, the confidence interval for the difference equation was constructed using non-parametric bootstrapped estimates with separate variances between the active disposal area (Mound B) versus the reference areas. The confidence interval for the difference between the mean maximum successional stage rank of the pooled reference areas (3.0 rank) versus the active disposal area (Mound B) (2.8 rank) was [0.17, 0.39] and was contained within the interval [-0.5, +0.5] (Table 3-9; Figure 3-26). It was concluded that the mean maximum successional stage rank at the active disposal area (Mound B) was statistically equivalent to that of the pooled reference areas (Table 3-9; Figure 3-26).

3.3.3 Mound A SPI/PV Stations

SPI/PV images were collected at six stations at Mound A, located in the southern portion of IOSN, where dredged material was placed during the 2020/2021 season (Tables 3-5 and 3-6; Figure 3-7). This area was previously surveyed in October 2021 with SPI/PV.

3.3.3.1 Physical Sediment Characteristics

Sediment grain size major mode at Mound A was consistently classified as very fine sand over silt/clay at all stations sampled (Table 3-5; Figure 3-8). Camera prism penetration depths ranged from 12.8 cm at Station 013 to 18.5 cm at Station 016, averaging 16.2 cm across the Mound A area (Table 3-5; Figure 3-9).

Boundary roughness values at Mound A ranged from 1.1 cm at Stations 013, 014, and 016 to 1.4 cm at Station 017, with an average of 1.2 cm (Table 3-5; Figure 3-11). Consistent boundary roughness at Mound A was attributed to biological processes, such as burrow openings, pits, and mounds (Appendix D).

Evidence of dredged material was documented in all SPI replicates collected at Mound A (Table 3-5, Figures 3-18 through 3-20; Appendices D and E). The dredged material signature at Mound A was characterized as a layer of oxidized, very fine sand

overlying a thick layer of organically enriched silt/clay (Figure 3-27). Dredged material measurement depths extended to the bottom of the SPI prism at Stations 013, 014, and 017, indicating that dredged material thickness may not have been fully measured to depth due to penetration limitations (Table 3-5; Figures 3-18 and 3-27A). Stations 016 and 018 had penetration greater than the dredged material measurement depth, displaying the native silt/clay below the dredged material (Figures 3-18 and 3-27B). At least one replicate at Stations 014 and 015 also displayed native sediment beneath the measured dredged material layer (Appendix D).

3.3.3.2 Biological Conditions

Tubes and burrows were observed at all locations sampled in the Mound A area (Table 3-6; Figure 3-23). Tracks were observed in at least one replicate at all stations, with the exception of Station 013 (Table 3-6). Epifauna were observed in three of the six stations sampled at Mound A, with shrimp and bryozoa/hydroids being the most observed groups (Table 3-6).

The average aRPD depth at Mound A was 1.5 cm, with little variability across stations, ranging from 1.3 cm at Station 014 to 1.6 cm at Station 016 (Table 3-6; Figure 3-13). No indications of low dissolved oxygen, methane, or *Beggiatoa* were observed at stations at Mound A (Appendices D and E).

Successional Stage 2 on 3 (mapped as Stage 3 present) was the most frequently observed classification among replicates at Mound A (Table 3-6; Figure 3-15). Sediment profile images from Mound A displayed benthic community characteristics that were generally not as advanced as the communities at the reference areas, with Stage 2 and Stage 2 transitioning to Stage 3 communities observed in more replicates than at the reference areas (Table 3-6; Figures 3-15 and 3-28).

3.3.3.3 Statistical Comparisons

Statistical comparisons of data collected at Mound A were conducted on two variables: aRPD depth and successional stage rank. Both variables are quantifiable metrics indicative of the health of a benthic community. Generally, deeper aRPD depths and high infaunal successional stage ranks are indications of a healthy and functioning benthic community. These statistical analyses explored two hypotheses related to the 2022 survey objectives at Mound A:

1. The benthic community at Mound A in 2022 was ecologically dissimilar to the benthic community at the reference areas in 2022, based on aRPD depths and successional stage ranks.

2. The benthic community at Mound A in 2022 was ecologically dissimilar to the benthic community at Mound A in 2021, at stations where dredged material was observed, based on aRPD depths and successional stage ranks.

Area mean aRPD depth at Mound A in 2022 was 1.5 cm, which was lower than the 2022 grand mean of reference areas (2.8 cm) (Tables 3-2 and 3-6; Figure 3-25). Mound A had less variability in aRPD depth compared to reference areas (SD of 0.1 and 0.4, respectively). A confidence interval was calculated between Mound A in 2022 and the 2022 reference areas. Residuals for each area were normally distributed (Shapiro-Wilk's test p-value = 0.05, $\alpha = 0.05$), but Levene's test for equality of variances was rejected, so separate variances were used (Levene's test, $p = 0.01$, $\alpha = 0.05$). The confidence interval for the difference between the mean aRPD depth of the pooled reference areas (2.8 cm) versus Mound A (1.5 cm) was [1.09 to 1.55 cm] (Table 3-8; Figure 3-25), indicating that the mean aRPD depths between Mound A and reference areas were significantly inequivalent, ecologically dissimilar and not contained in the bounds of the interval [-1.00 to +1.00 cm].

The maximum successional stage rank among replicates was used to represent the station values and used in the statistical comparisons for Mound A (see Section 2.2.7.1). The confidence interval for the difference equation between the mean maximum successional stage at Mound A versus the pooled reference areas was constructed in the same manner as Mound B (Section 3.3.2.3), using non-parametric bootstrapped estimates with separate variances. The confidence interval for the difference between the mean maximum successional stage rank of the pooled reference areas (3.0 rank) versus Mound A (2.9 rank) was [0.08, 0.19] and was contained within the interval [-0.5, +0.5] (Table 3-9; Figure 3-26). Therefore, it was concluded that the mean maximum successional stage rank at Mound A was statistically equivalent to that of the pooled reference areas (Table 3-9; Figure 3-26).

Area mean aRPD depths at Mound A in 2021 and 2022 were 2.1 and 1.5 cm, respectively, with a decrease of 0.66 cm over time (Table 3-10; Figure 3-29). Measured aRPD depths were more variable in 2021 than in 2022 (SD of 0.49 and 0.11, respectively). The confidence interval for the change in aRPD depth over time (2021 minus 2022) was calculated for Mound A. The residuals for this area within each time period were normally distributed (Shapiro-Wilk's test p-value = 0.65, $\alpha = 0.05$). Levene's test for equality of

variances was rejected, so separate variances were used (Levene's test, $p = 0.02$, $\alpha = 0.05$). The confidence interval for the change over time at Mound A was [0.26 to 1.07 cm] (Table 3-10; Figure 3-29). This indicated that the mean aRPD depths at Mound A between the two survey years were significantly inequivalent and ecologically different, as the confidence interval was not contained within the bounds of the interval [-1.00 to +1.00 cm].

Area mean maximum successional stage ranks at Mound A in 2021 and 2022 were 2.7 and 2.9, respectively, with an increase of 0.2 over time (Table 3-10; Figure 3-30). Maximum successional stage ranks in 2021 were more variable than in 2022 (SD of 0.5 and 0.2, respectively). Results for the normality test indicated that mean maximum successional stage ranks were significantly different from a normal distribution (Shapiro-Wilk's test, p-value 0.005). Levene's test for equality of variances was rejected, so separate variances were used (Levene's test, p-value = 0.007). Therefore, the confidence interval for the difference equations was constructed using non-parametric bootstrapped estimates with separate variances between the mean maximum successional stage at Mound A in 2021 (2.7 rank) versus 2022 (2.9 rank). The confidence interval for the change over time at Mound A was [-0.56, 0.59] and was not contained within the interval [-0.5, +0.5] (Table 3-10; Figure 3-30), indicating that the mean maximum successional stage rank at Mound A between the two surveys were significantly inequivalent and ecologically different (Figure 3-30).

3.3.4 Short-Dump SPI/PV Stations

Fifteen single-drop, SPI/PV image pairs were collected along a transect running northeast to southwest in the area of the reported short dump. Data collected during the acoustic survey, described in Section 3.1, provided information about the suspected area where the dredged material was likely to be present which helped guide the planning and collection of SPI/PV images to ground truth this expectation (Table 3-7; Figures 3-3 and 3-7).

Camera prism penetration depths at stations along the short-dump investigation transect ranged from 13.8 to 19.9 cm (Table 3-7; Figure 3-9). Dredged material was identified at the sediment-water interface (not buried) at twelve of the fifteen locations sampled along the short-dump transect and was identified as a buried layer beneath the sediment–water interface at one station (Table 3-7; Figures 3-18 through 3-20).

The distribution and thickness of dredged material in the sediment column along the short-dump transect followed a spatial gradient. The southwestern-most stations exhibited trace dredged material that transitioned to much thicker dredged material layers in the central

portion of the transect, and then decreased at stations towards the northeast end of the transect (Figures 3-18, 3-20, 3-31, and 3-32). The dredged material signature at the short dump consisted of white clay similar to that seen at stations at the active portion of the site (Mound B) (Figures 3-31 and 3-32). The white clay was seen in the SPI images ranging from trace patches to the entire imaged sediment column (Figure 3-31). Where a dredged material layer was distinguishable, dredged material thickness in the sediment column ranged from a minimum of 3.0 cm at Station T1-12 to a maximum of 17.0 cm at Station T1-09, which equated to a range of 17% to 100%, respectively, of the visible sediment column (dredged material thickness relative to prism penetration depth) (Table 3-7; Figures 3-18 and 3-20). Dredged material was also captured in the PV images as compact clasts of white clay on the sediment surface (Figure 3-32).

Table 3-1.

Summary of IOSN Reference Area Sediment Profile and Plan View Imaging Physical Results, September 2022

Station ID	SPI Replicate (n)	Mean Prism Penetration Depth (cm)	Mean Boundary Roughness (cm)	SPI Predominant Sediment Type	PV Replicate (n)	PV Predominant Sediment Type
REF-A-101	3	18.6	1.0	Silt/clay	3	Sandy Mud
REF-A-102	3	19.4	1.1	Silt/clay	3	Sandy Mud
REF-A-103	3	17.9	1.1	Silt/clay	3	Sandy Mud
REF-A-104	3	18.5	0.6	Silt/clay	3	Sandy Mud
REF-B-105	3	18.0	1.1	Silt/clay	3	Sandy Mud
REF-B-106	3	18.8	1.1	Silt/clay	3	Sandy Mud
REF-B-107	3	19.7	1.0	Silt/clay	3	Sandy Mud
REF-B-108	3	17.7	0.8	Silt/clay	3	Sandy Mud
REF-C-109	3	11.4	1.5	Silt/clay	3	Clayey Mud
REF-C-110	3	11.1	2.7	Silt/clay	3	Varies
REF-C-111	3	10.3	1.5	Silt/clay	3	Clayey Mud
REF-C-112	3	9.5	2.4	Silt/clay	3	Clayey Mud
	n = 12					
	Max	19.7	2.7			
	Min	9.5	0.6			
	Mean	15.9	1.3			
	SD	4.0	0.6			

Dredged material was not present in SPI or PV images at the reference area; dredged material-related results were not included in the table.

Table 3-2.

Summary of IOSN Reference Area Sediment Profile and Plan View Imaging Biological Results, September 2022

Station ID	SPI Replicate (n)	Mean aRPD Depth (cm)	Mean Maximum Bioturbation Depth (cm)	Sediment Oxygen Demand	Void Presence	Successional Stage (by replicate)[1,2]			PV Replicate (n)	Predominant Burrow Abundance	Predominant Track Abundance	Predominant Tube Abundance	Epifauna Present
REF-A-101	3	3.2	16.7	Low	Yes	1 on 3	1 on 3	1 on 3	3	Present (10-25%)	Varies	Present (10-25%)	None
REF-A-102	3	3.4	18.2	Low	Yes	1 on 3	1 on 3	1 on 3	3	Sparse (<10%)	Abundant (25-75%)	Present (10-25%)	Shrimp
REF-A-103	3	2.8	14.3	Low	Yes	1 on 3	1 on 3	2 on 3	3	Varies	Present (10-25%)	Sparse (<10%)	None
REF-A-104	3	2.5	17.9	Low	Yes	1 on 3	1 on 3	2 on 3	3	Sparse (<10%)	Abundant (25-75%)	Sparse (<10%)	None
REF-B-105	3	2.0	16.6	Low	Yes	1 on 3	1 on 3	2 on 3	3	Present (10-25%)	Abundant (25-75%)	Sparse (<10%)	None
REF-B-106	3	2.9	14.5	Low	Yes	1 on 3	1 on 3	2 on 3	3	Varies	Varies	Present (10-25%)	None
REF-B-107	3	3.2	18.2	Low	Yes	1 on 3	1 on 3	1 on 3	3	Varies	Present (10-25%)	Present (10-25%)	None
REF-B-108	3	3.2	14.9	Low	Yes	1 on 3	1 on 3	2 on 3	3	Present (10-25%)	Abundant (25-75%)	Sparse (<10%)	None
REF-C-109	3	2.6	10.3	Low	Yes	2 -> 3	2 on 3	2 on 3	3	Present (10-25%)	Sparse (<10%)	Present (10-25%)	Bryozoa/ Hydroids
REF-C-110	3	2.6	8.8	Low	Yes	2 on 3	2 on 3	2 on 3	3	Present (10-25%)	Varies	Present (10-25%)	Anemone, Bryozoa /Hydroids, Shrimp

Station ID	SPI Replicate (n)	Mean aRPD Depth (cm)	Mean Maximum Bioturbation Depth (cm)	Sediment Oxygen Demand	Void Presence	Successional Stage (by replicate)[1,2]			PV Replicate (n)	Predominant Burrow Abundance	Predominant Track Abundance	Predominant Tube Abundance	Epifauna Present
REF-C-111	3	2.5	9.2	Low	Yes	1 on 3	2 on 3	2 on 3	3	Present (10-25%)	Sparse (<10%)	Present (10-25%)	Anemone, Bryozoa/ Hydroids
REF-C-112	3	2.6	7.8	Low	Yes	2 on 3	2 on 3	2 on 3	3	Present (10-25%)	Sparse (<10%)	Present (10-25%)	Bryozoa/ Hydroids
	n = 12												
	Max	3.4	18.2										
	Min	2.0	7.8										
	Mean	2.8	14.0										
	SD	0.4	3.9										

IND=Indeterminate

1 Successional Stage: “on” indicates one Stage is found on top of another Stage (i.e., 1 on 3); “->” indicates one Stage is progressing to another Stage (i.e., 2 -> 3).

2 Variable determined from combined SPI/PV analysis.

Table 3-3.

Summary of IOSN Active Area Mound B Sediment Profile and Plan View Imaging Physical Results, September 2022

Station ID	SPI Replicate (n)	Mean Prism Penetration Depth (cm)	Mean Boundary Roughness (cm)	SPI Predominant Sediment Type	SPI Dredged Material Presence	Mean Dredged Material Thickness (cm)[1]	Dredged Material > Penetration[1]	Buried Dredged Material Presence	Mean Dredged Material Depth (cm)	PV Replicate (n)	PV Predominant Sediment Type	PV Dredged Material Presence
005	3	8.4	1.7	Varies	Yes	8.4	Yes	No	0.0	3	Sand	Yes
006	3	0.0	IND	IND	Yes	IND	No	IND	IND	3	Boulder	Yes
007	3	6.2	1.1	Fine sand over silt/clay	Yes	6.2	Yes	No	0.0	3	Sand	Yes
008	3	0.0	IND	IND	Yes	IND	No	IND	IND	3	Cobble	Yes
009	3	6.2	1.8	Very fine sand over coarse sand	Yes	6.2	Yes	No	0.0	3	Varies	Yes
010	3	7.7	1.4	Coarse sand and very fine sand mix	Yes	7.7	Yes	No	0.0	3	Sand	Yes
011	3	10.7	1.0	Very fine sand over silt/clay	Yes	10.7	Yes	No	0.0	3	Clay	Yes
012	3	10.0	0.9	Fine sand over silt/clay	Yes	10.0	Yes	No	0.0	3	Sand	Yes
	n = 8											
	Max	10.7	1.8			10.7			0.0			
	Min	0.0	0.9			6.2			0.0			
	Mean	6.2	1.3			8.2			0.0			
	SD	4.1	0.4			1.9			0.0			

IND=Indeterminate

1 Mean dredged material thickness (cm) measurements are dependent on penetration depths. Inferences cannot be made about the absolute thickness of dredged material using SPI if dredged material extends below the penetration of the prism (i.e., DM > penetration). Therefore, the mean calculation for DM thickness is biased low.

Table 3-4.

Summary of IOSN Active Area Mound B Sediment Profile and Plan View Imaging Biological Results, September 2022

Station ID	SPI Replicate (n)	Mean aRPD Depth (cm)	Mean Maximum Bioturbation Depth (cm)	Sediment Oxygen Demand	Void Presence	Successional Stage (by replicate)[1,2]			PV Replicate (n)	Predominant Burrow Abundance	Predominant Track Abundance	Predominant Tube Abundance	Epifauna Present
005	3	IND	8.2	Low	Yes	2	2 on 3	2 on 3	3	Sparse (<10%)	Sparse (<10%)	Varies	Shrimp
006	3	IND	IND	IND	IND	IND	IND	IND	3	None	None	Abundant (25-75%)	Bryozoa/Hydroids, Hermit Crab, Lobster, Shrimp
007	3	IND	5.7	Low	Yes	2	2	2	3	Sparse (<10%)	Present (10-25%)	Abundant (25-75%)	None
008	3	IND	IND	IND	IND	IND	IND	IND	3	None	None	Present (10-25%)	Bryozoa/Hydroids, Shrimp
009	3	2.1	6.5	Low	Yes	2	2	2 on 3	3	Sparse (<10%)	None	Present (10-25%)	Bryozoa/Hydroids, Shrimp
010	3	IND	8.2	Low	Yes	2	2	2 on 3	3	Sparse (<10%)	Varies	Present (10-25%)	Bryozoa/Hydroids
011	3	1.8	9.4	Medium	Yes	2	1 on 3	2 on 3	3	Sparse (<10%)	Present (10-25%)	Sparse (<10%)	Bryozoa/Hydroids, Crab
012	3	IND	8.9	Low	Yes	2 -> 3	2 on 3	2 on 3	3	Present (10-25%)	Present (10-25%)	Abundant (25-75%)	None
	n = 8												
	Max	2.1	9.4										
	Min	1.8	5.7										
	Mean	1.9	7.8										
	SD	0.3	1.4										

IND=Indeterminate

1 Successional Stage: "on" indicates one Stage is found on top of another Stage (i.e., 1 on 3); "->" indicates one Stage is progressing to another Stage (i.e., 2 -> 3).

2 Variable determined from combined SPI/PV analysis.

Table 3-5.

Summary of IOSN Mound A Sediment Profile and Plan View Imaging Physical Results, September 2022

Station ID	SPI Replicate (n)	Mean Prism Penetration Depth (cm)	Mean Boundary Roughness (cm)	SPI Predominant Sediment Type	SPI Dredged Material Presence	Mean Dredged Material Thickness (cm)[1]	Dredged Material > Penetration[1]	Buried Dredged Material Presence	Mean Dredged Material Depth (cm)	PV Replicate (n)	PV Predominant Sediment Type	PV Dredged Material Presence
013	3	12.8	1.1	Very fine sand over silt/clay	Yes	12.8	Yes	No	0.0	3	Sand	Yes
014	3	16.5	1.1	Very fine sand over silt/clay	Yes	16.1	Yes	No	0.0	3	Sand	Yes
015	3	16.8	1.3	Very fine sand over silt/clay	Yes	16.0	No	No	0.0	3	Sand	Yes
016	3	18.5	1.1	Very fine sand over silt/clay	Yes	12.4	No	No	0.0	3	Sand	Yes
017	3	15.4	1.4	Very fine sand over silt/clay	Yes	15.4	Yes	No	0.0	3	Gravelly Sand	Yes
018	3	17.3	1.2	Very fine sand over silt/clay	Yes	13.3	No	No	0.0	3	Sand	Yes
	n = 6											
	Max	18.5	1.4			16.1			0.0			
	Min	12.8	1.1			12.4			0.0			
	Mean	16.2	1.2			14.3			0.0			
	SD	2.0	0.1			1.7			0.0			

1 Mean dredged material thickness (cm) measurements are dependent on penetration depths. Inferences cannot be made about the absolute thickness of dredged material using SPI if dredged material extends below the penetration of the prism (i.e., DM > penetration). Therefore, the mean calculation for DM thickness is biased low.

Table 3-6.

Summary of IOSN Mound A Sediment Profile and Plan View Imaging Biological Results, September 2022

Station ID	SPI Replicate (n)	Mean aRPD Depth (cm)	Mean Maximum Bioturbation Depth (cm)	Sediment Oxygen Demand	Void Presence	Successional Stage (by replicate)[1,2]			PV Replicate (n)	Predominant Burrow Abundance	Predominant Track Abundance	Predominant Tube Abundance	Epifauna Present
013	3	1.5	8.9	Medium	Yes	2 -> 3	2 on 3	2 on 3	3	Sparse (<10%)	None	Abundant (25-75%)	Bryozoa/Hydroids, Shrimp
014	3	1.3	6.4	Medium	No	2 -> 3	2 -> 3	2 -> 3	3	Sparse (<10%)	Abundant (25-75%)	Abundant (25-75%)	None
015	3	1.4	12.3	Medium	Yes	2 -> 3	1 on 3	2 on 3	3	Abundant (25-75%)	Abundant (25-75%)	Abundant (25-75%)	None
016	3	1.6	9.6	Medium	Yes	2 on 3	2 on 3	2 on 3	3	Present (10-25%)	Varies	Present (10-25%)	None
017	3	1.5	5.5	Medium	Yes	2 -> 3	2 -> 3	2 on 3	3	Present (10-25%)	Sparse (<10%)	Present (10-25%)	Bryozoa/Hydroids, Crab, Gastropod
018	3	1.4	8.3	Medium	Yes	2	2	2 on 3	3	Abundant (25-75%)	Present (10-25%)	Abundant (25-75%)	Shrimp
	n = 6												
	Max	1.6	12.3										
	Min	1.3	5.5										
	Mean	1.5	8.5										
	SD	0.1	2.4										

1 Successional Stage: “on” indicates one Stage is found on top of another Stage (i.e., 1 on 3); “->” indicates one Stage is progressing to another Stage (i.e., 2 -> 3).
2 Variable determined from combined SPI/PV analysis.

Table 3-7

Summary of IOSN Short-Dump Location Sediment Profile and Plan View Imaging Physical Results, September 2022

Station ID	SPI Replicate (n)	Mean Prism Penetration Depth (cm)	SPI Dredged Material Presence	Mean Dredged Material Thickness (cm)[1]	Dredged Material > Penetration[1]	Buried Dredged Material Presence	Mean Dredged Material Depth (cm)	PV Replicate (n)	PV Dredged Material Presence
T1-01	1	18.1	Trace	0.0	No	No	0.0	1	Trace
T1-02	1	18.5	Yes	6.1	No	No	0.0	1	Trace
T1-03	1	18.6	Yes	6.3	No	No	0.0	1	Yes
T1-04	1	19.1	Yes	8.1	No	No	0.0	1	Yes
T1-05	1	13.8	Yes	13.8	Yes	No	0.0	1	Yes
T1-06	0	-	-	-	-	-	-	1	Yes
T1-07	1	14.6	Yes	14.6	Yes	No	0.0	1	Yes
T1-08	1	14.6	Yes	8.6	No	No	0.0	1	Yes
T1-09	1	17.0	Yes	17.0	Yes	No	0.0	1	Yes
T1-10	1	15.4	Yes	3.8	No	No	0.0	1	IND
T1-11	1	17.1	Yes	7.1	No	Yes	3.0	1	Yes
T1-12	1	17.3	Yes	3.0	No	No	0.0	1	Yes
T1-13	1	17.4	Yes	3.1	No	No	0.0	1	Yes
T1-14	1	19.3	No	N/A	N/A	N/A	N/A	1	Trace
T1-15	1	19.9	Trace	0.0	No	No	0.0	1	Trace
	n = 15								
	Max	19.9		17.0			3.0		
	Min	13.8		0.0			0.0		
	Mean	17.2		7.0			0.2		
	SD	1.9		5.4			0.8		

N/A=Not Applicable
IND=Indeterminate
"-" Replicate image not analyzed.
1 Mean dredged material thickness (cm) measurements are dependent on penetration depths. Inferences cannot be made about the absolute thickness of dredged material using SPI if dredged material extends below the penetration of the prism (i.e., DM > penetration). Therefore, the mean calculation for DM thickness is biased low.

Table 3-8.

Summary Statistics and Results of Inequivalence Hypothesis Testing for aRPD Values

Difference Equation	Observed Difference ($\hat{d}$)	SE $\hat{d}$	*df* for SE	Confidence Bounds (D_L to D_U)[1]	Results[2]	n (REF)	n (Mounds)
$Mean_{REF} - Mean_{MoundA}$	1.32	0.12	7.0	1.09 to 1.55	d	12	6
$Mean_{REF} - Mean_{MoundB}$	0.84	N/A	N/A	N/A	N/A	12	2

1 DL and DU as defined in [Eq. 3].
2 s = Reject the null hypothesis of inequivalence: the two group means are significantly equivalent, within ± 1.0 cm.
d = Fail to reject the null hypothesis of inequivalence: the two group means are different.

Table 3-9.

Summary Statistics and Results of Inequivalence Hypothesis Testing for Successional Stage Values

Difference Equation	Observed Difference ($\hat{d}$)	SE $\hat{d}$	*df* for SE	Number of Bootstrap Replicates	Confidence Bounds (D_L to D_U)[1]	Results[2]	n (REF)	n (Mounds)
$Mean_{REF} - Mean_{MoundA}$	0.08	0.08	5.0	1000	0.08 to 0.19	s	12	6
$Mean_{REF} - Mean_{MoundB}$	0.17	0.17	5.0	1000	0.17 to 0.39	s	12	6

1 DL and DU as defined in [Eq. 3].

2 s = Reject the null hypothesis of inequivalence: the two group means are significantly equivalent, within ± 0.5.
d = Fail to reject the null hypothesis of inequivalence: the two group means are different.

Table 3-10.

Summary Statistics and Results of Inequivalence Hypothesis Testing for Temporal Change in aRPD and Successional Stage Values at Mound A

Difference Equation	Observed Difference ($\hat{d}$)	SE $\hat{d}$	*df* for SE	Number of Bootstrap Replicates	Confidence Bounds (D_L to D_U)[1]	Results[2]	n (2021)	n (2022)
aRPD: $Mean_{2021} - Mean_{2022}$	0.66	0.20	5.5	N/A	0.26 to 1.07	d	6	6
SS: $Mean_{2021} - Mean_{2022}$	-0.25	0.23	6.5	1000	-0.56 to 0.59	d	6	6

1 DL and DU as defined in [Eq. 4].

2 s = Reject the null hypothesis of inequivalence: the two group means are significantly equivalent, within ± 1 cm (aRPD depth) or within ± 0.5 rank (Successional Stage).
d = Fail to reject the null hypothesis of inequivalence: the two group means are different.

4.0 DISCUSSION

The objective of the 2022 monitoring effort was to conduct a confirmatory survey over the active area of IOSN (Mounds B and C), the portion of the site that had not received new material since 2021 (Mound A), and the three reference areas. A multibeam acoustic survey was completed over the northwestern area of IOSN (Mounds B and C) that most recently received approximately 558,500 m³ of dredged material from improvement dredging of the Portsmouth Harbor and Piscataqua River FNP. SPI/PV images were collected at Mound B, Mound A, and the three reference areas. A focused investigation of a reported short dump that occurred just outside the western border of the site was also conducted using multibeam acoustic data collection and SPI/PV imagery collection.

4.1 Dredged Material Distribution and Seafloor Topography

The acoustic survey of the northwest portion of IOSN revealed a relatively flat seafloor except for two distinct mounds (Mounds B and C), where dredged material had recently been placed (Figure 4-1). The types of sediments expected to be found in this area from the Portsmouth Harbor and Piscataqua River FNP improvement dredging project consisted of glacial till composed of a mix of clean, coarse sand, gravel, and fine-grained material (USACE and New Hampshire State Port Authority 2014). The ambient sediments at IOSN are primarily fine grained (Guarinello et al. 2016). The placement of dredged material at IOSN that exhibited sediment characteristics that differed from the ambient substrate resulted in a more physically diverse and rugous environment on the seafloor relative to baseline conditions.

An elevation change comparison between the 2022 and 2015 bathymetric datasets showed a circular topographic feature that increased in elevation by approximately 7 to 8 m above the ambient seafloor at Mound B (Figure 3-5). This area of increased elevation coincided with the location of dredged material placement events (Figure 4-1). High-relief topographic features indicative of coarser materials can be seen in the acoustic relief model in the central part of Mound B and to the east and northeast of the mound (Figures 3-1, 3-3, and 3-5). SPI/PV images collected in these areas confirmed the placement of coarse-grained materials at Mound B, as was expected; this coarse-grained material inhibited the SPI camera prism penetration at two locations at the apex of the mound feature (Figures 3-8, 3-9, 3-21, and 3-22). An apron of material rising approximately 1 m above the ambient seafloor, extending approximately 400 m to the east of the center of Mound B, appears to be related to

placement material dispersion. The shape and location of this extended apron, eastward of the placement events, suggests it is likely related to the speed of the scows transiting from Portsmouth Harbor during material release activities (Figure 4-1). Backscatter collected at Mound B suggested a larger footprint of dredged material than observed in the bathymetric data (elevation change comparison) (Figures 3-3 and 3-5). This footprint discrepancy between bathymetric and backscatter datatypes suggests that a relatively thin layer of dredged material extends beyond the area where the elevation changed and was not thick enough to be detected in the bathymetric temporal comparison. Given the bias and error in the two bathymetric datasets, the elevation change detection was approximately +/- 0.5 m (Figure 3-5). As such, this thin layer of dredged material apparent in the backscatter but not observed in the bathymetric dataset comparison (elevation change) is likely less than 0.5 m in thickness.

The SPI/PV imagery collected at Mound B provided additional confirmatory evidence of dredged material presence and documented the physical characteristics of the dredged material. The dredged material placed at Mound B was more heterogeneous in grain size composition than the maintenance dredged material from Rye Harbor that was previously deposited at Mound A (discussed in Section 4.3) and as compared to the native homogeneous silt/clay sediments at the site (Figure 3-8; Guarinello et al. 2016). White clay, very fine sand, fine sand, coarse sand, and rock (ranging from pebbles to cobbles and boulders) were all observed at Mound B in 2022, all of which was considered dredged material (Table 3-3; Figures 3-8, 3-21, and 3-22). Surficial sediments at the stations where SPI was analyzed (i.e., penetration was achieved) were made up of a mixture of coarse to very fine sands, often resulting in porous textures (Figure 4-2). This chaotic mixture of poorly sorted sediments is typical of dredged material. The two stations near the center of Mound B had higher prevalence of coarser materials including pebbles, cobbles, and boulders, which were also considered non-native material. The three stations positioned on the apron of Mound B (Stations 007, 011, and 012) were characterized by fine-scale layering of sediment types, in which slightly coarser material was observed overlying white clay. Both the coarser material and the underlying white clay are characteristic of dredged material and different than the native light brown silt/clay observed at IOSN prior to disposal (Guarinello et al. 2016) and the native material at the reference areas (light brown silt/clay).

At Mound C, the elevation change since 2015 revealed a feature approximately 2 m above the ambient seafloor, which spatially coincided with the documented dredged material placement events (Figures 3-5 and 4-1). Similar to Mound B, a tail extending to the east of Mound C was observed in the backscatter data; however, this tail was not evident in the

bathymetric or elevation change datasets (Figures 3-1, 3-3, and 3-5). The less pronounced tail at Mound C compared to the extended apron to the east of Mound B is likely due to the fact that less material, and coarser material, such as cobbles and boulders that settle more quickly to the seafloor compared to finer material, were placed at Mound C (Table 1-2; Figure 4-1). Due to time constraints during field collection, no SPI/PV sampling occurred at Mound C to ground-truth the acoustic data collected in 2022.

At the short-dump location, acoustic and SPI/PV data confirmed the placement of dredged material outside of the western IOSN boundary. This is discussed in more detail in Section 4.4.

4.2 Status of the Benthic Community at the Recently Active Portion of IOSN (Mounds B and C)

In 2022, SPI/PV imaging was used to assess the recolonization status of benthic organisms and to characterize surficial sediments at the active area of IOSN (Mound B). Conducting SPI/PV imaging at Mound C was also planned for the 2022 survey, but due to time constraints during the survey these planned stations were not sampled.

At Mound B there were several lines of evidence derived from SPI/PV suggesting benthic recovery was progressing as expected following dredged material disposal. SPI/PV imagery revealed the presence of relatively deep bioturbation activity, carpets of small surficial tubes at many of the stations, and successional stage classifications equivalent to the reference areas. Surficial tubes were present at Mound B in high abundances relative to the reference areas, indicating the recolonization by Stage 2 taxa in this area (Figure 3-15). Additionally, evidence of Stage 3 taxa, including feeding voids and deep burrowing polychaetes, was present at five of the six stations at Mound B where the SPI prism penetrated the seafloor (i.e., where penetration was not inhibited by cobbles and boulders) (Figure 3-15).

Conventionally, the DAMOS Program uses biological indicators relevant to soft sediment environments (aRPD depth and successional stage) to assess the recovery of the benthic habitat after dredged material is placed at disposal sites (Germano et al. 2011). The prevalence of coarser grained substrate deposited at Mound B (Figure 4-2) limited the evaluation of biological recovery using aRPD depth, however the results of other metrics suggest benthic recovery is underway. Due to limited prism penetration depths and the inability to distinguish aRPD depths in the porous mixture of fine and coarse sands, the sample size for aRPD depth measurements at Mound B was not sufficient to support the

statistical tests generally run to investigate recovery (Table 3-4). However, mean maximum successional stage rank at Mound B was statistically equivalent to that of the reference areas, which suggests benthic recovery is proceeding following disturbance, as described above.

4.3 Benthic Recolonization at Mound A

One of the objectives of the 2022 IOSN SPI/PV survey was to continue the investigation into the biological recovery timeline at this newly designated disposal site. To obtain a better understanding of the timeframe in which recovery takes place at IOSN, SPI/PV imagery was collected in 2022 at Mound A, one year after it was previously surveyed.

Mound A received dredged material during the 2020 – 2021 disposal season, which marked the first placement events at the newly designated IOSN disposal site. The DAMOS Program conducted the first confirmatory monitoring survey of Mound A in October 2021, eight months after disposal events were completed (USACE 2022). Mound A was sampled again, a year later, approximately 20 months after completion of disposal activities, during the September 2022 IOSN survey. These two surveys created a temporal dataset that could be used to investigate the progression of benthic recolonization following dredged material placement at IOSN. Results of the SPI/PV imagery from Mound A in 2022 were compared to both the results from the reference areas in 2022, as well as to the 2021 data from Mound A (including only stations where dredged material was observed in 2021), to assess the current benthic recolonization status and to further understand the temporal trajectory of recovery in this environment.

Approximately two years after dredged material placement at Mound A, the signature of dredged material persisted (Figure 4-3); however, signs of biological recovery were evident. Biological metrics derived from SPI/PV imagery, specifically aRPD depths and successional stage, were used as indicators of benthic recovery and benthic functioning. In soft sediment environments, deeper aRPD depths and more advanced successional stages are indicative of a healthier, higher functioning, more recovered, and resilient benthic community (Germano et al. 2011).

There were several biological indicators observed at Mound A that suggested benthic recovery was progressing as expected. The 2022 maximum infaunal successional stage at the Mound A disposal area was statistically similar to the reference areas, and statistically higher than it was at Mound A in 2021 (Tables 3-9 and 3-10; Figure 3-30). The increase in successional stage between years follows the successional stage paradigm, with more

advanced successional stages developing over time since disturbance (Figure 2-5). In addition to the successional stage classifications derived from SPI, the presence and relative abundance of biological features observed in PV including burrows, tracks, and tubes provided further evidence of biological recovery at this site. The percent cover of burrows, tracks, and tubes on the sediment surface were generally higher at stations at Mound A compared to the reference areas, suggesting high biological activity at this location (Figure 3-23).

Despite evidence of biological recovery described above, the aRPD depths at Mound A remained lower compared to the three reference areas, consistent with what was reported in 2021 (Table 3-8; Figure 3-29) (USACE 2022). The shallower aRPD depths at Mound A compared to the reference areas indicate higher sediment oxygen demand at the disposal site, suggesting additional time is necessary at IOSN for the biological community to fully rework the surface sediments through bioturbation and bioirrigation. The aRPD depths at Mound A were also significantly lower in 2022 compared to 2021 (Table 3-10; Figure 3-29). However, the difference in mean aRPD depths between these two years at Mound A was minimal (0.6 cm), and a similar temporal shift in mean aRPD depths was observed at the reference areas (a decrease of 0.4 cm). This spatially broad reduction in aRPD depth measurements may suggest regional processes could have contributed to the decrease in aRPD depths at the Site and Reference Areas. It is also possible that the shallower aRPD depths in 2022 compared with 2021 at Mound A were driven by a lag in the bioturbation activity by Stage 3 taxa, relative to the increased sediment oxygen demand driven by the microbial breakdown of organic matter sourced from the introduced coastal sediments (i.e., the dredged material). As more organisms, particularly large and long-lived deep burrowing Stage 3 infauna continue colonizing these sediments, the aRPD depths are expected to increase as bioturbation counteracts the drawdown of oxygen by microbial respiration. Additionally, it is likely that the organic content of the sediments will decrease over time as it continues to be consumed by Stage 3 organisms, decreasing microbial sediment oxygen demand, and allowing for increased aRPD depths and general benthic recovery over time. This paradigm has been well documented at DAMOS sites in the past, such as at Cape Cod Bay Disposal Site (CCBDS; USACE 2021b) and at Rhode Island Sound Disposal Site (RISDS; USACE 2021c).

4.4 Short-Dump Investigation

Coupled acoustic and SPI/PV data were used to investigate and confirm the location of a short dump outside of the IOSN boundary. Targeted SPI/PV data were collected based

on the preliminary acoustic data at the reported location of the short dump. The SPI/PV images successfully ground-truthed the presence of dredged material indicated in the 2022 acoustic data.

The acoustic survey at the short-dump site revealed a discrete signature of stronger backscatter returns relative to the surrounding seafloor within the central portion of the short-dump survey area (Figure 3-3). The footprint of the relatively strong backscatter return at the short-dump survey area was approximately 49,000 m² (circular footprint with a 250-m diameter) and aligned with the reported short-dump location from the scow logs and the dredged material signature recorded from the SPI analysis (Figures 4-4 and 4-5). The majority of this footprint was characterized by a thin spread of dredged material, within the elevation change model error range of +/-0.5 m, extending beyond the central impact point. Using the measured dredged material depth from the SPI dataset, an average depth of dredged material in this apron area was estimated at 7.0-cm thick within the short-dump backscatter footprint.

The single scow load of material released at the short-dump location (~ 3,800 m^3 [(5,000 yd^3)] created a small (~20.0 m diameter) crater impact area with detectable elevation change between the 2015 and 2022 bathymetric datasets (Figure 3-5). This small area of scour or compaction with a low berm surrounding it was apparent in the bathymetric relief and measured approximately -0.6 m below the ambient seafloor (2015 bathymetric dataset) (Figures 3-1, 3-5, and 4-1). This berm surrounded a circular area that was approximately 100 to 150 m in diameter (Figure 4-6) and is consistent with impact crater dimensions mapped during the Massachusetts Bay Disposal Site Demonstration Project which were created from the placement of similar volumes and types of dredged material released in similar water depths and ambient seafloor conditions as the IOSN short-dump (USACE 2015).

The single-drop SPI/PV transect sampling approach confirmed the presence of dredged material on the seafloor at the short-dump location. The SPI/PV sampling design was informed by the preliminary acoustic dataset, which displayed a signature of the short-dump disposal in the relief, backscatter, and side-scan sonar data. The target SPI/PV transect intersected the acoustic footprint of the short dump. Fifteen single-drop SPI/PV image pairs were collected along the transect line, beginning prior to the acoustic signature to the west and traversing through the footprint and beyond the acoustic signature to the northeast. This SPI/PV sampling design captured a gradient of dredged material prevalence in the sediments, with trace amounts displayed in the images at either end of the transect and dredged material spanning the entire sediment column (100% of the prism penetration) at stations in the

central part of the transect (Figures 3-31 and 4-5). This gradient aligned closely with the signature of the dredged material in the acoustic data (Figure 4-6). Using the average value of measured dredged material thickness from SPI across the transect of stations (7.0-cm) (Table 3-7) and the measured dredged material footprint from backscatter (250-m diameter circular feature), the estimated volume of dredged material from the short dump detected on the seafloor was approximately 3,400 m^3. This volume estimate closely aligns with the approximate barge disposal volume of 3,800 m^3 and provides additional support for the method approach.

The physical characteristics of the dredged material observed at the short-dump site were similar to the dredged material observed at Mound B, which was sourced from the same dredging project (Portsmouth Harbor and Piscataqua River FNP). The dredged material at both the short-dump site and Mound B was distinct from the native sediment, appearing as white clay seen both in the sediment column (SPI) and on the sediment surface (PV) (Figures 3-31 and 3-32).

A combination of MBES data and SPI/PV image collection is an effective strategy to identify and delineate dredged material associated with short-dump events. A similar approach was taken to investigate a short-dump event to the northeast of RISDS in 2021 (USACE 2023). At the RISDS associated short-dump location, the dredged material was very similar in composition to that of the surrounding native sediments, which made it challenging to clearly identify the footprint of the disposal event in the MBES data. However, at IOSN, the dredged material was distinct from the native sediments, allowing the MBES data to clearly distinguish the distribution of non-native material on the seafloor. Therefore, the survey design of the SPI/PV stations could be developed using the preliminary MBES data layers, aiming to traverse the area where relatively high backscatter was observed. This approach should continue to be employed in the future to investigate distribution of dredged material that has been inadvertently placed outside of a designated disposal site.

5.0 CONCLUSIONS AND RECOMMENDATIONS

The August 2022 acoustic and September 2022 SPI/PV surveys provided information on the distribution of recently placed dredged material at Mounds B and C, assessed benthic habitat recovery at Mound A, and investigated the short-dump location just outside of the IOSN western boundary. The overall findings of the 2022 surveys were:

- Dredged material was observed at the target area at Mound B, as confirmed by acoustic data and SPI/PV sampling results, resulting in an elevation increase of approximately 7 m above the ambient seafloor at the mound's highest point.
- Dredged material deposited at Mound B was disbursed on the seafloor and was visible as an oblong-shaped apron of sediment that trailed off to the east. This extension of dredged material from Mound B was potentially due to slightly higher scow speeds, which may have been necessary due to the local sea state and offshore conditions of IOSN.
- At Mound B, material deposited was of different composition than the ambient material at the site and at the reference areas. The mixture of poorly sorted, porous sediments at Mound B did not allow for statistical comparison of aRPD depths. However, successional stage rank at Mound B was statistically equivalent to that of the reference areas, which suggests a level of benthic recovery following disturbance.
- Dredged material was observed at the target area at Mound C, as confirmed by acoustic mapping results, resulting in an elevation increase of approximately 2 m above the ambient seafloor.
- Dredged material at Mound B ranged from boulder to clay, with mixtures of poorly sorted grain sizes within station locations, based on SPI/PV analysis. Mound C was comprised of coarser materials from blasted portions of the Piscataqua River, based on disposal logs and acoustic mapping results.
- The benthic conditions at Mound A suggest recovery is progressing, with measured aRPD depths progressing towards ecological equivalence with the reference areas. Successional stages at Mound A were equivalent to those observed at the reference areas.
- Dredged material was confirmed at the short-dump location using acoustic and SPI/PV data.

The following recommendations are provided based on the information collected during these surveys:

R1: Future dredged material can be placed throughout the disposal site and should continue to be targeted to specific areas to limit temporary impacts to the benthic community. Scow disposal speeds should be monitored for compliance with permit conditions and contract specifications to limit the spread of material beyond target areas.

R2: Mound B should be revisited to determine if aRPD depths are measurable after additional time has passed since disposal events. This will provide additional information on the time needed for mixed/porous dredged material to consolidate enough to generate measurable aRPD depths.

R3: Mound C should be monitored under a hard bottom habitat-specific recovery protocol, focusing on benthic colonization and species recruitment of the harder substrate at this mound.

R4: Another SPI/PV survey at Mound A paired with the next monitoring survey, prior to placing additional dredged material in this area, would provide further temporal resolution on the recovery timeline at the Site.

R5: Targeted acoustic data collection, coupled with SPI/PV sampling, should continue to be used to investigate any future short-dump events.

6.0 REFERENCES

Fredette, T. J.; French, G. T. 2004. Understanding the physical and environmental consequences of dredged material disposal: history in New England and current perspectives. Mar. Pollut. Bull. 49:93–102.

Germano, J. D. 1983. Infaunal succession in Long Island Sound: animal sediment interactions and the effects of predation [dissertation]. New Haven (CT): Yale University.

Germano, J. D. 1999. Ecology, statistics, and the art of misdiagnosis: The need for a paradigm shift. Environ. Rev. 7(4):167–190.

Germano, J. D.; Rhoads, D. C.; Lunz, J. D. 1994. An Integrated, Tiered Approach to Monitoring and Management of Dredged Material Disposal Sites in the New England Regions. DAMOS Contribution No. 87. U.S. Army Corps of Engineers, New England Division, Waltham, MA, 67 pp.

Germano, J. D.; Rhoads, D. C.; Valente, R. M.; Carey, D. A.; Solan, M. 2011. The use of sediment-profile imaging (SPI) for environmental impact assessments and monitoring studies: lessons learned from the past four decades. Oceanogr. Mar. Biol. Ann. Rev. 49:235–285.

Guarinello, M. L.; Carey, D. A.; Wright, C. 2016. Data Summary Report for the Monitoring Survey at the Isles of Shoals Disposal Site North, September 2015. U.S. Army Corps of Engineers, New England District, Concord, MA, 63 pp.

INSPIRE Environmental. 2019. Standard Operating Procedure (SOP) for Sediment Profile and Plan View Imaging Sample Collection and Image Analysis. Prepared by INSPIRE Environmental, Newport, RI. Revision 1 March 2019.

INSPIRE Environmental. 2020. Quality Assurance Project Plan (QAPP) for the Disposal Area Monitoring System (DAMOS) Program. Prepared for the U.S. Army Corps of Engineers, New England District under Contract No. W912WJ-19-D-0010. Submitted by INSPIRE Environmental, Newport, RI. September 2020.

INSPIRE Environmental. 2021. Image Analysis Results for the 2020 Historic Area Remediation Site (HARS) ROV Survey, Data Report. Prepared for the U.S. Environmental Protection Agency. Submitted by RTI International. July 2021.

McBride, G. B. 1999. Equivalence tests can enhance environmental science and management. Aust. New Zeal. J. Stat. 41(1):19–29.

Pearson, T. H.; Rosenberg, R. 1978. Macrobenthic succession in relation to organic enrichment and pollution of the marine environment. Oceanogr. Mar. Biol. 16: 229-311.

Rhoads, D. C.; Boyer, L. F. 1982. The effects of marine benthos on physical properties of sediments. In: McCall, P.L. and M.J.S. Tevesz, editors. Animal-sediment relations. New York (NY): Plenum Press. p. 3-52.

Rhoads, D. C.; Germano, J. D. 1982. Characterization of organism-sediment relations using sediment profile imaging: an efficient method of remote ecological monitoring of the seafloor (REMOTS System). Mar. Ecol. Progr. 8: 115-128.

Rosenberg, R., H.C. Nilsson, and R.J. Diaz. 2001. Response of benthic fauna and changing sediment redox profiles over a hypoxic gradient. Estuar. Coast. Shelf Sci. 53: 343-350.

Satterthwaite, F. E. 1946. "An Approximate Distribution of Estimates of Variance Components", Biometrics Bulletin, Vol. 2, No. 6, pp. 110-114.

Schuirmann, D. J. 1987. A comparison of the two one-sided tests procedure and the power approach for assessing the equivalence of average bioavailability. J. Pharmacokinet. Biopharm. 15:657–680.

Sturdivant, S.K., R.J. Diaz., and G.R. Cutter. 2012. Bioturbation in a declining oxygen environment, in situ observations from Wormcam. PLoS ONE 7(4): e34539.

Substructure, Inc. 2022. Standard Operating Procedure (SOP) for Acoustic Multibeam Surveys. Prepared by Substructure, Inc., Portsmouth, NH. June 2022.

USACE. 2015. Massachusetts Bay Disposal Site Restoration Demonstration Report 2008–2009. DAMOS Contribution No. 198. U.S. Army Corps of Engineers, New England District, Concord, MA, 114 pp.

USACE. 2021a. Data Summary Report for the Baseline Surveys of the Isles of Shoals North Disposal Site, September/October 2019 and September 2020. Prepared by AECOM

and CR Environmental for the U.S. Army Corps of Engineers, New England District, Concord, MA. 53 pp. plus Appendices.

USACE. 2021b. Monitoring Survey at the Cape Cod Bay Disposal Site May/June 2020. DAMOS Contribution No. 209. Prepared by INSPIRE Environmental, Newport, RI. Prepared for the U.S. Army Corps of Engineers, New England District, Concord, MA. 56 pp. plus Figures and Appendices.

USACE. 2021c. Monitoring Survey at the Rhode Island Sound Disposal Site May/June 2020. DAMOS Contribution No. 210. Prepared by INSPIRE Environmental. Submitted to the U.S. Army Corps of Engineers, New England District, Concord, MA, 87 pp. plus Figures and Appendices.

USACE. 2022. Monitoring Survey at the Isles of Shoals North Disposal Site, October 2021. DAMOS Contribution No. 214. Prepared by INSPIRE Environmental, Newport, RI for the U.S. Army Corps of Engineers, New England District, Concord, MA. 46 pp. plus Figures and Appendices.

USACE. 2023. Monitoring Survey at the Rhode Island Sound Disposal Site, October 2021. DAMOS Contribution No. 215. Prepared by INSPIRE Environmental. Submitted to the U.S. Army Corps of Engineers, New England District, Concord, MA, 38 pp. plus Figures and Appendices.

USACE and New Hampshire State Port Authority. 2014. Portsmouth Harbor and Piscataqua River New Hampshire and Maine Navigation Improvement Project Addendum to Final Feasibility Report. Prepared by the U.S. Army Corps of Engineers, New England District and the New Hampshire State Port Authority. July 2014.

Wolf, S.; Fredette, T. J.; Loyd, R. B. 2012. Thirty-Five Years of Dredged Material Disposal Area Monitoring – Current Work and Perspectives of the DAMOS Program. WEDA Journal of Dredging Engineering, Vol. 12, No. 2, p. 24-41.

MONITORING SURVEY AT THE
ISLES OF SHOALS NORTH DISPOSAL SITE
AUGUST/SEPTEMBER 2022

FIGURES

CONTRIBUTION #217

December 2023

Contract No. W912WJ-19-D-0010

Funded and Managed by:
New England District
U.S. Army Corps of Engineers
696 Virginia Road
Concord, MA 01742-2751

Prepared by:
INSPIRE ENVIRONMENTAL
INSPIRE Environmental
513 Broadway
Newport, RI 02840

LIST OF FIGURES

Figure Page

Figure Page

Figure Page

Figure Page

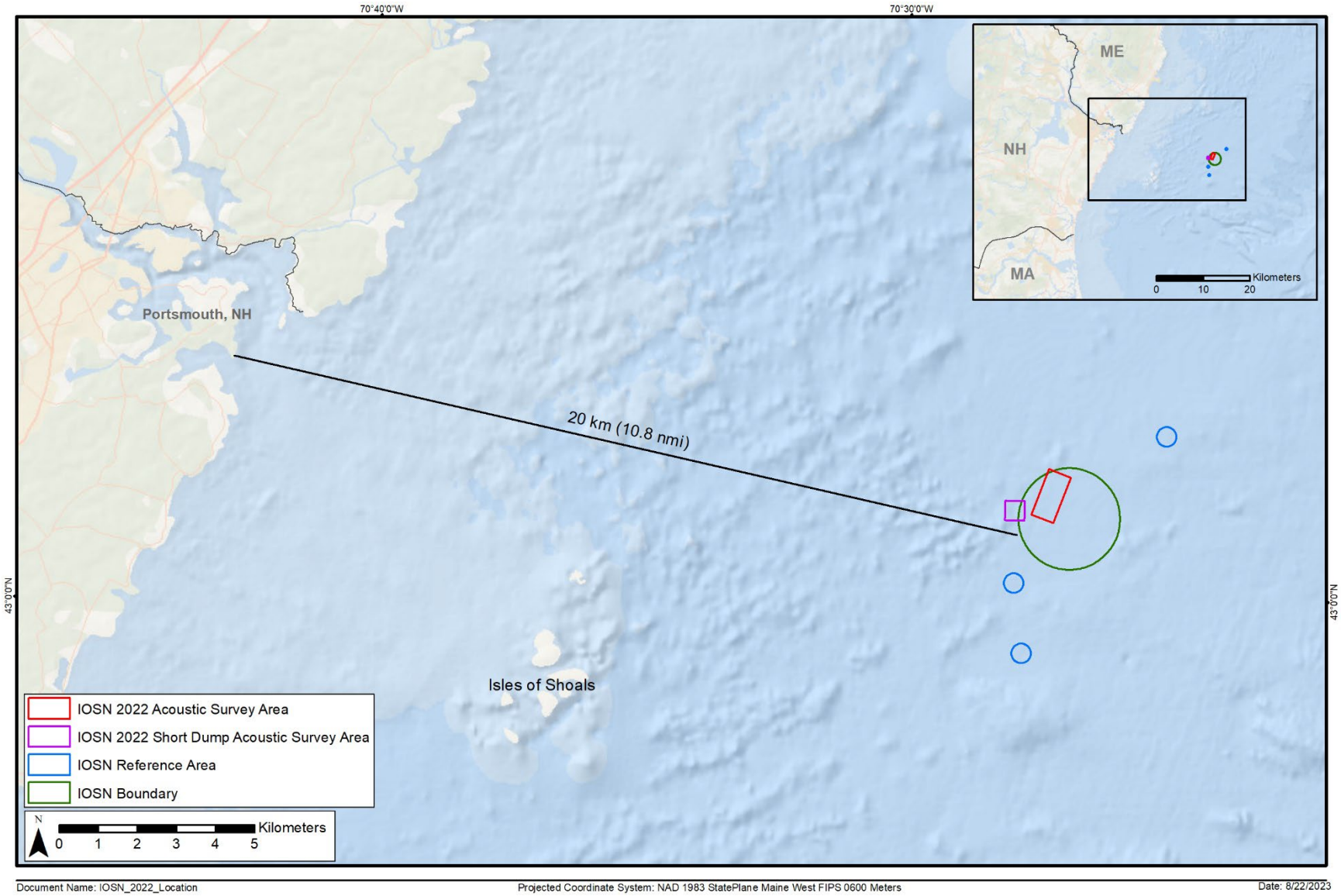

Figure 1-1. Location of the Isles of Shoals North Disposal Site (IOSN)

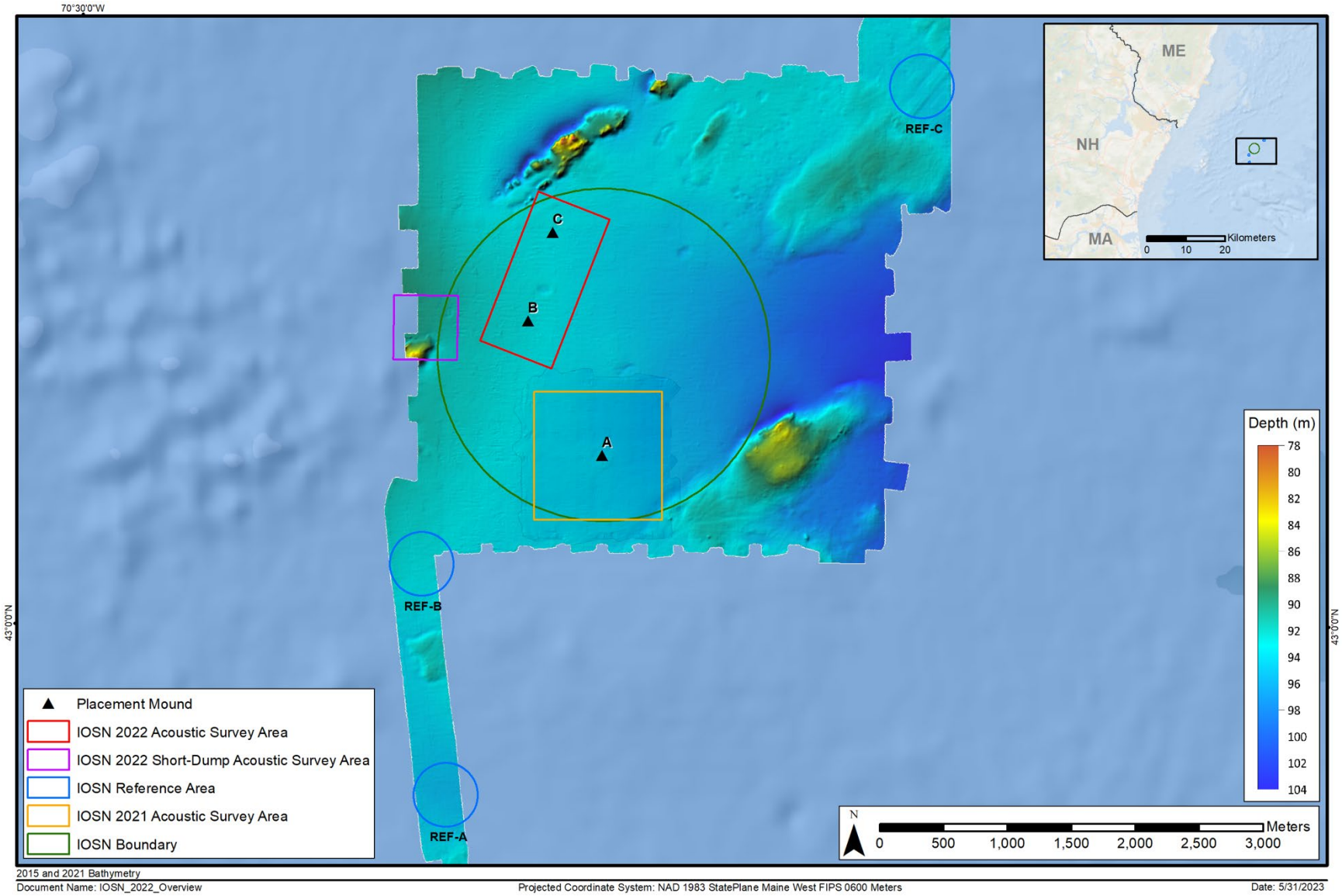

Figure 1-2. Overview of IOSN bathymetry (2015 and 2021) and 2022 sampling areas

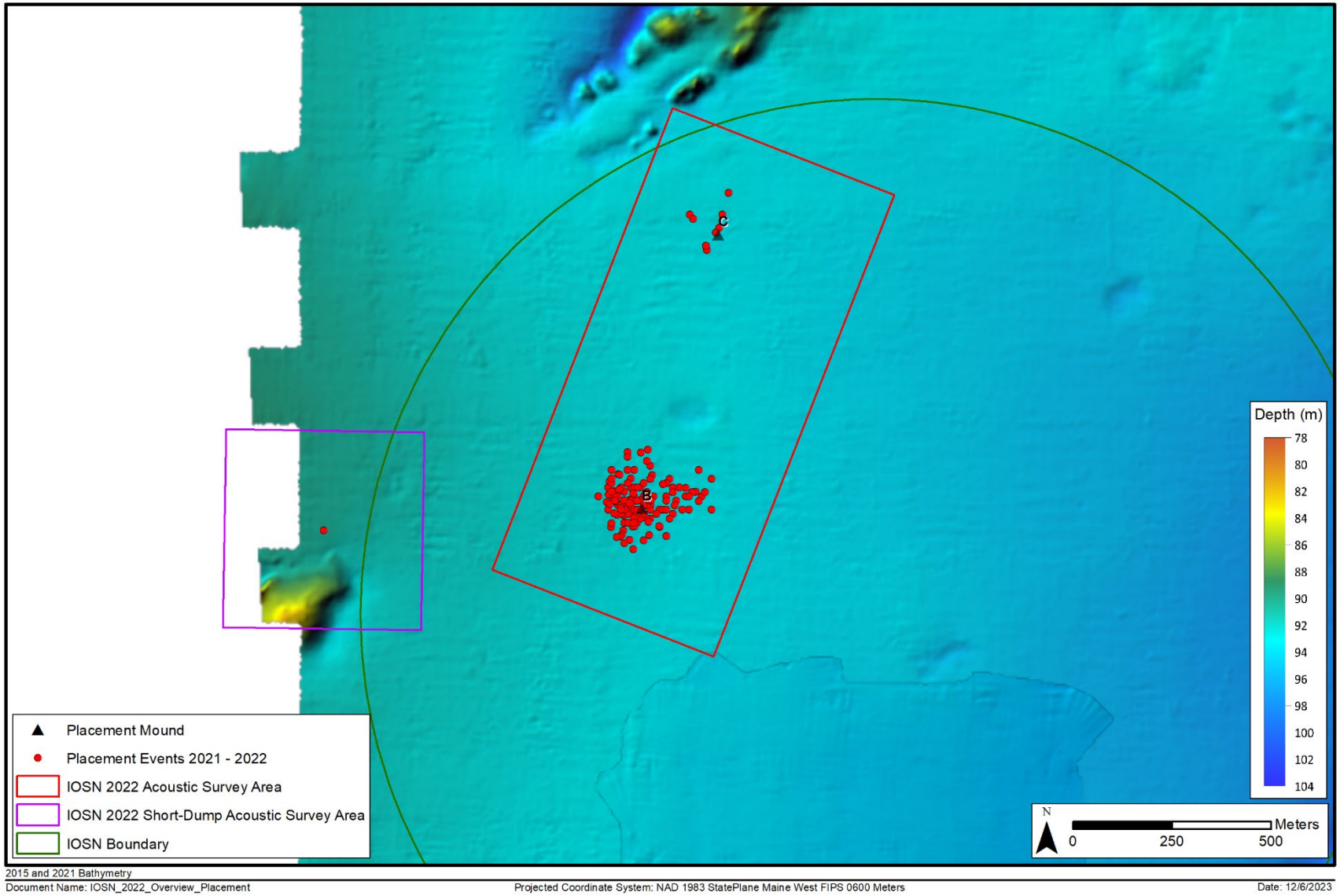

Figure 1-3. Recent dredged material disposal locations for the period November 2021 to April 2022 and short-dump location

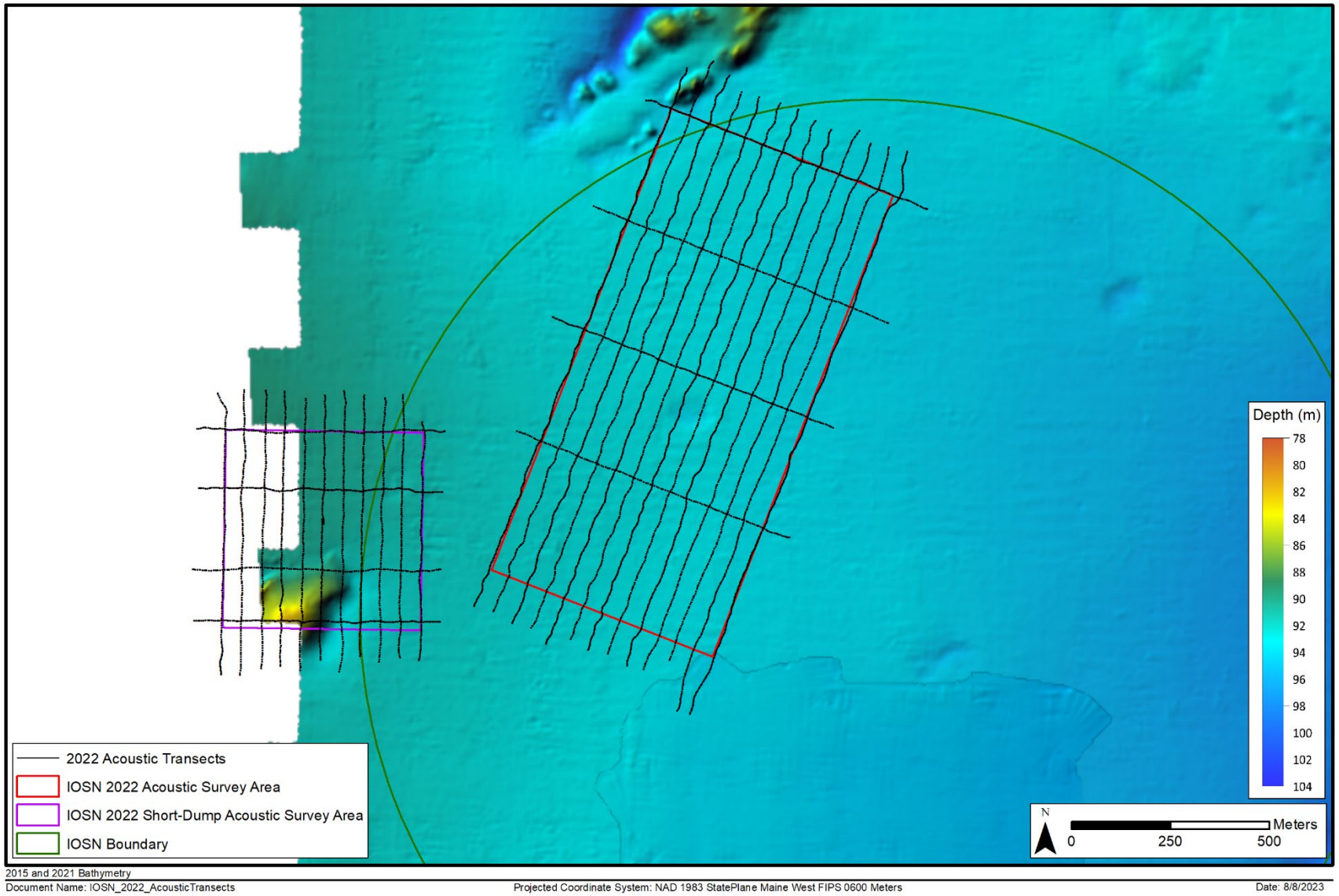

Figure 2-1. Actual acoustic survey tracklines at IOSN, August 2022

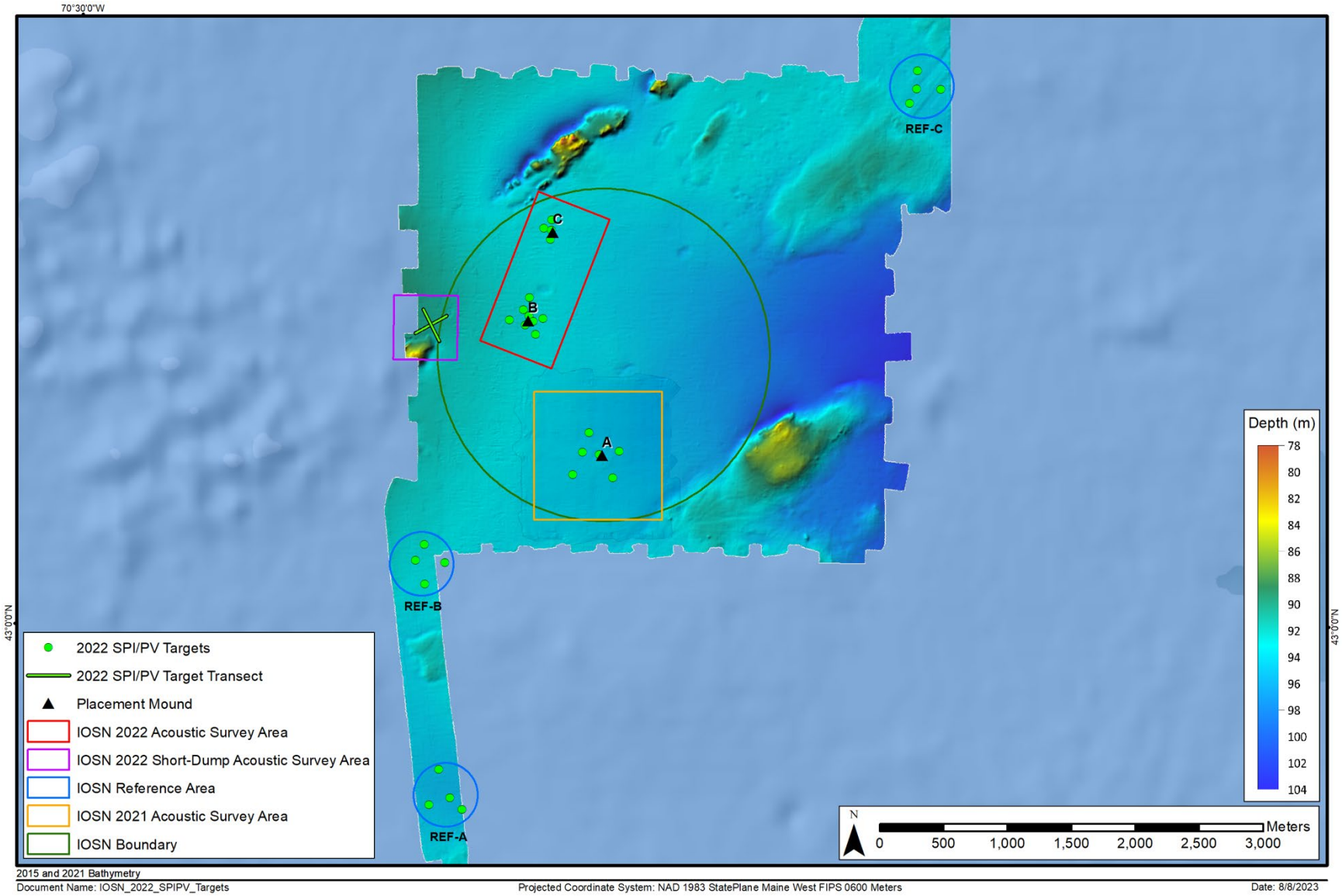

Figure 2-2. SPI/PV target station locations at the short dump, IOSN, and reference areas

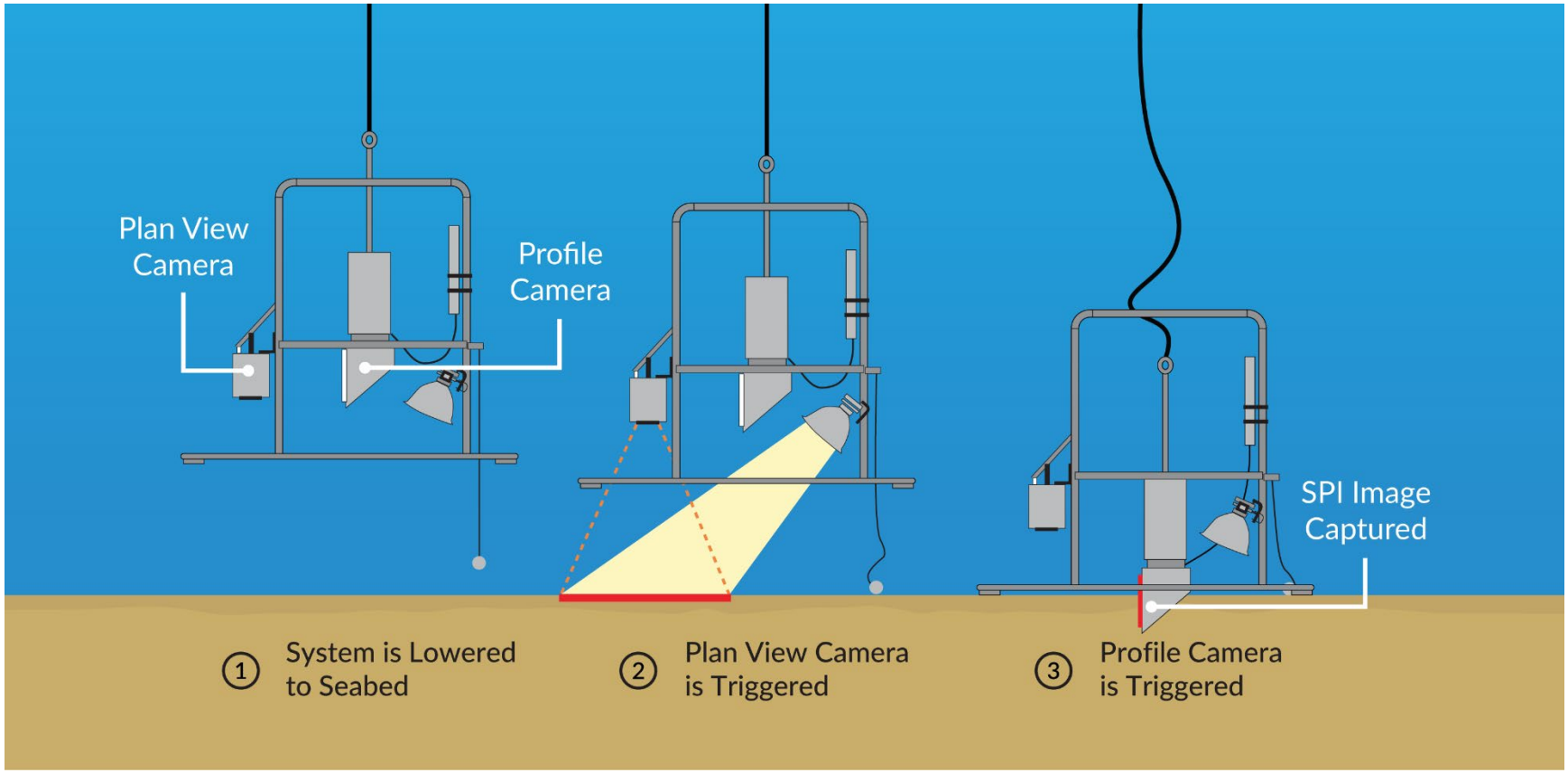

Figure 2-3. Schematic diagram of the operation of the sediment profile and plan view camera imaging system

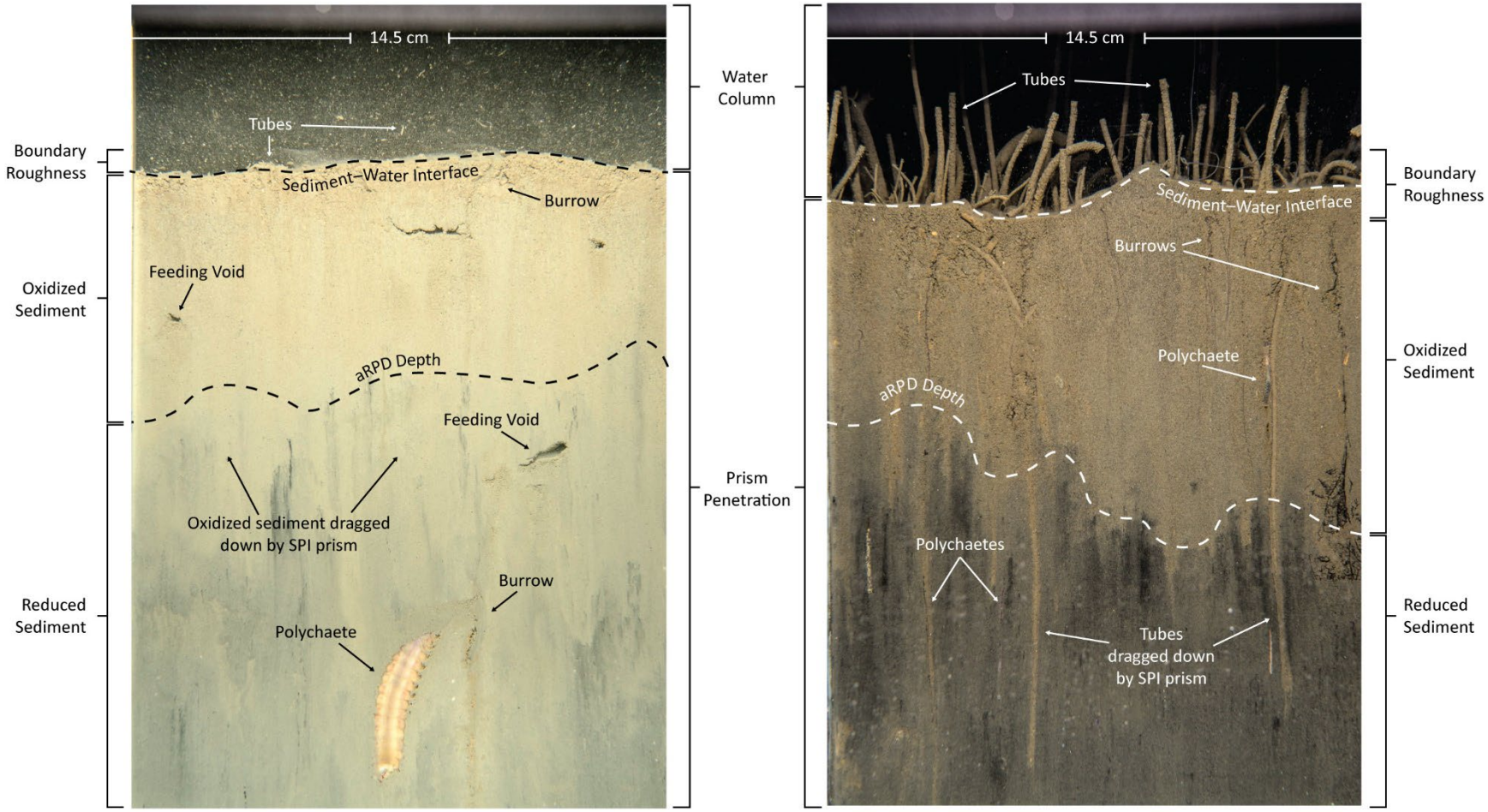

Figure 2-4. SPI images from soft bottom coastal and estuarine environments annotated with many standard variables derived from SPI images. The water column, depth of prism penetration, boundary roughness of the sediment–water interface, and zones of oxidized and reduced sediment are denoted with brackets. The apparent redox potential discontinuity (aRPD), the boundary between oxidized and reduced sediments, is marked with a dashed line. Infauna and related structures (tubes, burrows, feeding voids) are noted with arrows.

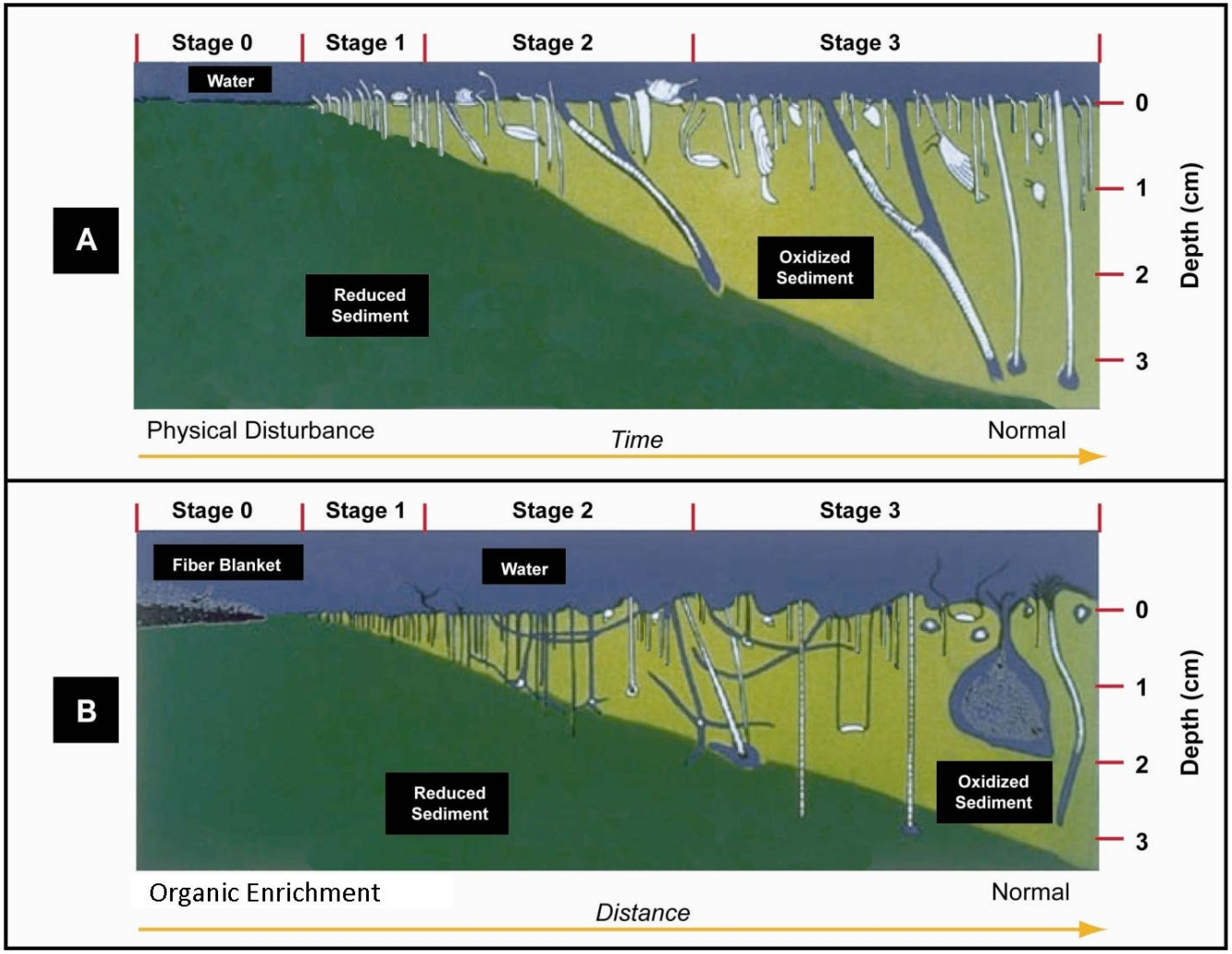

Figure 2-5. The stages of infaunal succession as a response of soft bottom benthic communities to (A) physical disturbance or (B) organic enrichment; from Rhoads and Germano (1982)

Figure 2-6. This representative plan view image shows the sampling relationship between plan view and sediment profile images. Note: plan view images differ between surveys and stations and the area covered by each plan view image may vary slightly between images and stations.

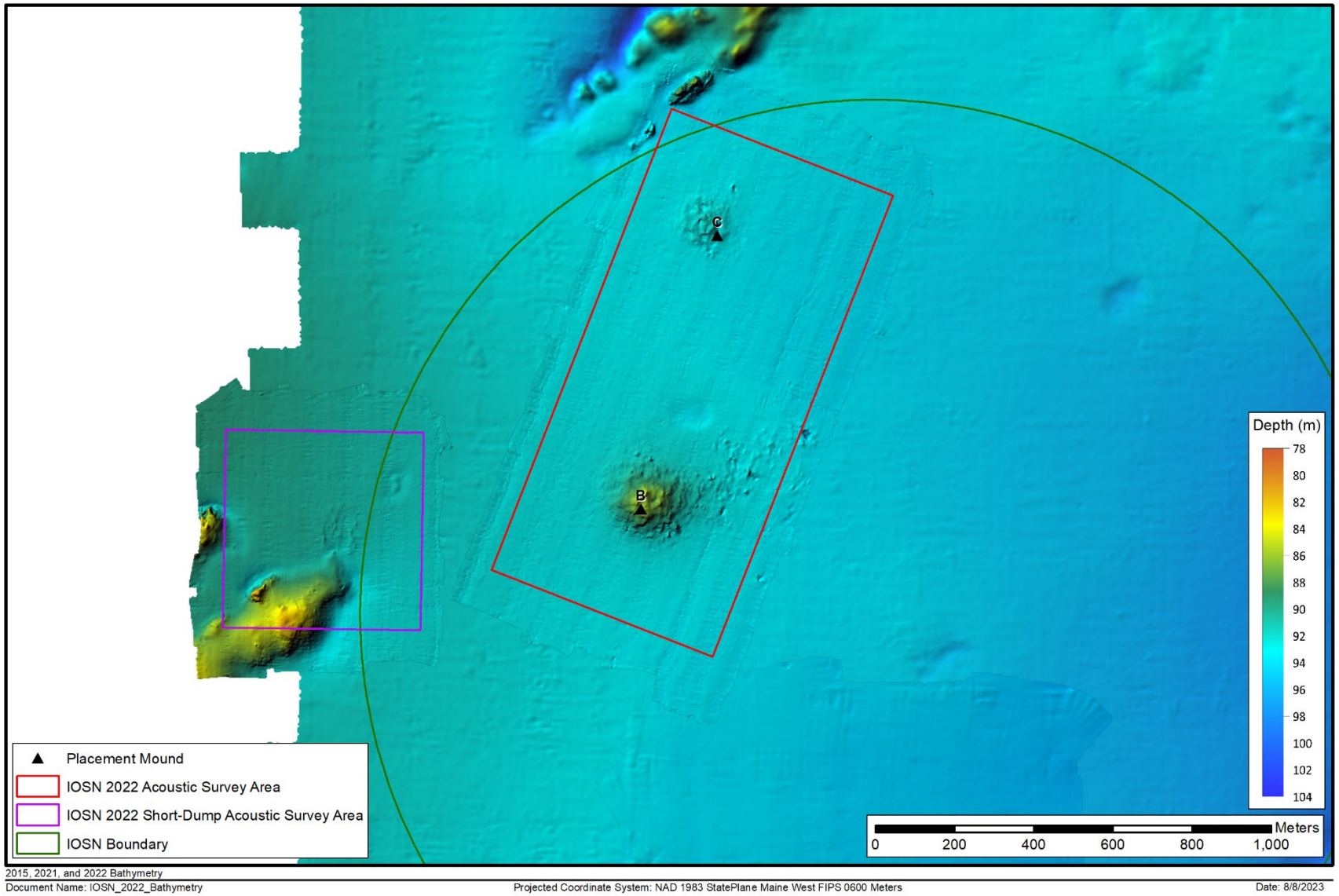

Figure 3-1. Bathymetric depth data over acoustic relief model of IOSN 2022 acoustic survey areas (Mounds B and C and short-dump area) - August 2022

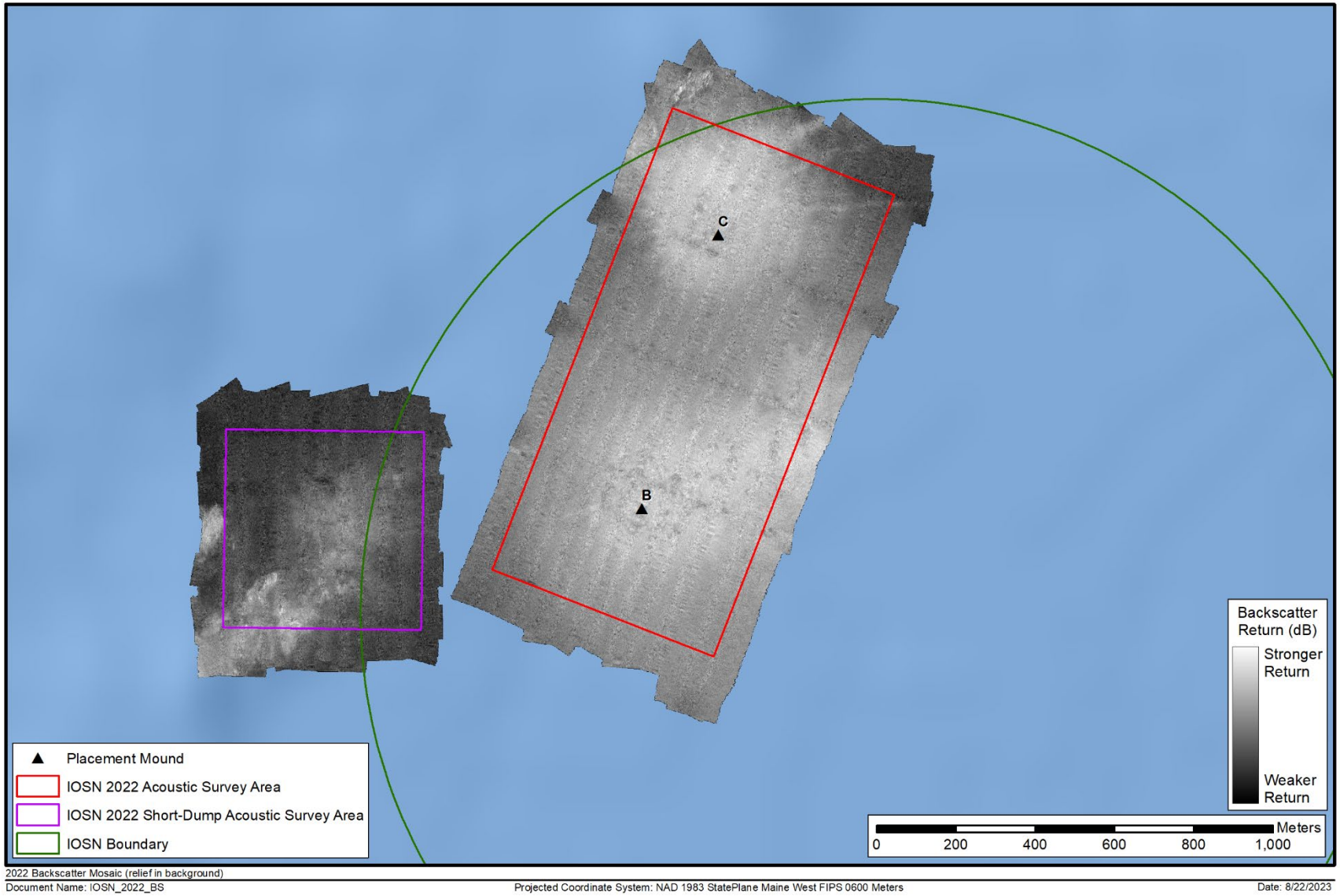

Figure 3-2. Mosaic of unfiltered backscatter data at IOSN acoustic survey areas (Mounds B and C and short-dump area) - August 2022

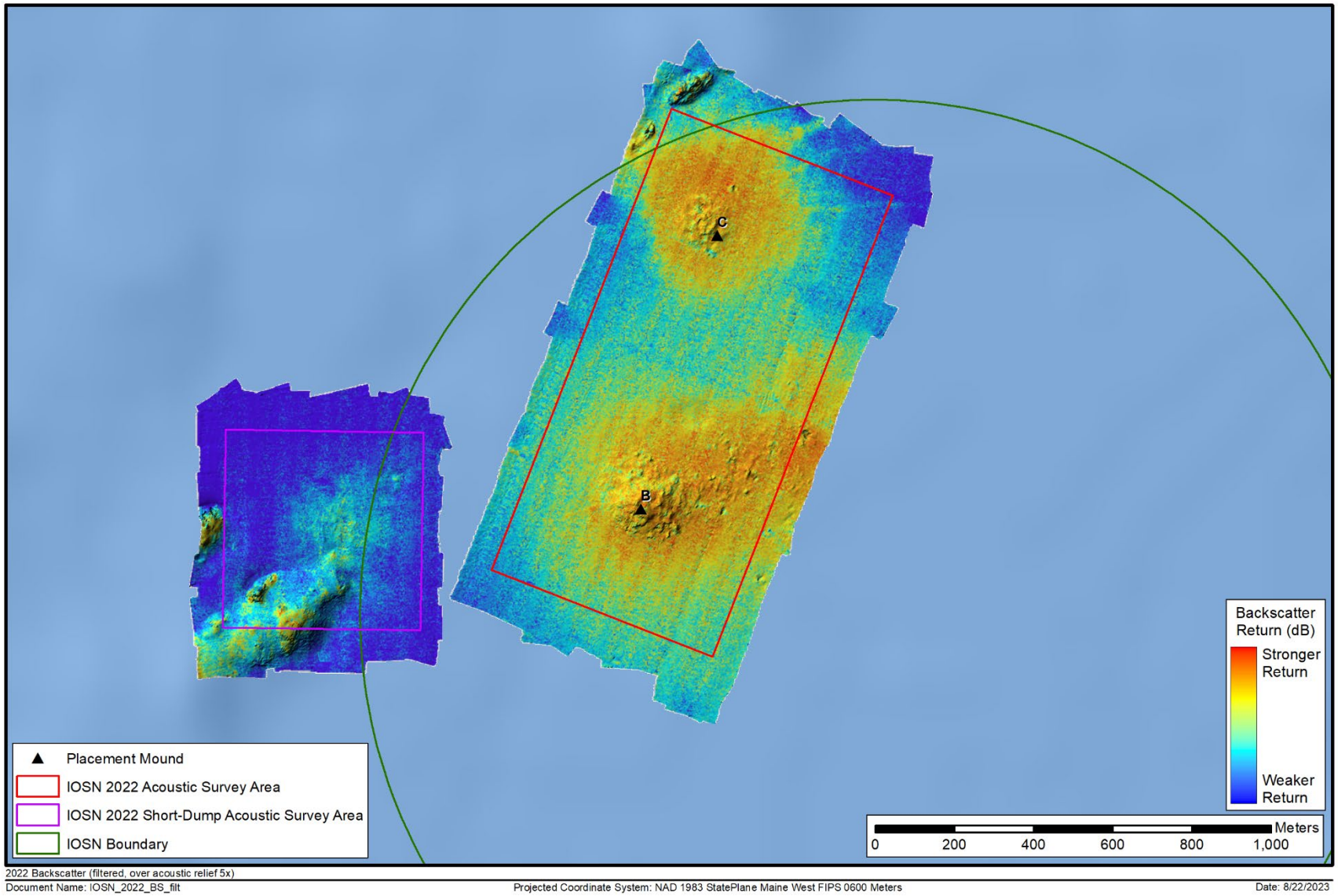

Figure 3-3. Filtered backscatter over acoustic relief model at IOSN acoustic survey areas (Mounds B and C and short-dump area) - August 2022

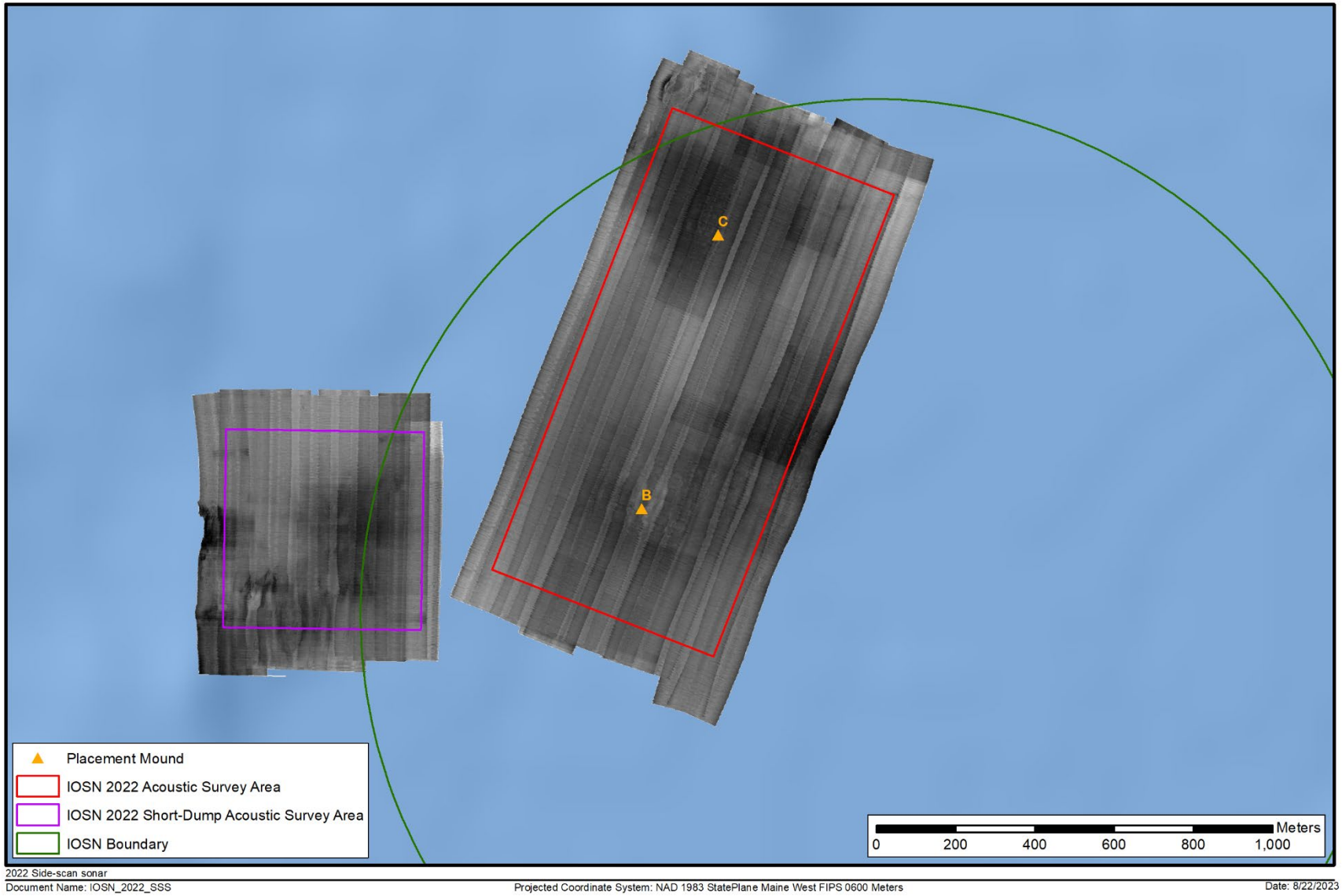

Figure 3-4. Side-scan sonar mosaic at IOSN acoustic survey areas (Mounds B and C and short-dump area) - August 2022

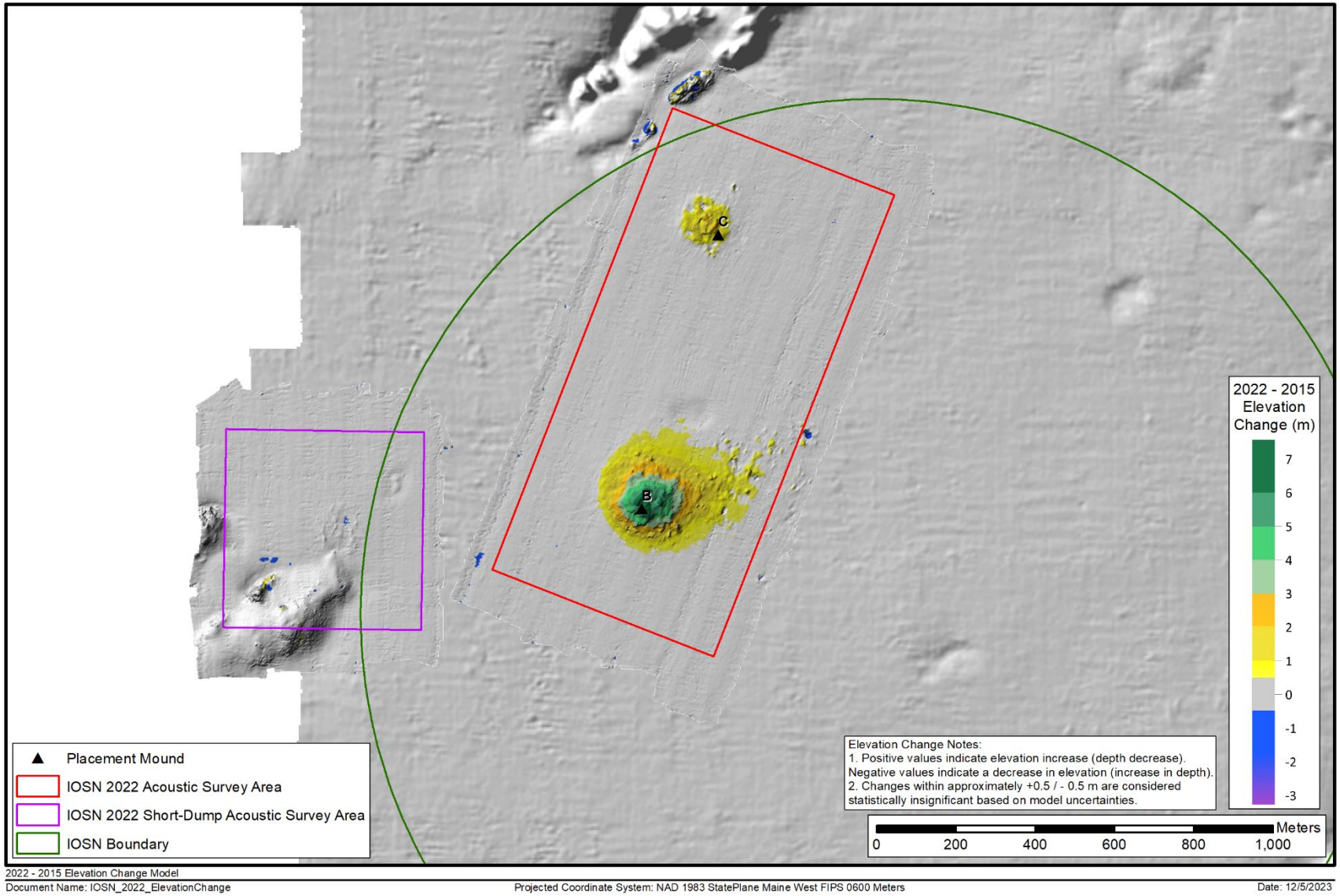

Figure 3-5. Elevation change September 2015 (baseline) vs. August 2022 at IOSN acoustic survey areas (Mounds B and C and short-dump area) - August 2022

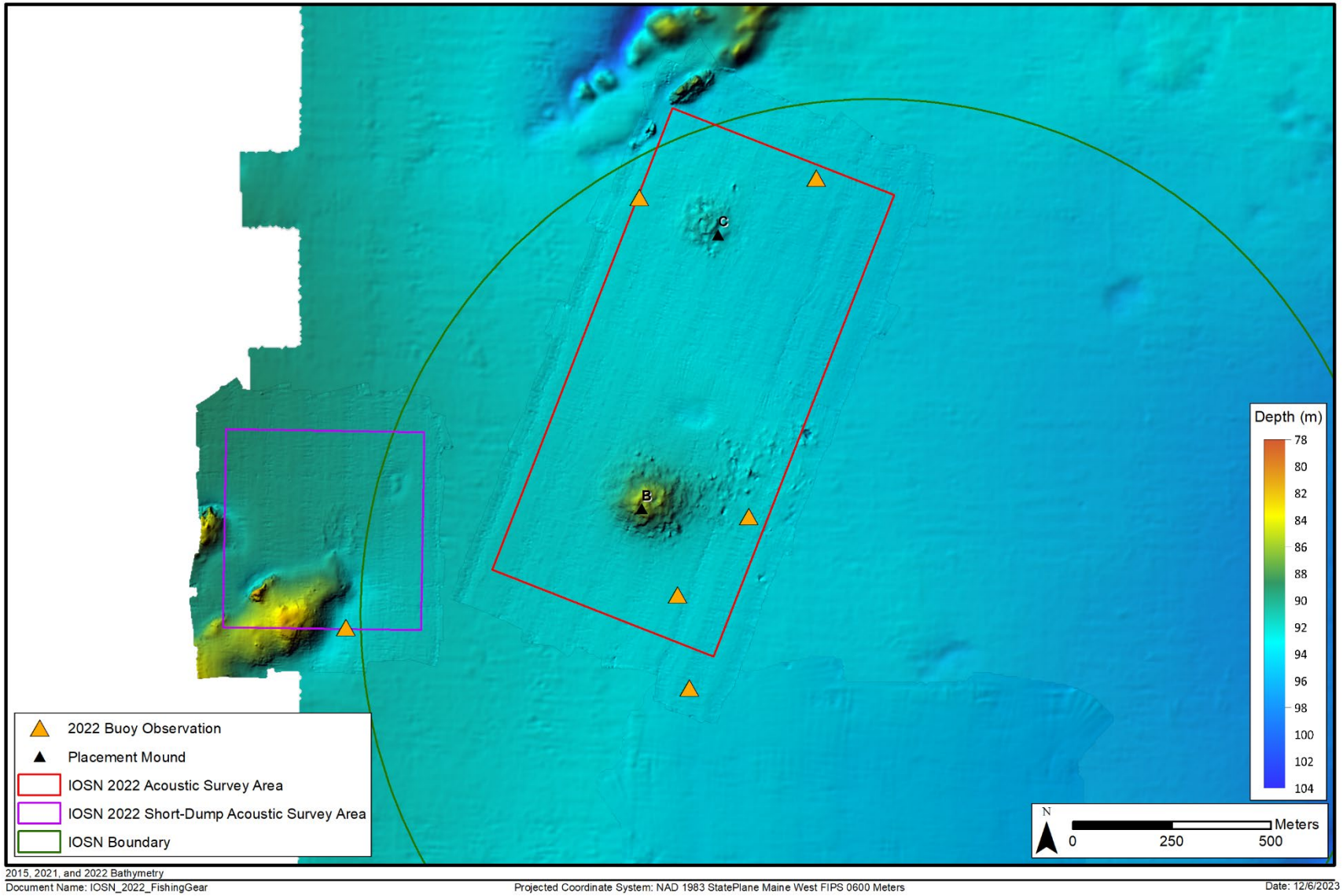

Figure 3-6. Fishing gear (buoy) observations made by hydrographers during the IOSN MBES survey - August 2022

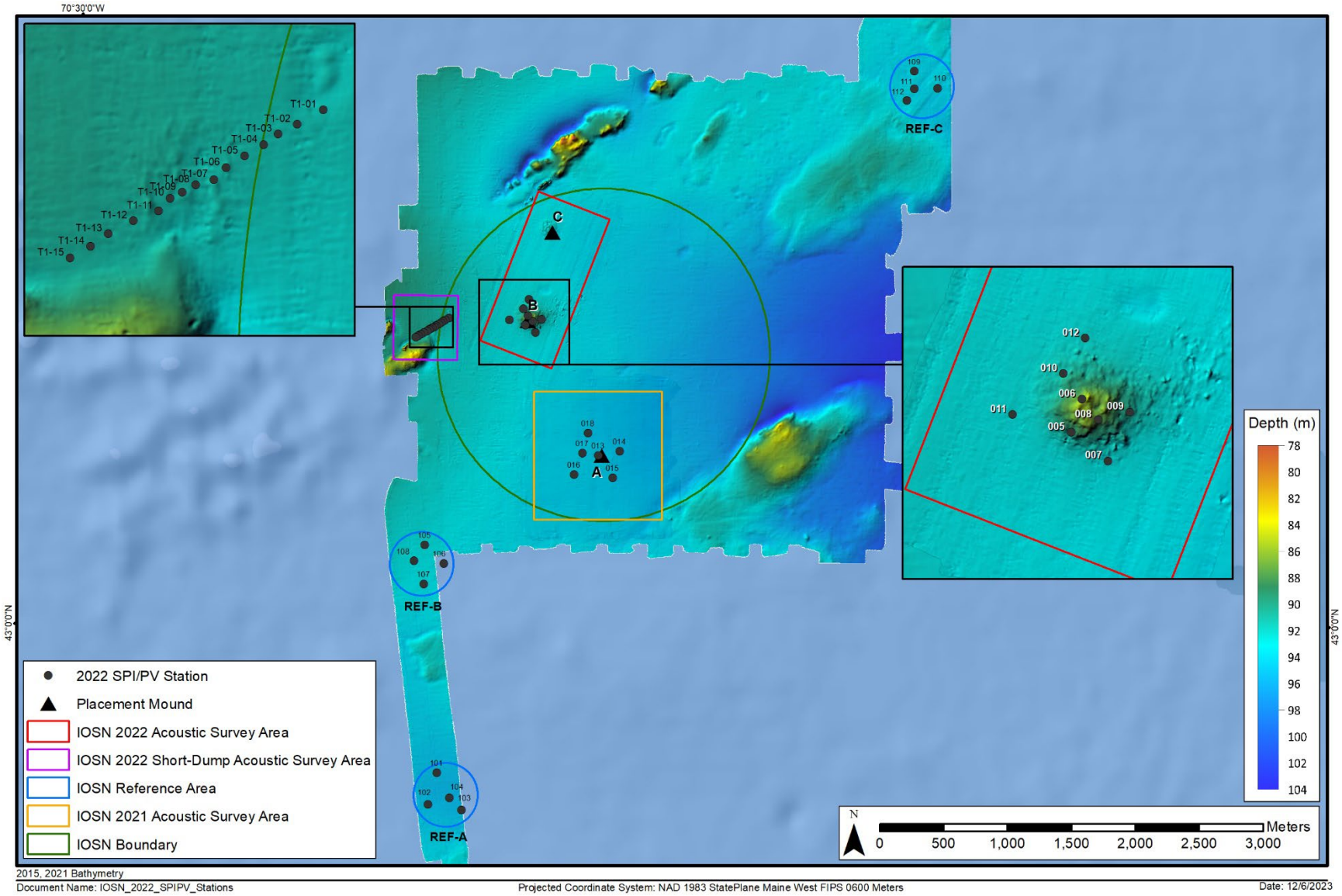

Figure 3-7. SPI/PV actual station locations at the 2022 active area of IOSN (Mound B), Mound A, reference areas, and short-dump investigation area

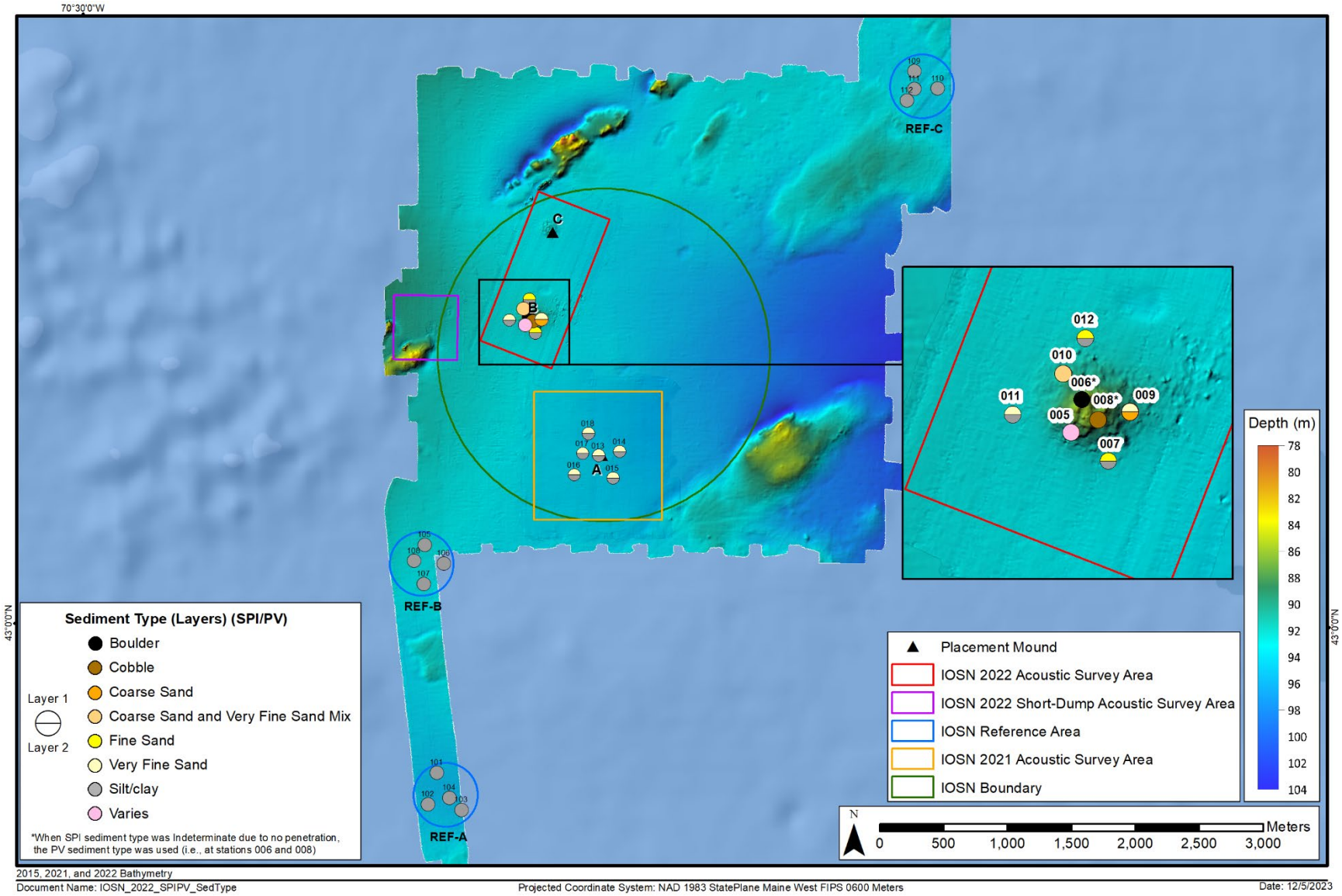

Figure 3-8. Sediment type derived from SPI and PV at the active portion of IOSN (Mound B), Mound A, and reference areas

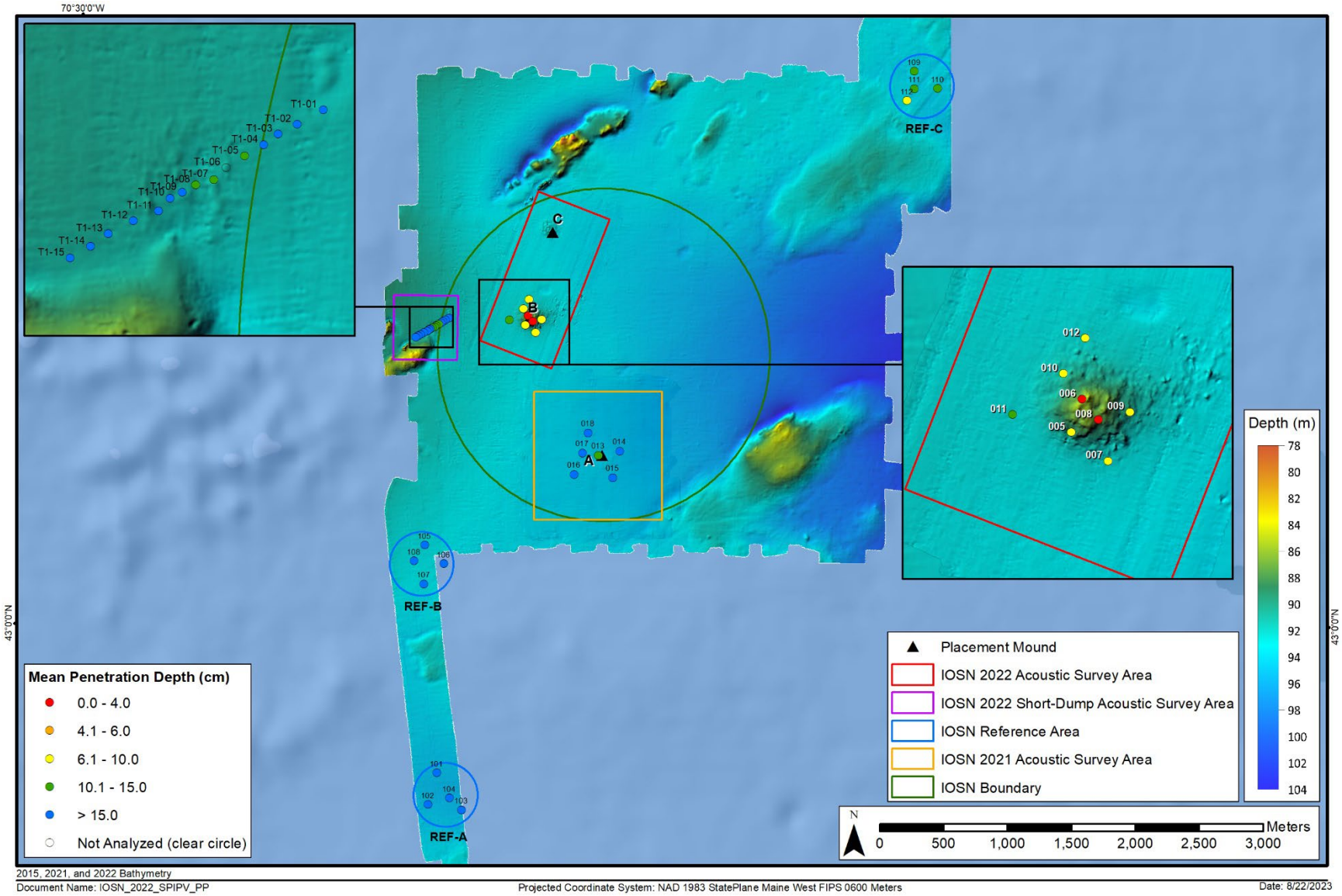

Figure 3-9. Mean station camera prism penetration depths (cm) at the active portion of IOSN (Mound B), Mound A, the short-dump area, and reference areas

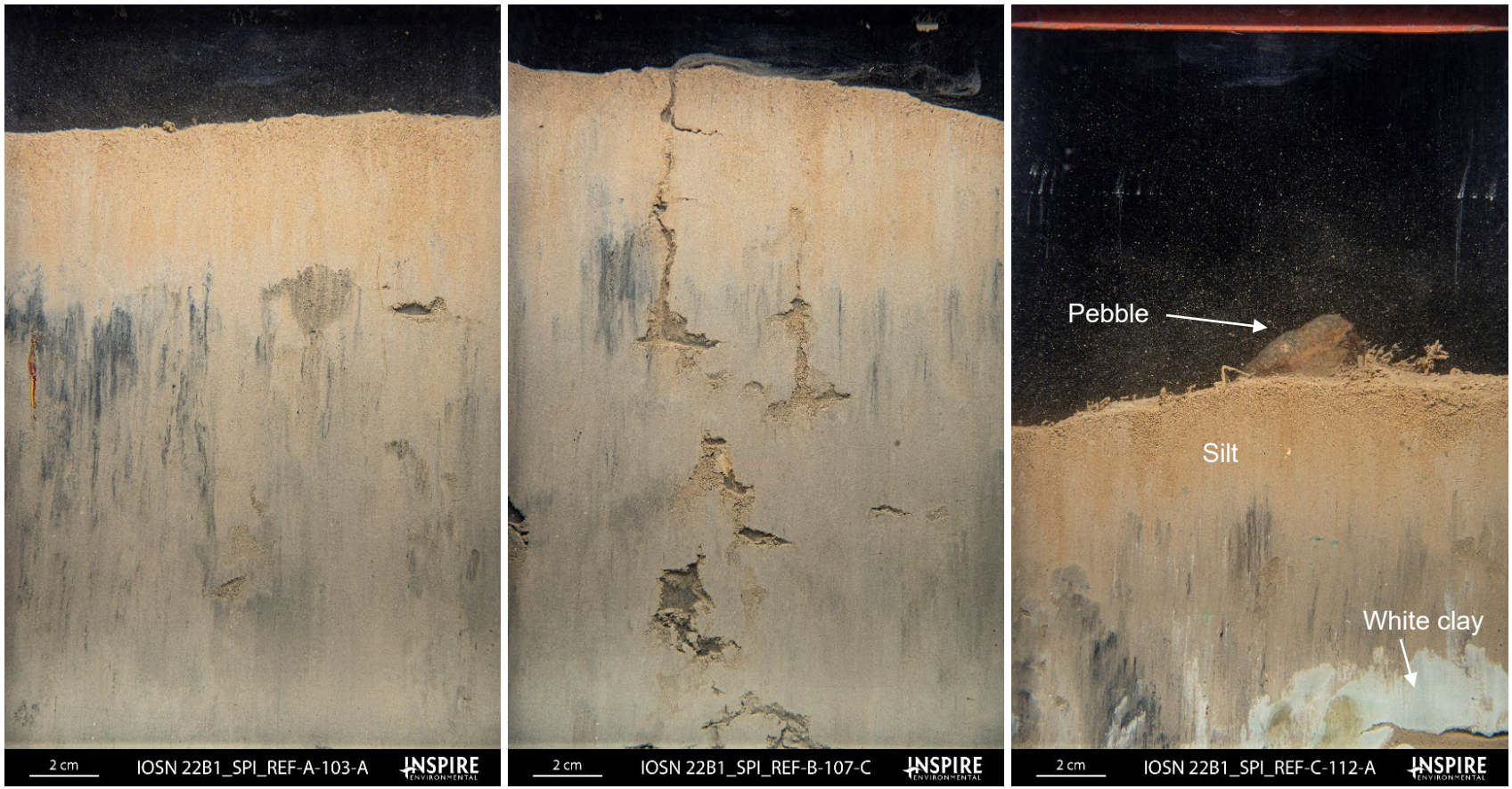

(A) Prism penetration = 18.4 cm (B) Prism penetration = 19.7 cm (C) Prism penetration = 10.5

Figure 3-10. Profile images depicting grain size (major mode), prism penetration, and boundary roughness at reference areas; (A) silt/clay at Station 103 at REF-A; (B) silt/clay at Station 107 at REF-B; and (C) silt over white clay at Station 112 at REF-C

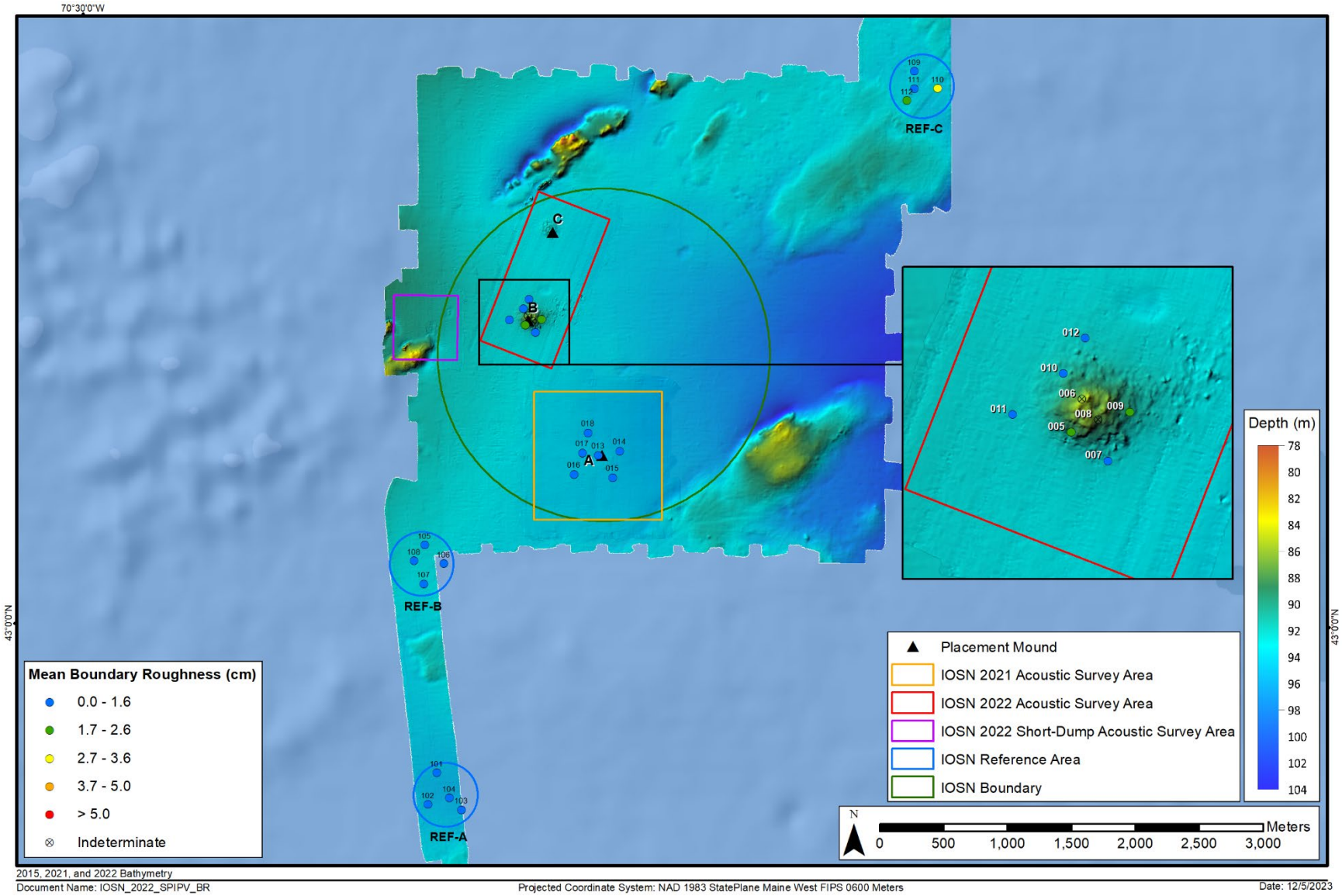

Figure 3-11. Mean station small-scale boundary roughness (cm) at the active portion of IOSN (Mound B), Mound A, and reference areas

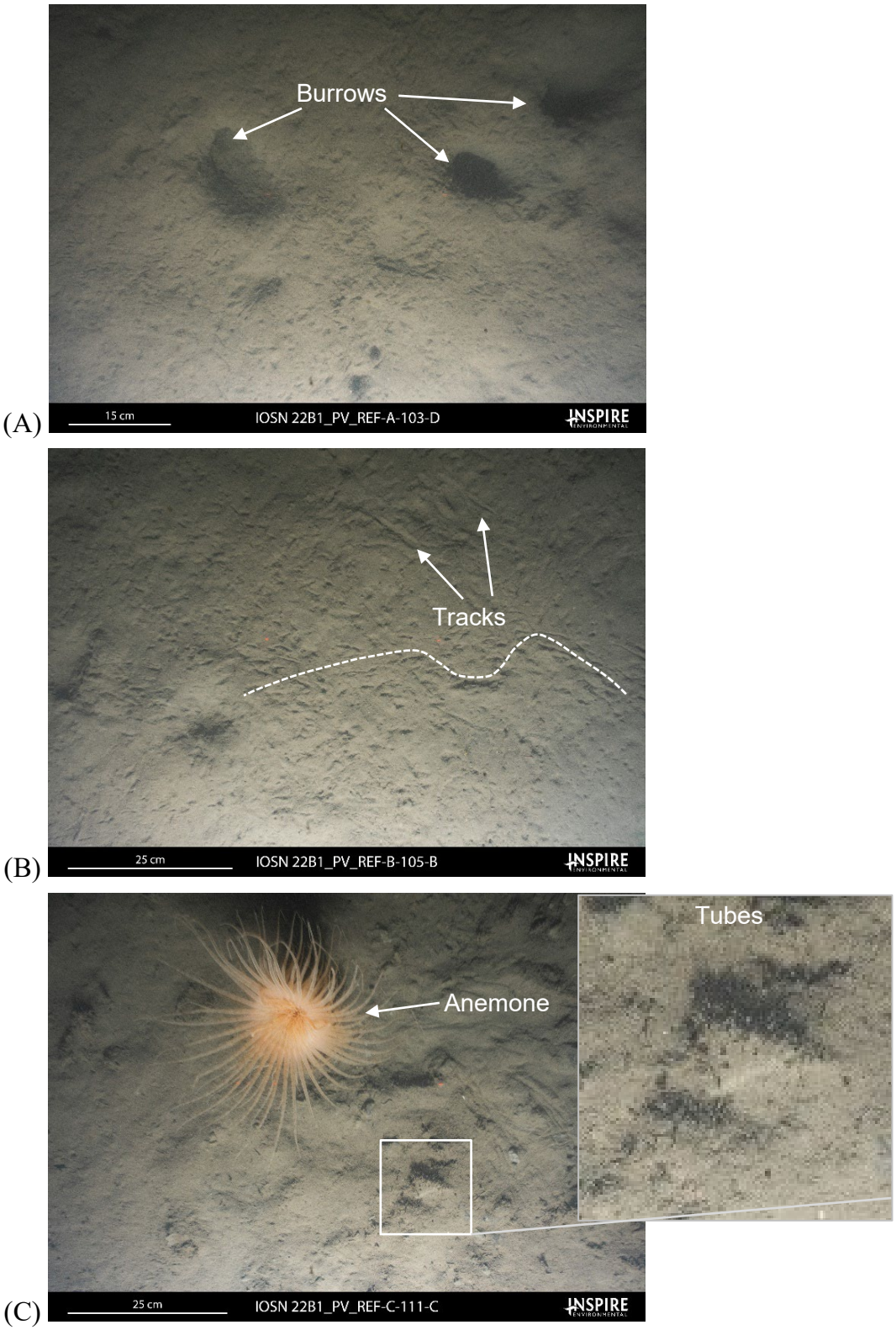

Figure 3-12. Plan view images depicting the range of biological features at the reference areas; (A) large burrows at Station 103 at REF-A; (B) tracks at Station 105 at REF-B; and (C) small tubes and an anemone at Station 111 at REF-C

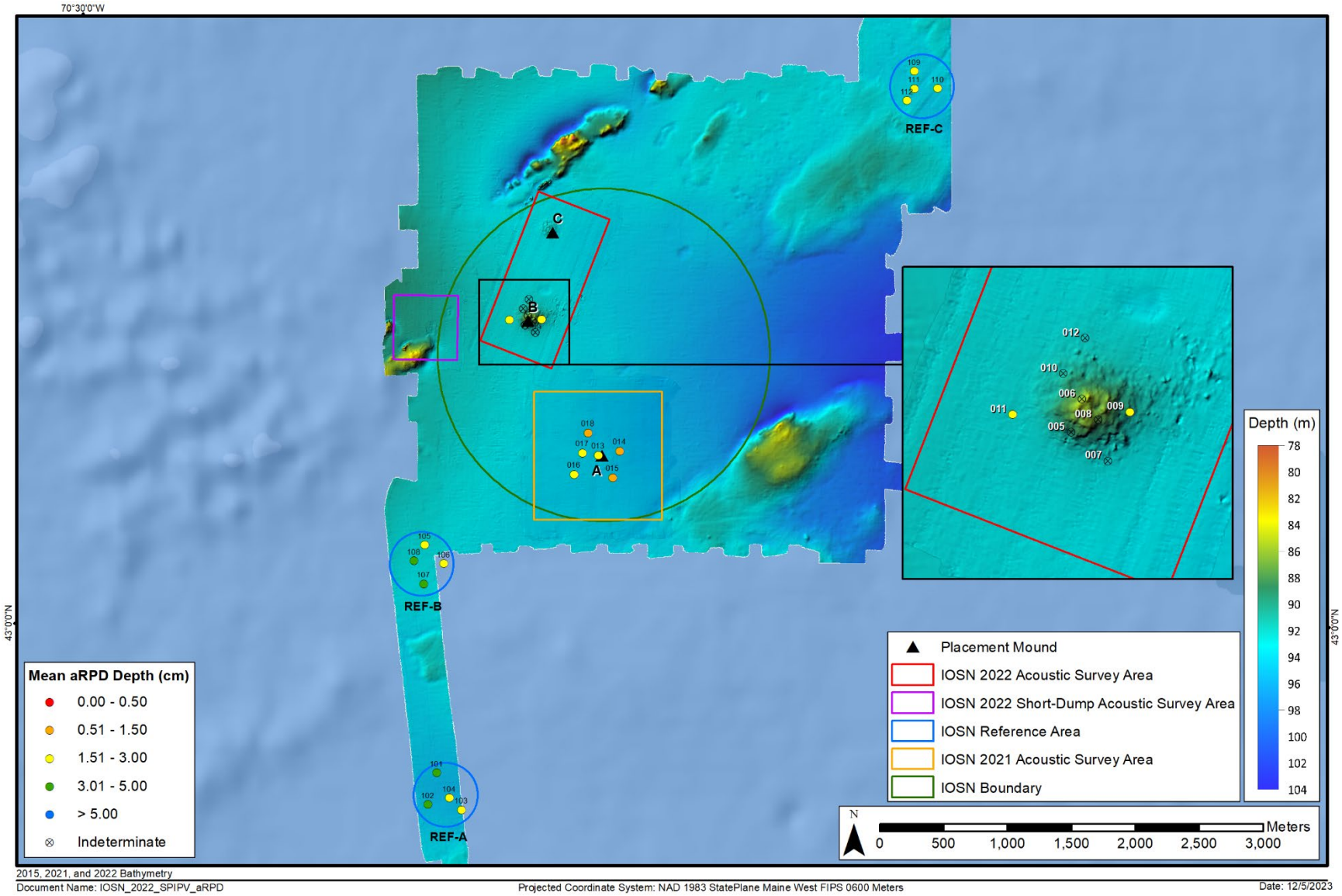

Figure 3-13. Mean station aRPD depth values (cm) at the active portion of IOSN (Mound B), Mound A, and reference areas

(A)

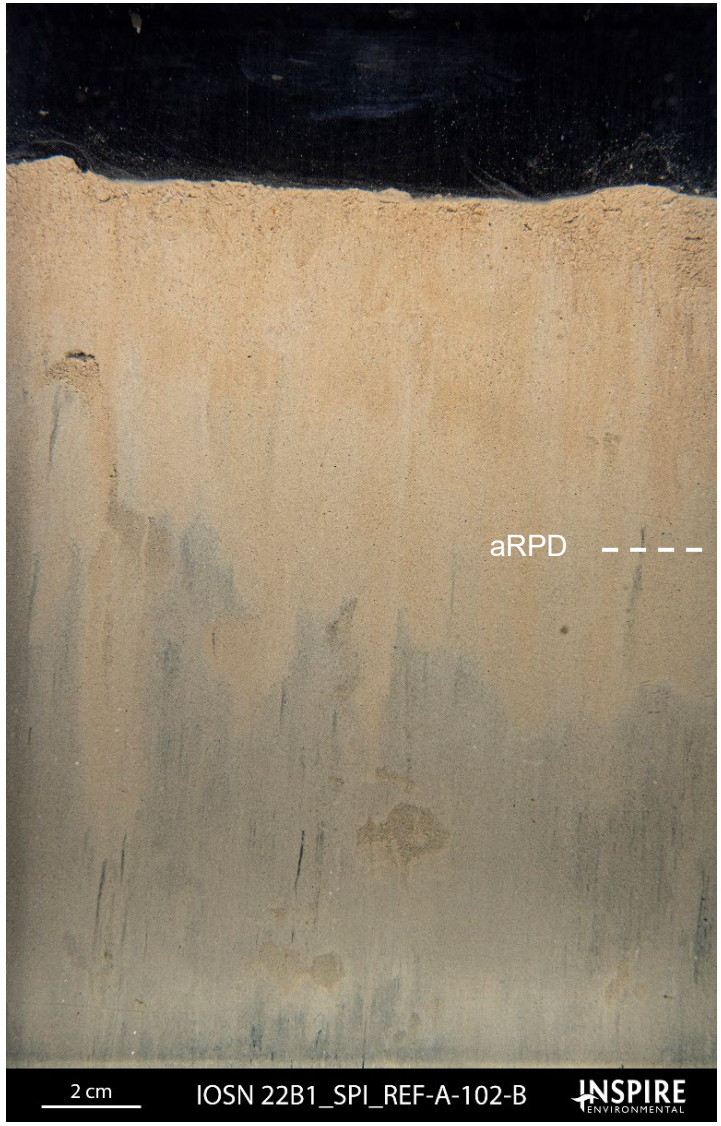

(B)

Figure 3-14. Profile images depicting well-developed aRPDs at the reference areas; (A) an aRPD of approximately 3.4 cm at Station 102 at REF-A; and (B) an aRPD of approximately 2.0 cm at Station 105 at REF-B

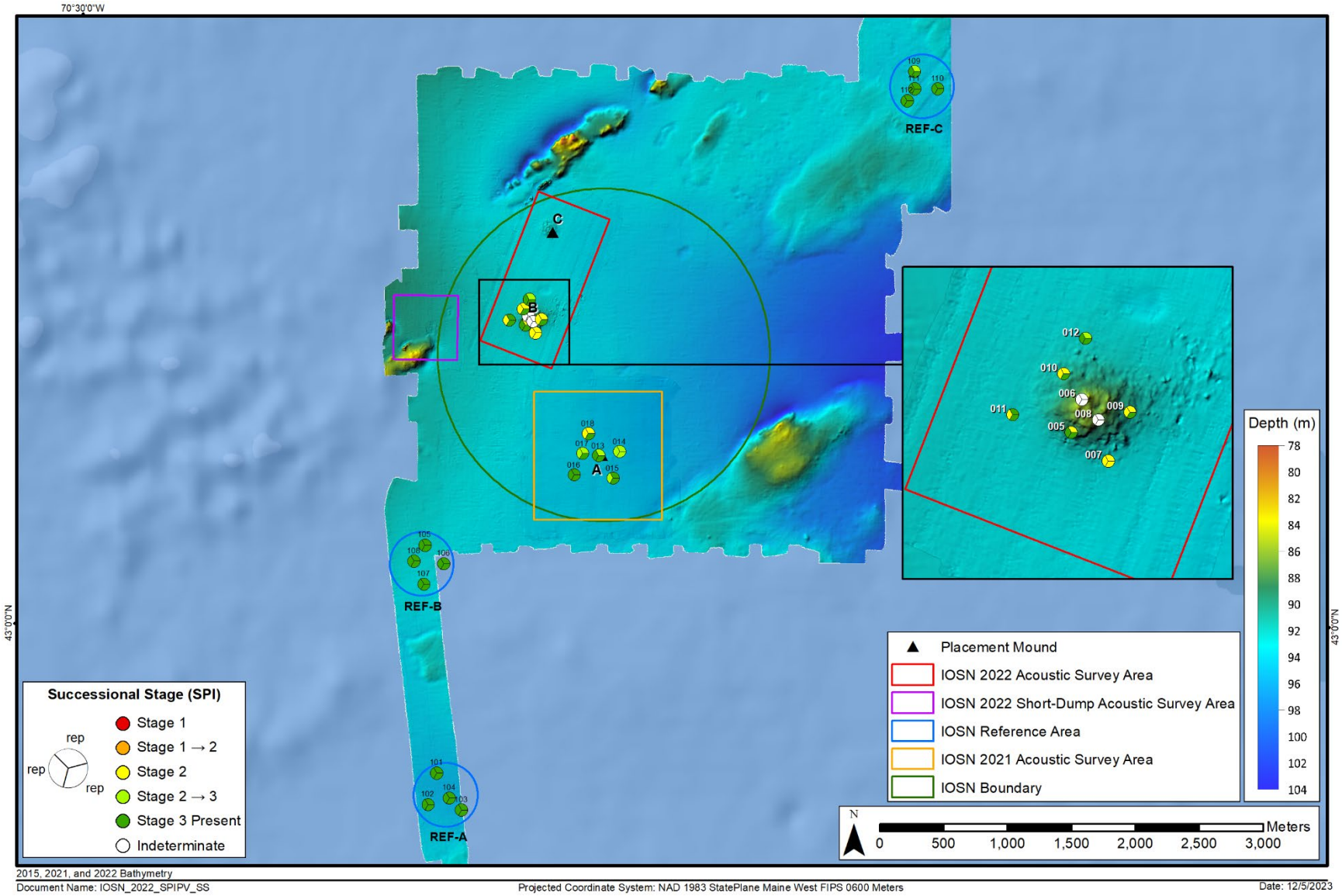

Figure 3-15. Infaunal successional stages at the active portion of IOSN (Mound B), Mound A, and reference areas. Results shown provide a value for each of three replicate images at each sampling station.

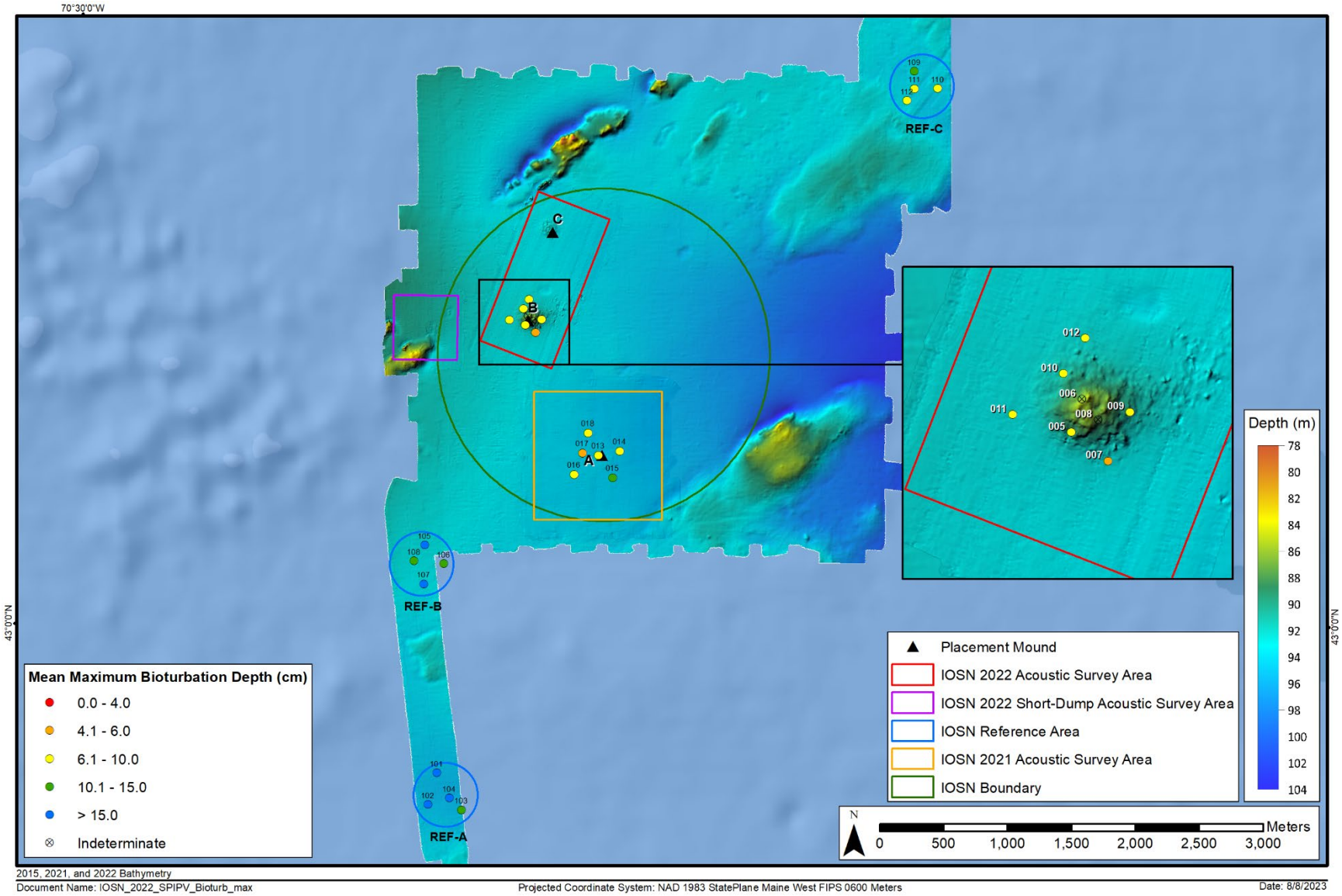

Figure 3-16. Mean Maximum bioturbation depth (cm) at the active portion of IOSN (Mound B), Mound A, and reference areas

(A)

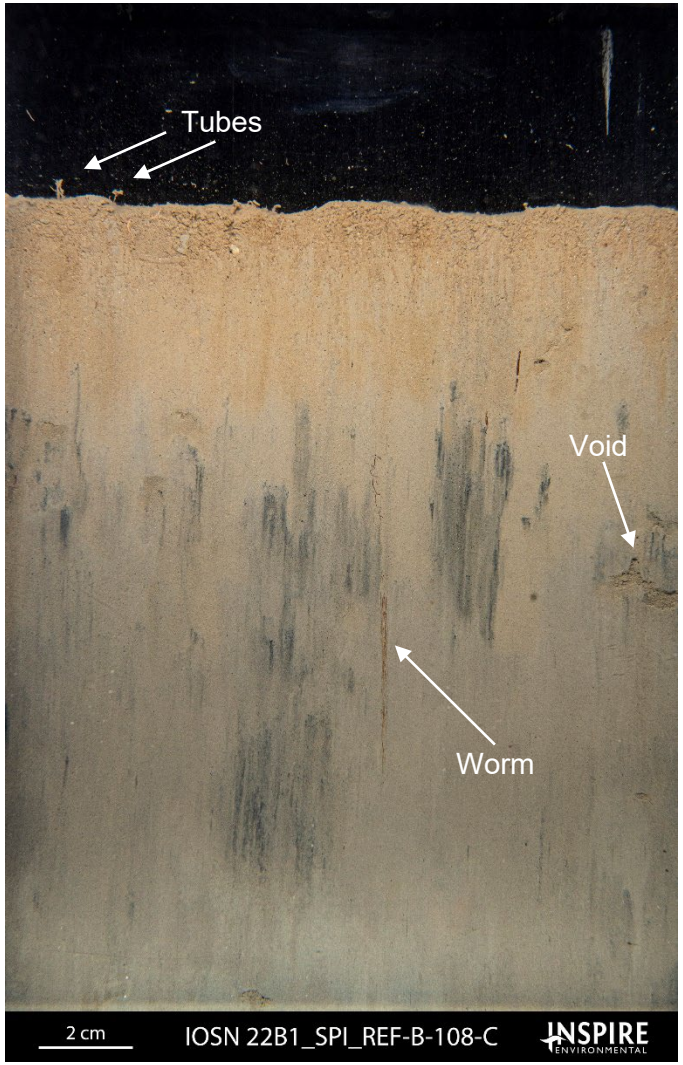

(B)

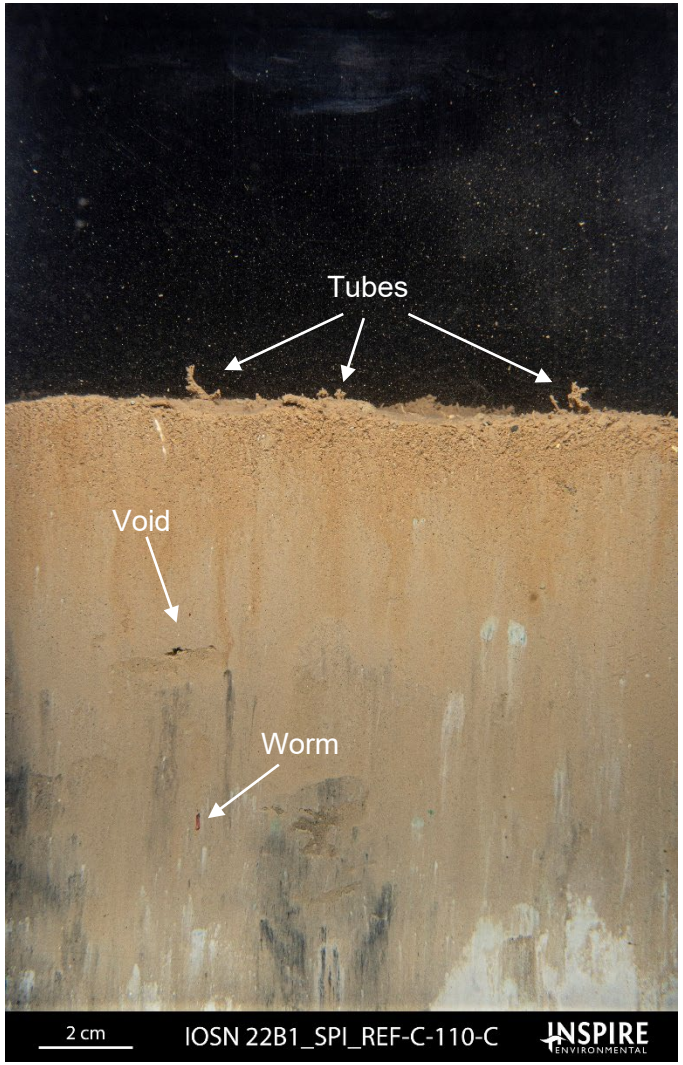

Figure 3-17. Profile images depicting the characteristics of Stage 3 succession at the Reference Areas; (A) deep feeding voids, a large worm in a burrow, and tubes at the sediment–water interface at REF-B 108; and (B) deep feeding voids and polychaete worms at depth, tubes at the sediment–water interface at REF-C 110

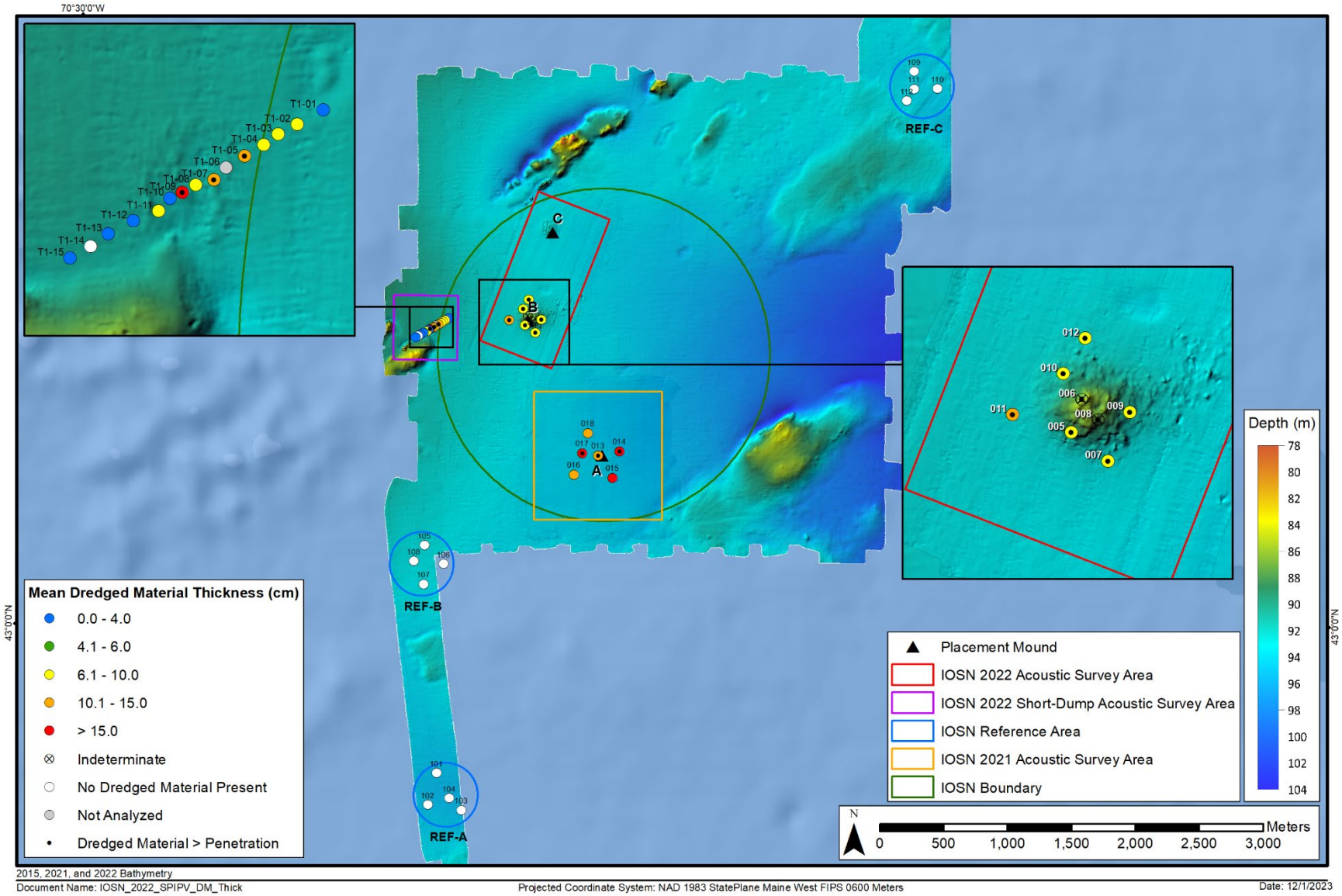

Figure 3-18. Mean dredged material thickness (cm) at the active portion of IOSN (Mound B), Mound A, the short-dump area, and reference areas

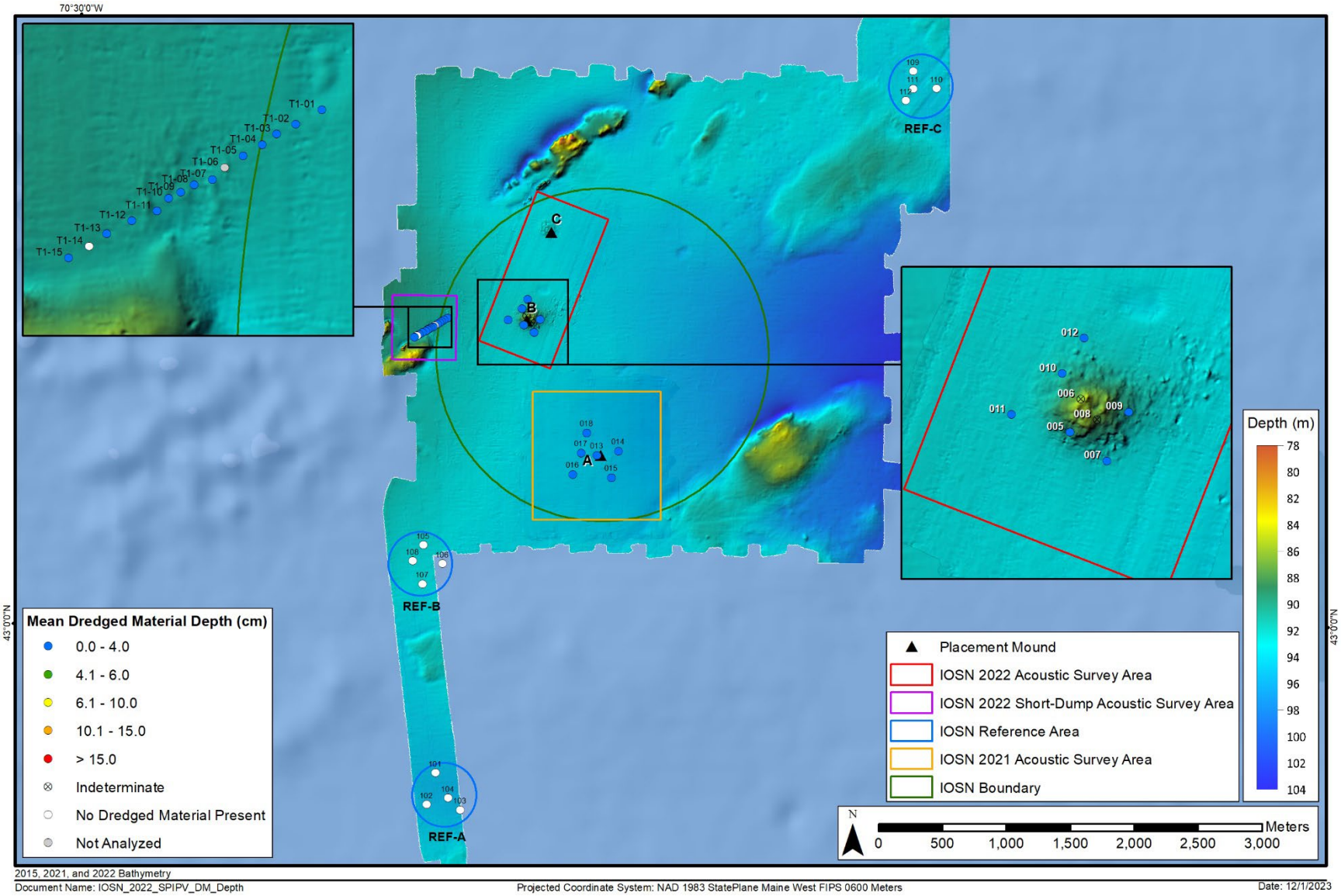

Figure 3-19. Mean dredged material depth (cm) at the active portion of IOSN (Mound B), Mound A, the short-dump area, and reference areas

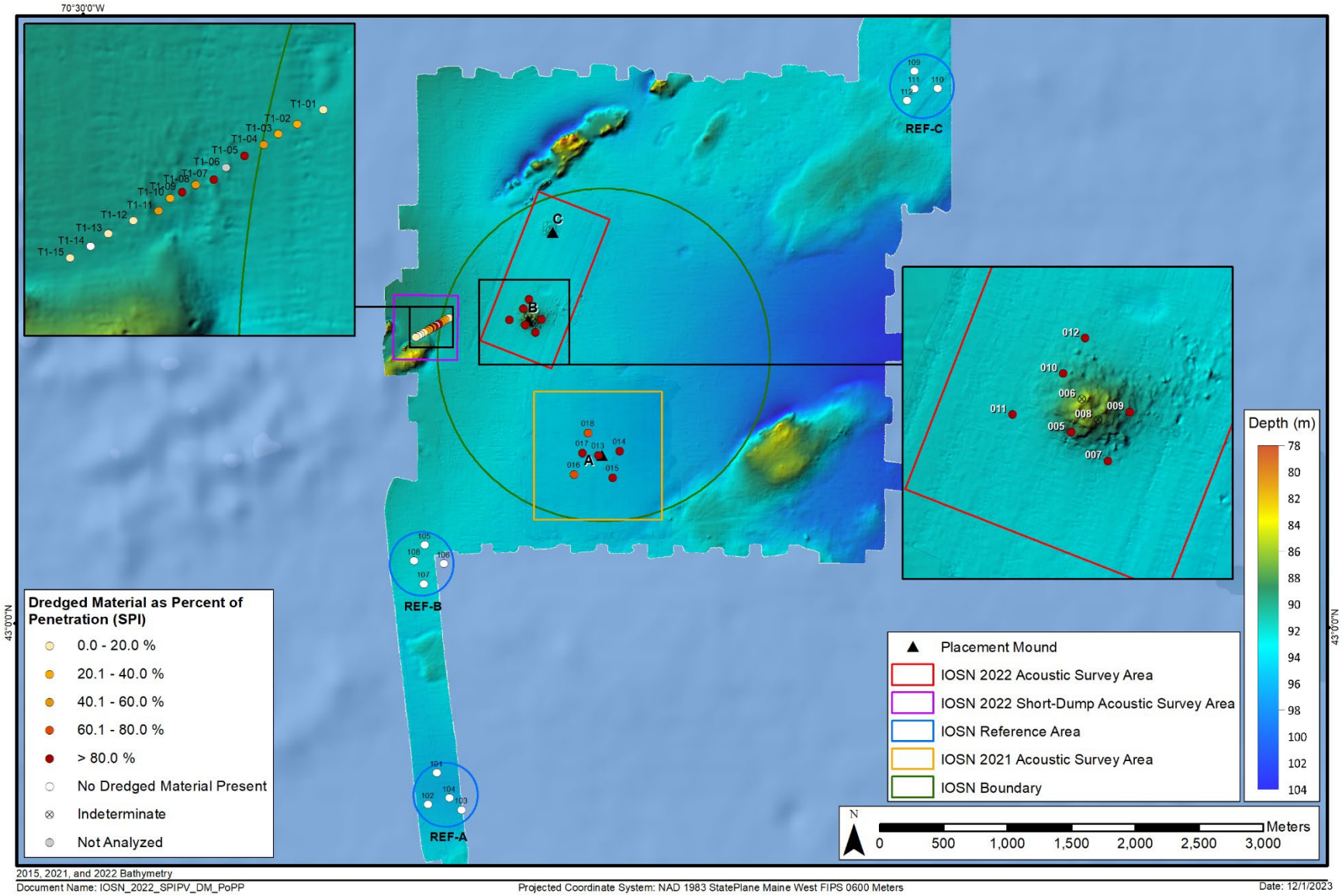

Figure 3-20. Percentage of penetration that is comprised of dredged material at the active portion of IOSN (Mound B), Mound A, the short-dump area, and reference areas

(A) (B) (C)

Figure 3-21. Profile images of the range of types of dredged material at Mound B; (A) rocks at the sediment surface at Station 008; (B) the entire imaged sediment column comprised of white clay at Station 011; and (C) fine sand overlaying white clay at Station 012

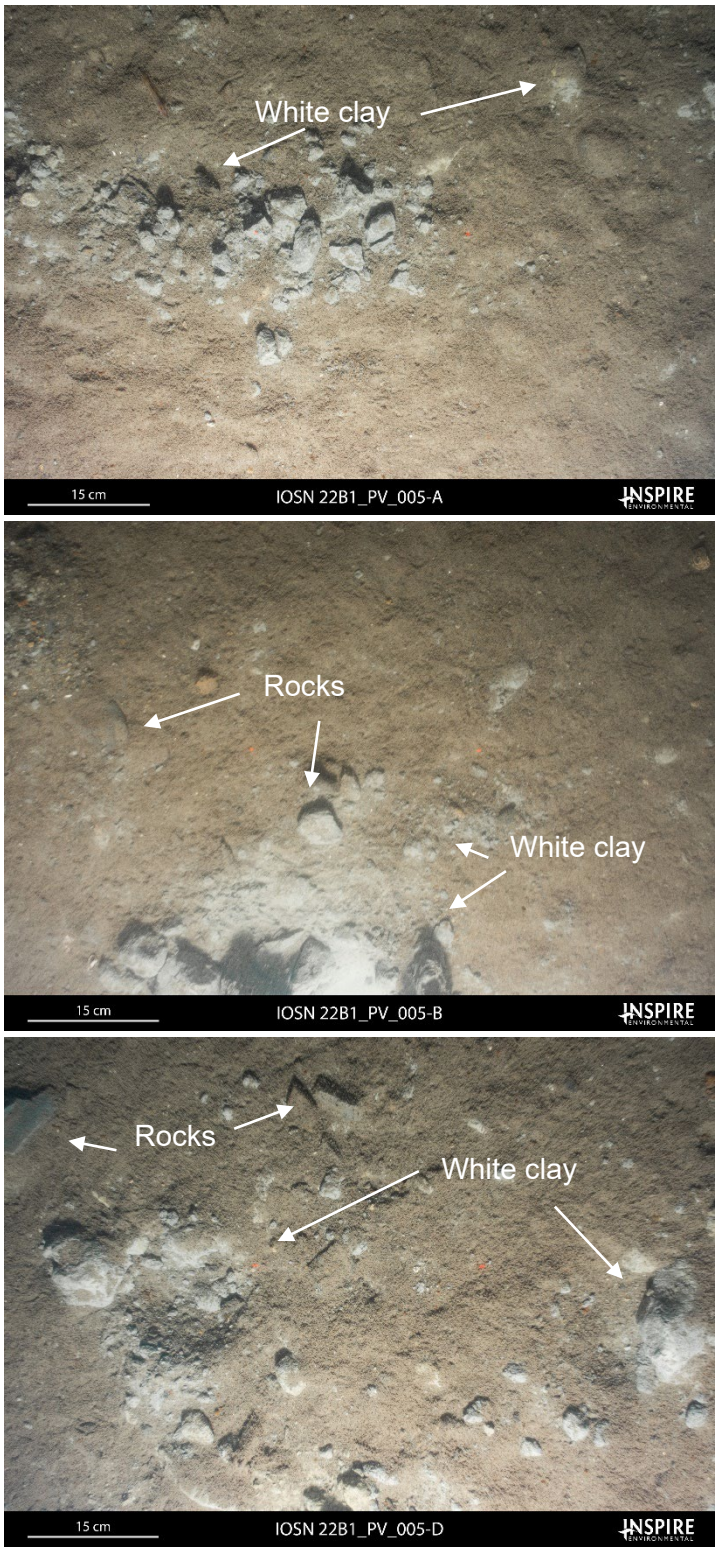

(A)

Figure 3-22. Plan view images of surficial dredged material and epifauna at Mound B; (A) clasts of white clay and small rocks at Station 005; (B) large rocks and white clay with a lobster at Station 006; and (C) white compact clay across the sediment surface with extensive epifaunal tracks and a crab at Station 011

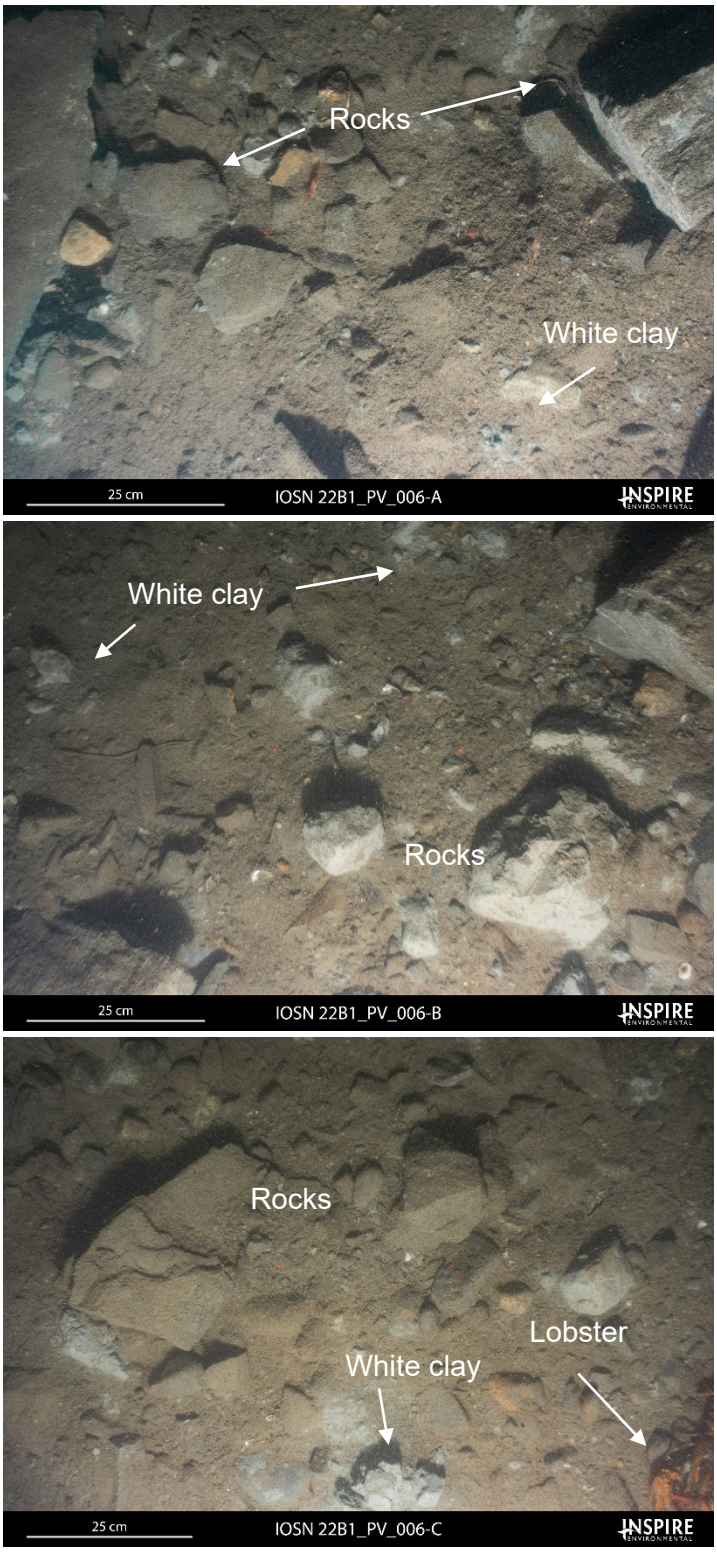

(B)

Figure 3-22 continued. Plan view images of surficial dredged material and epifauna at Mound B; (A) clasts of white clay and small rocks at Station 005; (B) large rocks and white clay with a lobster at Station 006; and (C) white compact clay across the sediment surface with extensive epifaunal tracks and a crab at Station 011

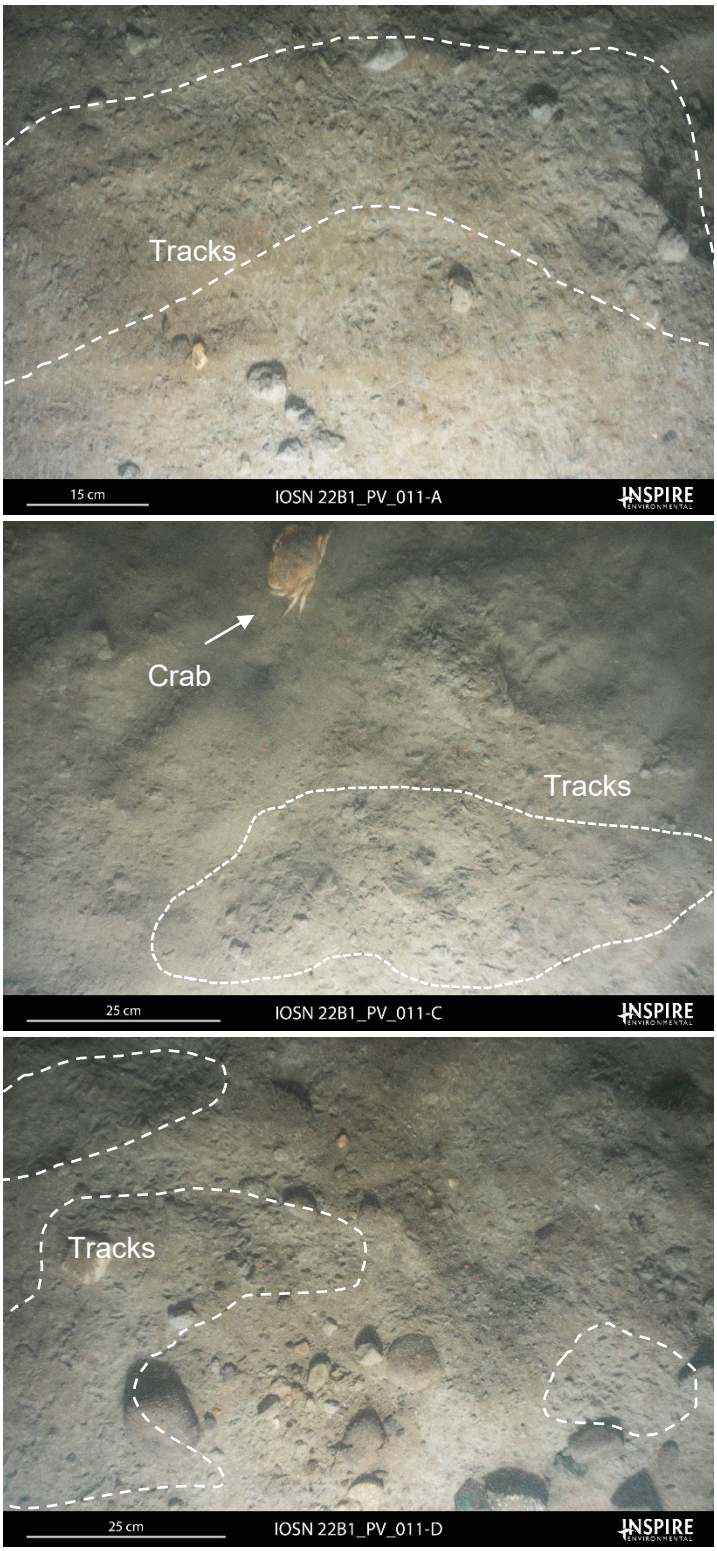

(C)

Figure 3-22 continued. Plan view images of surficial dredged material and epifauna at Mound B; (A) clasts of white clay and small rocks at Station 005; (B) large rocks and white clay with a lobster at Station 006; and (C) white compact clay across the sediment surface with extensive epifaunal tracks and a crab at Station 011

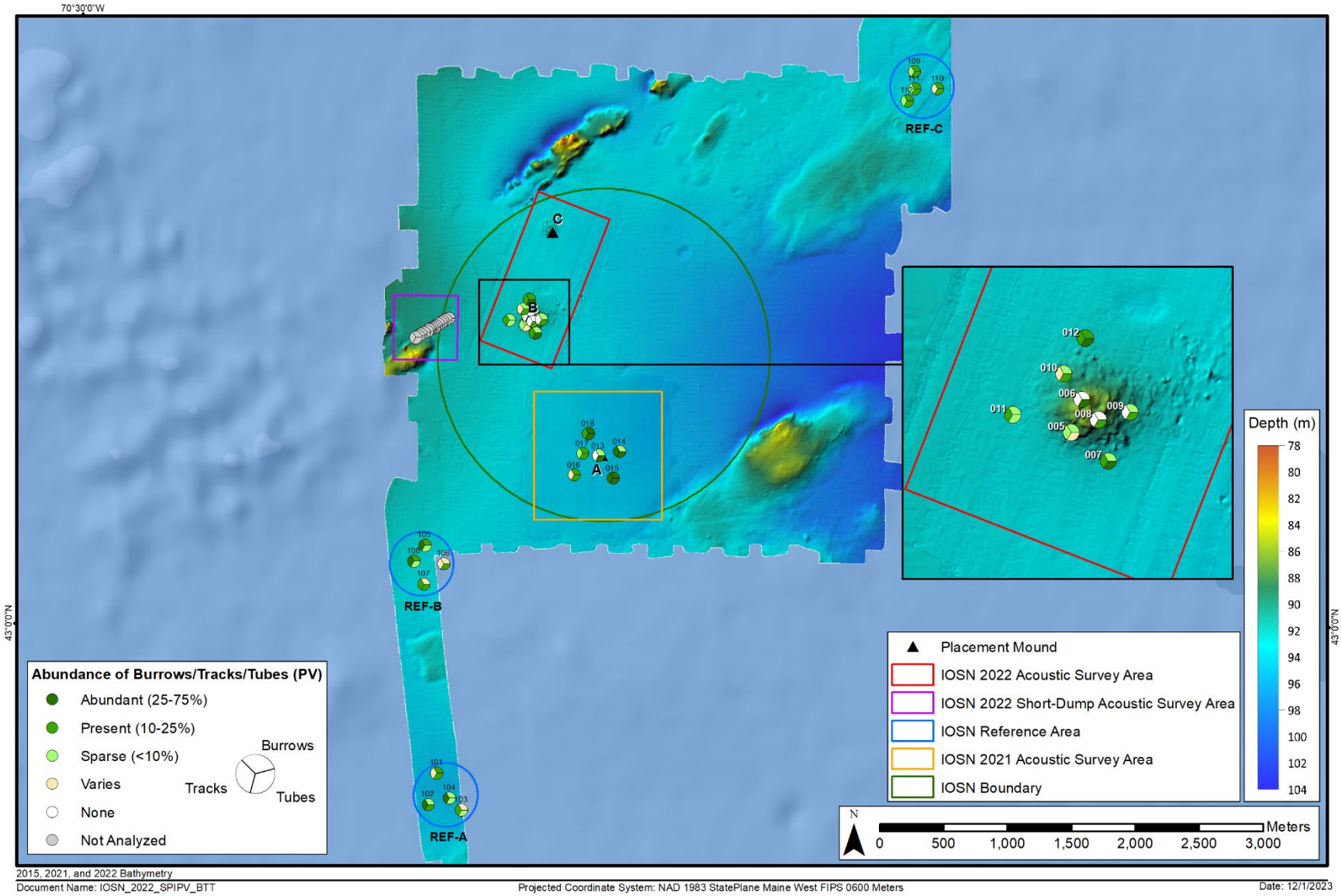

Figure 3-23. Percent cover of surficial tracks, tubes, and burrows observed in the plan view imagery at the active portion of IOSN (Mound B), Mound A, and reference areas

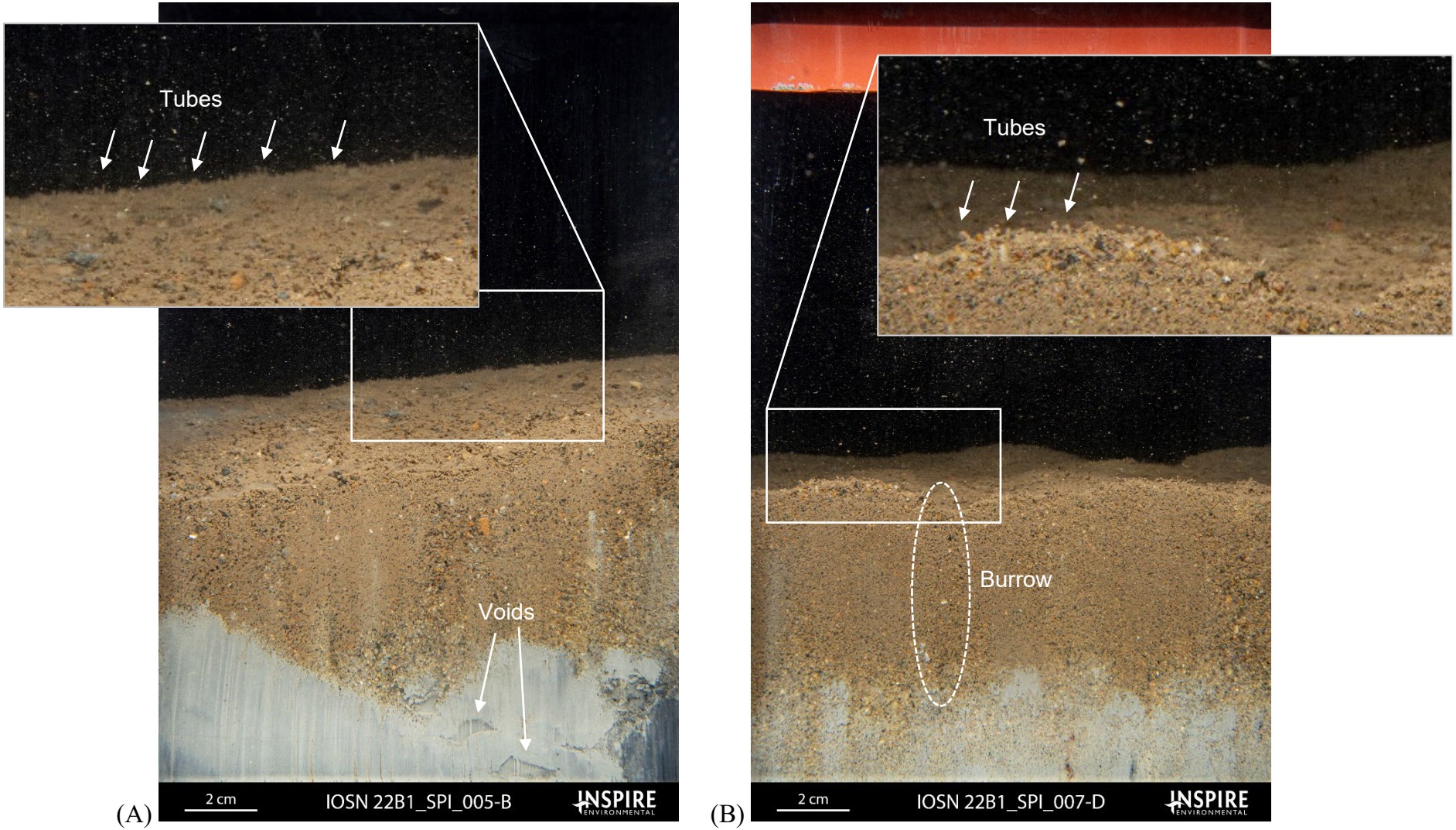

Figure 3-24. Profile images depicting common Successional Stages at Mound B, the active portion of the IOSN disposal area; (A) Stage 2 on 3 depicted by small tubes at the sediment–water interface and feeding voids within the buried white clay at Station 005; and (B) Stage 2 at Station 007 depicted by small tubes at the sediment–water interface and a burrow opening at the sediment–water interface

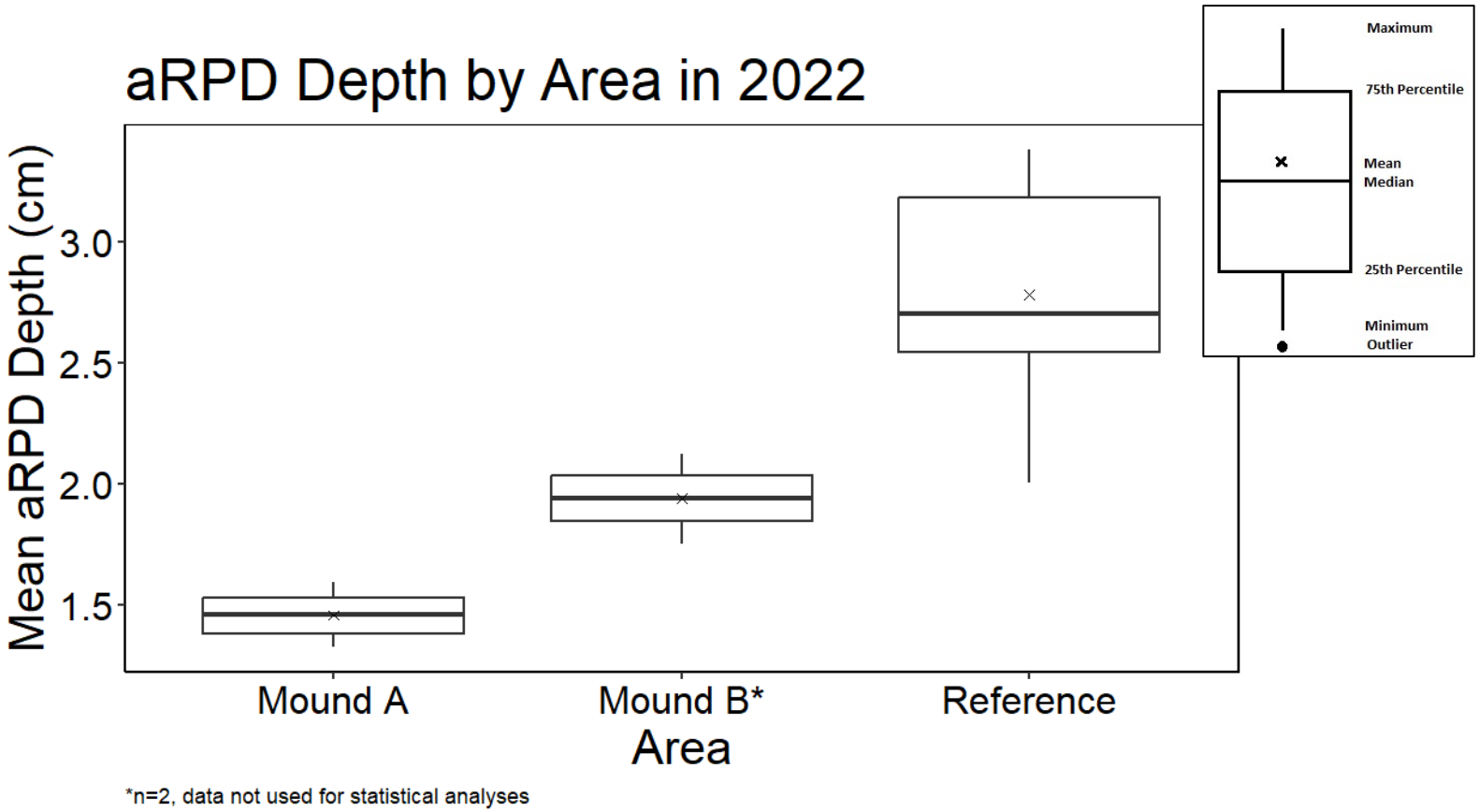

Figure 3-25. Distribution of aRPD depth measurements by sampling area at Mound A, Mound B, and the reference areas

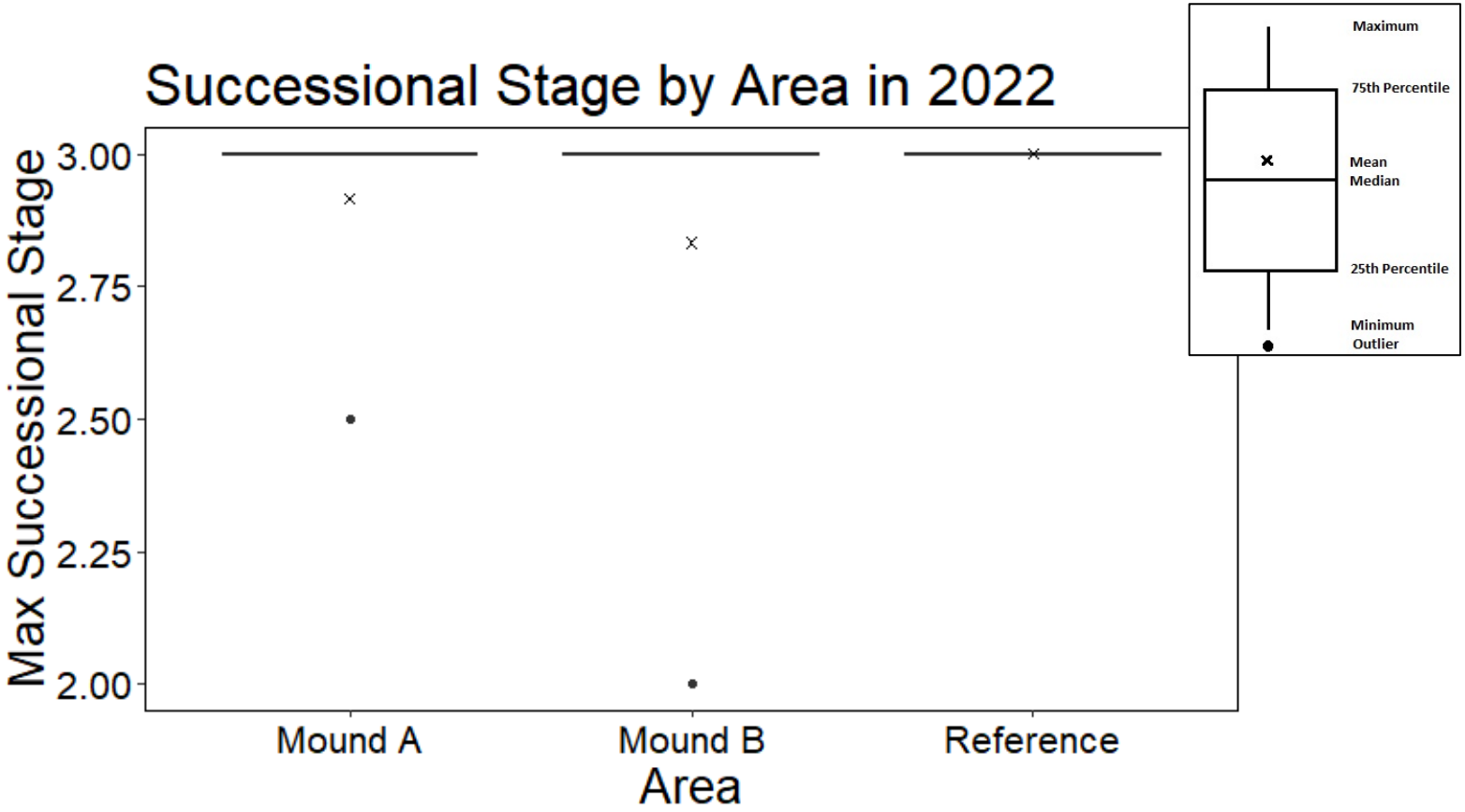

Figure 3-26. Distribution of maximum successional stage by sampling area at Mound A, Mound B, and the reference areas

(A)

(B)

Figure 3-27. Profile images of dredged material at the Mound A area; (A) the entire imaged sediment column at Station 017 depicting dredged material comprised of very fine sand over silt/clay; and (B) dredged material overlaying native silt/clay at Station 018

(A)

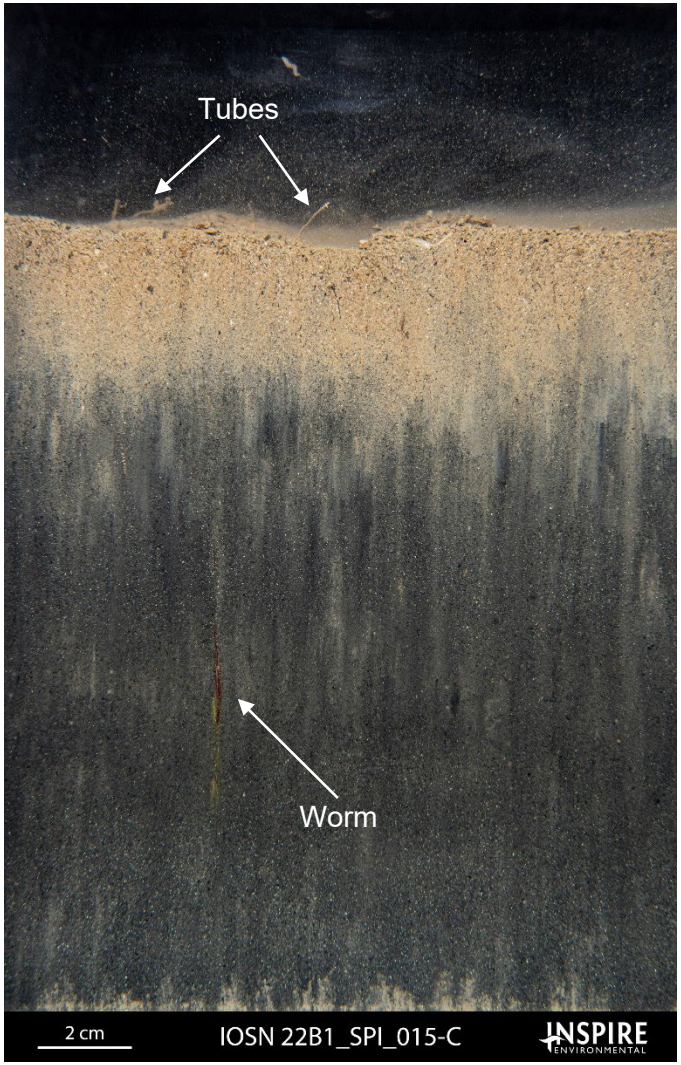

(B)

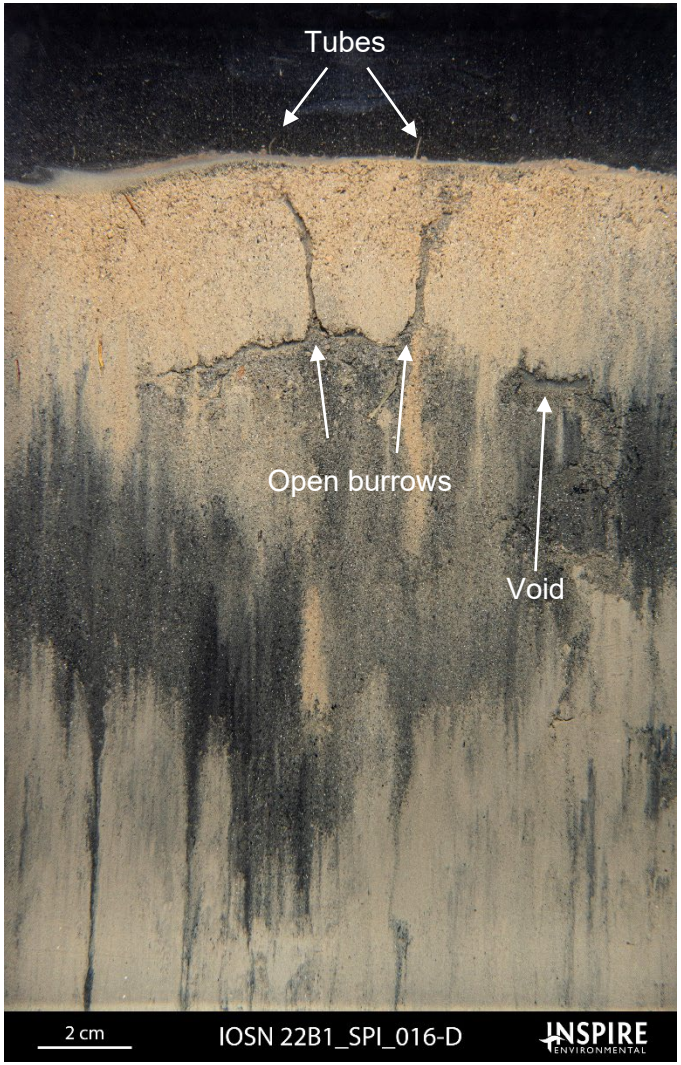

Figure 3-28. Profile images depicting common Successional Stages at Mound A; (A) Stage 2 on 3 at Station 015 depicted by small tubes at the sediment–water interface and a large worm in a burrow; and (B) Stage 2 on 3 depicted by small tubes and open burrows at the sediment–water interface and feeding voids within the sediment column at Station 016.

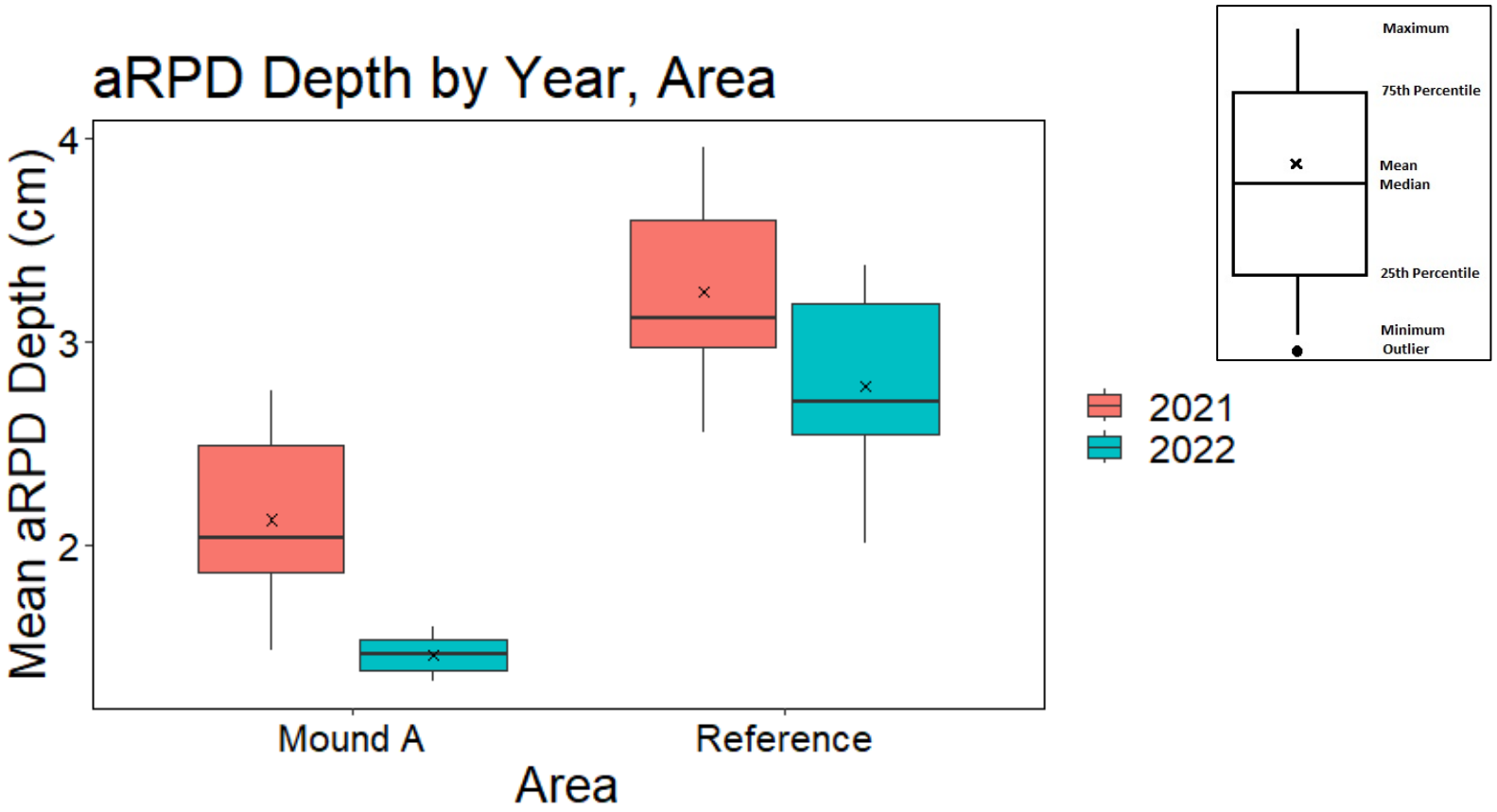

Figure 3-29. Distribution of aRPD depth measurements between 2021 and 2022 at Mound A and at the reference areas

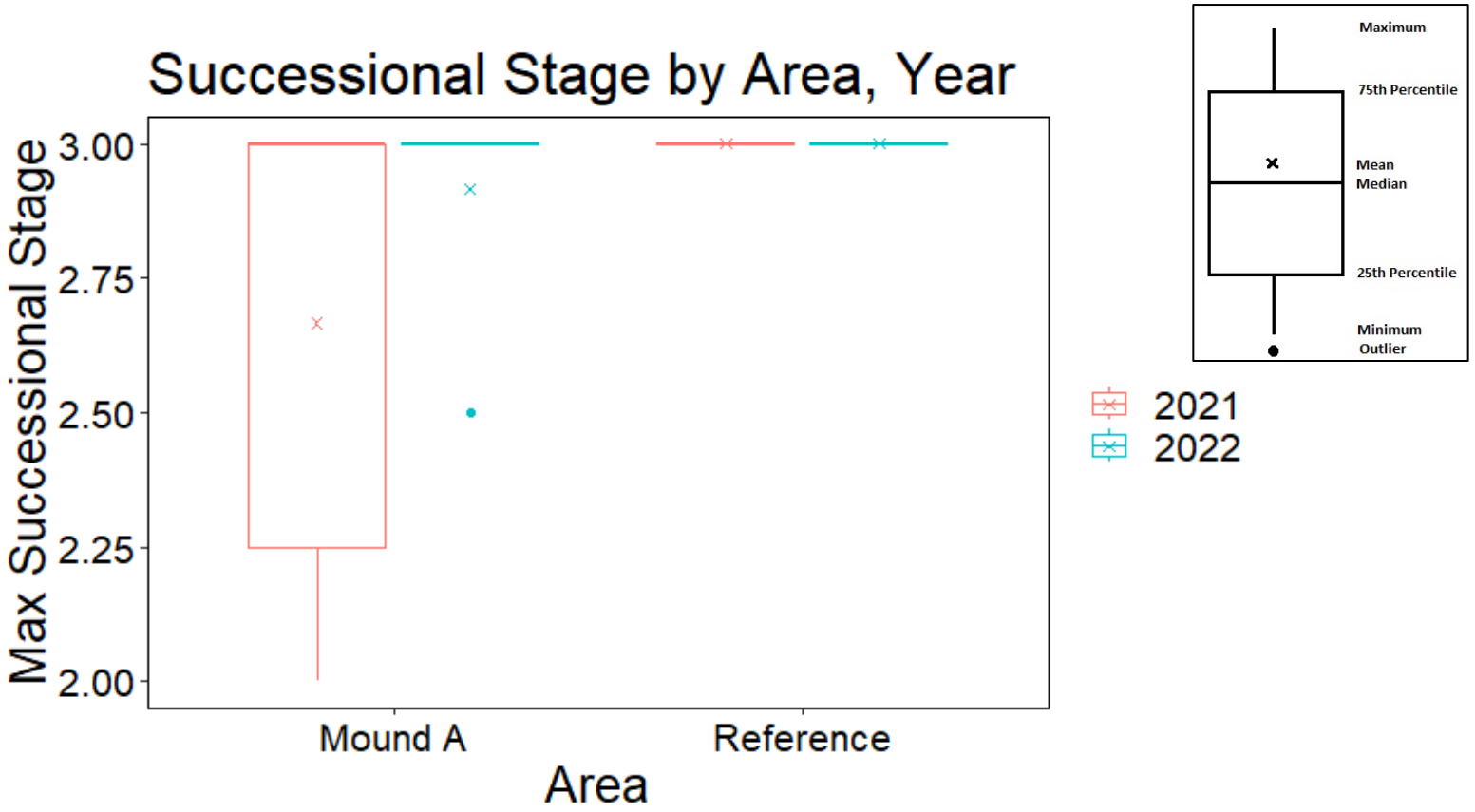

Figure 3-30. Distribution of maximum successional stage between 2021 and 2022 at Mound A and at the reference areas

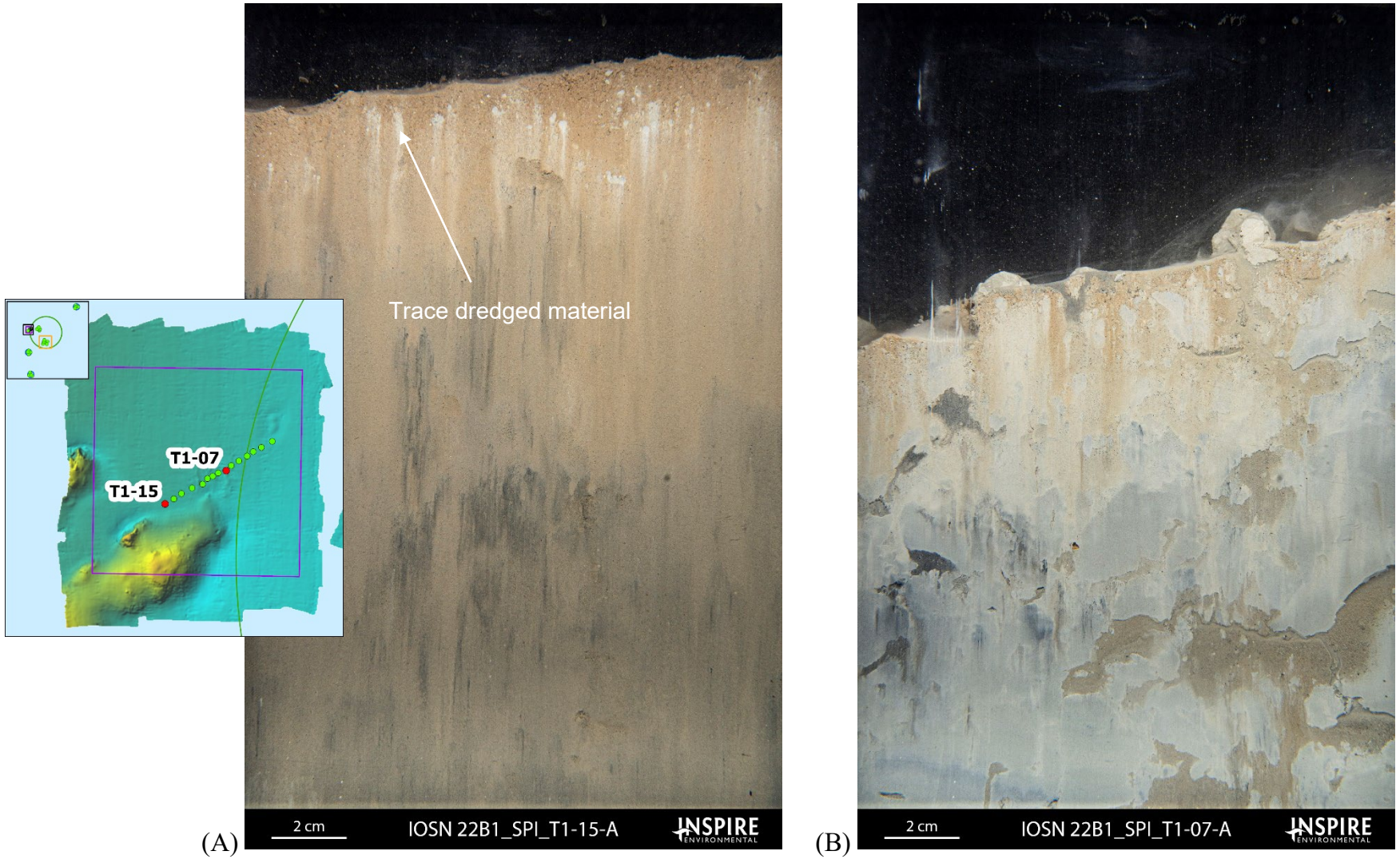

Figure 3-31. Profile images of dredged material along the short-dump transect; (A) trace white clay near the sediment–water interface at T1-15; and (B) the entire imaged sediment column comprised of white clay at T1-07

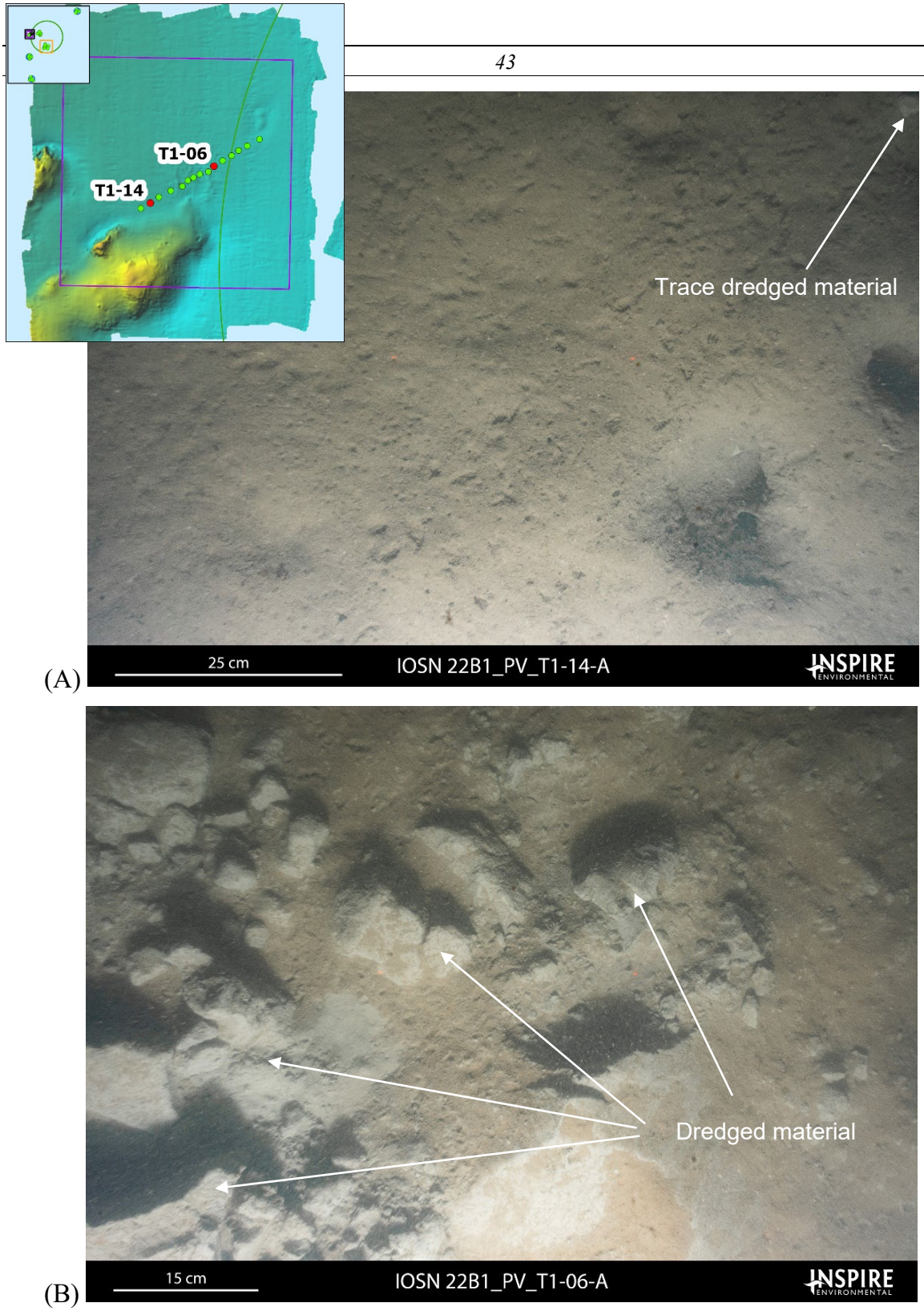

Figure 3-32. Plan view images of surficial dredged material along the short-dump transect; (A) trace white clay at T1-14; and (B) clasts of white clay at T1-06

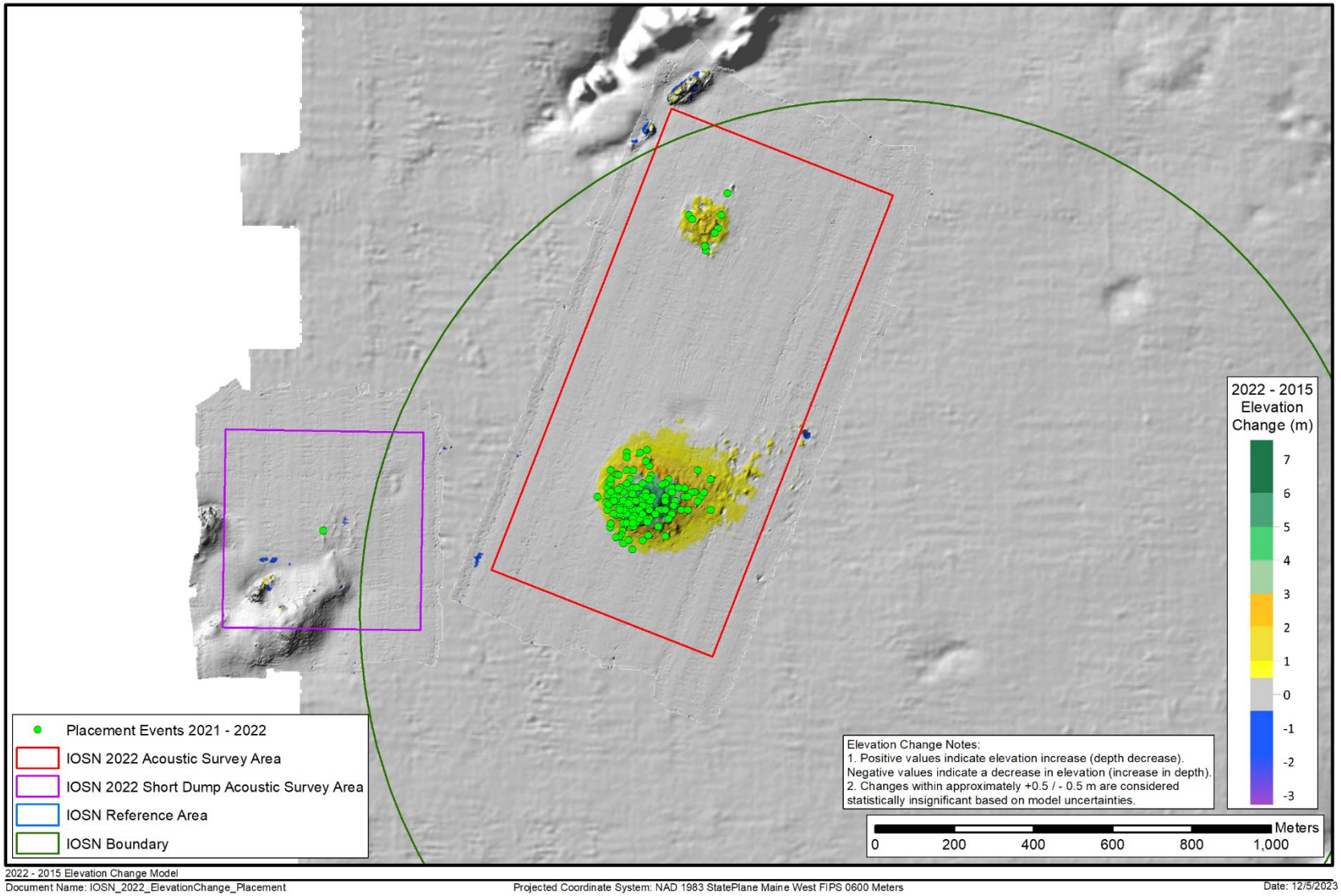

Figure 4-1. Recent dredged material disposal locations for the period November 2021 to April 2022 over elevation change September 2015 (baseline) vs. August 2022 at IOSN acoustic survey areas (Mounds B and C and short-dump area) - August 2022

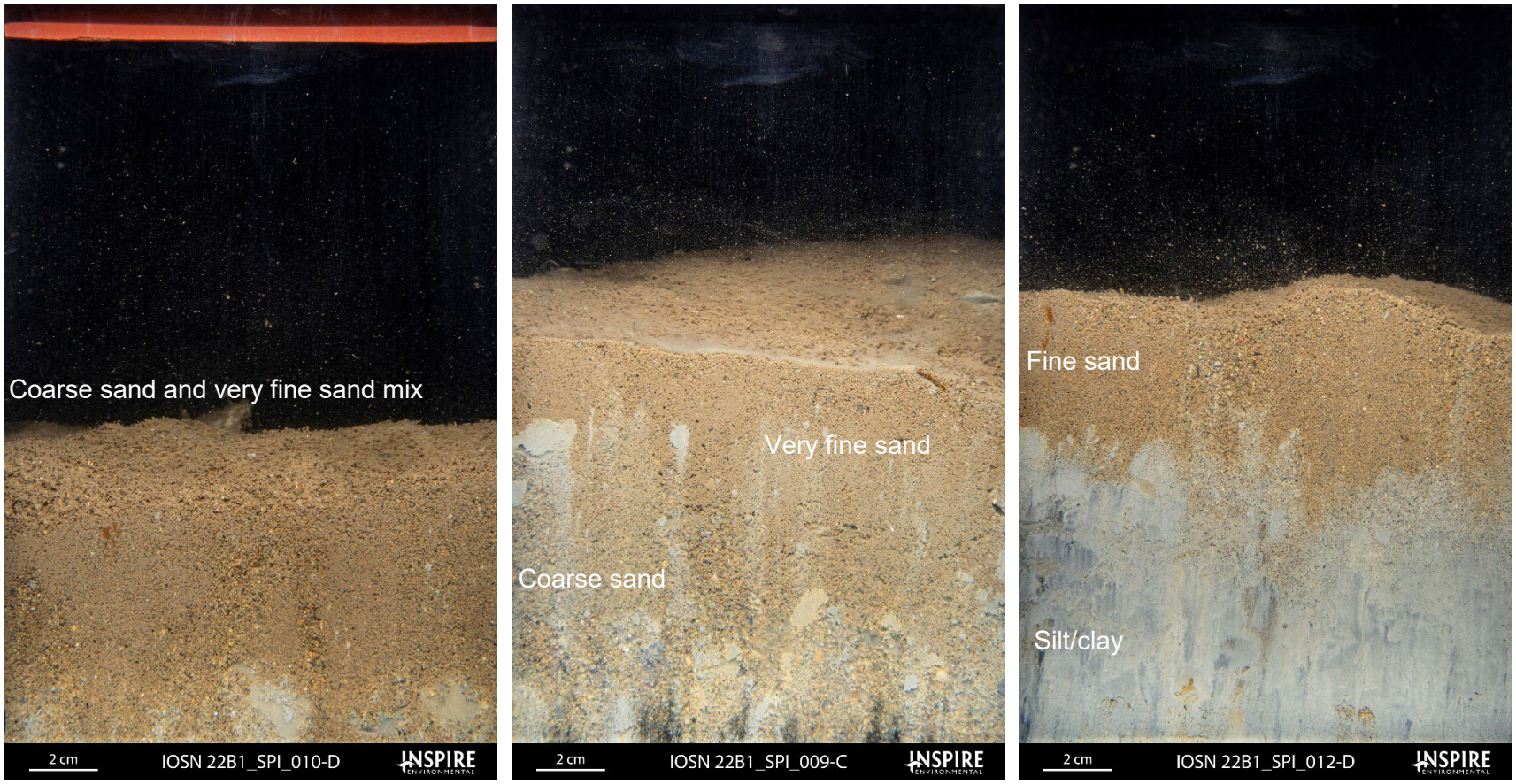

Figure 4-2. Representative sediment profile images collected at Mound B highlighting the mixture of grain sizes observed

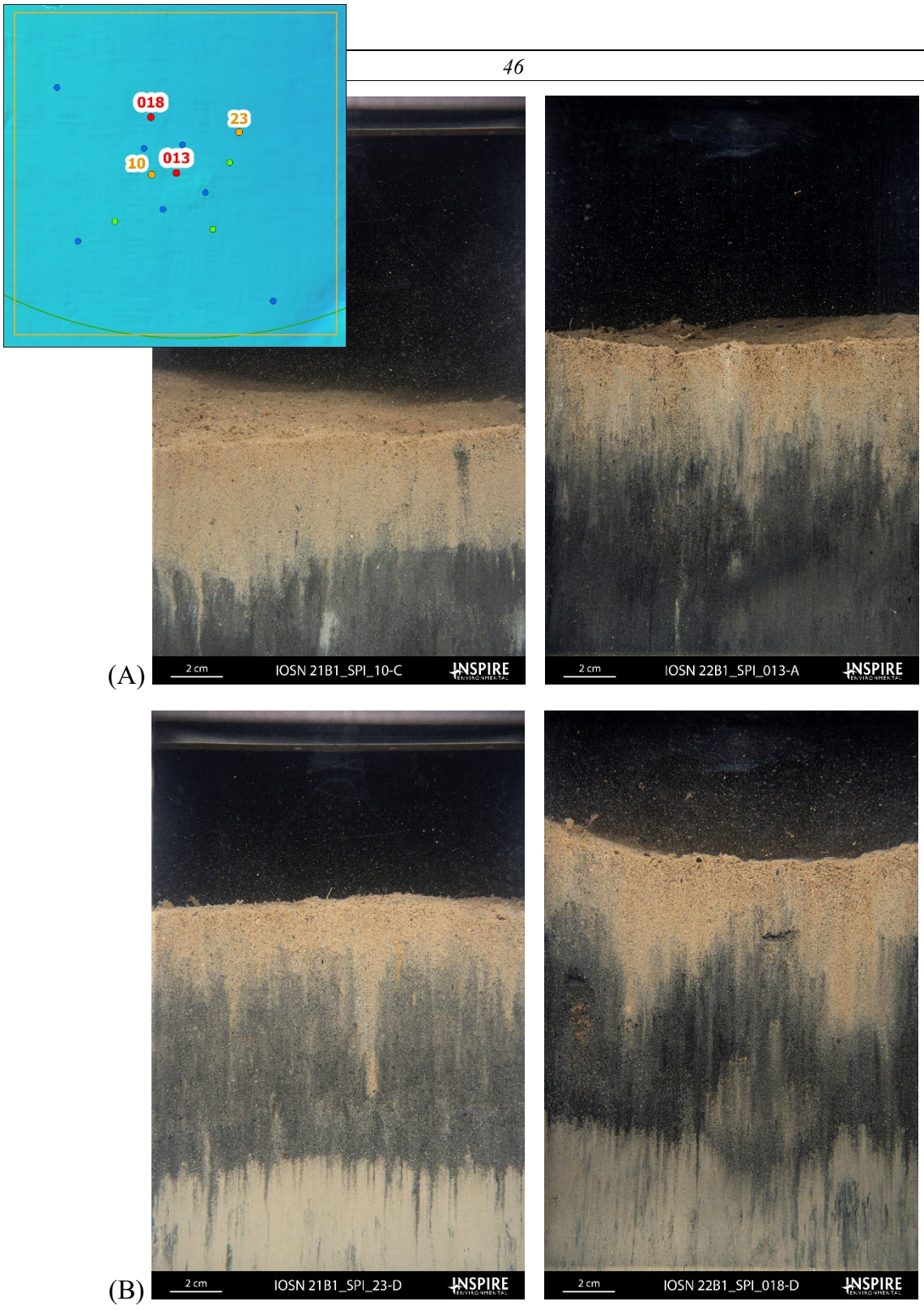

Figure 4-3. Profile images depicting the dredged material signature at Mound A between 2021 and 2022; (A) the entire imaged sediment column at Station 010 in 2021 and Station 013 in 2022 taken within the Mound A target area depicting dredged material comprised of silt/clay; and (B) dredged material overlaying ambient silt/clay at Station 23 in 2021 and Station 018 in 2022 collected on the apron of Mound A

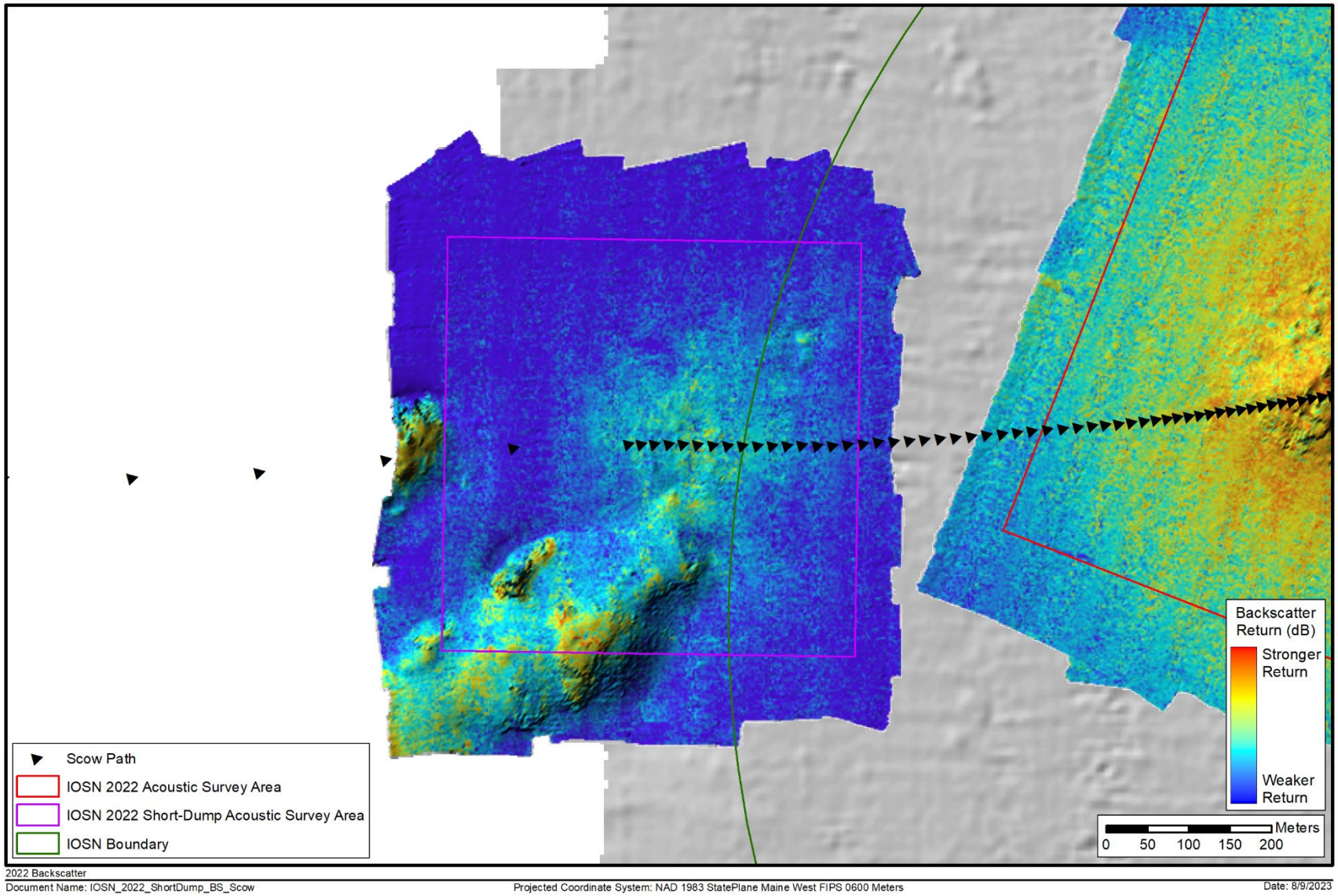

Figure 4-4. Filtered backscatter over acoustic relief model with scow path at short-dump area

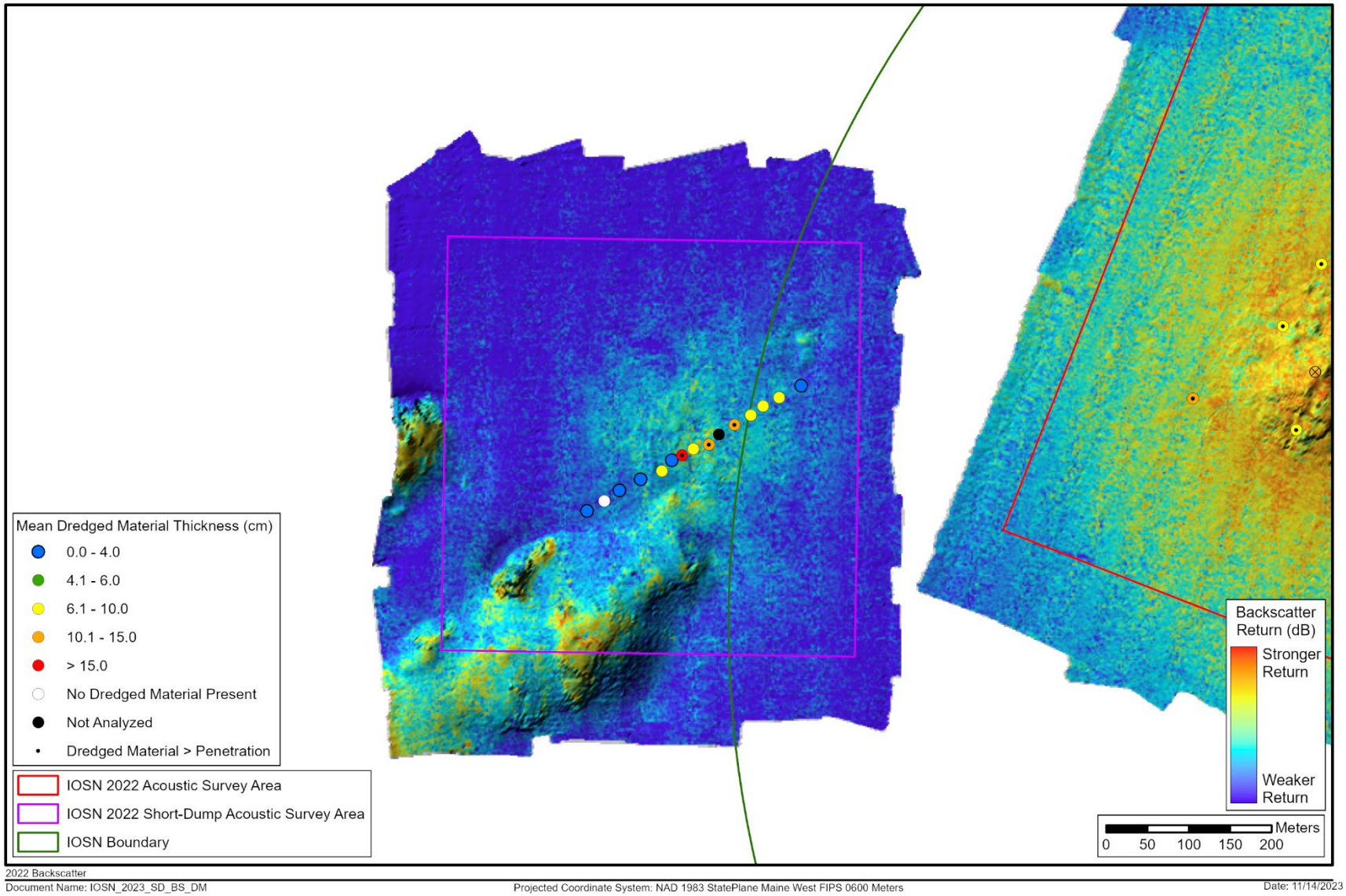

Figure 4-5. SPI/PV stations at the short-dump investigation area, displaying the mean dredged material thickness over 2022 backscatter

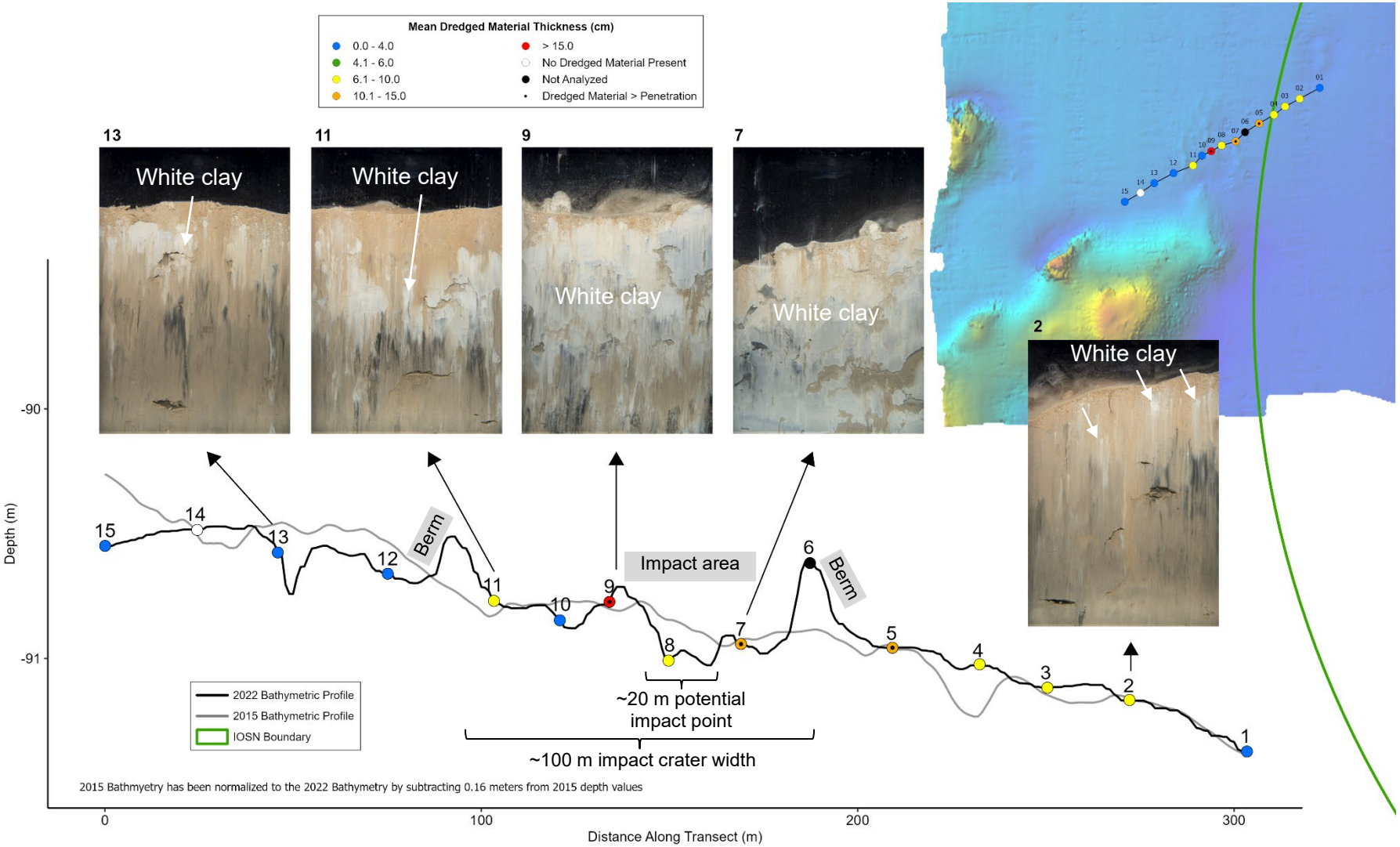

Figure 4-6. Bathymetric profiles (2015 and 2022) with selected SPI imagery and mean dredged material thickness data derived from SPI

MONITORING SURVEY AT THE
ISLES OF SHOALS NORTH DISPOSAL SITE
AUGUST/SEPTEMBER 2022

APPENDICES

CONTRIBUTION #217

December 2023

Contract No. W912WJ-19-D-0010
DAMOS PWS #04 - Task 3c

Funded and Managed by:
New England District
U.S. Army Corps of Engineers
696 Virginia Road
Concord, MA 01742-2751

Prepared by:
INSPIRE ENVIRONMENTAL
INSPIRE Environmental
513 Broadway
Newport, RI 02840

LIST OF APPENDICES

APPENDIX A - TABLE OF COMMON CONVERSIONS

APPENDIX A

TABLE OF COMMON CONVERSIONS

Metric Unit Conversion to English Unit		**English Unit Conversion to Metric Unit**	
1 meter	3.2808 ft	1 foot	0.3048 m
1 m		1 ft	
1 square meter	10.7639 ft^2	1 square foot	0.0929 m^2
1 m^2		1 ft^2	
1 kilometer	0.6214 mi	1 mile	1.6093 km
1 km		1 mi	
1 cubic meter	1.3080 yd^3	1 cubic yard	0.7646 m^3
1 m^3		1 yd^3	
1 centimeter	0.3937 in	1 inch	2.54 cm
1 cm		1 in	

APPENDIX B - IOSN DISPOSAL LOG DATA, NOV 2021 – APRIL 2022

Notes:

Disposal Log Data provided by USACE NAE, August 2022

Project Name	Scow ID	Load Volume (yd^3)	Load Volume (m^3)	Placement Date	Placement Latitude	Placement Longitude	Permit Number
Portsmouth Pisqatagua FNP	GL 601	5271	4030	2021-11-25	43.0219	-70.4562	W912WJ-21-C-0027
Portsmouth Pisqatagua FNP	GL 604	4613	3527	2021-11-26	43.022	-70.4564	W912WJ-21-C-0027
Portsmouth Pisqatagua FNP	GL 601	4834	3696	2021-11-26	43.021682	-70.458052	W912WJ-21-C-0027
Portsmouth Pisqatagua FNP	GL 604	5049	3860	2021-11-28	43.0227	-70.4572	W912WJ-21-C-0027
Portsmouth Pisqatagua FNP	GL 601	5178	3958	2021-11-29	43.0219	-70.4578	W912WJ-21-C-0027
Portsmouth Pisqatagua FNP	GL 604	4782	3656	2021-11-29	43.0227	-70.4576	W912WJ-21-C-0027
Portsmouth Pisqatagua FNP	GL 601	5054	3864	2021-11-30	43.0221	-70.4575	W912WJ-21-C-0027
Portsmouth Pisqatagua FNP	GL 604	4706	3598	2021-11-30	43.0212	-70.4572	W912WJ-21-C-0027
Portsmouth Pisqatagua FNP	GL 601	2658	2032	2021-12-02	43.021	-70.4566	W912WJ-21-C-0027
Portsmouth Pisqatagua FNP	GL 604	3884	2969	2021-12-02	43.0213	-70.4578	W912WJ-21-C-0027
Portsmouth Pisqatagua FNP	GL 601	4876	3728	2021-12-03	43.0215	-70.4571	W912WJ-21-C-0027
Portsmouth Pisqatagua FNP	GL 604	4755	3635	2021-12-04	43.0215	-70.4575	W912WJ-21-C-0027
Portsmouth Pisqatagua FNP	GL 601	3843	2938	2021-12-04	43.0219	-70.4582	W912WJ-21-C-0027
Portsmouth Pisqatagua FNP	GL 604	3298	2521	2021-12-05	43.0215	-70.4576	W912WJ-21-C-0027
Portsmouth Pisqatagua FNP	GL 601	4990	3815	2021-12-05	43.0216	-70.4573	W912WJ-21-C-0027
Portsmouth Pisqatagua FNP	GL 604	4215	3222	2021-12-08	43.0217	-70.4585	W912WJ-21-C-0027
Portsmouth Pisqatagua FNP	GL 604	4564	3489	2021-12-09	43.0217	-70.4558	W912WJ-21-C-0027
Portsmouth Pisqatagua FNP	GL 601	5222	3993	2021-12-15	43.0214	-70.4577	W912WJ-21-C-0027
Portsmouth Pisqatagua FNP	GL 601	4291	3281	2021-12-15	43.0214	-70.4576	W912WJ-21-C-0027
Portsmouth Pisqatagua FNP	GL 601	3645	2787	2021-12-16	43.0223	-70.4581	W912WJ-21-C-0027
Portsmouth Pisqatagua FNP	GL 601	5236	4003	2021-12-17	43.0215	-70.4571	W912WJ-21-C-0027
Portsmouth Pisqatagua FNP	GL 601	3537	2704	2021-12-18	43.021	-70.4581	W912WJ-21-C-0027
Portsmouth Pisqatagua FNP	GL 601	3186	2436	2021-12-19	43.0221	-70.4563	W912WJ-21-C-0027
Portsmouth Pisqatagua FNP	GL 601	3852	2945	2021-12-19	43.021513	-70.457912	W912WJ-21-C-0027
Portsmouth Pisqatagua FNP	GL 601	3542	2708	2021-12-20	43.0217	-70.4553	W912WJ-21-C-0027
Portsmouth Pisqatagua FNP	GL 601	5272	4030	2021-12-21	43.0217	-70.4564	W912WJ-21-C-0027
Portsmouth Pisqatagua FNP	GL 601	4920	3761	2021-12-22	43.0215	-70.457	W912WJ-21-C-0027
Portsmouth Pisqatagua FNP	GL 601	3608	2758	2021-12-22	43.0215	-70.4569	W912WJ-21-C-0027
Portsmouth Pisqatagua FNP	GL 601	4325	3306	2021-12-26	43.021323	-70.457572	W912WJ-21-C-0027
Portsmouth Pisqatagua FNP	GL 601	3622	2770	2021-12-27	43.021283	-70.457915	W912WJ-21-C-0027
Portsmouth Pisqatagua FNP	GL 604	3522	2693	2021-12-27	43.0212	-70.4573	W912WJ-21-C-0027
Portsmouth Pisqatagua FNP	GL 604	3370	2577	2021-12-28	43.021807	-70.4555	W912WJ-21-C-0027
Portsmouth Pisqatagua FNP	GL 604	4625	3536	2021-12-29	43.021807	-70.4555	W912WJ-21-C-0027
Portsmouth Pisqatagua FNP	GL 601	5147	3935	2021-12-30	43.0214	-70.4566	W912WJ-21-C-0027
Portsmouth Pisqatagua FNP	GL 604	5184	3964	2022-01-02	43.0211	-70.4573	W912WJ-21-C-0027
Portsmouth Pisqatagua FNP	GL 601	4056	3101	2022-01-03	43.0214	-70.4575	W912WJ-21-C-0027
Portsmouth Pisqatagua FNP	GL 604	1637	1252	2022-01-03	43.020925	-70.457723	W912WJ-21-C-0027
Portsmouth Pisqatagua FNP	GL 604	3694	2824	2022-01-04	43.0219	-70.4575	W912WJ-21-C-0027
Portsmouth Pisqatagua FNP	GL 604	4384	3352	2022-01-06	43.02181	-70.458028	W912WJ-21-C-0027
Portsmouth Pisqatagua FNP	GL 601	5141	3930	2022-01-07	43.021623	-70.457527	W912WJ-21-C-0027

Project Name	Scow ID	Load Volume (yd^3)	Load Volume (m^3)	Placement Date	Placement Latitude	Placement Longitude	Permit Number
Portsmouth Pisqatagua FNP	GL 604	5160	3945	2022-01-09	43.0217	-70.4574	W912WJ-21-C-0027
Portsmouth Pisqatagua FNP	GL 601	5148	3936	2022-01-10	43.0217	-70.4568	W912WJ-21-C-0027
Portsmouth Pisqatagua FNP	GL 604	3888	2973	2022-01-11	43.0219	-70.4572	W912WJ-21-C-0027
Portsmouth Pisqatagua FNP	GL 601	3048	2330	2022-01-13	43.0216	-70.4564	W912WJ-21-C-0027
Portsmouth Pisqatagua FNP	GL 604	3948	3018	2022-01-13	43.0219	-70.4574	W912WJ-21-C-0027
Portsmouth Pisqatagua FNP	GL 601	4418	3377	2022-01-14	43.0212	-70.4569	W912WJ-21-C-0027
Portsmouth Pisqatagua FNP	GL 604	5247	4012	2022-01-16	43.0215	-70.4569	W912WJ-21-C-0027
Portsmouth Pisqatagua FNP	GL 601	5207	3981	2022-01-19	43.0218	-70.457	W912WJ-21-C-0027
Portsmouth Pisqatagua FNP	GL 604	4971	3800	2022-01-20	43.0218	-70.4552	W912WJ-21-C-0027
Portsmouth Pisqatagua FNP	GL 604	4912	3756	2022-01-21	43.0218	-70.4556	W912WJ-21-C-0027
Portsmouth Pisqatagua FNP	GL 601	4288	3279	2022-01-21	43.027297	-70.455172	W912WJ-21-C-0027
Portsmouth Pisqatagua FNP	GL 604	4727	3614	2022-01-22	43.0217	-70.4571	W912WJ-21-C-0027
Portsmouth Pisqatagua FNP	GL 601	5260	4021	2022-01-22	43.0214	-70.455	W912WJ-21-C-0027
Portsmouth Pisqatagua FNP	GL 604	4990	3815	2022-01-23	43.0216	-70.4554	W912WJ-21-C-0027
Portsmouth Pisqatagua FNP	GL 604	3793	2900	2022-01-24	43.0214	-70.4566	W912WJ-21-C-0027
Portsmouth Pisqatagua FNP	GL 601	3790	2898	2022-01-25	43.021758	-70.457418	W912WJ-21-C-0027
Portsmouth Pisqatagua FNP	GL 604	5021	3839	2022-01-25	43.0216	-70.4561	W912WJ-21-C-0027
Portsmouth Pisqatagua FNP	GL 604	4938	3776	2022-01-26	43.0213	-70.4562	W912WJ-21-C-0027
Portsmouth Pisqatagua FNP	GL 604	5158	3943	2022-01-28	43.0217	-70.4557	W912WJ-21-C-0027
Portsmouth Pisqatagua FNP	GL 604	3604	2756	2022-02-01	43.021008	-70.457432	W912WJ-21-C-0027
Portsmouth Pisqatagua FNP	GL 604	3955	3024	2022-02-01	43.0223	-70.4554	W912WJ-21-C-0027
Portsmouth Pisqatagua FNP	GL 501	3721	2845	2022-02-02	43.0218	-70.4562	W912WJ-21-C-0027
Portsmouth Pisqatagua FNP	GL 604	4314	3299	2022-02-02	43.0219	-70.4558	W912WJ-21-C-0027
Portsmouth Pisqatagua FNP	GL 501	4830	3693	2022-02-03	43.022	-70.4571	W912WJ-21-C-0027
Portsmouth Pisqatagua FNP	GL 604	5303	4054	2022-02-03	43.02064	-70.457692	W912WJ-21-C-0027
Portsmouth Pisqatagua FNP	GL 501	4639	3547	2022-02-06	43.0214	-70.4572	W912WJ-21-C-0027
Portsmouth Pisqatagua FNP	GL 604	3323	2540	2022-02-06	43.0212	-70.457	W912WJ-21-C-0027
Portsmouth Pisqatagua FNP	GL 501	3886	2971	2022-02-07	43.0281	-70.4547	W912WJ-21-C-0027
Portsmouth Pisqatagua FNP	GL 604	2910	2225	2022-02-08	43.0286	-70.4545	W912WJ-21-C-0027
Portsmouth Pisqatagua FNP	GL 501	3574	2733	2022-02-09	43.0214	-70.4565	W912WJ-21-C-0027
Portsmouth Pisqatagua FNP	GL 604	2765	2114	2022-02-09	43.0278	-70.4548	W912WJ-21-C-0027
Portsmouth Pisqatagua FNP	GL 501	4517	3453	2022-02-10	43.0218	-70.457	W912WJ-21-C-0027
Portsmouth Pisqatagua FNP	GL 604	4946	3782	2022-02-10	43.0214	-70.4569	W912WJ-21-C-0027
Portsmouth Pisqatagua FNP	GL 501	2426	1855	2022-02-11	43.0216	-70.4571	W912WJ-21-C-0027
Portsmouth Pisqatagua FNP	GL 604	4140	3165	2022-02-11	43.0221	-70.4569	W912WJ-21-C-0027
Portsmouth Pisqatagua FNP	GL 604	5084	3887	2022-02-12	43.0213	-70.4575	W912WJ-21-C-0027
Portsmouth Pisqatagua FNP	GL 604	5222	3992	2022-02-13	43.0213	-70.4571	W912WJ-21-C-0027
Portsmouth Pisqatagua FNP	GL 502	4145	3169	2022-02-14	43.0274	-70.4552	W912WJ-21-C-0027
Portsmouth Pisqatagua FNP	GL 501	4115	3146	2022-02-15	43.0215	-70.457	W912WJ-21-C-0027
Portsmouth Pisqatagua FNP	GL 604	2298	1757	2022-02-15	42.7973	-70.8	W912WJ-21-C-0027

Project Name	Scow ID	Load Volume (yd^3)	Load Volume (m^3)	Placement Date	Placement Latitude	Placement Longitude	Permit Number
Portsmouth Pisqatagua FNP	GL 502	2628	2009	2022-02-15	43.0274	-70.4552	W912WJ-21-C-0027
Portsmouth Pisqatagua FNP	GL 604	5262	4023	2022-02-16	43.0213	-70.4567	W912WJ-21-C-0027
Portsmouth Pisqatagua FNP	GL 501	5054	3864	2022-02-16	43.02127	-70.457712	W912WJ-21-C-0027
Portsmouth Pisqatagua FNP	GL 604	4709	3600	2022-02-19	43.0216	-70.4569	W912WJ-21-C-0027
Portsmouth Pisqatagua FNP	GL 501	5272	4031	2022-02-19	43.0277	-70.4549	W912WJ-21-C-0027
Portsmouth Pisqatagua FNP	GL 604	5141	3931	2022-02-20	43.021572	-70.457577	W912WJ-21-C-0027
Portsmouth Pisqatagua FNP	GL 502	5050	3861	2022-02-20	43.0281	-70.4557	W912WJ-21-C-0027
Portsmouth Pisqatagua FNP	GL 604	4912	3755	2022-02-21	43.02161	-70.45687	W912WJ-21-C-0027
Portsmouth Pisqatagua FNP	GL 501	5154	3941	2022-02-21	43.028	-70.4556	W912WJ-21-C-0027
Portsmouth Pisqatagua FNP	GL 501	5125	3918	2022-02-28	43.0216	-70.4573	W912WJ-21-C-0027
Portsmouth Pisqatagua FNP	GL 502	4971	3800	2022-02-28	43.0213	-70.4576	W912WJ-21-C-0027
Portsmouth Pisqatagua FNP	GL 501	4193	3206	2022-03-01	43.0215	-70.4571	W912WJ-21-C-0027
Portsmouth Pisqatagua FNP	GL 502	5236	4003	2022-03-01	43.021613	-70.457203	W912WJ-21-C-0027
Portsmouth Pisqatagua FNP	GL 501	3752	2868	2022-03-02	43.0224	-70.4569	W912WJ-21-C-0027
Portsmouth Pisqatagua FNP	Thomas Desmond	2707	2070	2022-03-02	43.021532	-70.457757	W912WJ-21-C-0027
Portsmouth Pisqatagua FNP	GL 502	5202	3977	2022-03-02	43.0219	-70.456	W912WJ-21-C-0027
Portsmouth Pisqatagua FNP	GL 604	4161	3181	2022-03-03	43.0216	-70.4573	W912WJ-21-C-0027
Portsmouth Pisqatagua FNP	GL 501	4128	3156	2022-03-03	43.0215	-70.4577	W912WJ-21-C-0027
Portsmouth Pisqatagua FNP	Thomas Desmond	2738	2093	2022-03-03	43.021495	-70.456137	W912WJ-21-C-0027
Portsmouth Pisqatagua FNP	GL 502	4022	3075	2022-03-03	43.0214	-70.4573	W912WJ-21-C-0027
Portsmouth Pisqatagua FNP	GL 604	3393	2594	2022-03-04	43.0207	-70.4571	W912WJ-21-C-0027
Portsmouth Pisqatagua FNP	GL 501	3268	2499	2022-03-04	43.0223	-70.4574	W912WJ-21-C-0027
Portsmouth Pisqatagua FNP	GL 502	4580	3501	2022-03-04	43.0216	-70.4575	W912WJ-21-C-0027
Portsmouth Pisqatagua FNP	GL 604	4054	3100	2022-03-06	43.0216	-70.4577	W912WJ-21-C-0027
Portsmouth Pisqatagua FNP	GL 501	3478	2659	2022-03-06	43.0225	-70.457	W912WJ-21-C-0027
Portsmouth Pisqatagua FNP	GL 502	4081	3120	2022-03-07	43.0218	-70.4577	W912WJ-21-C-0027
Portsmouth Pisqatagua FNP	Thomas Desmond	2522	1928	2022-03-07	43.021452	-70.457712	W912WJ-21-C-0027
Portsmouth Pisqatagua FNP	GL 502	5163	3948	2022-03-08	43.021478	-70.457805	W912WJ-21-C-0027
Portsmouth Pisqatagua FNP	Thomas Desmond	2726	2084	2022-03-09	43.022037	-70.458163	W912WJ-21-C-0027
Portsmouth Pisqatagua FNP	GL 501	4200	3211	2022-03-09	43.022177	-70.456838	W912WJ-21-C-0027
Portsmouth Pisqatagua FNP	GL 604	4483	3427	2022-03-09	43.0219	-70.4573	W912WJ-21-C-0027
Portsmouth Pisqatagua FNP	Thomas Desmond	1071	819	2022-03-09	43.0214	-70.4582	W912WJ-21-C-0027
Portsmouth Pisqatagua FNP	GL 604	4607	3522	2022-03-10	43.021088	-70.458088	W912WJ-21-C-0027
Portsmouth Pisqatagua FNP	GL 502	5054	3864	2022-03-10	43.0222	-70.4579	W912WJ-21-C-0027
Portsmouth Pisqatagua FNP	GL 501	3828	2927	2022-03-11	43.0213	-70.4578	W912WJ-21-C-0027
Portsmouth Pisqatagua FNP	GL 502	4727	3614	2022-03-11	43.022187	-70.45785	W912WJ-21-C-0027
Portsmouth Pisqatagua FNP	GL 501	4909	3753	2022-03-12	43.0214	-70.4573	W912WJ-21-C-0027
Portsmouth Pisqatagua FNP	GL 604	4570	3494	2022-03-14	43.022	-70.4564	W912WJ-21-C-0027
Portsmouth Pisqatagua FNP	GL 502	3607	2758	2022-03-14	43.0214	-70.4574	W912WJ-21-C-0027
Portsmouth Pisqatagua FNP	GL 501	4804	3673	2022-03-15	43.0214	-70.4573	W912WJ-21-C-0027

Project Name	Scow ID	Load Volume (yd^3)	Load Volume (m^3)	Placement Date	Placement Latitude	Placement Longitude	Permit Number
Portsmouth Pisqatagua FNP	GL 63	3872	2961	2022-03-15	43.02083	-70.457768	W912WJ-21-C-0027
Portsmouth Pisqatagua FNP	GL 604	4553	3481	2022-03-15	43.0221	-70.455	W912WJ-21-C-0027
Portsmouth Pisqatagua FNP	GL 501	3888	2972	2022-03-16	43.0226	-70.4576	W912WJ-21-C-0027
Portsmouth Pisqatagua FNP	GL 63	4165	3184	2022-03-16	43.021773	-70.458052	W912WJ-21-C-0027
Portsmouth Pisqatagua FNP	GL 604	4475	3421	2022-03-16	43.0214	-70.4577	W912WJ-21-C-0027
Portsmouth Pisqatagua FNP	GL 63	4597	3514	2022-03-17	43.02168	-70.457967	W912WJ-21-C-0027
Portsmouth Pisqatagua FNP	GL 502	3444	2633	2022-03-17	43.0214	-70.4559	W912WJ-21-C-0027
Portsmouth Pisqatagua FNP	GL 604	4784	3658	2022-03-17	43.0215	-70.4571	W912WJ-21-C-0027
Portsmouth Pisqatagua FNP	GL 63	5141	3931	2022-03-18	43.0218	-70.4579	W912WJ-21-C-0027
Portsmouth Pisqatagua FNP	GL 604	4743	3626	2022-03-18	43.0215	-70.4578	W912WJ-21-C-0027
Portsmouth Pisqatagua FNP	GL 501	5229	3998	2022-03-18	43.022	-70.4576	W912WJ-21-C-0027
Portsmouth Pisqatagua FNP	GL 63	4704	3597	2022-03-19	43.0215	-70.4579	W912WJ-21-C-0027
Portsmouth Pisqatagua FNP	GL 502	4290	3280	2022-03-19	43.0212	-70.4572	W912WJ-21-C-0027
Portsmouth Pisqatagua FNP	GL 604	4977	3805	2022-03-19	43.0214	-70.4564	W912WJ-21-C-0027
Portsmouth Pisqatagua FNP	GL 63	3110	2377	2022-03-20	43.0217	-70.4579	W912WJ-21-C-0027
Portsmouth Pisqatagua FNP	GL 604	5141	3931	2022-03-20	43.0209	-70.467	W912WJ-21-C-0027
Portsmouth Pisqatagua FNP	GL 501	5077	3881	2022-03-21	43.0211	-70.4577	W912WJ-21-C-0027
Portsmouth Pisqatagua FNP	GL 63	4119	3149	2022-03-21	43.0215	-70.4578	W912WJ-21-C-0027
Portsmouth Pisqatagua FNP	GL 502	4127	3155	2022-03-21	43.0214	-70.4572	W912WJ-21-C-0027
Portsmouth Pisqatagua FNP	GL 604	1736	1328	2022-03-21	43.0219	-70.4578	W912WJ-21-C-0027
Portsmouth Pisqatagua FNP	GL 501	5089	3891	2022-03-22	43.0208	-70.4564	W912WJ-21-C-0027
Portsmouth Pisqatagua FNP	GL 63	5385	4117	2022-03-22	43.021572	-70.458243	W912WJ-21-C-0027
Portsmouth Pisqatagua FNP	GL 502	5288	4043	2022-03-23	43.021983	-70.45651	W912WJ-21-C-0027
Portsmouth Pisqatagua FNP	GL 63	4198	3209	2022-03-23	43.0215	-70.4575	W912WJ-21-C-0027
Portsmouth Pisqatagua FNP	GL 63	4401	3365	2022-03-24	43.0221	-70.4569	W912WJ-21-C-0027
Portsmouth Pisqatagua FNP	GL 501	4466	3415	2022-03-25	43.02102	-70.456612	W912WJ-21-C-0027
Portsmouth Pisqatagua FNP	GL 604	4426	3384	2022-03-26	43.021022	-70.457378	W912WJ-21-C-0027
Portsmouth Pisqatagua FNP	GL 604	638	488	2022-03-26	43.02050095	-70.457422	W912WJ-21-C-0027
Portsmouth Pisqatagua FNP	GL 502	4373	3343	2022-03-26	43.020787	-70.457822	W912WJ-21-C-0027
Portsmouth Pisqatagua FNP	GL 63	4394	3359	2022-03-26	43.021582	-70.457997	W912WJ-21-C-0027
Portsmouth Pisqatagua FNP	GL 501	3881	2967	2022-03-26	43.021255	-70.457358	W912WJ-21-C-0027
Portsmouth Pisqatagua FNP	GL 604	4717	3607	2022-03-27	43.020717	-70.45754	W912WJ-21-C-0027
Portsmouth Pisqatagua FNP	GL 502	4078	3118	2022-03-27	43.021207	-70.457407	W912WJ-21-C-0027
Portsmouth Pisqatagua FNP	GL 502	3014	2304	2022-03-28	43.021117	-70.456958	W912WJ-21-C-0027
Portsmouth Pisqatagua FNP	GL 604	4714	3604	2022-03-28	43.022	-70.4581	W912WJ-21-C-0027
Portsmouth Pisqatagua FNP	GL 501	3602	2754	2022-03-29	43.0212	-70.4563	W912WJ-21-C-0027
Portsmouth Pisqatagua FNP	GL 502	4489	3432	2022-03-29	43.021437	-70.457823	W912WJ-21-C-0027
Portsmouth Pisqatagua FNP	GL 604	3857	2949	2022-03-29	43.0211	-70.4576	W912WJ-21-C-0027
Portsmouth Pisqatagua FNP	Thomas Desmond	1964	1501	2022-03-30	43.020775	-70.45793	W912WJ-21-C-0027
Portsmouth Pisqatagua FNP	GL 502	2379	1819	2022-03-30	43.0211	-70.4574	W912WJ-21-C-0027

Project Name	Scow ID	Load Volume (yd^3)	Load Volume (m^3)	Placement Date	Placement Latitude	Placement Longitude	Permit Number
Portsmouth Pisqatagua FNP	GL 501	3587	2742	2022-03-31	43.0213	-70.4571	W912WJ-21-C-0027
Portsmouth Pisqatagua FNP	Thomas Desmond	2547	1948	2022-03-31	43.022757	-70.456978	W912WJ-21-C-0027
Portsmouth Pisqatagua FNP	GL 502	0	0	2022-03-31	43.021858	-70.457867	W912WJ-21-C-0027
Portsmouth Pisqatagua FNP	GL 604	3755	2871	2022-03-31	43.0217	-70.458	W912WJ-21-C-0027
Portsmouth Pisqatagua FNP	Thomas Desmond	2619	2002	2022-04-01	43.021743	-70.458182	W912WJ-21-C-0027
Portsmouth Pisqatagua FNP	GL 501	5156	3942	2022-04-01	43.021525	-70.458155	W912WJ-21-C-0027
Portsmouth Pisqatagua FNP	GL 604	1581	1209	2022-04-02	43.0216	-70.458	W912WJ-21-C-0027
Portsmouth Pisqatagua FNP	GL 502	5284	4040	2022-04-02	43.0221	-70.4581	W912WJ-21-C-0027
Portsmouth Pisqatagua FNP	Thomas Desmond	677	518	2022-04-02	43.020825	-70.45692	W912WJ-21-C-0027
Portsmouth Pisqatagua FNP	GL 501	4653	3557	2022-04-03	43.0216	-70.458	W912WJ-21-C-0027
Portsmouth Pisqatagua FNP	GL 604	4115	3146	2022-04-03	43.0223	-70.4576	W912WJ-21-C-0027
Portsmouth Pisqatagua FNP	GL 502	4103	3137	2022-04-03	43.0217	-70.457	W912WJ-21-C-0027
Portsmouth Pisqatagua FNP	GL 604	3846	2941	2022-04-04	43.0214	-70.4557	W912WJ-21-C-0027
Portsmouth Pisqatagua FNP	GL 604	4958	3791	2022-04-05	43.0214	-70.4578	W912WJ-21-C-0027
Portsmouth Pisqatagua FNP	GL 604	4851	3709	2022-04-06	43.0216	-70.4573	W912WJ-21-C-0027
Portsmouth Pisqatagua FNP	Thomas Desmond	2429	1857	2022-04-07	43.021615	-70.457703	W912WJ-21-C-0027
Portsmouth Pisqatagua FNP	GL 501	419	320	2022-04-07	43.02131	-70.458007	W912WJ-21-C-0027
Portsmouth Pisqatagua FNP	GL 502	2894	2213	2022-04-09	43.0218	-70.4581	W912WJ-21-C-0027
Portsmouth Pisqatagua FNP	GL 501	839	642	2022-04-15	43.021548	-70.457543	W912WJ-21-C-0027

APPENDIX C - ACTUAL SPI/PV REPLICATE LOCATIONS

Area	Sample Type	Station ID	Replicate	Date	Time	X_MaineWestSP_m	Y_MaineWestSP_m	Latitude_NAD83_N	Longitude_NAD83_W
Mound B	SPI/PV	009	A	9/13/2022	9:23:03	870279.25	4773233.31	43.021518	-70.455909
Mound B	SPI/PV	009	B	9/13/2022	9:25:50	870277.87	4773232.57	43.021512	-70.455927
Mound B	SPI/PV	009	C	9/13/2022	9:28:20	870284.56	4773237.37	43.021552	-70.455841
Mound B	SPI/PV	009	D	9/13/2022	9:30:55	870284.82	4773237.81	43.021556	-70.455838
Mound B	SPI/PV	008	A	9/13/2022	9:54:52	870212.45	4773213.21	43.021370	-70.456740
Mound B	SPI/PV	008	B	9/13/2022	9:57:26	870215.26	4773209.17	43.021332	-70.456708
Mound B	SPI/PV	008	C	9/13/2022	9:59:45	870224.37	4773205.57	43.021296	-70.456599
Mound B	SPI/PV	008	D	9/13/2022	10:02:02	870217.22	4773208.09	43.021322	-70.456685
Mound B	SPI/PV	005	A	9/13/2022	10:07:29	870156.27	4773182.98	43.021126	-70.457447
Mound B	SPI/PV	005	B	9/13/2022	10:10:08	870141.54	4773180.91	43.021115	-70.457629
Mound B	SPI/PV	005	C	9/13/2022	10:12:46	870156.09	4773188.25	43.021173	-70.457446
Mound B	SPI/PV	005	D	9/13/2022	10:15:38	870157.35	4773180.63	43.021104	-70.457435
Mound B	SPI/PV	007	A	9/13/2022	10:22:45	870238.84	4773126.41	43.020578	-70.456474
Mound B	SPI/PV	007	B	9/13/2022	10:25:44	870238.1	4773116.14	43.020486	-70.456490
Mound B	SPI/PV	007	C	9/13/2022	10:28:24	870235.38	4773112.9	43.020458	-70.456526
Mound B	SPI/PV	007	D	9/13/2022	10:31:11	870242.42	4773111.59	43.020443	-70.456441
Mound B	SPI/PV	011	A	9/13/2022	10:41:01	870029.23	4773213.66	43.021463	-70.458981
Mound B	SPI/PV	011	B	9/13/2022	10:43:54	870029.47	4773213.3	43.021460	-70.458978
Mound B	SPI/PV	011	C	9/13/2022	10:46:54	870031.02	4773211.26	43.021441	-70.458961
Mound B	SPI/PV	011	D	9/13/2022	10:49:46	870032.39	4773205.08	43.021385	-70.458948
Mound B	SPI/PV	006	A	9/13/2022	10:59:02	870175.02	4773254.34	43.021758	-70.457170
Mound B	SPI/PV	006	B	9/13/2022	11:01:17	870180.92	4773262.82	43.021831	-70.457093
Mound B	SPI/PV	006	C	9/13/2022	11:03:36	870172.49	4773242	43.021648	-70.457210
Mound B	SPI/PV	006	D	9/13/2022	11:05:56	870168.3	4773268.66	43.021889	-70.457243
Mound B	SPI/PV	010	A	9/13/2022	11:13:13	870132.9	4773307.22	43.022253	-70.457651
Mound B	SPI/PV	010	B	9/13/2022	11:15:44	870127.59	4773293.54	43.022133	-70.457725
Mound B	SPI/PV	010	C	9/13/2022	11:18:14	870120.07	4773300.12	43.022195	-70.457812
Mound B	SPI/PV	010	D	9/13/2022	11:20:53	870135.34	4773310.46	43.022281	-70.457619
Mound B	SPI/PV	012	A	9/13/2022	11:27:51	870175.08	4773385.02	43.022931	-70.457083
Mound B	SPI/PV	012	B	9/13/2022	11:31:02	870187.18	4773397.36	43.023035	-70.456927
Mound B	SPI/PV	012	C	9/13/2022	11:33:58	870172.18	4773401.21	43.023077	-70.457108
Mound B	SPI/PV	012	D	9/13/2022	11:36:48	870164.74	4773394.93	43.023025	-70.457203
Short Dump	SPI/PV	T1-01	A	9/13/2022	12:09:26	869554.61	4773201.79	43.021587	-70.464796
Short Dump	SPI/PV	T1-02	A	9/13/2022	12:12:29	869528.9	4773185.86	43.021457	-70.465121
Short Dump	SPI/PV	T1-03	A	9/13/2022	12:16:40	869510.15	4773174.47	43.021364	-70.465358
Short Dump	SPI/PV	T1-04	A	9/13/2022	12:20:30	869496	4773162.62	43.021264	-70.465539

Area	Sample Type	Station ID	Replicate	Date	Time	X_MaineWestSP_m	Y_MaineWestSP_m	Latitude_NAD83_N	Longitude_NAD83_W
Short Dump	SPI/PV	T1-05	A	9/13/2022	12:24:31	869476.97	4773150.05	43.021161	-70.465780
Short Dump	SPI/PV	T1-06	A	9/13/2022	12:27:35	869458.87	4773137.23	43.021054	-70.466010
Short Dump	SPI/PV	T1-07	A	9/13/2022	12:30:37	869447.22	4773124.36	43.020945	-70.466161
Short Dump	SPI/PV	T1-08	A	9/13/2022	12:35:24	869428.79	4773117.94	43.020896	-70.466390
Short Dump	SPI/PV	T1-09	A	9/13/2022	12:37:59	869415.54	4773109.57	43.020827	-70.466558
Short Dump	SPI/PV	T1-10	A	9/13/2022	12:40:35	869403.49	4773102.79	43.020772	-70.466710
Short Dump	SPI/PV	T1-11	A	9/13/2022	12:45:07	869392.5	4773089.1	43.020655	-70.466853
Short Dump	SPI/PV	T1-12	A	9/13/2022	12:48:37	869367.26	4773077.67	43.020564	-70.467170
Short Dump	SPI/PV	T1-13	A	9/13/2022	12:51:40	869342.44	4773062.74	43.020442	-70.467483
Short Dump	SPI/PV	T1-14	A	9/13/2022	12:54:00	869324.85	4773048.86	43.020326	-70.467708
Short Dump	SPI/PV	T1-15	A	9/13/2022	12:57:13	869304.65	4773035.72	43.020218	-70.467964
Mound A	SPI/PV	016	A	9/13/2022	13:53:30	870605.44	4772034.55	43.010598	-70.452714
Mound A	SPI/PV	016	B	9/13/2022	13:56:11	870596.08	4772031.94	43.010579	-70.452830
Mound A	SPI/PV	016	C	9/13/2022	13:58:21	870588.34	4772029.69	43.010563	-70.452927
Mound A	SPI/PV	016	D	9/13/2022	14:00:46	870595.55	4772025.99	43.010526	-70.452841
Mound A	SPI/PV	015	A	9/13/2022	14:12:42	870911.07	4772026.94	43.010381	-70.448981
Mound A	SPI/PV	015	B	9/13/2022	14:14:52	870906.25	4772023.67	43.010354	-70.449042
Mound A	SPI/PV	015	C	9/13/2022	14:17:09	870904.94	4772016.33	43.010289	-70.449063
Mound A	SPI/PV	015	D	9/13/2022	14:19:12	870911.85	4772014.49	43.010269	-70.448979
Mound A	SPI/PV	014	A	9/13/2022	14:27:23	870951.05	4772237.61	43.012253	-70.448352
Mound A	SPI/PV	014	B	9/13/2022	14:29:28	870950.34	4772236.39	43.012242	-70.448361
Mound A	SPI/PV	014	C	9/13/2022	14:34:07	870925.91	4772284.44	43.012685	-70.448628
Mound A	SPI/PV	014	D	9/13/2022	14:36:18	870914.8	4772276.82	43.012622	-70.448769
Mound A	SPI/PV	013	A	9/13/2022	14:42:37	870787.95	4772195.77	43.011957	-70.450375
Mound A	SPI/PV	013	B	9/13/2022	14:45:15	870782.35	4772191.35	43.011920	-70.450446
Mound A	SPI/PV	013	C	9/13/2022	14:47:24	870785.13	4772185.67	43.011867	-70.450416
Mound A	SPI/PV	013	D	9/13/2022	14:49:29	870784.44	4772185.84	43.011869	-70.450424
Mound A	SPI/PV	017	A	9/13/2022	14:57:44	870662.08	4772205.86	43.012109	-70.451908
Mound A	SPI/PV	017	B	9/13/2022	14:59:53	870657.7	4772206.03	43.012112	-70.451961
Mound A	SPI/PV	017	C	9/13/2022	15:02:08	870647.74	4772205.91	43.012116	-70.452083
Mound A	SPI/PV	017	D	9/13/2022	15:04:07	870644.56	4772202.32	43.012085	-70.452124
Mound A	SPI/PV	018	A	9/13/2022	15:10:45	870698.21	4772363.72	43.013508	-70.451361
Mound A	SPI/PV	018	B	9/13/2022	15:13:05	870694.55	4772373.35	43.013596	-70.451399
Mound A	SPI/PV	018	C	9/13/2022	15:15:15	870685.7	4772371.49	43.013584	-70.451509
Mound A	SPI/PV	018	D	9/13/2022	15:17:27	870679.1	4772369.02	43.013565	-70.451591
Reference	SPI/PV	REF-B-106	A	9/13/2022	15:43:17	869625.69	4771280.01	43.004301	-70.465198

Area	Sample Type	Station ID	Replicate	Date	Time	X_MaineWestSP_m	Y_MaineWestSP_m	Latitude_NAD83_N	Longitude_NAD83_W
Reference	SPI/PV	REF-B-106	B	9/13/2022	15:45:22	869626.36	4771282.61	43.004324	-70.465188
Reference	SPI/PV	REF-B-106	C	9/13/2022	15:47:22	869634.61	4771278.75	43.004286	-70.465090
Reference	SPI/PV	REF-B-106	D	9/13/2022	15:49:26	869625.35	4771274.79	43.004255	-70.465206
Reference	SPI/PV	REF-B-105	A	9/13/2022	15:55:25	869470.36	4771416.83	43.005605	-70.467007
Reference	SPI/PV	REF-B-105	B	9/13/2022	15:57:25	869464.02	4771413.37	43.005577	-70.467087
Reference	SPI/PV	REF-B-105	C	9/13/2022	15:59:27	869459.87	4771414.59	43.005590	-70.467137
Reference	SPI/PV	REF-B-105	D	9/13/2022	16:01:33	869453.13	4771406.85	43.005524	-70.467225
Reference	SPI/PV	REF-B-108	A	9/13/2022	16:06:09	869391.56	4771287.21	43.004480	-70.468057
Reference	SPI/PV	REF-B-108	B	9/13/2022	16:08:31	869399.95	4771288.37	43.004486	-70.467954
Reference	SPI/PV	REF-B-108	C	9/13/2022	16:10:53	869388.17	4771280.35	43.004420	-70.468103
Reference	SPI/PV	REF-B-108	D	9/13/2022	16:12:55	869378.93	4771267.97	43.004313	-70.468224
Reference	SPI/PV	REF-B-107	A	9/13/2022	16:19:58	869486.98	4771115.21	43.002889	-70.467004
Reference	SPI/PV	REF-B-107	B	9/13/2022	16:22:09	869479.24	4771111.62	43.002861	-70.467101
Reference	SPI/PV	REF-B-107	C	9/13/2022	16:24:20	869470.03	4771099.65	43.002758	-70.467221
Reference	SPI/PV	REF-B-107	D	9/13/2022	16:27:06	869472.98	4771097.55	43.002738	-70.467187
Reference	SPI/PV	REF-A-101	A	9/13/2022	16:44:41	869664.81	4769641.52	42.989574	-70.465803
Reference	SPI/PV	REF-A-101	B	9/13/2022	16:47:14	869677.18	4769652.94	42.989671	-70.465645
Reference	SPI/PV	REF-A-101	C	9/13/2022	16:49:19	869665.62	4769653.74	42.989683	-70.465785
Reference	SPI/PV	REF-A-101	D	9/13/2022	16:51:39	869656.21	4769645.33	42.989612	-70.465906
Reference	SPI/PV	REF-A-102	A	9/13/2022	16:57:28	869633.71	4769398.59	42.987408	-70.466344
Reference	SPI/PV	REF-A-102	B	9/13/2022	16:59:43	869610.99	4769391.09	42.987352	-70.466627
Reference	SPI/PV	REF-A-102	C	9/13/2022	17:01:57	869612.3	4769391.79	42.987358	-70.466611
Reference	SPI/PV	REF-A-102	D	9/13/2022	17:04:07	869600.64	4769388.35	42.987332	-70.466755
Reference	SPI/PV	REF-A-104	A	9/13/2022	17:10:54	869774.52	4769451.56	42.987815	-70.464587
Reference	SPI/PV	REF-A-104	B	9/13/2022	17:13:04	869767.71	4769448.85	42.987794	-70.464673
Reference	SPI/PV	REF-A-104	C	9/13/2022	17:15:09	869773.92	4769451.72	42.987817	-70.464595
Reference	SPI/PV	REF-A-104	D	9/13/2022	17:17:18	869760.69	4769449.91	42.987807	-70.464758
Reference	SPI/PV	REF-A-103	A	9/13/2022	17:22:30	869874.22	4769363.81	42.986979	-70.463426
Reference	SPI/PV	REF-A-103	B	9/13/2022	17:24:38	869864.9	4769354.52	42.986900	-70.463547
Reference	SPI/PV	REF-A-103	C	9/13/2022	17:26:51	869864.82	4769362.07	42.986968	-70.463542
Reference	SPI/PV	REF-A-103	D	9/13/2022	17:29:01	869860.86	4769360.8	42.986959	-70.463592
Reference	SPI/PV	REF-C-109	A	9/14/2022	12:01:29	873085.4	4775339.16	43.039050	-70.420171
Reference	SPI/PV	REF-C-109	B	9/14/2022	12:04:01	873086.71	4775312.43	43.038809	-70.420173
Reference	SPI/PV	REF-C-109	C	9/14/2022	12:08:29	873098.85	4775375.85	43.039372	-70.419982
Reference	SPI/PV	REF-C-109	D	9/14/2022	12:10:24	873118.96	4775352.79	43.039155	-70.419751
Reference	SPI/PV	REF-C-111	A	9/14/2022	12:17:57	873093.71	4775204.17	43.037834	-70.420159

Area	Sample Type	Station ID	Replicate	Date	Time	X_MaineWestSP_m	Y_MaineWestSP_m	Latitude_NAD83_N	Longitude_NAD83_W
Reference	SPI/PV	REF-C-111	B	9/14/2022	12:20:01	873100.22	4775183.23	43.037643	-70.420094
Reference	SPI/PV	REF-C-111	C	9/14/2022	12:22:06	873090.13	4775162.97	43.037466	-70.420231
Reference	SPI/PV	REF-C-111	D	9/14/2022	12:26:14	873103.4	4775180.55	43.037617	-70.420057
Reference	SPI/PV	REF-C-112	A	9/14/2022	12:31:59	873041.19	4775107.6	43.036993	-70.420867
Reference	SPI/PV	REF-C-112	B	9/14/2022	12:33:59	873046.54	4775082.32	43.036763	-70.420818
Reference	SPI/PV	REF-C-112	C	9/14/2022	12:36:02	873049.7	4775060.09	43.036562	-70.420794
Reference	SPI/PV	REF-C-112	D	9/14/2022	12:37:48	873046.33	4775044.65	43.036425	-70.420846
Reference	SPI/PV	REF-C-110	A	9/14/2022	12:44:52	873275.37	4775215.08	43.037843	-70.417929
Reference	SPI/PV	REF-C-110	B	9/14/2022	12:46:44	873288.31	4775195.02	43.037656	-70.417784
Reference	SPI/PV	REF-C-110	C	9/14/2022	12:48:40	873295.93	4775175.9	43.037481	-70.417704
Reference	SPI/PV	REF-C-110	D	9/14/2022	12:50:29	873295.16	4775163.1	43.037366	-70.417722

APPENDIX D - SEDIMENT PROFILE IMAGE ANALYSIS RESULTS

Notes:

DM=Dredged Material

IND=Indeterminate

N/A=Not Applicable

SWI=Sediment–water interface

Grain Size: "/" indicates layer of one phi size range over another.

Successional Stage: "on" indicates one Stage is found on top of another Stage (i.e., 1 on 3).

Area	Station ID	Replicate	Date	Time	Stop Collar Setting (in)	Weights per Side (#)	Image Width (cm)	Grain Size Major Mode (phi)	Grain Size Minimum (phi)	Grain Size Maximum (phi)	Grain Size Range (phi)	Penetration Mean (cm)	Penetration Minimum (cm)	Penetration Maximum (cm)	Over-penetration?	Boundary Roughness (cm)	Boundary Roughness Type	aRPD Mean (cm)
Mound B	005	A	9/13/2022	10:08:15	14	3	14.63	4 to 3+1 to 0	>4	0	>4 to 0	9.72	9.16	10.20	No	1.05	Physical/ Biological	IND
Mound B	005	B	9/13/2022	10:10:54	14	3	14.63	4 to 3+1 to 0/>4	>4	0	>4 to 0	8.95	7.92	10.16	No	2.24	Physical/ Biological	IND
Mound B	005	D	9/13/2022	10:16:26	14	3	14.63	4 to 3/>4	>4	1	>4 to 1	6.58	5.79	7.48	No	1.69	Physical	IND
Mound B	006	A	9/13/2022	10:59:49	14	3	14.63	IND	IND	IND	IND to IND	0.00	0.00	0.00	No	IND	IND	IND
Mound B	006	B	9/13/2022	11:02:07	14	3	14.63	IND	IND	IND	IND to IND	0.00	0.00	0.00	No	IND	IND	IND
Mound B	006	C	9/13/2022	11:04:24	14	3	14.63	IND	IND	IND	IND to IND	0.00	0.00	0.00	No	IND	IND	IND
Mound B	007	A	9/13/2022	10:23:31	14	3	14.63	3 to 2/>4	>4	1	>4 to 1	5.00	3.97	5.69	No	1.72	Physical	IND
Mound B	007	C	9/13/2022	10:29:11	14	3	14.63	3 to 2/>4	>4	0	>4 to 0	5.30	4.83	5.62	No	0.79	Physical/ Biological	IND
Mound B	007	D	9/13/2022	10:31:58	14	3	14.63	3 to 2/>4	>4	1	>4 to 1	8.16	7.58	8.47	No	0.89	Physical/ Biological	IND
Mound B	008	A	9/13/2022	9:55:39	14	3	14.63	IND	IND	-6	IND to -6	0.00	0.00	0.00	No	IND	IND	IND
Mound B	008	B	9/13/2022	9:58:13	14	3	14.63	IND	IND	-6	IND to -6	0.00	0.00	0.00	No	IND	IND	IND
Mound B	008	D	9/13/2022	10:02:49	14	3	14.63	IND	IND	-6	IND to -6	0.00	0.00	0.00	No	IND	IND	IND
Mound B	009	A	9/13/2022	9:23:50	14	3	14.63	4 to 3/1 to 0	>4	-1	>4 to -1	5.87	5.59	6.26	No	0.67	Physical/ Biological	IND
Mound B	009	B	9/13/2022	9:26:37	14	3	14.63	>4	>4	<-8	>4 to <-8	1.29	0.00	2.88	No	2.88	Physical	IND
Mound B	009	C	9/13/2022	9:29:06	14	3	14.63	4 to 3/1 to 0	>4	0	>4 to 0	11.33	10.19	12.00	No	1.81	Physical/ Biological	2.13
Mound B	010	A	9/13/2022	11:14:01	14	3	14.63	4 to 3/1 to 0	>4	0	>4 to 0	9.99	9.40	10.52	No	1.12	Physical/ Biological	IND
Mound B	010	B	9/13/2022	11:16:33	14	3	14.63	4 to 3+1 to 0	>4	0	>4 to 0	5.67	4.63	6.08	No	1.46	Physical/ Biological	IND
Mound B	010	D	9/13/2022	11:21:40	14	3	14.63	4 to 3+1 to 0	>4	0	>4 to 0	7.38	6.61	8.27	No	1.66	Physical/ Biological	IND
Mound B	011	A	9/13/2022	10:41:50	14	3	14.63	4 to 3/>4	>4	2	>4 to 2	10.92	10.57	11.40	No	0.83	Physical/ Biological	IND
Mound B	011	B	9/13/2022	10:44:42	14	3	14.63	4 to 3/>4	>4	1	>4 to 1	13.01	12.62	13.40	No	0.78	Physical/ Biological	1.76
Mound B	011	D	9/13/2022	10:50:34	14	3	14.63	4 to 3	>4	-5	>4 to -5	8.09	7.45	8.71	No	1.26	Physical/ Biological	IND
Mound B	012	A	9/13/2022	11:28:37	14	3	14.63	3 to 2/>4	>4	1	>4 to 1	7.29	6.93	7.66	No	0.74	Biological	IND
Mound B	012	C	9/13/2022	11:34:47	14	3	14.63	3 to 2/>4	>4	0	>4 to 0	9.67	9.31	10.04	No	0.72	Biological	IND

Area	Station ID	Replicate	Date	Time	Stop Collar Setting (in)	Weights per Side (#)	Image Width (cm)	Grain Size Major Mode (phi)	Grain Size Minimum (phi)	Grain Size Maximum (phi)	Grain Size Range (phi)	Penetration Mean (cm)	Penetration Minimum (cm)	Penetration Maximum (cm)	Over-penetration?	Boundary Roughness (cm)	Boundary Roughness Type	aRPD Mean (cm)
Mound B	012	D	9/13/2022	11:37:37	14	3	14.63	3 to 2/>4	>4	0	>4 to 0	12.89	12.06	13.45	No	1.38	Biological	IND
Mound A	013	A	9/13/2022	14:43:23	14	3	14.63	4 to 3/>4	>4	1	>4 to 1	12.23	11.82	12.60	No	0.78	Biological	1.37
Mound A	013	B	9/13/2022	14:46:03	14	3	14.63	4 to 3/>4	>4	1	>4 to 1	13.58	12.91	14.47	No	1.55	Biological	1.52
Mound A	013	D	9/13/2022	14:50:17	14	3	14.63	4 to 3/>4	>4	1	>4 to 1	12.54	12.33	13.19	No	0.86	Biological	1.72
Mound A	014	A	9/13/2022	14:28:12	14	3	14.63	4 to 3/>4	>4	2	>4 to 2	15.93	15.62	16.28	No	0.66	Biological	1.82
Mound A	014	B	9/13/2022	14:30:17	14	3	14.63	4 to 3/>4	>4	2	>4 to 2	16.91	16.37	17.39	No	1.02	Biological	0.95
Mound A	014	C	9/13/2022	14:34:54	14	3	14.63	4 to 3/>4	>4	2	>4 to 2	16.70	15.77	17.51	No	1.75	Biological	1.21
Mound A	015	A	9/13/2022	14:13:29	14	3	14.63	4 to 3/>4	>4	2	>4 to 2	17.48	17.18	17.76	No	0.58	Biological	1.12
Mound A	015	C	9/13/2022	14:17:51	14	3	14.63	4 to 3/>4	>4	2	>4 to 2	16.95	16.59	17.33	No	0.75	Biological	1.40
Mound A	015	D	9/13/2022	14:19:59	14	3	14.63	4 to 3/>4	>4	2	>4 to 2	16.03	14.49	16.98	No	2.49	Physical/ Biological	1.72
Mound A	016	A	9/13/2022	13:54:16	14	3	14.63	4 to 3/>4	>4	2	>4 to 2	19.80	19.24	20.54	No	1.31	Biological	1.74
Mound A	016	B	9/13/2022	13:56:59	14	3	14.63	4 to 3/>4	>4	1	>4 to 1	17.52	17.00	18.27	No	1.28	Biological	1.67
Mound A	016	D	9/13/2022	14:01:24	14	3	14.63	4 to 3/>4	>4	2	>4 to 2	18.29	17.84	18.55	No	0.71	Biological	1.38
Mound A	017	A	9/13/2022	14:58:33	14	3	14.63	4 to 3/>4	>4	2	>4 to 2	15.45	14.40	16.30	No	1.90	Biological	1.46
Mound A	017	B	9/13/2022	15:00:41	14	3	14.63	4 to 3/>4	>4	2	>4 to 2	16.15	15.68	16.45	No	0.76	Biological	1.04
Mound A	017	C	9/13/2022	15:02:57	14	3	14.63	4 to 3/>4	>4	2	>4 to 2	14.67	13.97	15.51	No	1.54	Physical/ Biological	2.05
Mound A	018	A	9/13/2022	15:11:34	14	3	14.63	4 to 3/>4	>4	2	>4 to 2	17.18	16.78	17.91	No	1.13	Biological	1.11
Mound A	018	C	9/13/2022	15:16:04	14	3	14.63	4 to 3/>4	>4	2	>4 to 2	18.49	18.06	18.75	No	0.69	Biological	1.23
Mound A	018	D	9/13/2022	15:18:14	14	3	14.63	4 to 3/>4	>4	2	>4 to 2	16.36	15.89	17.55	No	1.66	Physical/ Biological	1.78
Reference	REF-A-101	A	9/13/2022	16:45:31	14	3	14.63	>4	>4	3	>4 to 3	18.87	18.46	19.27	No	0.81	Biological	3.29
Reference	REF-A-101	B	9/13/2022	16:47:58	14	3	14.63	>4	>4	0	>4 to 0	18.26	17.73	18.84	No	1.11	Biological	3.22
Reference	REF-A-101	C	9/13/2022	16:50:06	14	3	14.63	>4	>4	3	>4 to 3	18.59	17.99	19.09	No	1.10	Biological	3.04
Reference	REF-A-102	B	9/13/2022	17:00:29	14	3	14.63	>4	>4	3	>4 to 3	18.10	17.77	18.71	No	0.94	Biological	4.91
Reference	REF-A-102	C	9/13/2022	17:02:44	14	3	14.63	>4	>4	2	>4 to 2	20.13	19.73	20.65	No	0.91	Biological	3.07
Reference	REF-A-102	D	9/13/2022	17:04:54	14	3	14.63	>4	>4	3	>4 to 3	19.98	19.20	20.64	No	1.44	Biological	2.17
Reference	REF-A-103	A	9/13/2022	17:23:17	14	3	14.63	>4	>4	3	>4 to 3	18.44	18.11	18.79	No	0.68	Biological	3.20
Reference	REF-A-103	B	9/13/2022	17:25:26	14	3	14.63	>4	>4	3	>4 to 3	17.98	16.77	18.52	No	1.75	Physical/ Biological	2.20
Reference	REF-A-103	C	9/13/2022	17:27:38	14	3	14.63	>4	>4	3	>4 to 3	17.21	16.87	17.86	No	1.00	Biological	2.96

Area	Station ID	Replicate	Date	Time	Stop Collar Setting (in)	Weights per Side (#)	Image Width (cm)	Grain Size Major Mode (phi)	Grain Size Minimum (phi)	Grain Size Maximum (phi)	Grain Size Range (phi)	Penetration Mean (cm)	Penetration Minimum (cm)	Penetration Maximum (cm)	Over-penetration?	Boundary Roughness (cm)	Boundary Roughness Type	aRPD Mean (cm)
Reference	REF-A-104	A	9/13/2022	17:11:42	14	3	14.63	>4	>4	3	>4 to 3	17.33	16.87	17.78	No	0.91	Biological	3.18
Reference	REF-A-104	B	9/13/2022	17:13:52	14	3	14.63	>4	>4	3	>4 to 3	18.14	17.94	18.41	No	0.47	Biological	2.45
Reference	REF-A-104	D	9/13/2022	17:18:05	14	3	14.63	>4	>4	3	>4 to 3	20.10	19.84	20.26	No	0.43	Biological	1.88
Reference	REF-B-105	A	9/13/2022	15:56:11	14	3	14.63	>4	>4	3	>4 to 3	17.88	17.60	18.27	No	0.66	Biological	1.03
Reference	REF-B-105	B	9/13/2022	15:58:13	14	3	14.63	>4	>4	3	>4 to 3	18.20	17.91	18.68	No	0.76	Biological	2.23
Reference	REF-B-105	C	9/13/2022	16:00:14	14	3	14.63	>4	>4	3	>4 to 3	17.85	16.91	18.67	No	1.76	Physical/ Biological	2.76
Reference	REF-B-106	A	9/13/2022	15:44:05	14	3	14.63	>4	>4	2	>4 to 2	18.47	17.58	19.43	No	1.85	Physical/ Biological	3.01
Reference	REF-B-106	B	9/13/2022	15:46:08	14	3	14.63	>4	>4	3	>4 to 3	20.37	20.11	20.86	No	0.75	Biological	2.90
Reference	REF-B-106	D	9/13/2022	15:50:14	14	3	14.63	>4	>4	3	>4 to 3	17.68	17.26	17.88	No	0.62	Biological	2.66
Reference	REF-B-107	B	9/13/2022	16:22:57	14	3	14.63	>4	>4	3	>4 to 3	19.47	19.14	19.71	No	0.57	Biological	2.61
Reference	REF-B-107	C	9/13/2022	16:25:07	14	3	14.63	>4	>4	3	>4 to 3	19.66	18.50	20.28	No	1.79	Physical/ Biological	3.41
Reference	REF-B-107	D	9/13/2022	16:27:52	14	3	14.63	>4	>4	3	>4 to 3	19.89	19.43	20.18	No	0.75	Physical/ Biological	3.56
Reference	REF-B-108	A	9/13/2022	16:06:57	14	3	14.63	>4	>4	3	>4 to 3	17.73	17.21	18.46	No	1.25	Biological	2.64
Reference	REF-B-108	B	9/13/2022	16:09:20	14	3	14.63	>4	>4	3	>4 to 3	17.68	17.26	17.97	No	0.71	Biological	4.23
Reference	REF-B-108	C	9/13/2022	16:11:39	14	3	14.63	>4	>4	3	>4 to 3	17.54	17.33	17.78	No	0.45	Biological	2.76
Reference	REF-C-109	A	9/14/2022	12:02:01	14	3	14.63	>4	>4	3	>4 to 3	11.41	10.21	12.13	No	1.92	Physical/ Biological	3.23
Reference	REF-C-109	C	9/14/2022	12:09:01	14	3	14.63	>4	>4	3	>4 to 3	11.84	11.23	12.23	No	1.00	Biological	2.55
Reference	REF-C-109	D	9/14/2022	12:10:55	14	3	14.63	>4	>4	2	>4 to 2	10.85	10.00	11.47	No	1.48	Biological	2.07
Reference	REF-C-110	A	9/14/2022	12:45:24	14	3	14.63	>4	>4	2	>4 to 2	8.77	5.51	9.92	No	4.41	Physical/ Biological	2.21
Reference	REF-C-110	C	9/14/2022	12:49:11	14	3	14.63	>4	>4	2	>4 to 2	13.07	12.79	13.42	No	0.63	Biological	3.39
Reference	REF-C-110	D	9/14/2022	12:51:01	14	3	14.63	>4	>4	1	>4 to 1	11.50	8.83	11.93	No	3.10	Physical/ Biological	2.05
Reference	REF-C-111	A	9/14/2022	12:18:28	14	3	14.63	>4	>4	2	>4 to 2	10.75	8.79	11.70	No	2.92	Physical/ Biological	1.69
Reference	REF-C-111	B	9/14/2022	12:20:32	14	3	14.63	>4	>4	1	>4 to 1	9.73	9.40	10.03	No	0.63	Biological	2.76
Reference	REF-C-111	D	9/14/2022	12:26:45	14	3	14.63	>4	>4	3	>4 to 3	10.49	10.03	11.09	No	1.06	Biological	3.12
Reference	REF-C-112	A	9/14/2022	12:32:31	14	3	14.63	>4	>4	3	>4 to 3	10.47	9.41	11.02	No	1.61	Physical/ Biological	2.53
Reference	REF-C-112	C	9/14/2022	12:36:34	14	3	14.63	>4	>4	2	>4 to 2	7.93	5.05	9.56	No	4.51	Physical/ Biological	IND
Reference	REF-C-112	D	9/14/2022	12:38:20	14	3	14.63	>4	>4	2	>4 to 2	9.95	9.51	10.53	No	1.02	Biological	2.62

Station ID	Replicate	aRPD > Pen	Mud Clast Number	Mud Clast State	Sediment Feature Anomalies	Dredged Material Present?	Dredged Material Layer Mean Thickness (cm)	Dredged Material Layer Minimum Thickness (cm)	Dredged Material Layer Maximum Thickness (cm)	Buried Dredged Material?	Mean Dredged Material Depth (cm)	Dredged Material > Pen	Dredged Material Notes
005	A	No	0	None		Yes	9.72	9.16	10.20	No	0.00	Yes	Mixed sand with some clay material intermixed in sediment column.
005	B	No	0	None		Yes	8.95	7.92	10.16	No	0.00	Yes	Mixed sand, likely DM, with a thick layer of white clay that goes beyond penetration
005	D	No	4	Oxidized		Yes	6.58	5.79	7.48	No	0.00	Yes	White clay clasts at SWI. Very fine sand, likely DM, with a layer of white clay that goes beyond penetration.
006	A	No	0	None		IND	IND	IND	IND	IND	IND	No	Likely white clay clasts at SWI, barely visible due to low penetration.
006	B	No	6	Oxidized		Yes	IND	IND	IND	IND	IND	No	White clay clasts at SWI.
006	C	No	5	Oxidized		Yes	IND	IND	IND	IND	IND	No	White clay clasts at SWI.
007	A	No	0	None		Yes	5.00	3.97	5.69	No	0.00	Yes	Fine sand, likely DM, with a thick layer of white clay that goes beyond penetration.
007	C	No	0	None		Yes	5.30	4.83	5.62	No	0.00	Yes	Fine sand, likely DM, with what appears to be the beginning of a layer of white clay that goes beyond penetration.
007	D	No	0	None		Yes	8.16	7.58	8.47	No	0.00	Yes	Fine sand, likely DM, with a thick layer of white clay that goes beyond penetration.
008	A	No	IND	IND		Yes	IND	IND	IND	IND	IND	No	Large pebbles/small cobbles at SWI with attached fauna.
008	B	No	IND	IND		Yes	IND	IND	IND	IND	IND	No	Large pebbles/small cobbles at SWI with attached fauna.
008	D	No	IND	IND		Yes	IND	IND	IND	IND	IND	No	Large pebbles/small cobbles at SWI with attached fauna.
009	A	No	2	Oxidized		Yes	5.87	5.59	6.26	No	0.00	Yes	Surficial clay clasts with trace clay and very fine sand that is likely DM as well.
009	B	No	1	Reduced/ Oxidized		Yes	1.30	0.00	2.88	No	0.00	Yes	Large clay clast against faceplate. Large boulder. Clay intermixed with silt.
009	C	No	0	None		Yes	11.33	10.19	12.00	No	0.00	Yes	Sand likely DM. Trace clay intermixed with sand.
010	A	No	0	None		Yes	9.99	9.40	10.52	No	0.00	Yes	Sand likely DM. Trace clay intermixed with sand.
010	B	No	0	None		Yes	5.67	4.63	6.08	No	0.00	Yes	Sand likely DM. Trace clay intermixed with sand.
010	D	No	0	None		Yes	7.38	6.61	8.27	No	0.00	Yes	Sand likely DM. Trace clay intermixed with sand.
011	A	No	1	Oxidized		Yes	10.92	10.57	11.40	No	0.00	Yes	Sand likely DM. Clay intermixed with sand.
011	B	No	0	None		Yes	13.01	12.62	13.40	No	0.00	Yes	Very fine sand, likely DM, with a thick layer of white clay that goes beyond penetration.
011	D	No	0	None		Yes	8.10	7.45	8.71	No	0.00	Yes	Very fine sand, likely DM. Clay intermixed with sand. Pebbles at SWI.
012	A	No	0	None		Yes	7.29	6.93	7.66	No	0.00	Yes	Fine sand, likely DM, with a thick layer of white clay that goes beyond penetration.
012	C	No	0	None		Yes	9.67	9.31	10.04	No	0.00	Yes	Fine sand, likely DM, with a thick layer of white clay that goes beyond penetration.

Station ID	Replicate	aRPD > Pen	Mud Clast Number	Mud Clast State	Sediment Feature Anomalies	Dredged Material Present?	Dredged Material Layer Mean Thickness (cm)	Dredged Material Layer Minimum Thickness (cm)	Dredged Material Layer Maximum Thickness (cm)	Buried Dredged Material?	Mean Dredged Material Depth (cm)	Dredged Material > Pen	Dredged Material Notes
012	D	No	0	None		Yes	12.90	12.06	13.45	No	0.00	Yes	Fine sand, likely DM, with a thick layer of white clay that goes beyond penetration.
013	A	No	0	None		Yes	12.23	11.82	12.60	No	0.00	Yes	Very fine sand dissimilar from native sediment from reference areas.
013	B	No	0	None		Yes	13.58	12.91	14.47	No	0.00	Yes	Very fine sand dissimilar from native sediment from reference areas.
013	D	No	0	None		Yes	12.54	12.33	13.19	No	0.00	Yes	Very fine sand dissimilar from native sediment from reference areas.
014	A	No	0	None		Yes	15.93	15.62	16.28	No	0.00	Yes	Very fine sand dissimilar from native sediment from reference areas.
014	B	No	0	None		Yes	15.81	14.96	16.10	No	0.00	No	Very fine sand dissimilar from native sediment from reference areas.
014	C	No	0	None		Yes	16.63	15.75	17.51	No	0.00	No	Very fine sand dissimilar from native sediment from reference areas.
015	A	No	0	None		Yes	16.48	15.98	16.92	No	0.00	No	Very fine sand dissimilar from native sediment from reference areas.
015	C	No	0	None		Yes	16.77	16.24	17.33	No	0.00	No	Very fine sand dissimilar from native sediment from reference areas.
015	D	No	0	None		Yes	14.64	12.66	16.43	No	0.00	No	Very fine sand dissimilar from native sediment from reference areas.
016	A	No	0	None		Yes	12.72	12.07	13.39	No	0.00	No	Very fine sand dissimilar from native sediment from reference areas.
016	B	No	0	None		Yes	12.47	10.77	15.10	No	0.00	No	Very fine sand dissimilar from native sediment from reference areas.
016	D	No	0	None		Yes	12.12	9.50	15.12	No	0.00	No	Very fine sand dissimilar from native sediment from reference areas.
017	A	No	0	None		Yes	15.45	14.40	16.30	No	0.00	Yes	Very fine sand dissimilar from native sediment from reference areas.
017	B	No	0	None		Yes	16.15	15.68	16.45	No	0.00	Yes	Very fine sand dissimilar from native sediment from reference areas.
017	C	No	2	Oxidized		Yes	14.67	13.97	15.51	No	0.00	Yes	Very fine sand dissimilar from native sediment from reference areas. White clay layer and white clay clasts at SWI.
018	A	No	0	None		Yes	13.88	13.10	15.47	No	0.00	No	Very fine sand dissimilar from native sediment from reference areas.
018	C	No	0	None		Yes	14.29	12.66	18.75	No	0.00	No	Very fine sand dissimilar from native sediment from reference areas.
018	D	No	0	None		Yes	11.66	10.87	12.42	No	0.00	No	Very fine sand dissimilar from native sediment from reference areas.
REF-A-101	A	No	0	None		No	N/A	N/A	N/A	N/A	N/A	N/A	
REF-A-101	B	No	0	None		No	N/A	N/A	N/A	N/A	N/A	N/A	
REF-A-101	C	No	0	None		No	N/A	N/A	N/A	N/A	N/A	N/A	
REF-A-102	B	No	0	None		No	N/A	N/A	N/A	N/A	N/A	N/A	
REF-A-102	C	No	0	None		No	N/A	N/A	N/A	N/A	N/A	N/A	
REF-A-102	D	No	0	None		No	N/A	N/A	N/A	N/A	N/A	N/A	
REF-A-103	A	No	0	None		No	N/A	N/A	N/A	N/A	N/A	N/A	
REF-A-103	B	No	0	None		No	N/A	N/A	N/A	N/A	N/A	N/A	
REF-A-103	C	No	0	None		No	N/A	N/A	N/A	N/A	N/A	N/A	

Station ID	Replicate	aRPD > Pen	Mud Clast Number	Mud Clast State	Sediment Feature Anomalies	Dredged Material Present?	Dredged Material Layer Mean Thickness (cm)	Dredged Material Layer Minimum Thickness (cm)	Dredged Material Layer Maximum Thickness (cm)	Buried Dredged Material?	Mean Dredged Material Depth (cm)	Dredged Material > Pen	Dredged Material Notes
REF-A-104	A	No	0	None		No	N/A	N/A	N/A	N/A	N/A	N/A	
REF-A-104	B	No	0	None		No	N/A	N/A	N/A	N/A	N/A	N/A	
REF-A-104	D	No	0	None		No	N/A	N/A	N/A	N/A	N/A	N/A	
REF-B-105	A	No	0	None		No	N/A	N/A	N/A	N/A	N/A	N/A	
REF-B-105	B	No	0	None		No	N/A	N/A	N/A	N/A	N/A	N/A	
REF-B-105	C	No	0	None		No	N/A	N/A	N/A	N/A	N/A	N/A	
REF-B-106	A	No	0	None		No	N/A	N/A	N/A	N/A	N/A	N/A	
REF-B-106	B	No	0	None		No	N/A	N/A	N/A	N/A	N/A	N/A	
REF-B-106	D	No	0	None		No	N/A	N/A	N/A	N/A	N/A	N/A	
REF-B-107	B	No	0	None		No	N/A	N/A	N/A	N/A	N/A	N/A	
REF-B-107	C	No	0	None		No	N/A	N/A	N/A	N/A	N/A	N/A	
REF-B-107	D	No	0	None		No	N/A	N/A	N/A	N/A	N/A	N/A	
REF-B-108	A	No	0	None		No	N/A	N/A	N/A	N/A	N/A	N/A	
REF-B-108	B	No	0	None		No	N/A	N/A	N/A	N/A	N/A	N/A	
REF-B-108	C	No	0	None		No	N/A	N/A	N/A	N/A	N/A	N/A	
REF-C-109	A	No	0	None	Buried layer of white clay.	No	N/A	N/A	N/A	N/A	N/A	N/A	
REF-C-109	C	No	0	None	Trace buried white clay.	No	N/A	N/A	N/A	N/A	N/A	N/A	
REF-C-109	D	No	0	None	Trace buried white clay.	No	N/A	N/A	N/A	N/A	N/A	N/A	
REF-C-110	A	No	0	None	Trace buried white and green clay.	No	N/A	N/A	N/A	N/A	N/A	N/A	
REF-C-110	C	No	0	None	Trace buried white and green clay.	No	N/A	N/A	N/A	N/A	N/A	N/A	
REF-C-110	D	No	0	None	Trace buried white clay.	No	N/A	N/A	N/A	N/A	N/A	N/A	
REF-C-111	A	No	0	None	Trace buried white and green clay.	No	N/A	N/A	N/A	N/A	N/A	N/A	
REF-C-111	B	No	0	None	Reworked buried white and green clay layer.	No	N/A	N/A	N/A	N/A	N/A	N/A	
REF-C-111	D	No	1	Oxidized	Trace buried white and green clay.	No	N/A	N/A	N/A	N/A	N/A	N/A	
REF-C-112	A	No	0	None	Reworked buried white and green clay layer.	No	N/A	N/A	N/A	N/A	N/A	N/A	
REF-C-112	C	No	0	None	Trace buried white clay.	No	N/A	N/A	N/A	N/A	N/A	N/A	
REF-C-112	D	No	0	None	Reworked buried white and green clay layer.	No	N/A	N/A	N/A	N/A	N/A	N/A	

Station ID	Replicate	Methane Present?	Low DO Present?	Sediment Oxygen Demand	Beggiatoa Present?	Beggiatoa Type/Extent	Voids Present?	Maximum Bioturbation Depth (cm)	Successional Stage	Comment
005	A	No	No	Low	No	None	IND	IND	2	Stage 2 tubes. Medium sand appears to have drag-down from prism penetration that makes bioturbation assessment difficult.
005	B	No	No	Low	No	None	Yes	9.53	2 on 3	Sand with intermixed silt overlaying white clay. Stage 2 tubes. Many feeding voids within white clay.
005	D	No	No	Medium	No	None	Yes	6.86	2 on 3	
006	A	IND	IND	IND	IND	IND	IND	IND	IND	No penetration.
006	B	IND	IND	IND	IND	IND	IND	IND	IND	No penetration. Large white clay chunks at sediment surface.
006	C	IND	IND	IND	IND	IND	IND	IND	IND	No penetration. Large white clay chunks at sediment surface.
007	A	No	No	Low	No	None	No	4.13	2	
007	C	No	No	Low	No	None	Yes	4.90	2	
007	D	No	No	Low	No	None	No	8.03	2	
008	A	IND	IND	IND	IND	IND	IND	IND	IND	No penetration. Hard bottom at SWI.
008	B	IND	IND	IND	IND	IND	IND	IND	IND	No penetration. Hard bottom at SWI.
008	D	IND	IND	IND	IND	IND	IND	IND	IND	No penetration. Hard bottom at SWI.
009	A	No	No	Low	No	None	IND	IND	2	Sand appears to have drag-down from prism penetration that makes bioturbation assessment difficult.
009	B	No	No	IND	No	None	No	1.43	2	Boulder in background of image. Large clay clast against faceplate.
009	C	No	No	Low	No	None	Yes	11.56	2 on 3	
010	A	No	No	Low	No	None	IND	9.01	2	Either clay or cobble in background of image with attached fauna. Prism penetration drag-down makes void determination difficult.
010	B	No	No	Low	No	None	IND	IND	2	Prism penetration obscures possible void determination.
010	D	No	No	Low	No	None	Yes	7.40	2 on 3	
011	A	No	No	Medium	No	None	Yes	9.96	2 on 3	Entire sediment column sandy/silty clay.
011	B	No	No	Medium	No	None	Yes	11.18	1 on 3	
011	D	No	No	Medium	No	None	No	7.06	2	
012	A	No	No	Low	No	None	No	6.25	2 -> 3	Thin worm in burrow visible against faceplate within clay layer. Oxygenated sediment coincides mostly with change in grain size, aRPD is IND.
012	C	No	No	Low	No	None	Yes	8.09	2 on 3	Voids and visible worms in burrows within clay layer. Oxygenated sediment generally coincides mostly with change in grain size, aRPD is IND.

Station ID	Replicate	Methane Present?	Low DO Present?	Sediment Oxygen Demand	Beggiatoa Present?	Beggiatoa Type/Extent	Voids Present?	Maximum Bioturbation Depth (cm)	Successional Stage	Comment
012	D	No	No	Low	No	None	Yes	12.28	2 on 3	Voids and visible worms in burrows within clay layer. Oxygenated sediment generally coincides mostly with change in grain size, aRPD is IND.
013	A	No	No	Medium	No	None	Yes	7.99	2 on 3	
013	B	No	No	Medium	No	None	No	6.37	2 on 3	Worm in burrow visible against faceplate beneath aRPD boundary.
013	D	No	No	Low	No	None	No	12.35	2 -> 3	
014	A	No	No	Medium	No	None	No	9.66	2 -> 3	Layer of medium sand beneath silt/clay layer at depth.
014	B	No	No	Medium	No	None	No	4.62	2 -> 3	Tubes and amphipods at SWI. Multiple layering within sediment column.
014	C	No	No	Medium	No	None	No	4.86	2 -> 3	Layering within sediment column.
015	A	No	No	Medium	No	None	Yes	11.08	1 on 3	Layering within sediment column.
015	C	No	No	Medium	No	None	No	12.15	2 on 3	Layering within sediment column.
015	D	No	No	Medium	No	None	No	13.60	2 -> 3	Layering within sediment column.
016	A	No	No	Medium	No	None	No	6.21	2 on 3	Layering within sediment column. Relict void at depth. Worms visible.
016	B	No	No	Medium	No	None	Yes	10.36	2 on 3	Layering within sediment column.
016	D	No	No	Medium	No	None	Yes	12.27	2 on 3	Layering within sediment column. Large voids partially infilled, possibly by prism penetration.
017	A	No	No	Medium	No	None	No	3.78	2 -> 3	Layering within sediment column. Large burrow at SWI causing boundary roughness.
017	B	No	No	Medium	No	None	No	6.22	2 -> 3	Layering within sediment column.
017	C	No	No	Medium	No	None	Yes	6.56	2 on 3	Layering within sediment column.
018	A	No	No	Medium	No	None	No	2.63	2	Layering within sediment column.
018	C	No	No	Medium	No	None	No	16.50	2	Layering within sediment column.
018	D	No	No	Medium	No	None	Yes	5.62	2 on 3	Layering within sediment column.
REF-A-101	A	No	No	Low	No	None	Yes	14.80	1 on 3	Open and infilled voids in sediment column.
REF-A-101	B	No	No	Low	No	None	Yes	18.22	1 on 3	Open and infilled voids in sediment column.
REF-A-101	C	No	No	Low	No	None	Yes	16.97	1 on 3	Open and infilled voids in sediment column.
REF-A-102	B	No	No	Low	No	None	Yes	17.39	1 on 3	
REF-A-102	C	No	No	Low	No	None	Yes	18.31	1 on 3	
REF-A-102	D	No	No	Low	No	None	Yes	19.03	1 on 3	Large worm in burrow.
REF-A-103	A	No	No	Low	No	None	Yes	13.94	2 on 3	Stage 2 tube.
REF-A-103	B	No	No	Low	No	None	Yes	15.01	1 on 3	
REF-A-103	C	No	No	Low	No	None	Yes	14.00	1 on 3	

Station ID	Replicate	Methane Present?	Low DO Present?	Sediment Oxygen Demand	Beggiatoa Present?	Beggiatoa Type/Extent	Voids Present?	Maximum Bioturbation Depth (cm)	Successional Stage	Comment
REF-A-104	A	No	No	Low	No	None	Yes	16.62	1 on 3	
REF-A-104	B	No	No	Low	No	None	Yes	17.28	1 on 3	
REF-A-104	D	No	No	Low	No	None	Yes	19.74	2 on 3	Stage 2 tubes.
REF-B-105	A	No	No	Low	No	None	Yes	15.19	1 on 3	
REF-B-105	B	No	No	Low	No	None	Yes	18.13	1 on 3	
REF-B-105	C	No	No	Low	No	None	Yes	16.53	2 on 3	Stage 2 tube.
REF-B-106	A	No	No	Low	No	None	Yes	12.78	2 on 3	Stage 2 tube at left at SWI and in background at right.
REF-B-106	B	No	No	Low	No	None	Yes	20.20	1 on 3	
REF-B-106	D	No	No	Low	No	None	Yes	10.54	1 on 3	
REF-B-107	B	No	No	Low	No	None	Yes	15.10	1 on 3	
REF-B-107	C	No	No	Low	No	None	Yes	19.76	1 on 3	
REF-B-107	D	No	No	Low	No	None	Yes	19.72	1 on 3	Large worm in burrow.
REF-B-108	A	No	No	Low	No	None	Yes	11.70	1 on 3	
REF-B-108	B	No	No	Low	No	None	Yes	15.67	1 on 3	
REF-B-108	C	No	No	Low	No	None	Yes	17.34	2 on 3	Stage 2 tube at center, far field.
REF-C-109	A	No	No	Low	No	None	No	9.55	2 -> 3	Relict voids. Worms in burrow visible. Tubes at SWI. Possible clay clast at SWI.
REF-C-109	C	No	No	Low	No	None	Yes	11.33	2 on 3	Stage 2 tubes.
REF-C-109	D	No	No	Low	No	None	Yes	10.13	2 on 3	Open voids. Larger Stage 2 tubes.
REF-C-110	A	No	No	Low	No	None	Yes	8.65	2 on 3	Open voids. Larger Stage 2 tubes.
REF-C-110	C	No	No	Low	No	None	Yes	10.83	2 on 3	Large Stage 2 tubes.
REF-C-110	D	No	No	Low	No	None	Yes	7.01	2 on 3	Large Stage 2 tubes. Possible attachment to clast or pebble at SWI.
REF-C-111	A	No	No	Low	No	None	Yes	10.58	2 on 3	Large Stage 2 tubes in far field.
REF-C-111	B	No	No	Low	No	None	Yes	9.53	2 on 3	Stage 2 tubes.
REF-C-111	D	No	No	Low	No	None	Yes	7.42	1 on 3	Attached fauna on a feature at SWI, cannot identify.
REF-C-112	A	No	No	Low	No	None	Yes	10.61	2 on 3	Large Stage 2 tubes. Unable to determine feature in background of SWI. Possible pebble or epifauna.
REF-C-112	C	No	No	Low	No	None	Yes	8.46	2 on 3	Stage 2 tubes near burrow opening. Large burrow and physical disturbance at SWI make aRPD determination difficult. Lots of white clay streaks on prism.
REF-C-112	D	No	No	Low	No	None	Yes	4.40	2 on 3	Stage 2 tubes.

Area	Station ID	Replicate	Date	Time	Stop Collar Setting (in)	Weights per Side (#)	Image Width (cm)	Penetration Mean (cm)	Penetration Minimum (cm)	Penetration Maximum (cm)	Over-penetration?	Dredged Material Present?	Dredged Material Layer Mean Thickness (cm)	Dredged Material Layer Minimum Thickness (cm)
Short Dump	T1-01	A	9/13/2022	12:10:14	14	3	14.71	18.14	15.78	19.61	No	Trace	0.00	0.00
Short Dump	T1-02	A	9/13/2022	12:13:16	14	3	14.71	18.50	17.66	18.92	No	Yes	6.08	3.44
Short Dump	T1-03	A	9/13/2022	12:17:27	14	3	14.71	18.62	18.19	18.82	No	Yes	6.28	3.90
Short Dump	T1-04	A	9/13/2022	12:21:18	14	3	14.71	19.11	18.45	19.74	No	Yes	8.12	6.07
Short Dump	T1-05	A	9/13/2022	12:25:18	14	3	14.71	13.85	12.82	15.06	No	Yes	13.85	12.82
Short Dump	T1-07	A	9/13/2022	12:31:25	14	3	14.71	14.55	12.46	16.38	No	Yes	14.55	12.46
Short Dump	T1-08	A	9/13/2022	12:36:13	14	3	14.71	14.57	13.72	15.63	No	Yes	8.61	6.60
Short Dump	T1-09	A	9/13/2022	12:38:48	14	3	14.71	16.98	16.66	17.63	No	Yes	16.98	16.66
Short Dump	T1-10	A	9/13/2022	12:41:22	14	3	14.71	15.45	14.60	16.10	No	Yes	3.82	0.20
Short Dump	T1-11	A	9/13/2022	12:45:56	14	3	14.71	17.14	16.86	17.53	No	Yes	7.08	4.24
Short Dump	T1-12	A	9/13/2022	12:49:25	14	3	14.71	17.30	16.79	18.18	No	Yes	3.05	1.48
Short Dump	T1-13	A	9/13/2022	12:52:26	14	3	14.71	17.38	16.81	17.84	No	Yes	3.05	1.17
Short Dump	T1-14	A	9/13/2022	12:54:45	14	3	14.71	19.34	18.71	19.96	No	No	N/A	N/A
Short Dump	T1-15	A	9/13/2022	12:58:01	14	3	14.71	19.89	18.99	20.66	No	Trace	0.00	0.00

Station ID	Replicate	Dredged Material Layer Maximum Thickness (cm)	Buried Dredged Material?	Mean Dredged Material Depth (cm)	Dredged Material > Pen	Dredged Material Notes	Comment
T1-01	A	0.00	No	0.00	No	Small deposits of white material present just below SWI.	
T1-02	A	8.65	No	0.00	No	Depositional brown fines at SWI, inclusions of white/gray material that becomes thicker deposits and extends halfway down image.	
T1-03	A	8.14	No	0.00	No	Depositional brown fines at SWI, small inclusions of white/gray material that become thicker deposits and extend 1/3 down image.	Several feeding voids about halfway down sediment column.
T1-04	A	11.06	No	0.00	No	Depositional brown fines at SWI with inclusions of white/gray material that becomes thicker deposits and extends through 3/4 of image.	Several feeding voids throughout sediment column.
T1-05	A	15.06	No	0.00	Yes	Gray and white material present throughout sediment column.	Several polychaetes and feeding voids deep in sediment column.
T1-07	A	16.35	No	0.00	Yes	Gray and white material present throughout sediment column.	Numerous voids, possibly due to deposition of DM not necessarily biological.
T1-08	A	11.85	No	0.00	No	Depositional fines at SWI, inclusions of white/gray material that becomes thicker deposits and extends through 3/4 of image.	Large voids within the DM.
T1-09	A	17.63	No	0.00	Yes	Gray, white, and black material present throughout sediment column in disorganized chaotic fabric.	
T1-10	A	7.83	No	0.00	No	Depositional brown fines at SWI. White and gray material present below SWI and extends halfway down image.	
T1-11	A	12.42	Yes	2.98	No	Depositional layer of fines at SWI, with inclusions of white/gray material that becomes thicker deposits and extend through 3/4 of image.	
T1-12	A	4.99	No	0.00	No	Depositional layer of fines at SWI, with white/gray inclusions that become thicker deposits and extend through 1/4 of image.	
T1-13	A	4.90	No	0.00	No	Depositional brown fines at SWI, with white/gray clay inclusions that become thicker deposits and extend through 1/4 of image.	
T1-14	A	N/A	N/A	N/A	N/A		
T1-15	A	0.00	No	0.00	No	Trace DM near SWI, several small white clay inclusions.	

APPENDIX E - PLAN VIEW IMAGE ANALYSIS RESULTS

Notes:

DM=Dredged Material

IND=Indeterminate

N/A=Not Applicable

Area	Station ID	Replicate	Date	Time	Image Width (cm)	Image Height (cm)	Field of View (m2)	Sediment Type	Surface Oxidation	Bedforms	Beggiatoa Present?	Beggiatoa Type/Extent	Dredged Material Present?	Dredged Material Notes	Debris
Mound B	005	A	9/13/2022	10:07:55	87.39	58.26	0.51	Sand	Oxidized	None	No	None	Yes	Chunky white clay at surface. Sand as well, likely to be DM.	None
Mound B	005	B	9/13/2022	10:10:34	81.21	54.14	0.44	Sand	Oxidized	None	No	None	Yes	Chunky white clay at surface. Sand as well, likely to be DM.	None
Mound B	005	D	9/13/2022	10:16:06	81.42	54.28	0.44	Sand	Oxidized	None	No	None	Yes	Chunky white clay at surface. Sand as well, likely to be DM. Also what looks like chunks of blasted rock at sediment surface.	None
Mound B	006	A	9/13/2022	10:59:28	89.86	59.91	0.54	Boulder	Oxidized	None	No	None	Yes	Blasted rock and sand. Some white clay between rock.	None
Mound B	006	B	9/13/2022	11:01:47	99.62	66.41	0.66	Boulder	Oxidized	None	No	None	Yes	Blasted rock and sand. Some white clay between rock.	None
Mound B	006	C	9/13/2022	11:04:04	107.29	71.53	0.77	Boulder	Oxidized	None	No	None	Yes	Blasted rock and sand. Some white clay between rock.	None
Mound B	007	A	9/13/2022	10:23:11	93.41	62.28	0.58	Sand	Oxidized	None	No	None	Yes	Chunky white clay at surface. Sand as well, likely to be DM.	None
Mound B	007	C	9/13/2022	10:28:51	94.95	63.30	0.60	Sand	Oxidized	None	No	None	Yes	Small chunk of white clay at bottom of image. Sand likely to be DM.	None
Mound B	007	D	9/13/2022	10:31:38	92.36	61.57	0.57	Sand	Oxidized	Divots	No	None	Yes	Sand and trace white clay.	None
Mound B	008	A	9/13/2022	9:55:17	93.64	62.42	0.58	Cobble	Oxidized	None	No	None	Yes	Blasted rock and sand.	None
Mound B	008	B	9/13/2022	9:57:53	91.93	61.28	0.56	Boulder	Oxidized	None	No	None	Yes	Blasted rock and sand.	None
Mound B	008	D	9/13/2022	10:02:29	96.06	64.04	0.62	Cobble	Oxidized	None	No	None	Yes	Blasted rock and sand.	None
Mound B	009	A	9/13/2022	9:23:29	96.18	64.12	0.62	Sandy Gravel	Oxidized	None	No	None	Yes	Clay and pebble/cobble. Sand also likely DM.	None
Mound B	009	B	9/13/2022	9:26:17	79.96	53.31	0.43	Boulder	Oxidized	None	No	None	Yes	Boulder and cobble on sand.	None
Mound B	009	C	9/13/2022	9:28:47	74.04	49.36	0.37	Sand	Oxidized	None	No	None	Yes	Clay and pebble/cobble. Sand also likely DM.	None
Mound B	010	A	9/13/2022	11:13:41	95.65	63.76	0.61	Sand	Oxidized	None	No	None	Yes	Large clay chunks and sand.	None
Mound B	010	B	9/13/2022	11:16:13	74.96	49.98	0.37	Sand	Oxidized	None	No	None	Yes	Sand and a large clay chunk or blasted rock, mostly buried.	None
Mound B	010	D	9/13/2022	11:21:20	90.54	60.36	0.55	Sand	Oxidized	None	No	None	Yes	Sand and smaller chunks of clay.	None
Mound B	011	A	9/13/2022	10:41:29	87.44	58.30	0.51	Clay	IND	IND	No	None	Yes	Sandy clay bottom with occasional chunk/pebble.	None
Mound B	011	C	9/13/2022	10:47:19	91.76	61.18	0.56	Clay	IND	IND	No	None	Yes	Sandy clay bottom with occasional chunk/pebble.	None
Mound B	011	D	9/13/2022	10:50:14	89.40	59.60	0.53	Gravelly Clay	IND	None	No	None	Yes	Sandy clay bottom with occasional chunks. Pebbles and cobbles at surface.	None
Mound B	012	A	9/13/2022	11:28:17	93.02	62.02	0.58	Sand	Oxidized	Divots	No	None	Yes	Sand likely to be DM. Very small discrete bits of clay.	None
Mound B	012	C	9/13/2022	11:34:25	95.59	63.73	0.61	Sand	Oxidized	Divots	No	None	Yes	Sand likely to be DM. Very small discrete bits of clay.	None

Area	Station ID	Replicate	Date	Time	Image Width (cm)	Image Height (cm)	Field of View (m2)	Sediment Type	Surface Oxidation	Bedforms	Beggiatoa Present?	Beggiatoa Type/Extent	Dredged Material Present?	Dredged Material Notes	Debris
Mound B	012	D	9/13/2022	11:37:17	90.38	60.25	0.54	Sand	Oxidized	Divots	No	None	Yes	Clay and sand likely to be DM.	None
Mound A	013	A	9/13/2022	14:43:03	89.45	59.63	0.53	Sand	Oxidized	None	No	None	Yes	Pebbles/cobbles and possible wood debris. Sand likely to be DM.	Possible wood
Mound A	013	B	9/13/2022	14:45:42	94.37	62.92	0.59	Sand	Oxidized	None	No	None	Yes	Sand likely to be DM.	None
Mound A	013	C	9/13/2022	14:47:52	90.91	60.61	0.55	Sand	Oxidized	None	No	None	Yes	Sand likely to be DM.	None
Mound A	014	A	9/13/2022	14:27:52	94.20	62.80	0.59	Sand	Oxidized	None	No	None	Yes	Sand likely to be DM.	None
Mound A	014	C	9/13/2022	14:34:35	92.75	61.83	0.57	Sand	Oxidized	None	No	None	Yes	Sand likely to be DM.	None
Mound A	014	D	9/13/2022	14:36:46	90.43	60.29	0.55	Sand	Oxidized	None	No	None	Yes	Sand likely to be DM.	None
Mound A	015	A	9/13/2022	14:13:09	91.98	61.32	0.56	Sand	Oxidized	None	No	None	Yes	Sand likely to be DM.	None
Mound A	015	C	9/13/2022	14:17:32	90.12	60.08	0.54	Sand	Oxidized	None	No	None	Yes	Sand likely to be DM.	None
Mound A	015	D	9/13/2022	14:19:39	90.75	60.50	0.55	Sand	Oxidized	None	No	None	Yes	Sand likely to be DM.	None
Mound A	016	A	9/13/2022	13:53:56	89.55	59.70	0.53	Sand	Oxidized	None	No	None	Yes	Sand likely to be DM.	None
Mound A	016	B	9/13/2022	13:56:40	89.45	59.63	0.53	Sand	Oxidized	None	No	None	Yes	Sand likely to be DM.	None
Mound A	016	D	9/13/2022	14:01:05	92.09	61.39	0.57	Sand	Oxidized	None	No	None	Yes	Sand likely to be DM.	None
Mound A	017	A	9/13/2022	14:58:13	91.76	61.18	0.56	Gravelly Sand	Oxidized	None	No	None	Yes	Sand, cobbles, and pebbles.	None
Mound A	017	B	9/13/2022	15:00:20	89.35	59.56	0.53	Sand	Oxidized	None	No	None	Yes	Sand likely to be DM.	None
Mound A	017	C	9/13/2022	15:02:37	91.39	60.93	0.56	Gravelly Sand	Oxidized	None	No	None	Yes	Sand, cobbles, and pebbles.	None
Mound A	018	A	9/13/2022	15:11:14	90.80	60.54	0.55	Sand	Oxidized	None	No	None	Yes	Sand likely to be DM.	None
Mound A	018	B	9/13/2022	15:13:34	90.49	60.32	0.55	Sand	Oxidized	None	No	None	Yes	Sand likely to be DM.	None
Mound A	018	D	9/13/2022	15:17:54	91.33	60.89	0.56	Sand	Oxidized	None	No	None	Yes	Sand likely to be DM.	None
Reference	REF-A-101	A	9/13/2022	16:45:10	77.77	51.84	0.40	Sandy Mud	Oxidized	None	No	None	No		None
Reference	REF-A-101	B	9/13/2022	16:47:39	92.20	61.47	0.57	Sandy Mud	Oxidized	None	No	None	No		None
Reference	REF-A-101	C	9/13/2022	16:49:46	94.43	62.95	0.59	Sandy Mud	Oxidized	None	No	None	No		None
Reference	REF-A-102	B	9/13/2022	17:00:09	88.54	59.02	0.52	Sandy Mud	Oxidized	None	No	None	No		None
Reference	REF-A-102	C	9/13/2022	17:02:24	91.39	60.93	0.56	Sandy Mud	Oxidized	None	No	None	No		None
Reference	REF-A-102	D	9/13/2022	17:04:34	87.99	58.66	0.52	Sandy Mud	Oxidized	None	No	None	No		None

Area	Station ID	Replicate	Date	Time	Image Width (cm)	Image Height (cm)	Field of View (m2)	Sediment Type	Surface Oxidation	Bedforms	Beggiatoa Present?	Beggiatoa Type/Extent	Dredged Material Present?	Dredged Material Notes	Debris
Reference	REF-A-103	A	9/13/2022	17:22:56	100.39	66.92	0.67	Sandy Mud	Oxidized	Depression	No	None	No		None
Reference	REF-A-103	C	9/13/2022	17:27:19	88.49	58.99	0.52	Sandy Mud	Oxidized	None	No	None	No		None
Reference	REF-A-103	D	9/13/2022	17:29:28	87.84	58.56	0.51	Sandy Mud	Oxidized	None	No	None	No		None
Reference	REF-A-104	A	9/13/2022	17:11:22	92.69	61.79	0.57	Sandy Mud	Oxidized	None	No	None	No		None
Reference	REF-A-104	B	9/13/2022	17:13:31	85.29	56.86	0.48	Sandy Mud	Oxidized	None	No	None	No		None
Reference	REF-A-104	C	9/13/2022	17:15:37	90.91	60.61	0.55	Sandy Mud	Oxidized	None	No	None	No		None
Reference	REF-B-105	A	9/13/2022	15:55:51	89.04	59.36	0.53	Sandy Mud	Oxidized	None	No	None	No		None
Reference	REF-B-105	B	9/13/2022	15:57:53	90.59	60.39	0.55	Sandy Mud	Oxidized	None	No	None	No		None
Reference	REF-B-105	C	9/13/2022	15:59:54	89.30	59.53	0.53	Sandy Mud	Oxidized	None	No	None	No		None
Reference	REF-B-106	A	9/13/2022	15:43:46	91.39	60.93	0.56	Sandy Mud	Oxidized	None	No	None	No		None
Reference	REF-B-106	B	9/13/2022	15:45:48	92.25	61.50	0.57	Sandy Mud	Oxidized	IND	IND	IND	IND		IND
Reference	REF-B-106	D	9/13/2022	15:49:53	96.12	64.08	0.62	Sandy Mud	Oxidized	None	No	None	No		None
Reference	REF-B-107	B	9/13/2022	16:22:36	90.02	60.01	0.54	Sandy Mud	Oxidized	Depression	No	None	No		None
Reference	REF-B-107	C	9/13/2022	16:24:46	92.86	61.90	0.57	Sandy Mud	Oxidized	None	No	None	No		None
Reference	REF-B-107	D	9/13/2022	16:27:31	91.60	61.07	0.56	Sandy Mud	Oxidized	None	No	None	No		None
Reference	REF-B-108	A	9/13/2022	16:06:38	88.84	59.23	0.53	Sandy Mud	Oxidized	Depression	No	None	No		None
Reference	REF-B-108	C	9/13/2022	16:11:19	92.36	61.57	0.57	Sandy Mud	Oxidized	None	No	None	No		None
Reference	REF-B-108	D	9/13/2022	16:13:24	91.23	60.82	0.55	Sandy Mud	Oxidized	None	No	None	No		None
Reference	REF-C-109	A	9/14/2022	12:01:41	89.04	59.36	0.53	Clayey Mud	Oxidized	None	No	None	No		None
Reference	REF-C-109	C	9/14/2022	12:08:41	94.20	62.80	0.59	Clayey Mud	Oxidized	Depression	No	None	No		None
Reference	REF-C-109	D	9/14/2022	12:10:36	93.69	62.46	0.59	Clayey Mud	Oxidized	None	No	None	No		None
Reference	REF-C-110	A	9/14/2022	12:45:05	93.41	62.28	0.58	Clayey Mud	Oxidized	None	No	None	No		None
Reference	REF-C-110	C	9/14/2022	12:48:51	77.53	51.69	0.40	Sandy Mud	Oxidized	None	No	None	No		None
Reference	REF-C-110	D	9/14/2022	12:50:41	91.55	61.03	0.56	Gravelly Mud	Oxidized	Depression	No	None	No		None

Area	Station ID	Replicate	Date	Time	Image Width (cm)	Image Height (cm)	Field of View (m2)	Sediment Type	Surface Oxidation	Bedforms	Beggiatoa Present?	Beggiatoa Type/Extent	Dredged Material Present?	Dredged Material Notes	Debris
Reference	REF-C-111	A	9/14/2022	12:18:09	95.06	63.38	0.60	Sandy Mud	Oxidized	None	No	None	No		None
Reference	REF-C-111	B	9/14/2022	12:20:12	96.53	64.36	0.62	Clayey Mud	Oxidized	None	No	None	No		None
Reference	REF-C-111	C	9/14/2022	12:22:17	93.75	62.50	0.59	Clayey Mud	Oxidized	None	No	None	No		None
Reference	REF-C-112	A	9/14/2022	12:32:12	92.31	61.54	0.57	Clayey Mud	Oxidized	None	No	None	No		None
Reference	REF-C-112	B	9/14/2022	12:34:11	97.87	65.24	0.64	Clayey Mud	Oxidized	None	No	None	No		None
Reference	REF-C-112	C	9/14/2022	12:36:15	85.95	57.30	0.49	Clayey Mud	Oxidized	None	No	None	No		None

Station ID	Replicate	Tube Abundance	Burrow Abundance	Track Abundance	Epifauna	Macroalgae	Number of Fish	Comment
005	A	Abundant (25-75%)	Sparse (<10%)	Present (10-25%)	Shrimp	None	0	
005	B	Present (10-25%)	Sparse (<10%)	Sparse (<10%)	None	None	0	Some larger-grained pebbles in upper left corner of image.
005	D	Dense (>75%)	Sparse (<10%)	Sparse (<10%)	None	None	0	
006	A	Abundant (25-75%)	None	None	Bryozoa/Hydroids, Shrimp	None	0	Multiple shrimp among blasted rock.
006	B	Abundant (25-75%)	None	None	Hermit Crab	None	0	Boulders and smaller cobble and pebble at sediment surface amongst sand.
006	C	Present (10-25%)	None	None	Lobster	None	0	Boulders and smaller cobble and pebble at sediment surface amongst sand. Larger chunks of clay also present. Lobster in bottom right corner.
007	A	Abundant (25-75%)	None	Present (10-25%)	None	None	0	
007	C	Abundant (25-75%)	Sparse (<10%)	Abundant (25-75%)	None	None	0	Small chunk of white clay near bottom of image.
007	D	Dense (>75%)	Sparse (<10%)	Present (10-25%)	None	None	0	
008	A	Present (10-25%)	None	None	Bryozoa/Hydroids, Shrimp	None	0	Shrimp in bottom right corner of image. Bryozoa/Hydroids attached to cobble in center of image.
008	B	Present (10-25%)	None	None	Bryozoa/Hydroids	None	0	Mostly cobble with large boulder and some pebble on sandy surface. Bryozoa/Hydroids attached to hard bottom.
008	D	Abundant (25-75%)	None	None	Bryozoa/Hydroids, Shrimp	None	0	Shrimp left of image.
009	A	Present (10-25%)	Sparse (<10%)	None	Bryozoa/Hydroids	None	0	
009	B	Present (10-25%)	None	None	Bryozoa/Hydroids	None	0	Large boulder.
009	C	Dense (>75%)	None	None	Shrimp	None	0	Shrimp lower left. Small pebble/granule and large clay chunks.
010	A	Present (10-25%)	None	Sparse (<10%)	None	None	0	
010	B	Abundant (25-75%)	Sparse (<10%)	None	None	None	0	Pebble/Granule also present at sediment surface
010	D	Present (10-25%)	Sparse (<10%)	Abundant (25-75%)	Bryozoa/Hydroids	None	0	Bryozoa/Hydroids growth on cobble/clay in image.
011	A	Sparse (<10%)	None	None	None	None	0	Very unique clay bottom. Possible suggestion of hydrodynamics based on contours of clay and sand at surface.
011	C	Sparse (<10%)	Sparse (<10%)	Present (10-25%)	Crab	None	0	Similar bottom to 11-A. Crab in top of image.
011	D	Sparse (<10%)	Sparse (<10%)	Present (10-25%)	Bryozoa/Hydroids	None	0	Bryozoa/Hydroids growth on cobble/clay in image.
012	A	Abundant (25-75%)	Present (10-25%)	Present (10-25%)	None	None	0	Surface pocked with small divots.
012	C	Abundant (25-75%)	Present (10-25%)	Present (10-25%)	None	None	0	Surface pocked with small divots.

Station ID	Replicate	Tube Abundance	Burrow Abundance	Track Abundance	Epifauna	Macroalgae	Number of Fish	Comment
012	D	Abundant (25-75%)	Present (10-25%)	Sparse (<10%)	None	None	0	Large chunks of white clay.
013	A	Abundant (25-75%)	Sparse (<10%)	None	Bryozoa/Hydroids	None	0	Bryozoa/Hydroids growth on what appears to be wood debris in image.
013	B	Abundant (25-75%)	Sparse (<10%)	None	Shrimp	None	0	Pebble/Granule also present at sediment surface. Blue mussel shells.
013	C	Abundant (25-75%)	Sparse (<10%)	None	Shrimp	None	0	Pebble/Granule also present at sediment surface. Blue mussel shells.
014	A	Abundant (25-75%)	Sparse (<10%)	Present (10-25%)	None	None	0	
014	C	Abundant (25-75%)	Sparse (<10%)	Abundant (25-75%)	None	None	0	
014	D	Abundant (25-75%)	Present (10-25%)	Abundant (25-75%)	None	None	0	
015	A	Abundant (25-75%)	Abundant (25-75%)	Abundant (25-75%)	None	None	0	
015	C	Abundant (25-75%)	Present (10-25%)	Abundant (25-75%)	None	None	0	
015	D	Abundant (25-75%)	Abundant (25-75%)	Abundant (25-75%)	None	None	0	
016	A	Present (10-25%)	Abundant (25-75%)	Sparse (<10%)	None	None	0	
016	B	Abundant (25-75%)	Present (10-25%)	Present (10-25%)	None	None	0	
016	D	Present (10-25%)	Present (10-25%)	Abundant (25-75%)	None	None	0	
017	A	Abundant (25-75%)	Present (10-25%)	Sparse (<10%)	None	None	0	Unidentified greenish discoloration in hummock in left of image.
017	B	Present (10-25%)	Present (10-25%)	Present (10-25%)	None	None	0	
017	C	Present (10-25%)	Sparse (<10%)	Sparse (<10%)	Bryozoa/Hydroids, Crab, Gastropod	None	0	Many gastropod shells on sediment surface, some possibly alive. Cobbles and pebbles scattered on sediment surface. Crab in burrow in lower right.
018	A	Abundant (25-75%)	Sparse (<10%)	Present (10-25%)	None	None	1	One small fish in upper right of image.
018	B	Abundant (25-75%)	Abundant (25-75%)	Present (10-25%)	Shrimp	None	0	
018	D	Present (10-25%)	Abundant (25-75%)	Sparse (<10%)	Shrimp	None	0	
REF-A-101	A	Present (10-25%)	Abundant (25-75%)	Sparse (<10%)	None	None	0	Several large pits or burrows.
REF-A-101	B	Present (10-25%)	Present (10-25%)	Present (10-25%)	None	None	0	
REF-A-101	C	Present (10-25%)	Present (10-25%)	Abundant (25-75%)	None	None	0	
REF-A-102	B	Present (10-25%)	Present (10-25%)	Present (10-25%)	None	None	0	Sediment plume obscures portion of image.
REF-A-102	C	Present (10-25%)	Sparse (<10%)	Abundant (25-75%)	None	None	0	
REF-A-102	D	Present (10-25%)	Sparse (<10%)	Abundant (25-75%)	Shrimp	None	0	

Station ID	Replicate	Tube Abundance	Burrow Abundance	Track Abundance	Epifauna	Macroalgae	Number of Fish	Comment
REF-A-103	A	Sparse (<10%)	Sparse (<10%)	Present (10-25%)	None	None	0	Large rectangular depression in sediment surface. Possibly from fish activity.
REF-A-103	C	Sparse (<10%)	Present (10-25%)	Present (10-25%)	None	Unidentified	0	Unknown object/flora on sediment surface. Possibly macroalgal debris/detritus.
REF-A-103	D	Sparse (<10%)	Abundant (25-75%)	Sparse (<10%)	None	None	0	Large burrows.
REF-A-104	A	Sparse (<10%)	Present (10-25%)	Abundant (25-75%)	None	None	0	Very large burrow.
REF-A-104	B	Sparse (<10%)	Sparse (<10%)	Abundant (25-75%)	None	None	0	
REF-A-104	C	Sparse (<10%)	Sparse (<10%)	Present (10-25%)	None	None	1	Fish.
REF-B-105	A	Sparse (<10%)	Present (10-25%)	Abundant (25-75%)	None	None	0	
REF-B-105	B	Sparse (<10%)	Present (10-25%)	Abundant (25-75%)	None	None	0	
REF-B-105	C	Sparse (<10%)	Present (10-25%)	Abundant (25-75%)	None	None	0	
REF-B-106	A	Present (10-25%)	Present (10-25%)	Present (10-25%)	None	None	0	
REF-B-106	B	IND	IND	IND	IND	IND	IND	Turbidity obscures most of image except center, where sand a few small burrows are visible.
REF-B-106	D	Present (10-25%)	Abundant (25-75%)	Abundant (25-75%)	None	None	1	Small fish with head in sediment, in lower left.
REF-B-107	B	Sparse (<10%)	Present (10-25%)	Present (10-25%)	None	None	0	Large depression in sediment surface. Possibly from fish activity.
REF-B-107	C	Present (10-25%)	Sparse (<10%)	Present (10-25%)	None	None	1	Fish at center of left edge.
REF-B-107	D	Present (10-25%)	Abundant (25-75%)	Abundant (25-75%)	None	None	0	
REF-B-108	A	Present (10-25%)	Present (10-25%)	Present (10-25%)	None	None	0	Large depression and burrows in sediment surface.
REF-B-108	C	Sparse (<10%)	Abundant (25-75%)	Abundant (25-75%)	None	None	0	
REF-B-108	D	Sparse (<10%)	Present (10-25%)	Abundant (25-75%)	None	None	0	Recently excavated large burrow with sediment forming a large mound around the burrow opening, evident given shadow.
REF-C-109	A	Present (10-25%)	Sparse (<10%)	Sparse (<10%)	Bryozoa/Hydroids	None	0	Bryozoa/Hydroids attached to clay on sediment surface. Chunks of clay visible at sediment surface.
REF-C-109	C	Present (10-25%)	Present (10-25%)	Sparse (<10%)	Bryozoa/Hydroids	None	0	Bryozoa/Hydroids attached to clay on sediment surface. Depression in upper right corner. Chunks of clay visible at sediment surface.
REF-C-109	D	Present (10-25%)	Present (10-25%)	Present (10-25%)	Bryozoa/Hydroids	None	0	Bryozoa/Hydroids attached to clay on sediment surface. Chunks of clay visible at sediment surface.
REF-C-110	A	Present (10-25%)	Sparse (<10%)	Present (10-25%)	Bryozoa/Hydroids	None	0	Bryozoa/Hydroids attached to clay on sediment surface. Chunks of clay visible at sediment surface.
REF-C-110	C	Present (10-25%)	Present (10-25%)	Abundant (25-75%)	Shrimp	None	0	Shrimp.
REF-C-110	D	Present (10-25%)	Present (10-25%)	Sparse (<10%)	Anemone	None	0	Bryozoa/Hydroids at center, along with large vertical tubes. Large burrow or depression in upper corner with tendrils of anemone visible. Small clay chunks at sediment surface.

Station ID	Replicate	Tube Abundance	Burrow Abundance	Track Abundance	Epifauna	Macroalgae	Number of Fish	Comment
REF-C-111	A	Sparse (<10%)	Present (10-25%)	Sparse (<10%)	None	None	0	Small clay chunks at sediment surface.
REF-C-111	B	Present (10-25%)	Present (10-25%)	Sparse (<10%)	None	None	0	Small clay chunks at sediment surface.
REF-C-111	C	Present (10-25%)	Sparse (<10%)	Sparse (<10%)	Anemone, Bryozoa/Hydroids	None	0	Large anemone in center of image. Small clay chunks at sediment surface; some bryozoa/hydroids attached to a few.
REF-C-112	A	Abundant (25-75%)	Present (10-25%)	Sparse (<10%)	Bryozoa/Hydroids	None	0	Chunks of clay visible at sediment surface. Bryozoa/Hydroids attached to clay chunks.
REF-C-112	B	Present (10-25%)	Present (10-25%)	Sparse (<10%)	Bryozoa/Hydroids	None	0	Very large tubes in left half of image. Chunks of clay visible at sediment surface. Bryozoa/Hydroids attached to clay chunks.
REF-C-112	C	Present (10-25%)	Sparse (<10%)	Abundant (25-75%)	Bryozoa/Hydroids	None	0	Chunks of clay visible at sediment surface. Bryozoa/Hydroids attached to clay chunks.

Area	Station ID	Replicate	Date	Time	Image Width (cm)	Image Height (cm)	Field of View (m2)	Dredged Material Present?	Dredged Material Notes	Comment
Short Dump	T1-01	A	9/13/2022	12:09:54	85.81	57.21	0.49	Trace	White fines present alongside burrows top right.	
Short Dump	T1-02	A	9/13/2022	12:12:56	89.04	59.36	0.53	Trace	White fines scattered center, small clast in top right.	
Short Dump	T1-03	A	9/13/2022	12:17:08	94.03	62.69	0.59	Yes	White fines and small clasts scattered throughout image center.	
Short Dump	T1-04	A	9/13/2022	12:20:59	88.74	59.16	0.52	Yes	White fines and small clasts scattered throughout image center.	
Short Dump	T1-05	A	9/13/2022	12:24:59	89.66	59.77	0.54	Yes	White fines and large clasts scattered throughout image.	
Short Dump	T1-06	A	9/13/2022	12:28:03	86.09	57.40	0.49	Yes	Large white/gray clasts and deposits throughout image .	
Short Dump	T1-07	A	9/13/2022	12:31:06	93.19	62.13	0.58	Yes	Large white/gray clasts and deposits throughout image .	
Short Dump	T1-08	A	9/13/2022	12:35:53	80.00	53.33	0.43	Yes	Large white/gray clasts and deposits throughout image .	
Short Dump	T1-09	A	9/13/2022	12:38:29	86.52	57.68	0.50	Yes	White/gray medium sized clasts and deposits throughout image.	
Short Dump	T1-10	A	9/13/2022	12:41:03	IND	IND	IND	IND	Turbid image.	
Short Dump	T1-11	A	9/13/2022	12:45:36	95.06	63.38	0.60	Yes	Large and small white/gray clasts and deposits throughout image.	Shrimp in bottom right.
Short Dump	T1-12	A	9/13/2022	12:49:05	88.74	59.16	0.52	Yes	White fines and small clasts scattered throughout image.	
Short Dump	T1-13	A	9/13/2022	12:52:07	84.55	56.37	0.48	Yes	White fines and small clasts scattered throughout image.	
Short Dump	T1-14	A	9/13/2022	12:54:25	91.55	61.03	0.56	Trace	Small white clast, top right.	
Short Dump	T1-15	A	9/13/2022	12:57:42	87.84	58.56	0.51	Trace	Trace white fines scattered.	

APPENDIX F - GRAIN SIZE SCALE FOR SEDIMENTS

APPENDIX F

GRAIN SIZE SCALE FOR SEDIMENTS

Phi (Φ) Size	**Size Range (mm)**	**Size Class (Wentworth Class)**
<-1	>2	Gravel
0 to –1	1 to 2	Very coarse sand
1 to 0	0.5 to 1	Coarse sand
2 to 1	0.25 to 0.5	Medium sand
3 to 2	0.125 to 0.25	Fine sand
4 to 3	0.0625 to 0.125	Very fine sand
>4	<0.0625	Silt/clay

APPENDIX G - NON-PARAMETRIC BOOTSTRAPPED CONFIDENCE LIMITS

APPENDIX G

Non-parametric Bootstrapped Confidence Limits

Bootstrapping is a statistical resampling procedure that uses the sample data to represent the entire population in order to construct confidence limits around population parameters. Bootstrapping assumes only that the sample data are representative of the underlying population, so random sampling is a prerequisite for appropriate application of this method.

Bootstrapping procedures entail resampling, with replacement, from the observed sample of size n. Each time the sample is resampled, a summary statistic (e.g., mean or standard deviation) of the bootstrapped sample is computed and stored. After repeating this procedure many times, a summary of the bootstrapped statistics is used to construct the confidence limit. For the bootstrap-*t* method (e.g., Manly 1997, pp. 56-59; or Lunneborg 2000, pp. 129-131), the bootstrapped statistic (T) is a pivotal statistic, which means that the distribution of T is the same for all values of the true mean (θ). The bootstrap-*t* is essentially the "Studentized" version (i.e., subtract the mean and divide by the standard error, as is done to obtain the Student *t*-distribution for the sample mean) of the statistic of interest. This approach is quite versatile, and can be applied to construct a confidence interval around any linear combination of means (Lunneborg 2000, p. 364).

For the purpose of constructing a confidence interval around the true value for the linear combination of means ($\Theta = \mu_{Ref} - \mu_{Mound}$) the pivotal statistic T for the true difference is defined as

$$T = \frac{d - \theta}{SE(d)} \qquad \text{(Eq. A-1)}$$

We assume that this is adequately approximated by the bootstrap sampling distribution of T, denoted T*:

$$T^* = \frac{d^* - \hat{\theta}}{SE(d^*)} \qquad \text{(Eq. A-2)}$$

This distribution is comprised of the studentized statistic (T^*_B) computed from a large number (B) of randomly chosen bootstrapped samples $y_1^*, y_2^*, \ldots y_B^*$ from each of the four groups or populations. Here, d^* is the linear combination of group means for the bootstrapped sample; $\hat{\theta}$ is the observed difference in sample means from the original samples; $SE(d^*)$ is the estimated standard error of the linear contrast.

The 5th and the 95th quantiles of the T^* distribution ($T^*_{0.05}$ and $T^*_{0.95}$, respectively) satisfy the equations:

$$\Pr[\frac{\theta - d}{SE(d)} > T^*_{0.05}] = 0.95 \quad \text{(Eq. A-3a)}$$

$$\Pr[\frac{\theta - d}{SE(d)} < T^*_{0.95}] = 0.95 \quad \text{(Eq. A-3b)}$$

Rearranging these equations yields 95% confidence in each of the following two inequalities:

$$\Pr[d + T^*_{0.05}\, SE(d) < \theta] = 0.95 \quad \text{(Eq. A-4a)}$$

$$\Pr[d + T^*_{0.95}\, SE(d) > \theta] = 0.95 \quad \text{(Eq. A-4b)}$$

Bootstrapping is used to estimate the values $T^*_{0.05}$, $T^*_{0.95}$ and $SE(d)$. The left side of equation A-4a represents the 95% lower confidence limit on the difference equation ($\mu_y - \mu_x$); the left side of equation A-4b is the 95% upper confidence limit on the difference equation. Based on the two one-sided testing (TOST) approach presented in McBride (1999), if the bounds computed by Equations A-4a and A-4b are fully contained within the interval [–δ , +δ], then we conclude equivalence within δ units.

The specific steps used to compute the 95% upper and 95% lower confidence limits on the difference between two means using the bootstrap-*t* method are described below.

1. Bootstrap (sample with replacement from the original sample of size n) B = 10,000 samples from each of the four populations (1 pooled reference group and 3 mounds) separately.
2. Compute the T^*_B statistic for each bootstrapped set of independent samples. T^*_i is the bootstrapped-*t* statistic computed from the i^{th} bootstrap sample, defined by the following equation

$$T^*_i = \frac{\sum_{j=1}^4 c_j \bar{y}^*_{ji} - \sum_{j=1}^4 c_j \bar{y}_j}{SE\left(\sum_{j=1}^4 c_j \bar{y}^*_{ji}\right)} = \frac{\sum_{j=1}^4 c_j \bar{y}^*_{ji} - \sum_{j=1}^4 c_j \bar{y}_j}{\sqrt{\sum_{j=1}^4 s^2_{y^*_{ji}} c_j^2 / n_j}} \quad \text{(Eq. A-5)}$$

   where $\bar{y}^*_{ji}$, and $s^2_{y^*_{ji}}$ are the means and variances for the i^{th} bootstrapped sample from the j^{th} group (j=1 to 4); and $\bar{y}_j$ is the observed mean for the j^{th} group. Multiplying these group means by their respective coefficients c_j (1/3, -1, -1, -1) and summing the products yields the difference equation we wish to test (Equation 1). This step produces 10,000 values of the bootstrapped-*t* statistic which comprise the "bootstrap-*t* distribution".
3. Compute the standard deviation of the 10,000 bootstrapped linear combinations, $\sum_{j=1}^4 c_j\, \bar{y}^*_{ji}$ and save it as $SE(d)$. This is the bootstrap estimate of the true standard error.
4. Find $T^*_{0.05}$ and $T^*_{0.95}$, the 5th and 95th quantiles of the bootstrap-*t* distribution generated in Step 2. These values satisfy Equations A- 3a and A-3b.

5. Applying Equations A-4a and A-4b using the values $T^*_{0.05}$ and $T^*_{0.95}$ found in Step 4 gives the bootstrap-*t* estimate of the 95% lower and upper confidence limits on the difference equation, i.e.,

$$95\%\ \text{LCL} = \sum_{j=1}^{4} c_j\, \bar{y}_j + T *_{0.05}\, SE(d) \qquad \text{(Eq. A-6a)}$$

$$95\%\ \text{UCL} = \sum_{j=1}^{4} c_j \bar{y}_j + T *_{0.95}\, SE(d) \qquad \text{(Eq. A-6b)}$$

where $(\sum_{j=1}^{4} c_j \bar{y}_j)$ is the linear combination expressing the difference between the mean of the reference group and the mean of the three disposal mounds based on the original sample observations, and *SE(d)* is the standard deviation of the bootstrapped differences computed in Step 3.

References

Lunneborg, Clifford E. 2000. Data Analysis by Resampling: Concepts and Applications. Duxbury. 556 pp. + Appendices.

Manly, Bryan F.J. 1997. Randomization, Bootstrap and Monte Carlo Methods in Biology. Second edition. Chapman & Hall, London. 340 pp. + Appendices